



Comparative analysis of European vertical landing reusable first stage concepts

Jascha Wilken¹ · Sven Stappert¹

Received: 23 January 2024 / Accepted: 21 March 2024 / Published online: 17 April 2024
© The Author(s) 2024, corrected publication 2024

Abstract

Reusable launch systems have the potential to significantly impact the space launch service market if both a high reliability and low refurbishment costs can be achieved. This study delves into the Vertical Takeoff and Vertical Landing (VTVL) methodology, as currently employed by SpaceX, and forms a segment of the ENTRAIN study by DLR. This broader study encompasses an examination of both Vertical Takeoff Horizontal Landing (VTHL) and VTVL reusable first stages, exploring their performance across high-level design parameters. This manuscript's primary objective is to assess the quantitative impact of high-level design factors on launch vehicle performance, particularly in relation to the development of a future European reusable launch system featuring a VTVL first stage. For a two-stage vehicle with a payload performance of 7.5t into GTO, the effect of varying propellant combinations, staging velocities and engine cycles are assessed. The study encompasses an iterative, multidisciplinary analysis and sizing process for ten different configurations. Each design iteration not only entails a structural design analysis but also includes optimization of the ascent and descent trajectories. Finally, the developed vehicle concepts are compared to derive quantitative insights into the trade-offs associated with key design choices.

Keywords Reusable launch vehicle · VTVL · Multidisciplinary analysis

1 Introduction

As the Ariane 6 nears completion, the future trajectory of launcher development in Europe remains unclear. It currently appears likely that the next large launcher will be partially reusable. Yet, other aspects of the architecture were unclear when this study was initiated in 2018 and continue to be undefined. This includes critical aspects such as the vehicle staging, the fuel selection and the engine cycle. Although qualitative arguments for various choices are well-established, their quantitative impact on the overall vehicle system is less clear. For example, it is known that hydrogen offers extremely high performance with regard to the specific impulse but comes with the challenges associated with extremely low boiling temperature and low density. In contrast, hydrocarbon fuels, though denser, are associated with lower specific impulses.

The resulting quantitated effect of these conflicting qualitative trends on launcher performance is not well established and may differ significantly across various use cases. Accurately determining this impact requires a comprehensive, multidisciplinary evaluation of the entire launcher system for each considered option.

Multidisciplinary Design Optimization (MDO) for Vertical Takeoff and Vertical Landing (VTVL) first stages using various propellant combinations is established in current literature [1, 2]. However, these studies simplify subdiscipline models to facilitate actual optimization without excessive computational costs. For instance, rather than simulating ascent and descent trajectories, Δv budgets are typically used to assess launcher performance.

In contrast, studies with more detailed subdiscipline modeling usually focus on a limited selection of reference vehicles. The RETALT project [3], for example, conducted an in-depth investigation of two reference VTVL vehicles, particularly in terms of technologies required for the propulsive return of the stage.

Older system studies like FESTIP [4] that compared different options for European reusable vehicles only considered a hydrogen-fueled VTVL Single Stage to Orbit (SSTO).

✉ Jascha Wilken
jascha.wilken@dlr.de

¹ Deutsches Zentrum für Luft- und Raumfahrt, System Analysis for Space Transportation, Institute for Space Systems, Bremen, Germany

There exists a notable gap in published literature regarding the comparison of high-level design options based on a multidisciplinary design analysis, especially within the current European context.

The Europe's NexT Reusable Ariane (ENTRAIN) study by the DLR seeks to address this gap by quantitatively evaluating options for a partially reusable European launch system, laying a solid technical foundation for future discussions. While the extent of variations and iterations precludes the use of high-fidelity methods like Computational Fluid Dynamics (CFD) or Finite Element (FE) models, key sub-disciplines are modeled using specialized conceptual design tools. For example, the evaluation of each launcher in the study includes structural design analysis, optimization of both ascent and descent trajectories, and modeling of the propellant tank and associated feed, fill, and pressurization lines.

The study examines a range of design parameters, including staging velocity, fuel choice, engine cycle, and recovery method, to provide a comprehensive understanding of the trade-offs and potentials of various design choices.

The scope of the study is broad, and its findings are detailed in several publications. [5] provides an overview of the study's methodology and its relation to other European projects. [6] delves into propulsion datasets and the underlying rocket engine models. While this manuscript concentrates on the concepts employing a VTVL approach, the equivalent variants with the winged vehicles and horizontal landing are discussed in [7]. Finally, within [8] the different recovery approaches and compared in depth to each other.

While the study itself encompasses different recovery methods, this paper focusses on the modeling of launch vehicles employing the Downrange Landing (DRL) mode, first successfully used by SpaceX.

1.1 Study logic and high-level assumptions

The ENTRAIN study was structured into two parts: the first part concentrates on a comparative analysis of VTVL and VTHL launchers ensuring uniformity in the investigation level to prevent distortions from varied degrees of detail. Therefore, identical high-level requirements and assumptions are used for all return methods. This paper introduces the VTVL launchers investigated in this first part of the ENTRAIN study. They were all evaluated with regard to the following high-level requirements:

- 7000 kg + 500 kg margin payload to Geostationary Transfer Orbit (GTO) of $250 \text{ km} \times 35786 \text{ km} \times 6^\circ$ (standard Ariane 5 GTO) via a LEO parking orbit of $140 \text{ km} \times 330 \text{ km} \times 6^\circ$, see sect. 2.6.1 for details
- launch from Centre Spatial Guyanais (CSG), Kourou
- Two Stage to Orbit (TSTO) configurations

- same propellant combination in both stages
- same engines in both stages with exception of different nozzle expansion ratios

In the launchers detailed in sect. 3, an exception to the aforementioned two requirements is included: a hybrid launcher configuration. This unique model incorporates a methane-fueled lower stage and a hydrogen-fueled upper stage. The feasibility, potential advantages, and limitations of this hybrid launcher are discussed in sect. 4.

Based on these requirements, the following degrees of freedom were explored:

- Engine Cycles: Gas Generator (GG) and Staged Combustion (SC);
- VTVL with retropropulsion landing on downrange barge (DRL) or with Return-to-Launch-Site (RTLS);
- 2nd stage Δv of 6.2 km/s, 6.6 km/s, 7.0 km/s, 7.6 km/s.
- propellant combinations:
- Liquid oxygen (LOX)/ Liquid hydrogen (LH2);
- LOX/Liquid methane (LCH4);
- LOX/Liquid propane (LC3H8);
- LOX/kerosene, Rocket Propellant-1 (RP-1).

In the analysis of the staging variations, the upper stage Δv was chosen instead of the more commonly used separation Mach number. This decision was made to decouple the staging parameter from the variances caused by separation different altitudes, where atmospheric properties such as speed of sound can vary significantly. These variations limit the comparability exclusively via Mach number. For reference, the upper stage Δv of 6.2 km/s, 6.6 km/s, 7.0 km/s, 7.6 km/s approximately correspond to a separation Mach numbers of 15, 12, 10 and 7, respectively.

A comprehensive staging optimization would require a reliable cost function, which for reusable stages will depend on the cost of recovery and refurbishment of a used stage. Given the substantial uncertainties surrounding refurbishment and the impact of the stage separation velocity on these costs a full optimization was deemed impractical. Instead this parametric approach was chosen for this study.

In a preliminary design phase of the ENTRAIN study, when sizing the various combinations SI curves, it was found that the configurations with an upper stage Δv of 6.2 or 7.6 km/s resulted in excessively heavy and impractical launchers. The same result was found when trying to meet the required GTO performance with a first stage returning via RTLS. Fulfilling the total Δv requirement of the RTLS maneuver and the demanding GTO mission with a TSTO vehicle leads to excessive vehicle sizes, especially for the hydrocarbon-fueled concepts. Consequently, these options were excluded from the more detailed design study shown

hereafter. The results of the preliminary design phase are described in [9].

2 Methods

2.1 Launcher architecture

As described in [5], it was assumed that all launchers will be TSTO vehicles. Most launchers described hereafter share the same general layout: The same propellant combination in both stages as well as the same engines for both stages, albeit with a larger nozzle on the second stage. This is considered cost effective since only one engine core has to be developed and the high number of engines on the first stage results in a higher production rate, thus reducing both development and production cost per unit.

During the study, one exception to this architecture was added: The possibility of a hydrogen-fueled upper stage and a methane-fueled first stage was also evaluated, even though it does not strictly adhere to the above-mentioned logic. Even though this combination was found to be very performant, the need for two engine developments and the handling of two propellants at the launch pad has to be considered. This exception is hereafter referred to as the hybrid launcher.

2.2 Sizing logic

The design of launch vehicles is inherently iterative due to the interdependence of various subsystems. For each launcher, the initial design variables were the propellant loadings for both stages. Once these were determined, the vehicle geometry could be derived, assuming a constant

length-to-diameter ratio of ~ 15 for the entire launcher. With the geometry established, the aerodynamic coefficients can be estimated. Based on these inputs, the structural analysis, mass model, and trajectory optimization were addressed iteratively.

The main propulsion system was sized so that the thrust-to-weight (T/W) ratio at take-off was close to 1.4, with a number of engines that kept the T/W of the upper stage between 0.8 and 1.2.

The process then progressed to the optimization of ascent and descent trajectories to evaluate the total payload capacity and the Δv provided by the upper stage. The design of the launcher was considered to have converged once these values aligned closely with the targeted objectives, allowing for a margin of ± 150 kg for payload and ± 100 m/s for upper stage Δv . The sizing process used in this study is outlined in Fig. 1. The arrows to the left of a subsystem indicate the iterative loops necessary to achieve a convergent design.

2.3 Aerodynamic coefficients

The aerodynamic coefficients in this study were estimated using empirical methods similar to those in DATCOM [10], as implemented in the DLR tool cac [11]. With these methods, the aerodynamic properties of simple rotationally symmetric bodies with conic or ogive noses can be quickly assessed using analytical formulas supported by wind tunnel data.

While these methods are well suited for estimating coefficients for forward-flying launch vehicles, they do not inherently account for configurations like the engine-forward orientation during reentry. The complex geometry of the aft bay and multiple engine nozzles cannot be readily accounted for with cac. Therefore, for modeling the descent phase, the vehicle was represented within cac as a blunt cylinder. The

Fig. 1 Sketch of Launcher sizing process for ENTRAIN VTVL launch vehicles. The arrows to the left of a subsystem indicate the iterative loops necessary to achieve a convergent design

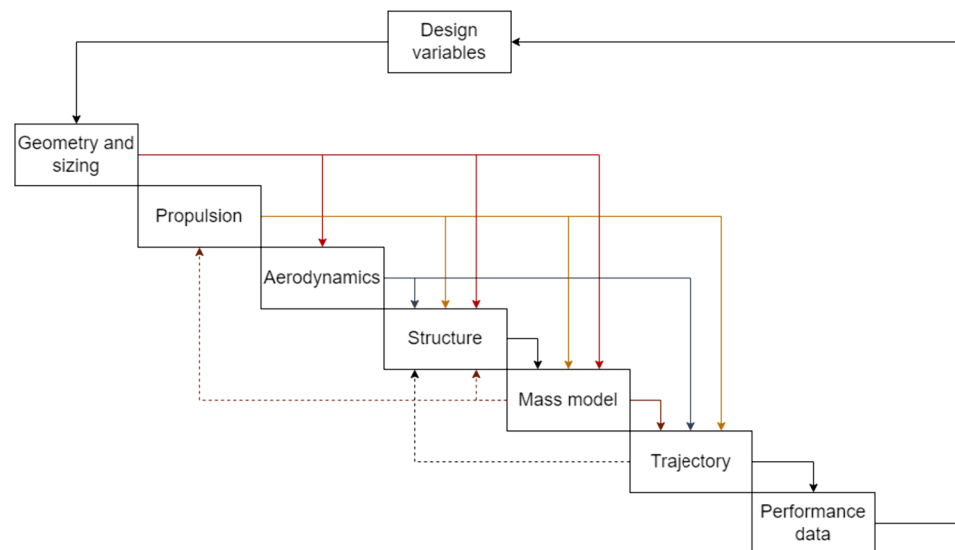


Fig. 2 Exemplary zero-lift drag coefficient used for both ascent and descent orientation, specifically for the CC GG Med configuration

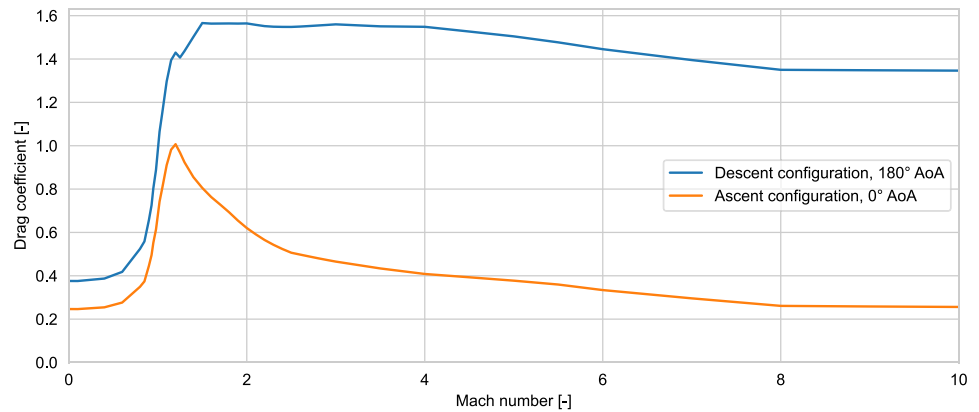


Table 1 LOX/RP-1, LOX/LC3H8, rocket engine data

Propellants	LOX/RP-1		LOX/LC3H8	
	1st stage	2nd stage	1st stage	2nd stage
Case	1st stage	2nd stage	1st stage	2nd stage
Engine cycle	GG	GG	GG	GG
Expansion ratio	20	120	20	120
Sea level Isp [s]	279	—	284	—
Vacuum Isp [s]	310	338	315	344
Engine T/W [-]	113	90	111	88

aerodynamic coefficients obtained from this model were then scaled to align with wind tunnel data for the zero-lift drag coefficient of blunt cylinders [12]. This approach was retroactively corroborated in subsequent studies, where similar aerodynamic configurations were analyzed using CFD calculations [13].

As an example, the thus derived zero-lift drag coefficients of both ascent and descent cases for a methane-fueled configuration are shown in Fig. 2.

2.4 Main propulsion rocket engines

The modeling of the engines and the derivation of the engine parameters such as specific impulse and T/W ratio and validation with existing engines are explained in-depth in [6].

The following Tables 1 and 2 summarize the resulting performance parameters used in this study.

For the landing burn of VTVL stages, the engines have to be throttled. The performance loss that occurs due to the reduced combustion chamber pressure necessary for throttling was not considered in the following trajectory optimization. As the landing burn only delivers a small amount of the overall Δv , it is expected that this impact is covered by the existing mass and performance margins.

2.5 Mass modeling

2.5.1 Structure

The structure mass was assessed with the DLR-SART tool *lsap* (Launcher Structure Analysis Program), which models the launcher structure as a beam. This allows the calculation of the global loads along the major structural components and the subsequent sizing of each segment to withstand the local loads. The global loads were evaluated on several load cases along the GTO trajectories. The load case of maximum product of dynamic pressure and Angle of Attack (AoA) had the biggest impact on the sizing of the structure. The analysis incorporated the change in effective AoA possible through steady winds and gusts. It was found that the loads during descent were not sizing for the main structures of the vehicles. While values such as the dynamic pressure or

Table 2 LOX/LCH4, LOX/LH2 rocket engine data

Propellants	LOX/LCH4				LOX/LH2			
	1st stage		2nd stage		1st stage		2nd stage	
Case	1st stage	2nd stage	1st stage	2nd stage	1st stage	2nd stage	1st stage	2nd stage
Engine cycle	GG	SC	GG	SC	GG	SC	GG	SC
Expansion ratio	20	23	120	120	20	23	120	120
Sea level Isp [s]	289	314	—	—	366	394	—	—
Vacuum Isp [s]	320	343	348	366	406	428	440	459
Engine T/W [-]	105	77	85	71	98	75	82	70

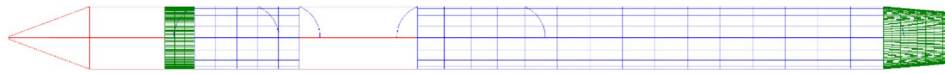
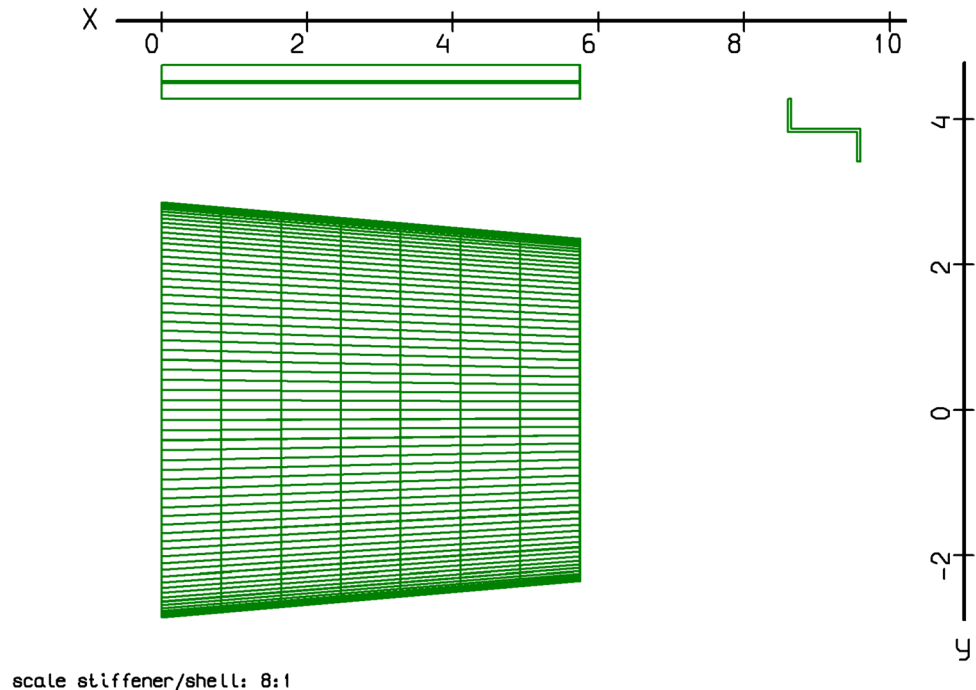


Fig. 3 Exemplary visualization of structure model for a LOX/LH₂ launcher, specifically the HH GG Med configuration

Fig. 4 Exemplary visualization of segment structure model for rear skirt of a LOX/LH₂ launcher, specifically the HH GG Med configuration. Stiffener geometry and size are shown in 8:1 scale compared to the shell



the axial or lateral acceleration might be higher during the descent, due to the reduced mass of the depleted stage, the actual loads within the structure are lower. This observation is further discussed in [14].

The fairing mass was not assessed with this tool, as the actual structural loads represent only one aspect that governs the fairing mass, and the others cannot be accurately assessed with this approach. Instead, the fairing mass was estimated by scaling the Ariane 5 fairing mass in proportion to surface area.

In the model, the interstage was represented as an Aluminum honeycomb structure, while other segments were depicted as conventional stringer/frame stiffened cylinders composed of AA 2219 alloy. An optimization process was applied to determine the precise number of stringers and frames for each segment, aiming to minimize total mass. The propellant tank's ullage pressure was set at 3 bar. A global safety factor of 1.25 was considered in the analysis, along additional margins for dynamic loads.

Figure 3 illustrates an example of the structural model. It depicts the stringer/frame stiffened propellant tanks in blue, the interstage and fairing in red, and the front and

Table 3 Design Matrix of ENTRAIN study with nomenclature abbreviations

Design parameter	Description	Nomenclature
Return method	VTVL Downrange Landing	VL DRL
	VTVL Return-to-Launch-Site	VL RTLS
	VTHL In-Air-Capturing	HL IAC
	VTHL Fly-Back	HL FB
Propellant	LOx-LH₂	H
	LOx-LCH₄	C
	LOx-LC₃H₈	P
	LOx-RP-1	K
Engine cycles	Staged combustion	SC
	Gas generator	GG
Upper stage Δv	6.6 km/s	Hi
	7.0 km/s	Med
	7.6 km/s	Lo

Options in bold are considered within this manuscript

rear skirts in green. A segment model for the rear skirt of a LOX/LH2 launcher is shown in Fig. 4 including the size and geometry of the optimized stiffener at 8:1 scale compared to the shell structure.

2.5.2 Propellant tanks and feedlines

The propellant system's modeling was conducted using the DLR-SART tool pmp (Propellant Management Program). This model includes the propellant tanks and incorporates the feed, fill, drain, and pressurization lines. The sizing of the hardware was determined through a simulation of the propellant and pressurization gas flow for the mission duration. This simulation facilitated the identification of the critical flow conditions within the lines, which then informed the sizing process.

A generic example of the propellant management system model for a LOX/LH2 launcher is shown in Fig. 5. The LOX tanks and feedlines are marked blue, the equivalent systems for LH2 market red. The pressurization lines are indicated in pink.

In addition to the usable propellant, a performance reserve of 0.9% and residuals of 0.36% were considered in the mass budget.

For all cryogenic propellants, an autogenous pressurization approach was assumed. Conversely, for the RP-1 tanks, helium pressurization was considered. Accordingly, the helium tanks required for this purpose were also sized and incorporated into the overall mass budget.

Cryogenic insulation of the propellant tanks was only considered for the LOX/LH2 launchers, for the hydrocarbon-fueled launchers no cryogenic insulation was included, following the example of the Falcon 9 with LOX/RP-1.

2.5.3 Recovery hardware

By definition the VTVL stages must include hardware that allows their safe and reliable return to earth, including a powered landing. While the engines are responsible for deceleration and control during propulsive phases, additional control surfaces are necessary for managing the vehicle's

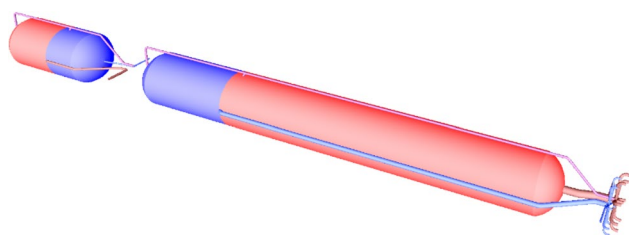


Fig. 5 Sketch of the model of propellant management system for both stages of a LOX/LH2 launcher, specifically the HH GG Med configuration

trajectory during non-propulsive descent phases within the atmosphere. These control surfaces also allow the returning stage to fly at small angles of attack. The lift and drag forces generated in this manner reduce the thermal loads on the stage, thereby allowing the reentry burn to be shorter. While different options exist for aerodynamic control surfaces (i.e., conventional fins would also be possible), for these study grid fins were chosen as the baseline design.

Alongside the control surfaces, landing legs are essential for the actual landing process. The mass of the recovery hardware in this study was estimated based on data from the Falcon 9. Although the exact values for Falcon 9 are not publicly available, their mass was estimated using in-house tools and reverse engineering techniques [15]. For the ENTRAIN RLV stages, the mass of the recovery hardware was estimated by linearly scaling the Falcon 9 recovery hardware mass in proportion to the dry mass of each stage.

In addition to the aforementioned recovery hardware, a thermal protection system is needed for the baseplate to protect the engine bay from the heat during reentry. A 2 cm thick layer of cork was chosen as a first guess, since there is little data available on the actual local heat loads. The generation of a comprehensive aerothermodynamic database would enable further optimization of this protective layer's thickness. It is presumed that the engine nozzle, which is designed to endure the thermal loads generated by the engine itself, is sufficiently robust to withstand the thermal stresses during reentry without the need for additional thermal protection.

2.5.4 Other subsystems/mass models

The mass model of the launchers was created using the SART tool stsm (Space Transport System Mass Estimation). This software applies empirical estimation formulas, which are grounded in historical data, to calculate the masses of various structural and subsystem elements. These elements include structural components such as the rear skirt, and subsystem masses such as engine equipment (including of engine controllers and wiring) as well as electrical systems including their harnesses. Other subsystems were sized based on the masses of corresponding components in the Ariane 6, including the power system and batteries, stage and fairing separation systems, avionics, the Reaction Control System (RCS), and the payload adapter.

Due to the inherently higher uncertainty in mass estimation for RLVs compared to ELVs, all first stage structures and subsystems were assigned a mass margin of 14%. The mass margin for the main engines for both stages was set at 12%. All other elements of the second stage were assigned a mass margin of 10%.

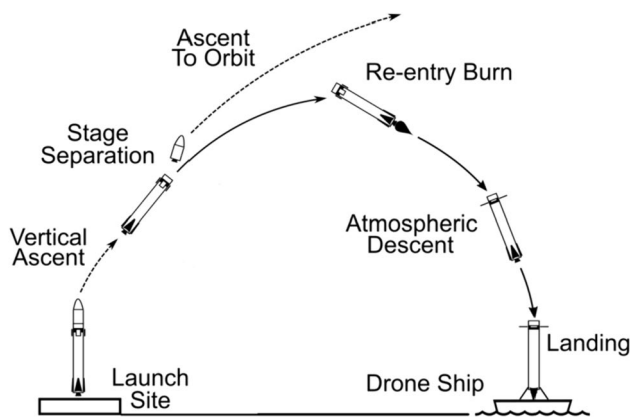


Fig. 6 Mission profile for downrange landing of first stage

2.6 Trajectory optimization

The mission profile for a mission including the recovery of the first stage via DRL is shown in Fig. 6. The assumptions used to optimize the ascent and descent phase are described in the following section. Due to constraints within the available trajectory optimization tools the two phases were optimized separately, however for the DRL mission type this approach yields sufficiently good results and agrees well with reverse-engineered trajectories from real vehicles [15]. Both ascent and descent trajectory optimizations were performed with the DLR tool *tosca*. It uses a direct single-shooting approach with a Runge–Kutta integration routine in combination with the optimization algorithm SLSQP [16]. For this type of performance assessment, the equations of motions are considered in three dimensions. The vehicle is modeled as point mass, no rotational dynamics are evaluated. The attitude of the vehicle is determined via the controls. The atmospheric model utilized in this study employs values of the NRLMSISE00 model [17] for Kourou.

2.6.1 Ascent

For the sizing of the launchers the performance into GTO was chosen, accordingly the ascent into a GTO with its perigee at 250 km was the reference ascent case. As CSG at Kourou in French Guyana was the designated launch location, the final GTO typically has an inclination of 6°.

To facilitate an efficient transfer of the payload into Geostationary Orbit (GEO), it is beneficial for the argument of perigee of the GTO to be approximately 0° or 180°, positioning it over the equator. To achieve this alignment, the upper stage is initially inserted into a 140×330 km parking orbit. It then raises its orbit to the final GTO configuration as it crosses the equator. This approach is necessitated by the relatively short burn time characteristic of the two-stage launchers, which would otherwise result in the Main Engine

Cut-Off (MECO) of the second stage occurring well before the stage reaches the vicinity of the equator.

This approach does have the drawback of requiring a second ignition of the second stage engine. However, given that the engines used in the second stage are identical to those in the first stage, the capability for reignition is inherently required. An additional consideration is the need to reserve some extra propellant for the chill-down of the engine prior to reignition. For this purpose, it was assumed that the mass flow equivalent to two seconds would be sufficient to adequately chill the engine for a successful reignition.

2.6.2 Descent

All launchers discussed hereafter use DRL on a barge (or some other landing platform in the Atlantic Ocean), to recover the first stage. As the barge can be freely positioned, no specific coordinates are targeted during optimization of the descent trajectory. The following landing conditions are targeted:

- Landing Flight Path Angle: $90^\circ \pm 2^\circ$
- Landing Velocity: 0 m/s–max. 2.5 m/s
- Landing Altitude: $0 \text{ m} \pm 10 \text{ m}$

In addition, the following constraints were imposed during the trajectory optimization:

- dynamic pressure of $< 200 \text{ kPa}$
- estimated heat flux of $< 200 \text{ kW/m}^2$ with respect to a (hypothetical) nose radius of 0.5 m
- lateral acceleration of $< 3 \text{ g}$

These constraints were chosen based on trajectories reverse engineered from SpaceX' Falcon 9 flights [15]. The high dynamic pressure encountered during reentry, in comparison to the ascent phase, is considered non-problematic. This is because, during reentry, the stage is significantly lighter due to the expended fuel. As a result, the global axial forces and bending moments generated during this phase are still lower than those experienced during the maximum dynamic pressure phase of the ascent, as shown in [14].

For the trajectory the heat flux is estimated with the following modified Chapman equation:

$$\dot{q} = 20254.4 \text{ W/cm}^2 \sqrt{\frac{\rho}{\rho_R} \frac{R_{N,r}}{R_N}} \left(\frac{v}{v_r} \right)^{3.05}$$

$R_{N,r}$ is reference nose radius (1 m), R_N is the vehicle nose radius (here 0.5 m for all vehicles), v is the vehicle's velocity and v_r is a reference velocity of 10000 m/s. In practice, the heat-flux constraint had the most impact on the Δv of the reentry boost.

As with the ascent, the descent trajectory optimization was also performed with the DLR tool *tosca*, with the optimization target being minimal propellant usage, while still respecting the above-mentioned constraints. For the entire trajectory the stage is simulated as a mass point without considering perturbations or rotational dynamics. While this approach is well suited to a performance estimation, it does not include the complexity of the control of the vehicle, especially during the reentry and landing phases.

3 Results

3.1 Nomenclature

The range of launchers considered in this study is categorized using a nomenclature that makes it easy to distinguish between vehicles based on key design space parameters, as outlined in Table 3. This nomenclature employs simple abbreviations for the return methods and engine cycles. In terms of propellants, each propellant combination is represented by a unique substitute letter. The first stage separation velocity is indicated by terms like "Hi" for high, "Med" for medium, and "Lo" for low separation velocity.

For example, a launcher featuring vertical landing with downrange landing, LOX/LH2 in both stages, gas generator engines and an upper stage Δv of 7.0 km/s would be dubbed: *VL DRL HH GG Med*. As this paper only discusses the VTVL stages, the "VL DRL" part is superfluous and is omitted in the following discussions.

3.2 Overview

Based on the assumptions and boundary conditions described in sect. 1.1 and the methods outlined in sect. 2, the propellant loading of the launchers was systematically varied. This iterative process continued until a viable solution was identified that aligned with the specific combination of upper stage Δv , fuel type and engine cycle being targeted. The key characteristics of the resulting launchers are given in Table 4. Not all possible combinations were investigated. For the reasons given in sect. 1.1 the RTLS return method and the upper stage Δv of 6.2 km/s and 7.6 km/s were discontinued. Also, the denser hydrocarbons, RP-1 and LC3H8, were only investigated for gas generator engines.

The following sections give an overview over the results with regard to geometry, mass, SI and inert mass ratio as well as the ascent and descent trajectories. The impact of the individual design degrees of freedom is discussed in sect. 4.

3.3 Size and geometry

Figure 7 presents a sketch illustrating the geometries of the resulting launchers from the study. A notable observation from this figure is that the launchers fueled by LCH4 are the largest in size, even surpassing their hydrogen-fueled counterparts significantly. Despite LCH4 having a higher density compared to hydrogen, the volume of these launchers is larger due to the substantially greater propellant loading required for LCH4. The difference in mass between the hydrogen and hydrocarbon-fueled launchers are explored in more detail in sect. 3.4.

Given the specified T/W at liftoff, it is observed that accommodating the engines beneath the stage becomes a challenge for the hydrocarbon-fueled launchers. In certain designs, this constraint leads to some engine nozzles slightly extending beyond the diameter of the fuselage. This issue is not encountered with the hydrogen-fueled launchers, primarily due to hydrogen's lower density, which allows for more spacious engine arrangement within the confines of the fuselage dimensions.

Generally, it is expected that this issue also stems from the sheer size of the launchers, since the base plate area does not increase linearly with the vehicle mass, which in turn is proportional to the thrust.

3.4 Mass

The Gross Lift-Off Mass (GLOM) of each configuration is shown in Fig. 8. At first sight, the difference between the hydrogen and hydrocarbon-fueled launchers is clearly apparent. This is expected due to the lower specific impulse of hydrocarbon-fueled stages.

Figure 9 shows the dry mass of the investigated launchers. The difference between hydrocarbon and hydrogen-fueled launchers is still significant but smaller than when only considering the GLOM. Within the hydrocarbon variants it is noteworthy that while the hydrocarbon-fueled launchers (for the same upper stage Δv) all exhibit similar GLOM, for the dry mass differences appear, favoring the denser hydrocarbons over the less dense LCH4.

The dry mass of the reusable first stages, with a particular focus on the portion comprised of the propulsion subsystem, is depicted in Fig. 10

3.5 Dimensionless parameters

To evaluate the performance of rocket stages, dimensionless parameters can be utilized. In the forthcoming paragraph, two such parameters will be used: The Structural Index (SI) excluding engine mass, and the Inert Mass Ratio (IMR). These parameters are defined as follows:

Table 4 Key parameters of investigated VTVL launchers

Fuel	LH2			LCH4			LC3H8			RP-1			Hybrid
	GG	GG	SC	GG	GG	SC	GG	GG	SC	GG	GG	GG	
Engine cycle	GG	GG	SC	GG	GG	SC	GG	GG	SC	GG	GG	GG	GG
2nd stage Δv [km/s]	6.6	7.0	7.0	6.6	7.0	7.0	6.6	6.6	7.0	6.6	7.0	7.0	7.0
Staging category	Hi	Med	Med	Hi	Med	Med	Hi	Hi	Med	Hi	Med	Med	Med
Designation	HH GG Hi	HH GG Med	HH SC Med	CC GG Hi	CC GG Med	CC SC Med	PP GG Hi	PP GG Hi	KK GG Hi	KK GG Hi	KK GG Med	CH GG Med	CH GG Med
1st stage													
Propellant loading [t]	392	311	250	1193	865	637	1251	1251	899	1221	899	441	441
Total dry mass [t]	47.9	41.7	35.9	98.1	73.2	57.3	94.2	94.2	68.1	88.4	68.1	41.2	41.2
Propulsion mass [t]	9.1	8	8.4	23.9	18.4	19	23.1	23.1	18	22.8	18	9.4	9.4
No. of engines [-]	9	9	9	17	15	11	15	15	13	15	13	9	9
Single Engine Thrust (sea level) [kN]	782	689	561	1165	1021	1062	1350	1350	1234	1352	1234	864	864
2nd stage													
Propellant loading [t]	63.8	77.7	66.3	125.6	151.8	128.7	137.2	137.2	169.2	135.9	169.2	72.1	72.1
Dry mass [t]	8.2	8.4	7.4	10.1	9.8	9.2	10.2	10.2	9.8	10	9.8	7.8	7.8
Propulsion mass [t]	1.3	1.2	1.1	1.9	1.6	2	2.1	2.1	1.9	2.1	1.9	1.1	1.1
Engine Thrust (vacuum) [kN]	942	829	652	1407	1229	1238	1629	1629	1495	1637	1495	777	777
Total Launcher													
Height [m]	86.5	79.9	75.1	91.3	83.6	76.2	88.9	88.9	77.3	82.8	77.3	69.7	69.7
Diameter [m]	5.4	5.3	5	6.1	5.7	5.1	5.9	5.9	5.4	5.8	5.4	5.0	5.0
Payload to GTO [t]	7.4	7.49	7.46	7.42	7.45	7.62	7.4	7.4	7.64	7.55	7.64	7.47	7.47
GLOM [t]	519	447	367	1434	1107	840	1500	1500	1153	1463	1153	570	570

Fig. 7 Sketch of investigated configurations with a VTVL first stage. Numbers above fairing indicate the staging via upper stage Δv

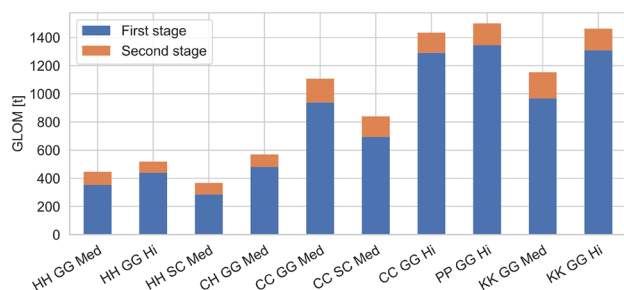
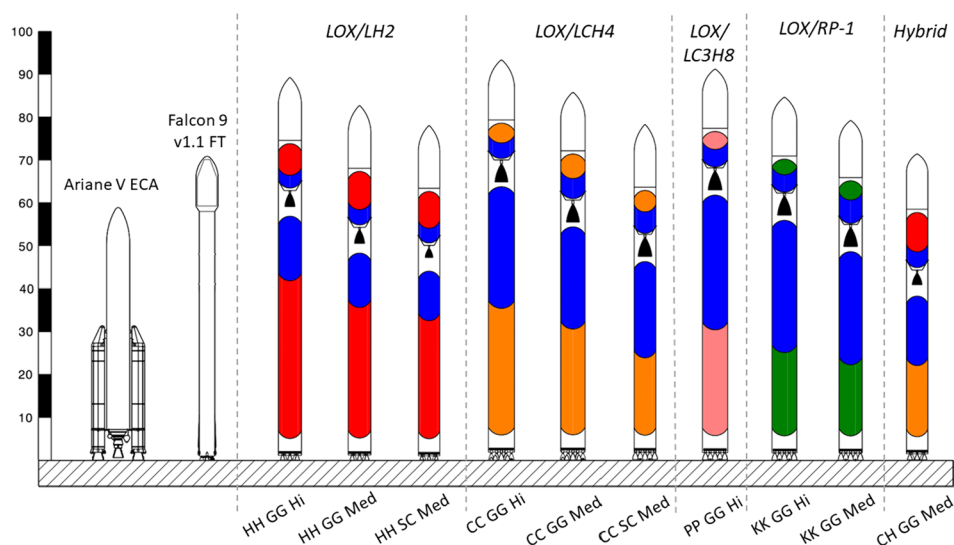


Fig. 8 GLOM of configurations with VTVL first stages with different propellant combination, staging velocities and engine cycles

$$\text{Structural index (SI)} = \frac{m_{\text{dry}} - m_{\text{engines}}}{m_{\text{propellant}}}$$

$$\text{Inert mass ratio (IMR)} = \frac{\text{GLOM}_{\text{stage}} - m_{\text{ascent propellant}}}{\text{GLOM}_{\text{stage}}}$$

While similar, the IMR is a better indicator of the ascent performance of the stage, since the descent propellant is essentially inert ballast during that phase. The SI is a good indicator of the overall efficiency of the stage design with regard to its dry mass.

Figure 11 shows the SI and IMR for all investigated reusable first stages as well as the Falcon 9. The comparison of the Falcon 9 to the launchers of this study is discussed in sect. 4.5.

The hydrocarbon stages have significantly lower SI's than hydrogen stages, mostly due to low density of LH2.

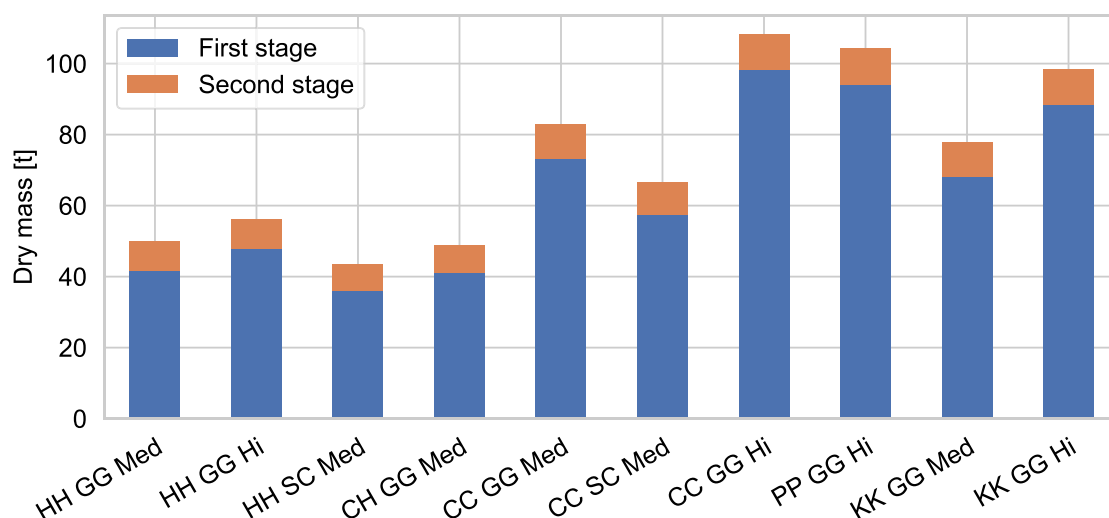


Fig. 9 Dry Mass of configurations with VTVL first stages with different propellant combination, staging velocities, and engine cycles

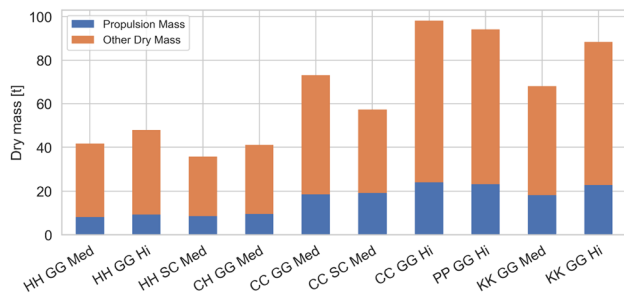


Fig. 10 Dry Mass of configurations with VTVL first stages with different propellant combinations, staging velocities and engine cycles, with the portion attributable to the propulsion subsystem highlighted

This is also true for the IMR, yet the difference appears reduced. The reduced disparity in IMR is primarily due to the increased requirement for descent propellant in hydrocarbon stages, which is a consequence of their lower engine efficiency. This additional propellant requirement partially offsets the benefits gained from having a lower SI.

The effect of the staging velocity can also be seen in these values. For launchers that have a lower upper stage Δv and consequently are the largest within their respective propellant group, there is a more significant disparity between the SI and IMR. This greater difference arises from the increased need for descent propellant in these stages with higher separation velocities. The additional propellant is required to decelerate the stage adequately, ensuring it does not exceed the heat-flux constraints during descent.

3.6 Trajectories

By their very nature, the ascent and descent trajectories contain many aspects that are of interest for the launch system, showing the evolution of all parameters is beyond the scope of this paper. In the context of this study the trajectories

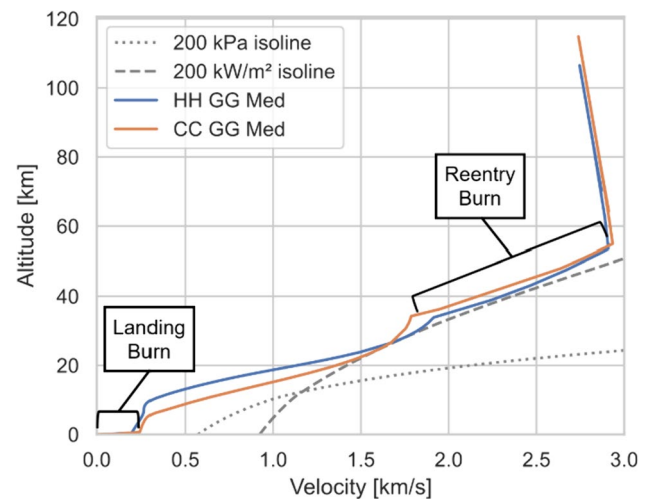


Fig. 12 Illustration of propulsive maneuvers in reentry profile (altitude over time)

primarily serve as a tool for determining the final sizing of the launchers. Therefore, the focus in this section will be on the return trajectory, as it represents the critical and novel element in these partially reusable launch concepts.

Two exemplary reentry profiles are illustrated in Fig. 12 with indication of the reentry and landing burns. These are characterized by sharp changes in the profile when the engines are ignited or extinguished. The two aforementioned constraints (200 kW/m² and 200 kPa) are indicated as well. It can be seen that the heat-flux constraint is the sizing constraint for this type of downrange reentry.

The ascent and descent during the ballistic arch after stage separation, but before the reentry burn, coincide in this perspective on the right edge of the figure.

Figure 13 illustrates the reentry profile (altitude over velocity) for all stages. It is observed that all stages exhibit a similar reentry trajectory, which aligns with expectations since the trajectory optimizer is designed to avoid regions of

Fig. 11 Structural Index and inert mass ratios over propellant mass of reusable VTVL first stages for different propellant combinations

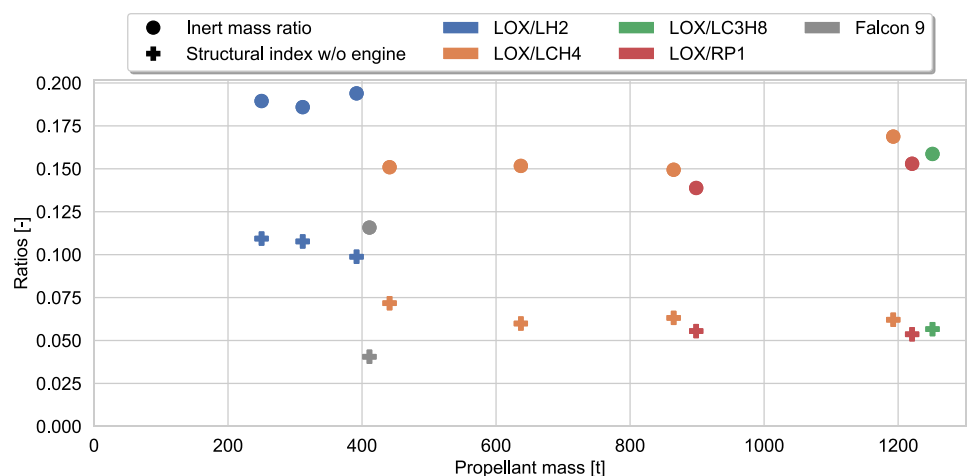
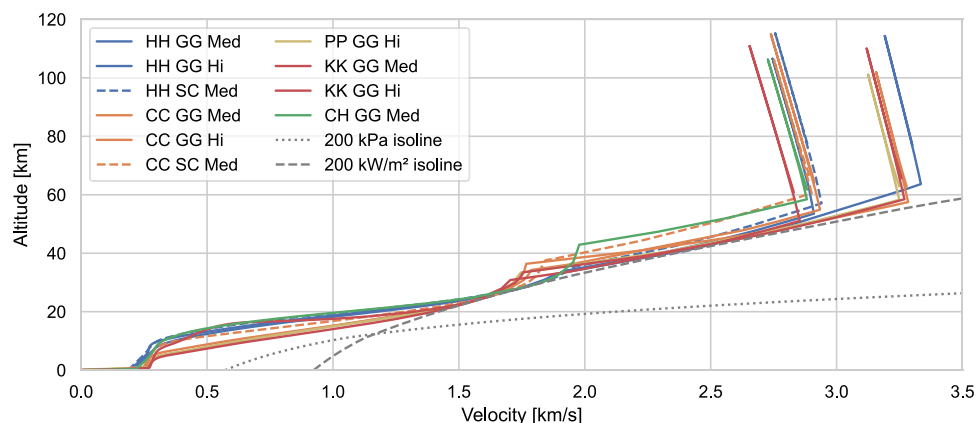


Fig. 13 Reentry profile of reusable VTVL first stages including the constraints for heat flux and dynamic pressure



high thermal loads while maximizing deceleration through aerodynamic forces. The clustering in the graph represents the two different staging velocities. The slight differences in initial conditions arise from variances in the ascent trajectory, as well as iteration limits applied with regard the upper stage Δv . Despite these initial discrepancies, the stages exhibit remarkably similar behavior post-reentry burn. The primary differentiator at this stage is the type of propellant used.

It can be seen that hydrogen stages are decelerated to ~ 1.9 km/s, whereas the hydrocarbon-fueled stages employ their engines to decelerate to ~ 1.75 km/s. Despite this difference in speeds at the end of the reentry burn, the maximum heat loads experienced by both types of stages are identical. The lower ballistic coefficient of the hydrogen stages enables them to achieve more deceleration through aerodynamic

means while still respecting the constraint set for maximum heat flux.

This difference is further illuminated when the cumulative forces acting on the returning stages over the entirety of the return trajectory are examined. Figure 14 presents these results for all evaluated stages. As anticipated, higher staging velocities necessitate additional engine Δv for deceleration during the reentry burn. A comparison between hydrogen and hydrocarbon-fueled stages reveals a greater impact of aerodynamic forces on the trajectory of hydrogen stages. Even near depletion the ballistic coefficient of the hydrogen stages is lower, which results in increased aerodynamic deceleration. Consequently, the engines of hydrogen-fueled stages are required to provide less Δv for both reentry and landing burns. Overall, this effect amounts to approximately 0.25 km/s less in

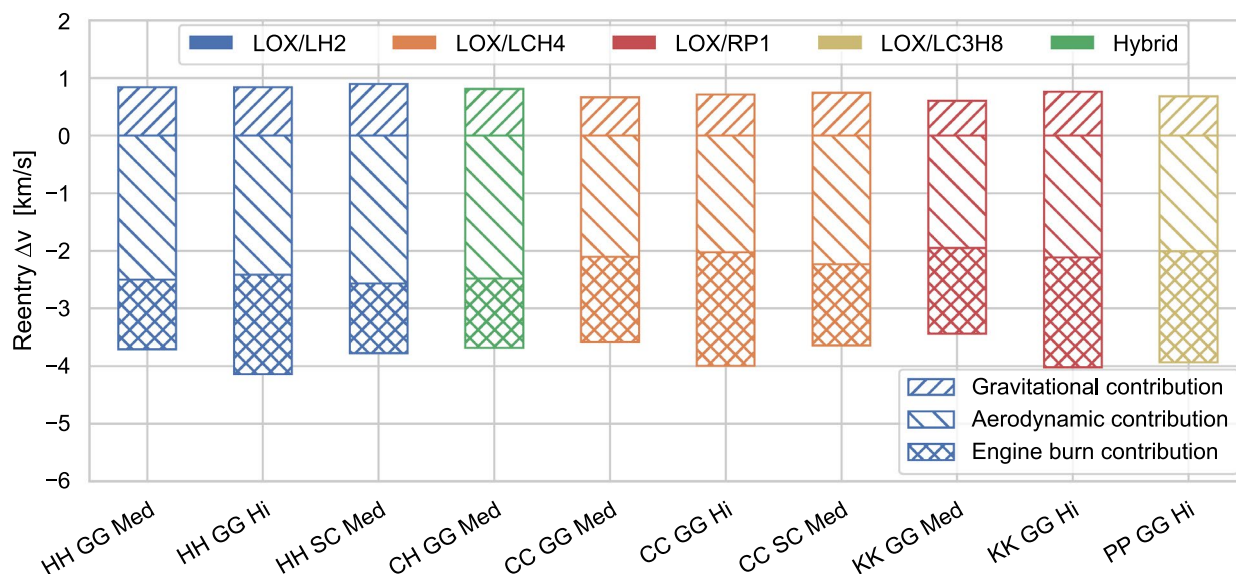


Fig. 14 Reentry velocity changes integrated of descent trajectory for returning VTVL stages

propulsive Δv . As a side effect of the decreased ballistic coefficient, the flight of the hydrogen-fueled stages has a longer duration, leading to slightly larger gravitational acceleration. This does not affect the propulsive budget, as it is compensated by a larger aerodynamic contribution as well.

The first stage of the hybrid launcher displays an unexpected behavior; despite being fueled with methane, it appears to follow the trends typically associated with hydrogen-fueled stages, as indicated in Figs. 13 and 14. This phenomenon can be attributed to two factors: First, the hydrogen upper stage is lighter than the equivalent methane upper stage, leading to less loads and thus potentially lighter structures. Second, due to the lighter upper stage the first stage itself also has a much smaller propellant loading (441 t) compared to the propellant loadings of the other methane stages (865 t). Assuming a similar SI, it is reasonable to infer that the dry mass of a stage is directly proportional to its volume. Meanwhile, the aerodynamic forces acting on the stage scale linearly with its cross-sectional area. This relationship results in heavier vehicles having higher ballistic coefficients, an example of the effects of the square–cube law. These two effects together lead to the first stage of the hybrid launcher having a reentry profile more similar to the hydrogen-fueled stages than the purely methane-fueled cases.

4 Discussion

As with every study, these results have to be seen in context with the underlying requirements and assumptions. The chosen reference orbit and the requirement of propulsively landing the first stage lead to considerable Δv needs. This, coupled with the TSTO architecture, leads to designs where each individual stage has to provide a substantial amount of Δv . Consequently, in this case, the specific impulse of the engines has an especially large impact on the overall vehicle size and mass, favoring solutions with higher specific impulses such as utilizing hydrogen as fuel or opting for staged combustion engines. For a lower energy reference orbit the comparison would yield different results, likely shifted toward the design choices with lower specific impulse. For now, the ability to lift significant payload mass into GTO remains a relevant for European launchers, but this might change if in-space tug services become economically viable or if the GTO market ceases to be relevant.

The subsequent sect. 4.1 delves into the comparison metrics for the various design options. Sections 4.2–4.4 each concentrate on a major design variable: fuel type, engine cycle, and staging velocity, respectively. Section 4.5 presents a comparison between the KK GG Med launcher and the

Falcon 9. Finally, in sect. 4.6 the limitations of the study are discussed.

4.1 Metrics of comparison

The primary objective of most contemporary launcher development programs, beyond simply ensuring access to space, is to reduce the cost of transporting payloads into orbit. This drive for cost reduction serves as the principal motivation behind the development of reusable stages. Thus, it is logical that the core metric of comparison should be the cost of the individual systems. However, cost estimation for launcher systems, even for ELV, remains an imprecise field, with a plethora of examples of programs exceeding their estimated costs. For RLV stages this is especially challenging, since no experience with the operation and refurbishment of these type of stages exists within Europe.

To navigate around these significant uncertainties, the upcoming sections will concentrate on GLOM and dry mass as comparison metrics. Of these two, the dry mass is considered a better indicator of the actual cost since the GLOM is dominated by the propellant mass. In the case of liquid propellant stages, the cost of the propellant typically constitutes only a small fraction of the total expenses.

While the dry mass is an imperfect surrogate, it should be noted that well-established cost estimation tools such as TRANSCOST rely on the dry mass to estimate the cost. Even more granular cost estimations methods that employ bottom-up approach usually estimate the cost of individual components based on their dry mass. In cases where the differences in dry mass are marginal, the final outcome of a cost comparison remains uncertain. However, in cases where there are significant disparities in the dry mass of the systems being compared, it is reasonable to anticipate that the cost comparison will yield a similar outcome.

4.2 Impact of fuel

For a more in-depth illustration of the impact of the fuel choice on the launcher mass, Figs. 15 and 16 shows the GLOM and dry mass for the launchers using gas generator cycle engines and an upper stage Δv of 6.6 km/s, since launchers with all investigated-fuel types were examined for this staging velocity.

For both GLOM and dry mass, the disparity between hydrogen and hydrocarbon fuels is significantly more pronounced than the differences among the various hydrocarbons, particularly in terms of GLOM. When it comes to dry mass, although the difference is less marked, it remains substantial. With respect to GLOM, the variances between the hydrocarbon fuels are relatively minor, yet in terms of dry mass, the denser hydrocarbons result in a noticeably lower mass. Notably, even though methane possesses the highest

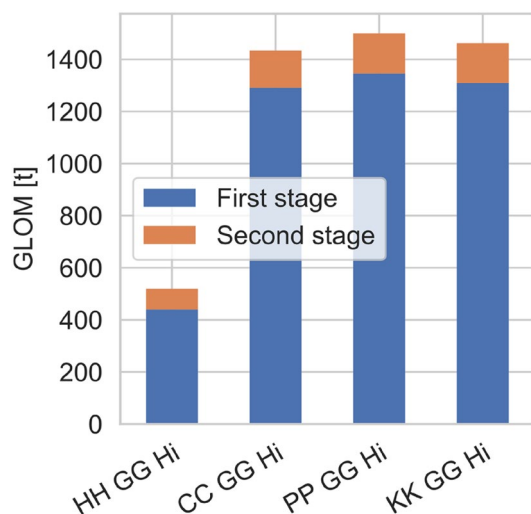


Fig. 15 GLOM of configurations with high separation velocity and gas generator cycle engines

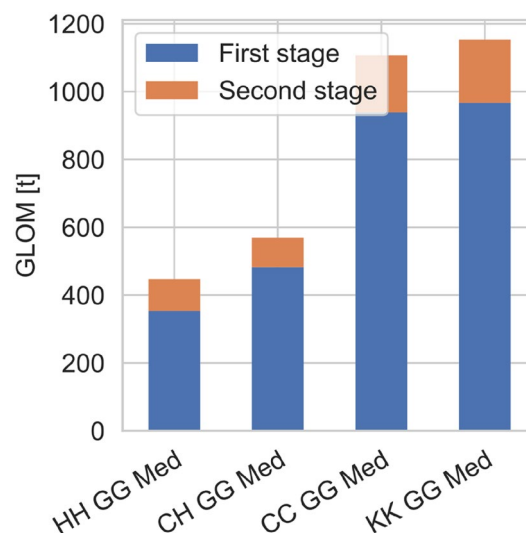


Fig. 17 GLOM of configurations with medium separation velocity and gas generator cycle engines

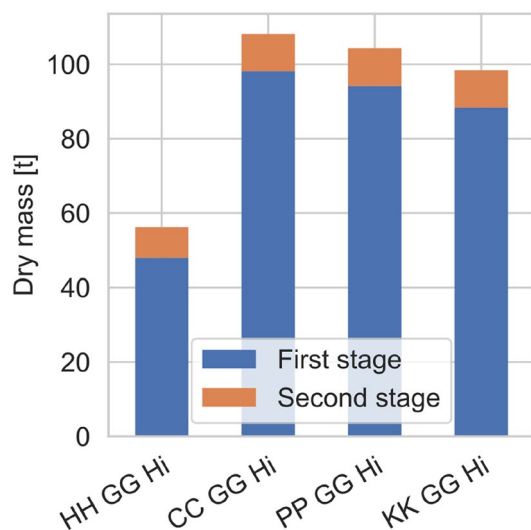


Fig. 16 Dry mass of configurations with high separation velocity and gas generator cycle engines

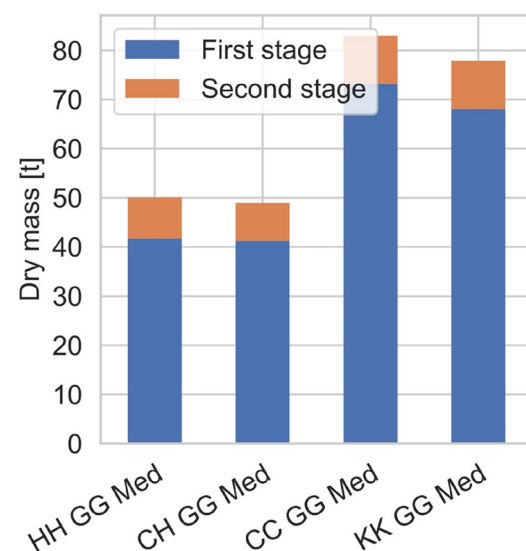


Fig. 18 Dry mass of configurations with medium separation velocity and gas generator cycle engines

specific impulse among the hydrocarbons examined in this study (see Tables 1 and 2 and [6]), its utilization as a fuel leads to the highest dry mass, almost twice the dry mass of the equivalent hydrogen-fueled launcher.

In the instances where the upper stage Δv is 7.0 km/s, as depicted in Figs. 17 and 18, the comparison between methane and hydrogen-fueled versions shows a slightly improved scenario. However, the dry mass of the reusable first stage of the methane-fueled launchers is still 76% heavier compared to their hydrogen-fueled counterparts. The primary contributor to this significant difference is the greater mass of the propulsion system in methane-fueled launchers, shown in Fig. 10, which in this case is 130% heavier

than the hydrogen-fueled counterpart. Although methane engines offer higher T/W ratios, the increased propellant load required for methane-fueled launchers leads to substantially higher thrust demands. This, in turn, results in a greater propulsion mass.

The hybrid launcher configuration, featuring a methane-fueled lower stage and a hydrogen-fueled upper stage, demonstrates the lowest dry mass among all configurations with gas generator engines. However, its GLOM is higher compared to an equivalent all-hydrogen stage. It is also important to consider that the hybrid launcher required two

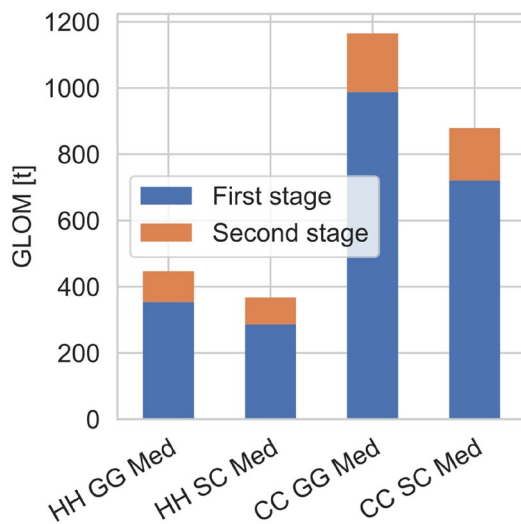


Fig. 19 GLOM of configurations with staged combustion cycle engines and counterparts with gas generator engines

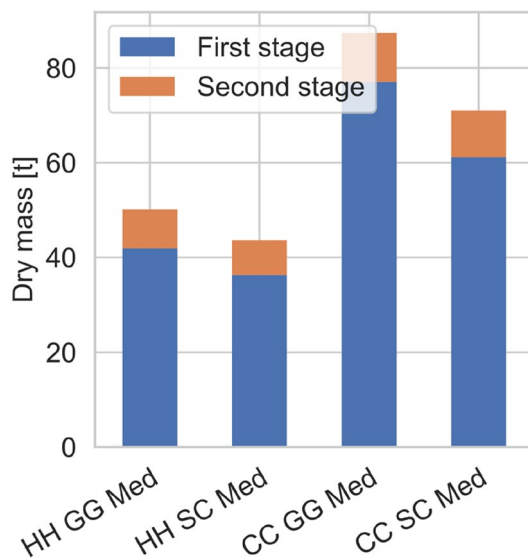


Fig. 20 Dry mass of configurations with staged combustion cycle engines and counterparts with gas generator engines

distinct rocket engines, one for each fuel. This is likely to increase development costs due to the complexities involved in designing, testing, and manufacturing two different propulsion systems.

4.3 Impact of engine cycle

Within this study two engine cycles were considered: gas generator and staged combustion. Historically, these are the two most common engine types for main rocket engines of orbital vehicles. An in-depth discussion of the assumptions for both cycles and their modeling can be found in [6].

In the following Fig. 19 and Fig. 20, the two launchers modeled with staged combustion engines are presented alongside their counterparts equipped with gas generator cycle engines. One of these launchers is fueled with hydrogen, while the other uses methane. As expected, the launchers with the closed engine cycles can fulfill the required mission with substantially less GLOM and dry mass. The difference is especially pronounced for the methane-fueled version. For the hydrogen-fueled launchers, those utilizing gas generator engines have a 22% higher GLOM compared to their counterparts with staged combustion engines. In the case of methane-fueled launchers, this difference increases to 32%. Regarding the dry mass of the reusable first stage, the hydrogen and methane variants show a difference of 16 and 27%, respectively, when comparing gas generator engines to staged combustion engines.

4.4 Impact of staging velocity

As previously discussed in sect. 1.1, only the high and medium separation velocities are included herein. The more extreme separation velocities, coinciding with upper stage Δv of 6.2 and 7.6 km/s, resulted in excessively large vehicles, especially for the hydrocarbons. Of the two remaining staging velocities, the medium separation velocities deliver lower GLOM and dry mass across all propellants, as can be seen in Fig. 8. It should be noted that with the higher staging velocity the reusable fraction of the launcher increases and thus that a cost-optimal staging will not necessarily coincide with the lowest mass optimum.

In contrast to VTHL return methods, the loads during reentry do not differ significantly between the different staging velocities. The reentry burn is optimized so that the same heat-flux constraints are respected. Consequently, higher separation velocities lead to higher Δv requirements for the descent and thus larger descent propellant masses.

4.5 Comparison with Falcon 9

Currently only one orbital launch vehicle with a reusable VTVL first stage is in operation, the Falcon 9. To assess the Falcon 9, the launcher was reverse-engineered on system level with publicly available data [15] with the tools described in chapter 3. The results from this reverse engineering have informed the methodology used to assess the VTVL stages within this study. The resulting values for the performance and mass of the Falcon 9 are in good agreement with the publicly available data including the broadcast of the trajectory. This indicates that the methodology described in chapter 3 is suited to the modeling of this type of vehicles.

In Figs. 21 and 22 the GLOM and the SI data of the Falcon 9 are shown compared to the KK GG Med configuration investigated within this study.

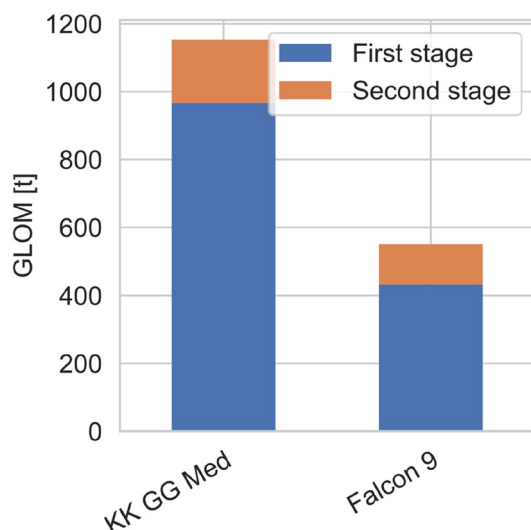


Fig. 21 GLOM comparison of the configuration KK GG Med with the Falcon 9

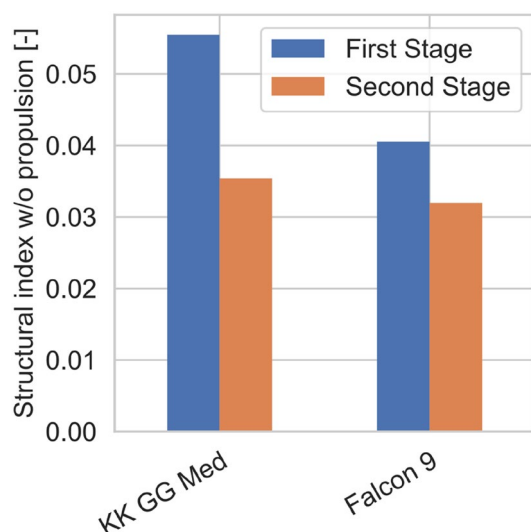


Fig. 22 Dry mass comparison of the configuration KK GG Med with the Falcon 9

At first glance, it becomes clear that the KK GG Med launcher is significantly larger and heavier than the Falcon 9. This is partially explained by the different payload performance into GTO while recovering the first stage on a barge (7.5t for the ENTRAIN launcher vs. ~5.5t for the Falcon 9). However, this difference accounts only for ~36% difference, while the total mass of the ENTRAIN launcher is more than twice the weight of the Falcon 9.

One major difference is found in the T/W of the engines. While the gas generator kerosene engine used in the first

stage of the KK GG Med configuration have a T/W of 105, for the Merlin 1D a value of ~160 was assumed for the Falcon 9 reverse engineering. As the performance with regard to specific impulse is similar, discussed in [6], the difference in T/W is almost entirely caused by differences in the estimated mass of the engines.

But even in the SI without the propulsion subsystems, shown in Fig. 22, differences between the two stages can be found. For both stages the ENTRAIN launcher has higher SI values than the Falcon 9. This difference is only compounded by the fact that the propellant loading of the Falcon 9 is significantly lower (411t vs 899t in the first stage) and thus the SI should be higher. Figure 11 shows the SI and the IMR over the propellant mass, where this factor is clearly apparent.

The underlying cause can be found in the design of the stages themselves. While on the surface the launchers share many characteristics, the Falcon 9 includes features that significantly lower the dry mass. Most importantly, the use of highly subcooled and thus densified propellants as well as the use of aluminum–lithium for the main structural elements.

This crosscheck with values reverse engineered from the Falcon 9 indicates that the launchers derived within this study are realistic and feasible. However, the challenge of actually achieving these values in a concrete design should not be underestimated, even if they are not as ambitious as the metrics of the Falcon 9.

4.6 Limitations

Any comparison of design options for launch vehicles (or any technical system) represents a compromise between the depth of the analysis, the breadth of scope and the available resources. To assess the effect of high-level design choices, such as propellant combination, engine cycle or staging velocity, the breadth of this study is necessarily large. While we believe sufficient depth was achieved to characterize the performance of the vehicles and their main subsystems, many details of an actual implementation were not directly evaluated.

In general, the uncertainties in the performance assessment are smaller than the uncertainties in the mass assessment. For a given mass budget the trajectory integration can be done precisely, with the main uncertainties lying in the propulsion performance and the aerodynamic properties. As discussed in [6], the propulsion datasets are cross-checked with existing engines where possible. With regard to the ascent aerodynamics, the engineering methods used are adapted to the typical ascent configuration and the impact on the overall performance is small. The largest uncertainty with regard to the performance assessment lies in

the aerodynamic properties during descent. The complex geometry resulting from flying engine first cannot be easily modeled with engineering approaches. While the chosen approach, described in sect. 2.3, is corroborated by wind tunnel and a-posteriori CFD results, the fact remains that no experience in flying this type of vehicle exists in Europe and thus some uncertainty is unavoidable with regard to the aerodynamic properties in engine-forward flight.

The larger uncertainties of the chosen methodology lie in the dry mass estimation of the launchers, especially for the reusable first stages. The mass estimations mostly rely on empirical relations based on historical data or conceptual design tools that cannot depict the full complexity of an actual launch vehicle. While the general suitability of the methodology is affirmed by its ability to replicate the Falcon 9, as discussed in sect 4.5, uncertainties remain with regard to an actual European implementation of such a vehicle.

Nonetheless, more detailed investigations of reduced scope but increased technical depth, performed within the scope of ENTRAIN2 for the hybrid launcher, essentially confirmed the results and did not identify any major inconsistencies [13, 18, 19].

On a broader scope, the chosen metrics of comparison, as discussed in the previous sections, don't account for all economical or operational aspects of the investigated design options. For example, the refurbishment or recovery effort per mass might vary depending on the staging velocity or propellant choice. However, even with this caveat, the assessment of the vehicle mass and performance is a necessary part of the full picture and essential in avoiding design choices that are optimal for a given aspect/subsystem without an understanding of the impact on the system level.

Finally, the launchers shown herein are not the result of a full multidisciplinary optimization. As discussed in sect. 1.1, the staging is varied parametrically and for many secondary parameters (for example the engine nozzle expansion ratio) are chosen based on previous experience or expert judgements. While this is sufficient to arrive at representative vehicle designs, it leaves some potential for optimization and might introduce some distortions into the comparison.

5 Conclusion

Within this paper ten different launchers, with a reusable VTVL first stage, were preliminarily sized using different assumptions for staging, fuel choice and engine cycle to achieve a payload performance of 7.5t into GTO. For all stages a reusable first stage, recovered via downrange landing, was assessed. For each launcher dedicated technical

models for the major subsystem were generated, including structure, propulsion, propellant tanks, feed-, fill- and pressurization lines as well as aerodynamics datasets for ascent and descent. The performance was assessed via trajectory optimization for both ascent and descent.

This effort lead to realistic and quantified data with regard to the effect of the investigated design options for a European reusable first stage which can serve as a technical foundation in discussions with regard to future European launchers.

The high Δv required to fulfill a GTO mission while also safely decelerating the reusable stage during reentry leads to substantial launcher sizes, especially for the hydrocarbon-fueled launchers, where the lower specific impulse has a large impact on the overall launcher mass even with the lower structural indexes. The methane-fueled VTVL stages exhibited a 76% higher dry mass than their hydrogen-fueled equivalents. With regard to GLOM, the entirely methane-fueled launcher with gas generator engines is almost two and a half times as heavy as its hydrogen counterpart.

Within the investigated hydrocarbons (RP-1, propane and methane), the RP-1 fueled cases result in the smallest and lowest dry mass launch vehicles. The GLOM of all vehicles fueled by hydrocarbons was fairly similar.

As expected, using staged combustion engines leads to noticeably reduced launcher sizes and masses. The dry mass of the reusable first stage for hydrogen and methane-fueled configurations is reduced by 14 and 22% respectively, compared to equivalent launchers with gas generator engines.

The use of methane (or likely any hydrocarbon) in the first stage with a hydrogen-fueled upper stage leads to a significantly lighter launcher than the use of methane in both stages. This hybrid configuration even has a slightly smaller dry mass than the entirely hydrogen-fueled version. However, this necessitates the development of two separate rocket engines for each fuel, and the handling of two different fuels on the launch pad.

Author contributions J.W. and S.S. performed the technical work, generated and analyzed the data described herein together. J.W. wrote the main manuscript text. All authors reviewed the manuscript.

Funding Open Access funding enabled and organized by Projekt DEAL.

Declarations

Conflict of interest The authors have no relevant financial or nonfinancial interests to disclose. During the preparation of this work, the authors used ChatGPT 4 to revise the text. After using this tool/service, the authors reviewed and edited the content as needed and take full responsibility for the content of the publication.

Open Access This article is licensed under a Creative Commons Attribution 4.0 International License, which permits use, sharing, adaptation, distribution and reproduction in any medium or format, as long

as you give appropriate credit to the original author(s) and the source, provide a link to the Creative Commons licence, and indicate if changes were made. The images or other third party material in this article are included in the article's Creative Commons licence, unless indicated otherwise in a credit line to the material. If material is not included in the article's Creative Commons licence and your intended use is not permitted by statutory regulation or exceeds the permitted use, you will need to obtain permission directly from the copyright holder. To view a copy of this licence, visit <http://creativecommons.org/licenses/by/4.0/>.

References

1. Dominguez Calabuig, G.J., Wilken, J.: Pre-conceptual staging trade-offs of reusable launch vehicles. 9th European Conference for aeronautics and space science, EUCASS 2022 (2022)
2. Dresia, K., et al.: Multidisciplinary design optimization of reusable launch vehicles for different propellants and objectives. *J. Spacecr. Rocket.* **58**(4), 1017–1029 (2021)
3. Marwege, A., Gülhan, A., Klevanski, J., et al.: RETALT: review of technologies and overview of design changes. *CEAS Space J.* **14**, 433–445 (2022). <https://doi.org/10.1007/s12567-022-00458-9>
4. Kuczera, H., Johnson, C.: The major results of the FESTIP system study. 9th International Space Planes and Hypersonic Systems and Technologies Conference (1999)
5. Dietlein, I., et al.: Overview of system study on recovery methods for reusable first stages of future European launchers, *CEAS space journal*, Submitted for publication (2024)
6. Sippel, M., Wilken, J.: Selection of propulsion characteristics for systematic assessment of future European RLV-options, *CEAS space journal*, Submitted for publication (2024)
7. Bussler, L., et al.: Comparative analysis of European horizontal-landing reusable first stage concepts, *CEAS space journal*, Submitted for publication (2024)
8. Stappert, S., et al.: Options for future European reusable booster stages: evaluation and comparison of VTHL and VTVL return methods, *CEAS space journal*, Submitted for publication (2024)
9. Stappert, S., Wilken, J., Sippel, M.: Evaluation of European Reusable VTVL Booster Stages. 2018 AIAA SPACE and astronautics forum and exposition. <https://elib.dlr.de/121912/> (2018)
10. Vukelich, S.R., Stoy, S.L., Burns, K.A., et al.: Missile DATCOM, volume I-final report, McDonnell Douglas, Technical report AFWAL-TR-86-3091
11. Klevanski, J., Sippel, M.: Beschreibung des Programms zur aerodynamischen Voranalyse CAC Version 2 (2003)
12. Nichols James, O., Edward, A.N.: Aerodynamic characteristics of blunt bodies. No. NASA-CR-59914 (1964)
13. Stappert, S., et al.: European next reusable ariane (ENTRAIN): a multidisciplinary study on a VTVL and a VTHL Booster Stage. In: Proceedings of the International Astronautical Congress, IAC (2019)
14. Sippel, M., Stappert, S., Bussler, L.: Systematic assessment of a reusable first-stage return options, IAC-17-D2.4.4, 68th International Astronautical Congress, Adelaide, Australia, <http://elib.dlr.de/114960/> (2017)
15. Stappert, S., Sippel, M.: Critical analysis of spaceX falcon 9 v1.2 launcher and missions, SART TN-009/2017 (2017)
16. Kraft, D., Schnepfer, K.: SLSQP—a nonlinear programming method with quadratic programming subproblems. *DLR, oberpfaffenhofen* 545 (1989)
17. Picone, J.M., et al.: NRLMSISE-00 empirical model of the atmosphere: Statistical comparisons and scientific issues. *J. Geophys. Res. Space Physics* (2002). <https://doi.org/10.1029/2002JA009430>
18. Wilken, J., Stappert, S.: Investigation of a European reusable VTVL first stage. 8th European Conference for aeronautics and space sciences (EUCASS), Madrid, Spain. <https://elib.dlr.de/135409/> (2019)
19. Wilken, J., et al.: Multidisciplinary design analysis of reusable European VTHL and VTVL Booster Stages. 2nd International Conference on High-Speed Vehicle Science Technology (HiSST), 11–15 September 2022, Bruges, Belgium

Publisher's Note Springer Nature remains neutral with regard to jurisdictional claims in published maps and institutional affiliations.



Overview of system study on recovery methods for reusable first stages of future European launchers

Ingrid Dietlein¹ · Leonid Bussler¹ · Sven Stappert¹ · Jascha Wilken¹ · Martin Sippel¹

Received: 22 December 2023 / Revised: 7 May 2024 / Accepted: 31 May 2024 / Published online: 1 July 2024
 © The Author(s) 2024

Abstract

The design of a reusable launch vehicle implies the need to provide for a means to safely retrieve the component to be re-used. Following economic considerations, reusable launch vehicle concepts tend to be designed such that large parts, like entire stages, are to be recovered. These are usually significant in size and weight and have acquired a considerable amount of energy during their primary mission. This poses the challenge of how to recover them in a way that makes it available for further re-uses. In the past and present, different methods were and are used. Depending on the selected recovery method, the system design is very different necessitating different technologies and competencies to be acquired for a successful design. Two major classes of recovery methods can be distinguished: those recovery methods ending with a vertical landing of the reusable stage and those ending with a horizontal landing. Both have their own benefits and drawbacks. In 2016, The German Aerospace Centre DLR has initiated a large in-house study with the aim of investigating, in a comparative manner on system level, both classes of recovery methods on a system level for two-stage-to-orbit launch vehicles with a reusable first stage and an expendable upper stage to be operated within a European context. Fuel choice and engine cycle were major design parameters that were considered during the study. The present paper presents the framework of this study describing the adopted study logic, providing an overview of the major findings obtained at the end of the first study phase and gives an outlook to the work of the second study phase. It ends with providing a view of a possible demonstrator and technology roadmap toward the realization of an operational two-stage-to-orbit launch system with a reusable first stage.

Keywords ENTRAIN · Horizontal landing · Reusability · RLV · Space transportation · Vertical landing

Abbreviations

3STO	Three stage to orbit	CFD	Computational Fluid Dynamics
AEDB	Aerodynamic database	CNES	Centre National d'Etudes Spatiales
AKIRA	Ausgewählte Kritische Technologien und Integrierte Systemuntersuchungen für RLV Anwendungen (specific critical technologies and integrated system investigations for RLV applications)	DLR	Deutsches Zentrum für Luft- und Raumfahrt (German Aerospace Centre)
BEO	Beyond Earth orbit	DRL	Downrange landing
CALLISTO	Cooperative Action Leading to Launcher Innovation for Stage Toss-back Operations	e. g.	<i>exempli gratia</i> (for example)
C	Carbon/methane	ENTRAIN	European Next Reusable Ariane
CFRP	Carbon fiber reinforced polymer	ESA	European Space Agency
		EU	European Union
		EVEREST	Evolved European Reusable Space Transportation
		FALCon	Formation flight for in-Air Launcher 1st stage Capturing Demonstration
		FB	Fly-back
		FESTIP	Future European Space Transportation Investigations Programme
		FLPP	Future Launcher Preparatory Programme
		GG	Gas generator
		GLOM	Gross lift-off weight
		GTO	Geostationary transfer orbit
		H	Hydrogen

✉ Ingrid Dietlein
ingrid.dietlein@dlr.de

¹ Deutsches Zentrum für Luft- und Raumfahrt, System Analysis for Space Transportation, Institute for Space Systems, Bremen, Germany

Hi	High
HL	Horizontal landing
IAC	In-air capturing
Isp	Specific impulse
JAXA	Japan Aerospace Exploration Agency
K	Kerosene
LEO	Low Earth orbit
LCH4	Liquid methane
LC3H8	Liquid propane
LH2	Liquid hydrogen
Lo	Low
Med	Medium
MEO	Medium Earth orbit
P	Propane
P/L	Payload
ReFEx	Reusability Flight Experiment
RETALT	Retro Propulsion Assisted Landing Technologies
RFA	Rocket Factory Augsburg
RLV	Reusable launch vehicle
RTLS	Return to launch site
SC	Staged combustion
SLME	SpaceLiner Main Engine
SSO	Sun synchronous orbit
SSTO	Single-stage-to-orbit
TRANSIENT	Thermalkontrollsystem für wiederverwendbare Träger (thermal control system for reusable launchers)
TRL	Technology readiness level
TSTO	Two-stage-to-orbit
T/W	Thrust-to-weight ratio
VL	Vertical landing
VTHL	Vertical take-off horizontal landing
VTVL	Vertical take-off vertical landing
w. r. t.	With respect to
Symbols	
ΔV	Velocity increment [m/s]

1 Introduction

In the past years, new launch system emerged that allowed reusing major parts, mostly the first stage. This re-introduction of reusability to the space transportation business potentially allows launch cost reductions, thus paving the way to create new markets based on the exploitation of space assets and innovations in space technology [1]. The launch vehicles developed and operated by Space X are the forerunners of this trend, whereas companies continue new developments, sometimes toward a reuse of each element. Further, actors are picking up this trend and develop own systems with the ability to re-fly parts of it.

Parts of the launch system that shall be re-used have to be recovered in a way that minimizes damage to it. This recovery, due to the high energy to be dissipated during recovery, is challenging. Several approaches for this recovery exist, some of them still in concept phase, a few however having been flight-proven.

SpaceX and Blue Origin have chosen the recovery via vertical landing as their baseline approach, a suitable choice considering that both companies plan to send their vehicles to the Moon or Mars where no or very little atmosphere exist which is incompatible with a winged horizontal landing on Moon or Mars surface. Other concepts pursue an approach of horizontal landing using wings for dissipating energy, see Sect. 2 for an overview of some major European studies on reusable launch systems (RLV). Both approaches have their advantages and drawbacks. For instance, where a vertically landing vehicle can do with a comparatively compact landing site, a horizontally landing vehicle needs a runway. In exchange, a horizontally landing vehicle has a higher potential for maneuverability and thus an increased flexibility to manage its flight path than unwinged vertically landing vehicles.

As it is currently unclear what choice would be best suited within a European context and considering this lack of a systematic comparison, DLR initiated in 2016 a system study named “European Next Reusable Ariane” (ENTRAIN) that aims at comparing various return and landing strategies on system level. Its focus is oriented toward two-stage-to-orbit systems (TSTO) with a reusable first stage and an expendable upper stage with vertical lift-off. The decision for or against a specific recovery method is probably one of the most significant development decisions made during the early concept phase of a launcher development program. It will determine the accompanying technology development roadmap and the tests to be performed to which significant financial resources will have to be dedicated. As such, there is a financial interest in consolidating the trust in this decision at an early stage as best as possible as later changes would come at significant costs and planning setbacks [2].

This paper gives an overview of the study approach, the adopted down-selection process and its major findings. It concludes with a brief overview of the DLR vision of a technology and demonstrator roadmap toward a European reusable launch vehicle considering current European technology and demonstrator development initiatives and an outlook on the continuation of the ENTRAIN study. Further papers are dedicated to provide more detail on the system design and specific technical aspects, see [3–6], and [7].

2 Related research

Several system studies in Europe for reusable space transportation systems were performed throughout the past decades. This section attempts to provide an overview of these studies without claiming to be exhaustive due to the wealth of studies performed in Europe.

The Future European Space Transportation Investigations Programme (FESTIP) launched by the European Space Agency (ESA) in 1994 compared various fully reusable concepts spanning from those foreseeing all stages being recovered to so-called “semi-reusable” ones for which some stages are not recoverable. The investigated concepts included two-stage-to-orbit (TSTO) concepts and single-stage-to-orbit (SSTO) concepts. All concepts but one belong to the vertical take-off horizontal landing (VTHL) category, the only exception being a vertical take-off vertical landing (VTVL) SSTO vehicle that was later dropped from further considerations due to the challenges imposed by the SSTO configuration. An overview of this study can be consulted in references [8, 9], and [10].

In 2001, the French space agency CNES attributed a contract to European space industry for the Evolved European Reusable Space Transportation (EVEREST) study of a fully reusable space transportation concept, [11, 12]. The first study phase aimed at identifying promising VTHL configurations with a payload capability of 7.5 metric tons into Geostationary transfer orbit (GTO) with staging velocity being one major trade-off parameter. One configuration was then selected and analyzed in-depth during the second phase of the EVEREST study.

In parallel to the EVEREST study, French industry under CNES contract has engaged in the system study of a partially reusable concept with a reusable first stage and an expendable second stage, [13]. This concept baptized “Reusable First Stage” or “RFS” is composed of a winged reusable booster stage and an expendable upper stage designed to lift 7.5 metric tons into GTO. While it was considered that from an economical point of view a fully reusable launch system like those studied in EVEREST was preferable, a mix of reusable and expendable stages appeared more easily accessible, see [13].

Other partially reusable concepts studied in Europe are those that foresaw the replacement of the solid boosters of the Ariane 5 launch system by two liquid “fly-back boosters”, like the French–Russian study on the Bargouzin concept, [13], the Russian Baikal concept [14] and the German ASTRA study (see Fig. 1), [15, 16]. Both concept proposals investigated liquid-propelled winged boosters which were to accelerate alongside the expendable central core stage of the Ariane 5 rocket and to return to Kourou after separation by making use of air-breathing propulsion.



Fig. 1 Artist's view of the ASTRA concept, [16]

Some RFS variants with a reusable first stage and one or more expendable upper stages were investigated as well, the reusable first stage being very similar in geometry to that proposed for the fly-back booster concepts [16].

With the successes of the VTVL approach adopted by SpaceX, several system studies in Europe focused on this recovery method. With its Ariane NEXT concept, [17], CNES proposes a VTVL space transportation system as a successor to Ariane 6 that follows a mixed expendable/reusable exploitation scheme, which is the first stage shall only be recovered in about 50% of the missions with the high-energetic missions such as GTO to be performed without recovery. The investigated concepts were TSTO configurations and configurations with liquid expendable boosters or with liquid recoverable boosters following a common core strategy with boosters and central core stage being, in principal, identical. All stages were to be propelled by liquid methane.

In [18], another building block concept based on the VTVL approach is developed and a critical comparison to a “big-size-fits-all” approach based on the VTHL launch and recovery method is performed. This latter concept, dubbed RLVC4 uses a winged first stage recovered with the in-air-capturing method and is sized big enough to transport large payloads but smaller payloads as well thus offering a wide range of payload transportation services. This is to be accomplished by exchanging the expendable stages adapted to the respective launch needs. Figure 2 presents three launcher architectures for this approach.

The EU-funded project RETALT investigated, among others, a VTVL two-stage-to-orbit concept, that could either perform a return to launch site (RTL) mission scenario where the reusable first stage performs a boost-back maneuver in order to return to the launch site for a vertical landing or a down range landing (DRL) where it will land on a ship positioned downrange of the launch trajectory, [19, 20].

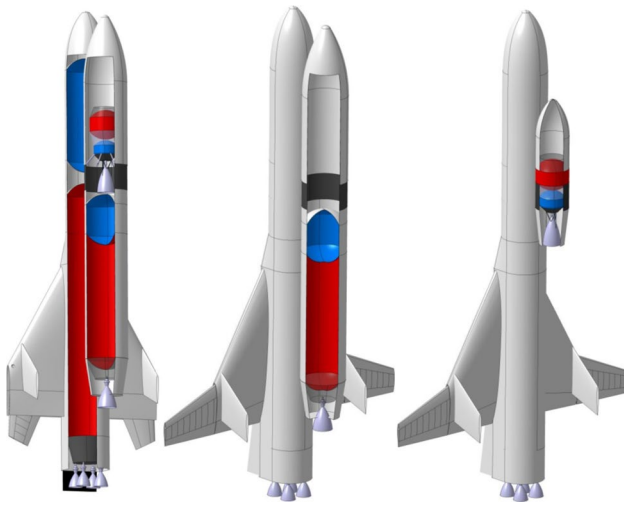


Fig. 2 Launcher architecture sketches of RLVC4-B configuration as 3STO (left), TSTO (center) and Mini-TSTO (right) [18]

A few studies investigated how various fuel choices impact the design of (partially) reusable launch vehicles. In 2004, results of a comparison between kerosene and methane for the reusable fly-back boosters performed in DLR were published, [21], on the basis of the liquid fly-back booster concept as presented in [15] and [16]. Another study performed in 2020 investigated VTVL TSTO concepts with a reusable first stage and the impact of propellant choice (LOX with LH₂, kerosene or liquid methane) on the overall architecture, making use of a multi-disciplinary optimization process and strongly simplified models [22].

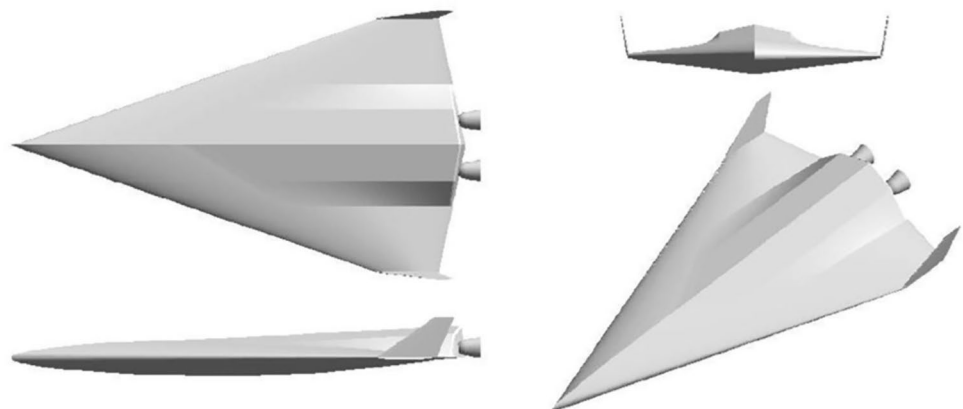
The overwhelming majority of these investigations in Europe are based on a pre-selection of the recovery methods pointing to the need of performing a more systematic comparison between those two fundamentally different recovery methods of vertical or horizontal landing. No

concept with horizontal take-off was considered as it is the vertical take-off that is already mastered in Europe and likely would preemptively exclude vertical landing as an option for such a vehicle. However, concepts with horizontal take-off and horizontal landing (HTHL) are part of the study portfolio of Europe, with the Sanger Concept of the 80 s (see [23]) and the Aurora concept (see Fig. 3) to name as a current project [24].

Of course, outside of Europe, a considerable amount of research activities on reusable launch vehicles exist, past and present. A good overview extending to non-European research on reusable launch vehicles under consideration of technology aspects is given by [25]. In the United States alone, the range and variety of research activities, past and present, is enormous, ranging from the first concept studies on the Space Shuttle [26] to the X-37 [27] as representative to winged reusable vehicles to the SpaceX Starship [28] as representative for vertically landing reusable vehicles and for a mixed approach in what concerns the orbital stage of the Starship.

The ENTRAIN study initiated in 2016 by DLR aimed at complementing the rich history of system studies in Europe with a systematic comparison of recovery methods for reusable first-stage TSTO concepts while considering the use of different fuel and engine cycles. It was considered essential for a reliable data basis to perform full system loops on a preliminary design level including coupled trajectory optimization for ascent and descent, mass estimation, and calculation for trimmed aerodynamics where necessary. Details of the design process can be found in [3] and [4]. A direct and detailed comparison of the results can be consulted in [6]. Just recently, cost estimations were completed and can be consulted in [7]. The results obtained by the time of the first milestone concluding the first study phase ENTRAIN 1 are presented in a series of papers of which this paper will lay out the framework of this study and a brief summary of the major findings.

Fig. 3 Preliminary geometry of the Aurora-R2 concept [24]



3 Study approach

The primary objective of the study is to systematically investigate, on system level, several recovery strategies for TSTO launch systems with a reusable first stage based on realistic data ensuring a feasible design. The considered recovery strategies can be declined into two categories with respect to their landing approach that is either vertical or horizontal and which has a considerable impact on the stage architecture.

In addition, it aims at providing data that shall help to identify those design choices that could contribute to a promising launch system with a reusable first stage, such as fuel choice and engine cycle. As elaborated below, this led to a considerable number of variants to be investigated. It was therefore decided to adopt a two-stage study approach in order to allow limiting the design effort without loss of quality of the results with respect to the primary objective of the study.

3.1 Principal study logic

During the first study phase (ENTRAIN 1), a parametric study was performed that aimed at evaluating the impact of major design drivers on system design and comparing the variants with respect to performance parameters, such as gross lift-off mass (GLOM), dry mass, encountered loads, and impact on launch costs. This way, certain key design choices (fuel combination, engine cycle...) should be evaluated and the most promising ones being identified.

To this end, other design parameters were kept identical irrespective of the considered launcher variant. These design parameters which were kept constant throughout this first study phase are:

- The design mission: GTO with a payload requirement of 7 T plus 500 kg performance margin,
- Vertical take-off from Kourou,
- The basic architecture being fixed to a two-stage-to-orbit (TSTO) concept with a reusable first stage and an expendable upper stage,
- Both stages using the same engine type albeit with a different nozzle to accommodate for the different operative environments (operation in atmosphere or vacuum), and
- No strap-on boosters.

Three different staging points, expressed as effective propulsive ΔV of the expendable upper stage, were fixed for each investigated variant. Each investigated variant underwent an iterative design process involving mass

estimation, aerodynamic data basis generation based on the geometry, engine system definition based on an inhouse engine data basis and coupled trajectory optimization both for ascent till orbit and return leg of the first stage. Ascent and return trajectories were subject to appropriate trajectory constraints such as maximum dynamic pressure or lateral load factor. The variants were iterated until the obtained performance hit the tolerance box of ± 150 kg about the target performance. After the completion of an initial preliminary design phase within this first ENTRAIN study, configurations that showed excessive sizes or did not converge were discarded from further detailing. Further details on the design process can be found in [3] and [4]. Details on the engine data base are provided by [5].

This approach of fixing certain parameters irrespective of the considered concept has a strong risk of not leading to the most optimal design per concept. This could hence conflict with the primary objective of this parametric study, which is to identify the impact of key design parameter on the launch system design and to compare the two recovery strategies under realistic conditions as this is not how a launch system would be optimized in real life for which key design parameters will be adapted to the specific needs of the individual design objective. For instance, fixing the system architecture to TSTO excluding three-stage-to-orbit configurations may penalize some variants more than others but was adopted nonetheless as it is expected to reduce complexity and reduce the relative portion of expendable parts. With this in mind, a second phase of the study, ENTRAIN 2 [29], followed with the purpose to compare an optimally designed VTVL launcher to an optimally designed VTHL launcher. This optimization should be performed within a European context and considering realistic boundaries and a mission scenario with a set of missions accessible to a European launcher.

A selection process was set up at the end of phase 1 in order to limit the number of launch concepts to be optimized while keeping in mind that the two fundamentally different return strategies of vertical and horizontal landing should be compared. This selection process aimed at identifying the most promising set of key design parameters within each of both return strategy categories. The outcome was the definition of a set of key design parameters for one VTVL and one VTHL launch concept to be further investigated in phase 2. Section 3.5 will provide details of the selection process and its results.

3.2 Adopted design process

The adopted design process globally follows the NASA launcher vehicle design process as laid out in [30] with some minor adaptations. The achieved design level partially

exceeds the state achieved during the Conceptual Design stage and, as such, contains already some relevant elements from the Preliminary Design stage, such as the Preliminary Design Concept and partially Refined Top-Level Requirements [30], and includes a concept design of major hardware subsystems up to the third level of the compartmentalization scheme (e. g. to aeroshell and tankage level) as described in [30].

Involved discipline functions following [30]) were:

- System,
- Trajectory,
- Aerodynamics,
- Control (simplified static trim analysis for VTHL only),
- Structures,
- Thermal, and
- Propulsion.

For details on the technical design process, it is recommended to refer to [3] and [4].

Certain disciplines mentioned by NASA in [30] were not involved in the ENTRAIN-study-design process as such. Since the objective was not to produce an operational launch vehicle, aspects such as manufacturing were not considered. Avionics and materials were not considered beyond mass considerations as well. Finally, while ascent and re-entry trajectories were optimized using algorithm-based optimal control theory, guidance and navigation were not part of the design process neither as perturbations and deviations from the nominal design point were not part of the study.

3.3 Investigated take-off mode and recovery strategies

The choice of take-off mode (horizontally or vertically or air-launch) is equally important for the necessary development

effort. However, for this study, it was decided to concentrate on the conventional vertical take-off from ground as this approach is well mastered in Europe, and no supplemental technology development effort is required besides the strict minimum to ensure recovery for the purpose of reusing the first stage. The designated launch site selected for this study is Kourou being the Europe's primary Spaceport.

As elaborated in the introduction, the return strategy and landing mode, alongside the take-off mode, is likely among the design choices with the largest impact on the development effort as ground and flight demonstration effort and specific technology development depends on this choice, whereas for a horizontally landing (or take-off), for instance, wings are needed that allow the vehicle to be safely operated throughout a wide range of Mach numbers, a vertically landing stage requires a highly reactive throttle capability for its rocket engines, among others. While both recovery approaches are mastered (by SpaceX and Blue Origin) or have been mastered in the past (as for the Space Shuttle), the associated technologies and the capabilities have to be acquired or further developed in Europe. This reasoning led the study team to place the focus on the return strategies and landing mode. Four different return strategies, sorted by their landing mode (horizontally or vertically), have been investigated as described below:

3.3.1 Vertical landing

- Return to launch site (RTLS), see Fig. 4 left side: This return strategy is identical to that used by Falcon 9 on low-performance missions and for the boosters of Falcon Heavy. After separation of the upper stage, the reusable stage performs a rotation maneuver and then fires its engines in order to reverse the flight direction thus reducing the distance to the launch site. After this boost-back maneuver, the stage is again rotated in order to orient the

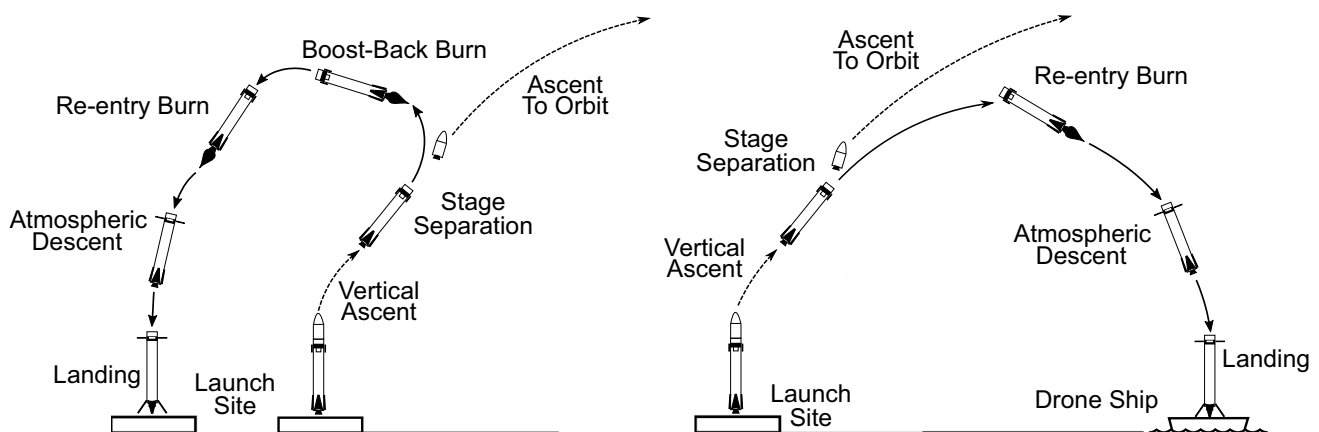


Fig. 4 Return strategies for VTVL: Return to launch site (left) and downrange landing (right)

stage that its engines point in-flight direction. Another engine boost phase may be programmed to decelerate the stage for load reduction. Above the landing platform, legs are extended and the stage is further decelerated by the landing boost until touchdown. At this point and anticipating study results, it shall be mentioned that RTLS investigation was discontinued as its performance was disappointing within the frame of the study constraint that limited the mission to the high-energy GTO mission and to a TSTO configuration. This result does not disqualify this specific recovery method for other launch scenarios or other architectural choices such as three stage to orbit.

- Downrange landing (DRL), see Fig. 4 right side: After separation, the lower stage is rotated before firing its engines in order to decelerate the stage to minimize reentry loads. Unlike RTLS, the flight direction is not reversed and the stage will land vertically on a platform placed downrange at a suitable position. In most cases, this platform is located on sea such as the drone ship used by SpaceX.

3.3.2 Horizontal landing

- Fly-back (FB), see Fig. 5 left side: After separation of the upper stage, the reusable stage will continue its flight downrange until the dynamic pressure is sufficient again to use the lift force generated by wings to point the flight direction to the landing site not far from the launch site. At a suitable point (subsonic), air-breathing engines are ignited in order to cover the remaining distance that separates the vehicle from its landing site.
- In-air capturing (IAC), see Fig. 5 right side: The initial phase of this return strategy is identical to that of a fly-back strategy. However, instead of using jet engines, a towing plane will capture the stage with an appropriate

device and tow it back to the landing site where the vehicle will be detached and automatically land on a runway. This strategy allows circumventing the need to install heavy jet engines and does not require additional fuel hence the potential interest of this approach. It shall be noted that the process of in-air capturing method has not been simulated within this study as little repercussions on the performance are expected. However, significant progress has been achieved recently by extensive simulations and lab-scale experiments in the European Commission-funded project FALCon with major results summarized in [31].

It shall be noted that other recovery methods were not considered for this study. Particularly, return methods that combine a boosted phase and a gliding phase such as the “dead leaf” concept were omitted as they showed to be less-performing than the fly-back option, see [32]. However, from a cost point of view, such return methods might still prove competitive as they simplify the recovered stage with respect to the winged concepts presented here.

3.4 Additional key design parameters

During the first study phase, further design choices were investigated which also have a considerable impact on technology development effort and on the system design:

- Fuel combinations: liquid hydrogen, liquid methane, and kerosene, all in combination to liquid oxygen, were considered. The impact of sub-cooling and the use of propane as fuel have been examined as well.
- Engine cycle: both gas generator cycles and staged combustion cycles were investigated as engine cycles.

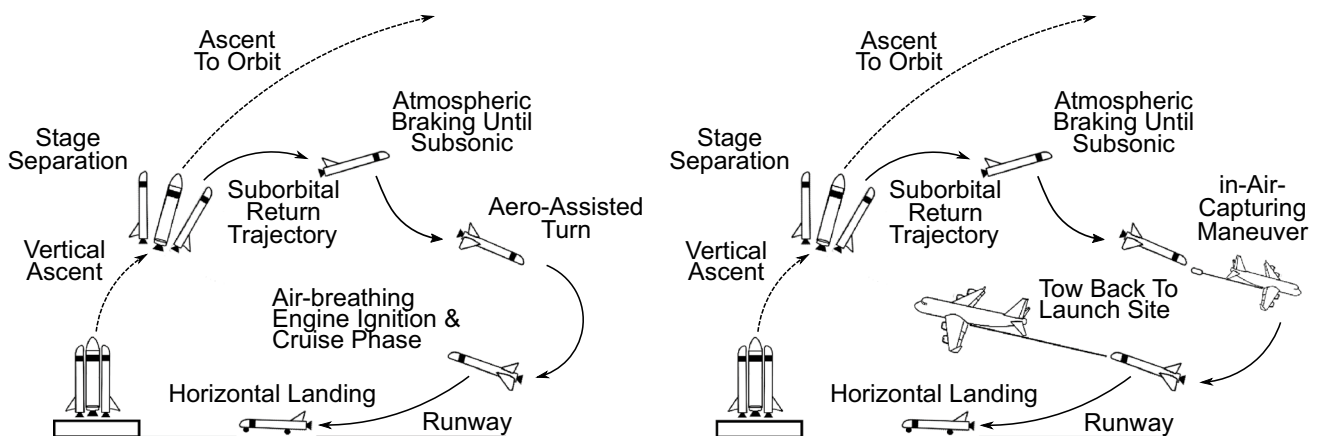


Fig. 5 Return strategies for VTHL: Fly-back (left) and in-air capturing (right)

In ENTRAIN 1, return strategies, fuel combinations, and engine cycle are the ingredients which make up the definition of a variant that is subjected to a preliminary design process aiming at sizing the launch system in such a way that it meets the mission requirements (minimum performance for a set of missions) and is compatible to applicable constraints such as maximum lateral or axial load factors or maximum dynamic pressures. These three key design parameters alone lead to 24 possible variants disregarding any sub-variants with sub-cooled propellant or more exotic fuels (propane) to be investigated.

Table 1 summarizes the design matrix, whereas Table 2 provides an overview of all investigated variants in the shape of a matrix. The design process was not performed for every variant however due to time constraints as long as the investigated variants allowed a deduction of the benefits or drawbacks on system level of the related design parameter.

For each variant, up to three staging points were used as design parameter. This parameter is expressed as propulsive ΔV of the upper stage, a higher ΔV equating to a bigger upper stage. This parameter is relevant as not only does the staging determine the overall launcher size as there exists a staging that allows maximizing the payload or alternatively

minimizing the take-off weight for a given mission requirement, but it also has an impact on the economic balance of a launcher with a reusable first stage. The additional cost benefits expected for a reusable launcher are strongly linked to the cost savings due to reusing a part of the launch system. It can be expected that the cost savings are larger if the re-used part represents a bigger part of the system. A small upper stage will require a larger first stage in order to compensate for the reduced ΔV of the upper stage hence a larger portion of the launcher is re-used in this case. However, at the same time, a larger first stage and a smaller upper stage increase the energy state of the first stage after separation from the second stage. This not only induces more effort to limit the reentry loads but may for some return strategies also lead to larger distances to the landing site. Both effects impact the launcher design and to some extent the maintenance and refurbishment effort for the reusable stage. In Table 1, the upper stage ΔV is depicted while the classification is with respect to the Mach number of the first stage separation. A launcher with a designation of Hi for “high” has a separation of the first stage at a Mach number between 10 and 12 while a Lo for “low” classified launcher separates its first stage at a Mach between 6 and 7.5.

3.5 Selection process

As indicated earlier, the number of variants investigated in the first study phase ENTRAIN 1 was quite large limiting the study approach to that of a parametric study with a limited detail level. A down-selection to two competing concepts was set up in order to increase the study detail level and allow an optimization process closer to operative mission requirements. To this end, a suitable selection process had to be established.

As a first step, appropriate selection criteria had to be identified. Out of 18 potential selection criteria candidates, seven were selected in a common team effort in order to smooth out any bias as much as possible. No threshold criteria were identified as all variants that did not meet the performance requirement of ENTRAIN 1 or which proved to be technically infeasible (e.g., unmanageably excessive loads) were dropped prior to be subjected to the selection process. The used selection criteria alongside indicative evaluation guidelines are presented by Table 3.

Table 1 Design Matrix of ENTRAIN study with nomenclature abbreviations

Design Parameter	Description	Nomenclature
Return Method	VTVL Downrange Landing	VL DRL
	VTVL Return-to-Launch-Site	VL RTLS
	VTHL In-Air-Capturing	HL IAC
	VTHL Fly-Back	HL FB
Propellant	LOx-LH2	H
	LOx-LCH4	C
	LOx-LC3H8	LC3H8
	LOx-RP-1	RP-1
	Hybrid	Hybrid
Engine Cycles	Staged Combustion	SC
	Gas Generator	GG
Upper Stage Δv (First stage separation Mach)	6.6 km/s (Mach 10–12)	Hi
	7.0 km/s (Mach 8.5–9.5)	Med
	7.6 km/s (Mach 6.0–7.5)	Lo

Table 2 Investigated variants

Return Strategy		LOX/LH2		LOX/LCH4		LOX/RP1		LOX/LC3H8	
		GG	SC	GG	SC	GG	SC	GG	SC
VL	RTLS	•	•	•	•	•	•	-	-
	DRL	•	•	•	•	•	-	•	-
HL	FB	•	•	•	•	•	•	-	-
	IAC	•	•	•	•	•	•	•	-

Table 3 Selection criteria and evaluation guidelines

Criteria	Evaluation guideline
Launch Costs	<i>Positive:</i> Lower expected costs: low dry mass, less expected maintenance (e. g. due to low TPS mass, few engines, less expected integration effort, high number of reuses) <i>Negative:</i> Higher expected costs: high dry mass, higher expected maintenance (e. g. due to high TPS mass, many engines, higher expected integration effort, low number of reuses)
Development Costs	<i>Positive:</i> Technologies predominantly high TRL, existing experience in Europe, low dry mass, relatively simple design, low number of testing required <i>Negative:</i> Technologies predominantly low TRL, lacking experience in Europe, high dry mass, relatively complex design, high number of testing required
Development Risk	<i>Positive:</i> Existing experience in Europe, proven techno (i.e., existing examples of use around the world), little in-flight testing required, simple switch to back-up solution w/o or little re-design, low operational or layout complexity; possibility for step-wise transition to concept <i>Negative:</i> lacking experience in Europe, unproven techno (i.e., no existing examples of usage around the world), intensive in-flight testing required, difficult switch to back-up solution w/ considerable re-design, high operational or layout complexity; disruptive transition to concept necessary
Growth/Shrink potential	<i>Positive:</i> High scalability of layout with comparatively simple re-design <i>Negative:</i> Low scalability of layout requiring large re-design
Mission flexibility	<i>Positive:</i> Limited impact on loads and structural layout; simple integration of additional performance-enhancers (e.g. boosters)/high potential for modularity; sufficient performance in other orbits <i>Negative:</i> Strong impact on loads and structural layout; difficult integration of additional performance-enhancers (e.g. boosters)/low potential for modularity; insufficient performance in other orbits
Reliability	<i>Positive:</i> Low complexity of concepts, ops & mission, large number of proven technologies, low number of moving parts <i>Negative:</i> high complexity of concepts, ops & mission, large number of little proven technologies, large number of moving parts
Environment	<i>Positive:</i> Environmentally friendly (production of hardware & fuel, exhaust gas, end-of-life disposal...) <i>Negative:</i> Not environmentally friendly (production of hardware & fuel, exhaust gas, end-of-life disposal...)

Special care had to be taken considering that this down-selection was to be performed at a very early stage when data and results are still subject to considerable uncertainties and the study approach was that of a parametric study during ENTRAIN 1. It should be avoided that principally promising concepts or key design parameters are prematurely discarded because another one was numerically slightly better but with a difference probably still within the error bar. With this in mind, it was decided to evaluate each variant qualitatively only by comparing pairs of variants considering their performance with respect to each selection criteria. This evaluation was performed as a team effort as well, again with the aim to smooth out possible biases of individual members of the evaluation team. Comparing each candidate pair-wise led to a ranking of the candidates with respect to the criteria under consideration. Finally, per criteria, the best and worst performing variants were identified with all other variants being classified as neutral. In the case of two candidates being evaluated as being very similar to each other during the pair-wise evaluation, they were considered to perform identically well with respect to the criteria under consideration.

Ideally, the resulting table performance vs criteria should show an accumulation of positive evaluation for one variant with further neutral and little or no negative evaluations. Both VTVL and VTHL variants were evaluated separately

yielding two tables. The results of the selection process are presented in 4.2.

Apart from the evaluation of the development costs for the engine, criteria were applied to the entire launch vehicle. For certain cases, this might lead to a better evaluation of the vehicle despite the engine cycle of that specific variant performing worse with respect to that criteria.

Since no work was performed on ground infrastructure or ground operations, these aspects could not be part of the evaluation at this stage. As such, the evaluation result is limited to the performance of the vehicle alone with respect to the selection criteria.

4 Results overview

In this section, we will present major findings of the first study phase ENTRAIN 1 including the results of the selection process prior to the beginning of the ENTRAIN 2 study phase. This will be complemented by a discussion of the major conclusions drawn from these results.

During this study phase, a total number of 19 configuration, disregarding any abandoned concepts such as RTLS, were investigated. For each concept, several design loops including coupled optimization and simulation of ascent of the launcher to orbit and re-entry of the first stage,

aerodynamic performance calculation, and mass estimations were run until a consistent design respecting the requirements was obtained. This meant that on average, a minimum of ten design loops were performed per concept with some concepts requiring significantly more iteration loops before reaching convergence. Details on the design loops can be consulted in [3] and [4].

These concepts could resort on an extensive propulsion database encompassing 36 engines for which performance and design parameters were calculated, see [5]. This database included:

- 19 gas generator cycle engines, and
- 17 staged combustion cycle engines.

Within these engines, four propellant combinations and seven nozzle expansion variations were considered and a total of ten thrust chamber geometries were defined. With a few exceptions, these cycles were analyzed with two independent cycle analysis tools in order to consolidate performance data.

4.1 Results of ENTRAIN phase 1

Several characteristic features of the investigated variants were identified as a relevant means of comparison (see [6]). Among these features, the Gross Lift-off Mass (GLOM) is a comparatively good indicator of the size of the launch configuration within a propellant type class. In between different propellant type classes, a comparison is more difficult due to different densities and mixture ratios since fuel mass has a different impact on launch costs and is a consumable,

whereas hardware, at least that of the first stage, is to be re-used.

Irrespective of this, a comparison over a variety of propellant type allows drawing a conclusion about the required take-off thrust and hence about the number, size and performance requirements for the propulsion system of the first stage. A higher number of engines increase the complexity and the cost of a system. As such, a system with lower thrust requirement is preferable when all others parameters were identical.

At this point, it shall be noted that all VTVL RTLS variants were discarded from further considerations at an early stage of the study as they led to excessively large launch systems due to the choice of GTO as reference mission. The high energy requirements of this mission led to increased fuel quantities required to perform the boost-back maneuver despite the fact that the trajectory optimization process used aimed at finding a suitable compromise between ascent and descent for this particular return method in order to maximize the performance. This left the downrange landing (DRL) as the preferred recovery method for the GTO mission and for all VTVL variants. RTLS was considered again in the second phase of this study ENTRAIN 2 as a potential recovery method for less energetic missions.

Figures 6 and 7 summarize selected mass characteristics of the investigated variants. For quick referencing, following nomenclature is adopted for variant identification. A variant is designated by its recovery attitude (VL: vertical landing, HL: horizontal landing) followed by precisely following the recovery method (DRL: downrange landing, RTLS: return to launch site, FB: fly-back, IAC: in-air capturing). The ensuing section describes the two stages by designating with

Fig. 6 Gross lift-off masses (without payload mass) of investigated variants

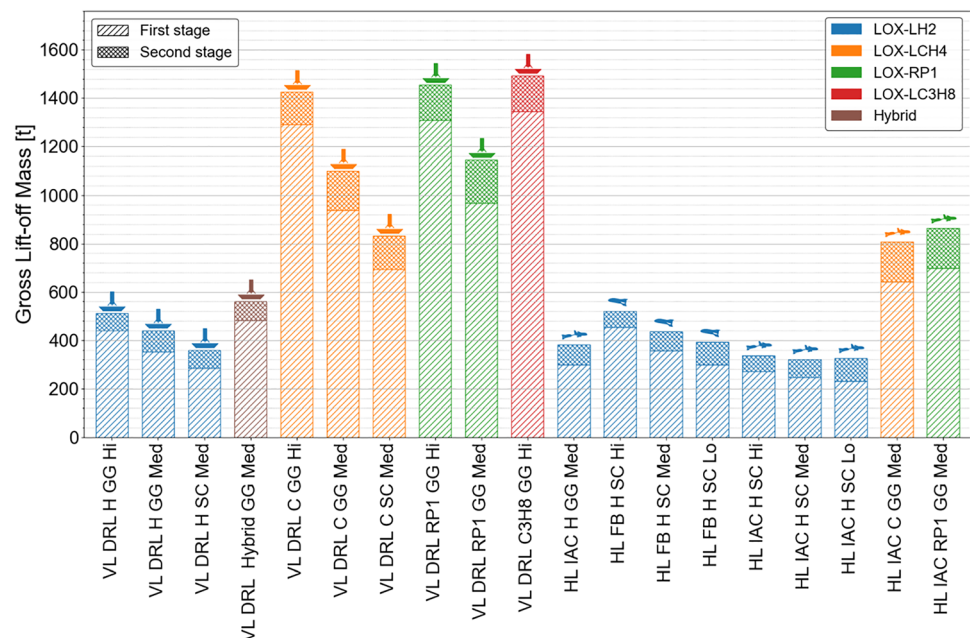
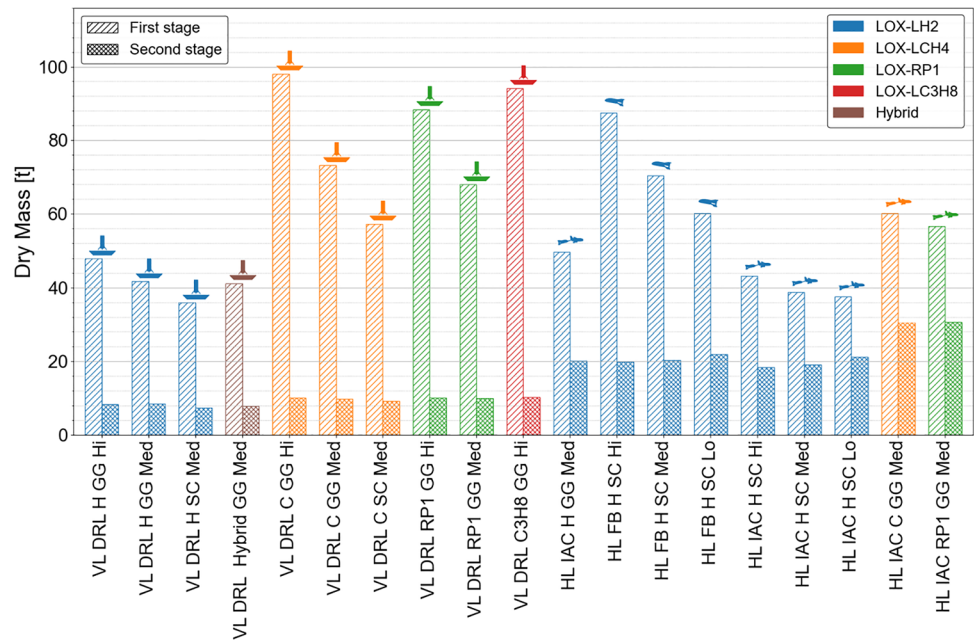


Fig. 7 Dry masses of investigated variants

the first letter the used fuel type (H: hydrogen, C: methane, P: propane, K: kerosene) in the first stage followed by the loaded propellant in metric tons. An identical logic applies to the second stage. Finally, the used engine cycle (GG: gas generator, SC: staged combustion) and the ΔV -class (see Table 1) of the upper stage are given.

Figure 6 shows the GLOM minus the payload mass allowing distinguishing the first stage and second stage contribution. As can be seen, the values for the total GLOM of hydrocarbon-fueled launchers exceed by far those relying on hydrogen fuel. A factor of two exists between a hydrogen-driven VTHL with an in-air capturing recovery strategy and a methane-driven one. This factor increases when comparing hydrogen VTVL to methane VTVL launch systems. This is due to the fact that hydrocarbon-based propulsion systems generate significantly lower specific impulses than hydrogen-based ones. This fact has multi-fold consequences on the design of a TSTO launch system with a reusable first stage:

- The lower specific impulse leads to increased fuel mass required to deliver the necessary ΔV . This will lead to larger and heavier stages, including a heavier upper stage compared to a hydrogen-fueled upper stage delivering the same ΔV .
- A heavier upper stage will result in reduced accelerations to be compensated by adding further fuel to the first stage. Consequently, the first stage has to increase in size and mass.
- Launch systems relying on recovery strategies that make use of the primary fuel will also suffer performance penalties when using hydrocarbon fuel instead of hydrogen.

This is particularly true for all VTVL concepts since a significant ΔV requirement for deceleration and landing boost has to be accounted for. This penalty is further aggravated by the fact that this fuel mass has to be accelerated during ascent thus further decreasing accelerations delivered by the first stage.

Figure 7 presents the obtained dry masses of both stages for each investigated variant. These figures are of interest as the production costs are to some extent related to this figure. When considering launch costs, it is also interesting to distinguish between production costs and fuel costs as the value of a kilogram hardware can be expected to be noticeably different from the value of a kilogram fuel. Furthermore, the treatment of hardware and fuel for launch cost evaluation has to be different for reusable launch systems, the hardware being purchased only once or for a limited number, whereas fuel has to be produced for each flight.

Comparing the VTVL DRL, all-hydrogen variant with a medium-sized upper stage (MED) with its equivalent using methane for the first stage and hydrogen for the upper stage indicates the impact that the switch from using hydrogen in the first stage to a hydrocarbon fuel has. The upper stage being in size and mass very close to each other as they deliver the same Δv and use the same fuel the difference in dry mass on the first stage is only related to the increase in fuel mass necessary to compensate for the lower specific impulse of methane. This underlines the negative effects hydrocarbon has on the performance of launchers.

It shall be emphasized that the limitation to a TSTO configuration has of course an impact on the mass budgets. Specifically, for GTO missions, a three-stage configuration or a

two-stage configuration with side boosters may be beneficial in terms of launcher size and mass. A switch to a different staging may prove specifically beneficial for the hydrocarbon variants performance-wise. This however was beyond the study scope. In [18], a family of launchers approach that includes TSTO and three stage to orbit (3STO) is discussed.

The same tendencies as for the GLOM can be observed for the dry mass of the first stage although to a lesser extent. Indeed, the more favorable structural index for the hydrocarbon-fueled variants alleviates to some extent the penalizing impact of the specific impulse—albeit not sufficiently to compensate it. The hydrogen-fueled variants continue to perform significantly better.

Whereas all-hydrogen variants maintain the edge in terms of performance, hydrocarbon has some interest particularly for a reusable first stage. The chances are good that when using hydrocarbon fuel no particular tank insulation is needed unlike for hydrogen. Ground handling and storage is also simplified; however, this benefit is mitigated to some extent when using a mixed fuel approach with hydrocarbon in the lower and hydrogen in the upper stage. Using two different fuel types for the first and upper stage also imposes the development of two separate engines and two separate production lines and increases launch installation and preparation complexity against which the performance benefit with respect to an all-hydrocarbon vehicle has to be traded.

Yet, an all-hydrogen launcher both has the better performance and avoids the need to handle two types of fuel but being a cryogenic liquid requires additional care.

Figure 8 provides an overview of selected VTVL and VTHL variants resulting from the system loop. For size comparison, Ariane 5 and the Falcon 9 launcher are represented as well.

4.2 Results of the selection process

The result of the evaluation process for the selection process as described in 3.5 is shown for the VTVL versions

Table 4 Evaluation of VTVL variants

Recovery method		DRL					
Fuel combination		C		H		RP1	
Engine cycle		GG	SC	GG	SC	GG	SC
Launch costs		⊗	○	○	⊗	⊗	○
Development costs	System	⊗	○	○	⊗	⊗	○
	Engine	○	⊗	⊗	○	○	○
Development risk		○	○	⊗	○	○	○
Growth/shrink potential		○	○	⊗	⊗	⊗	⊗
Mission flexibility		○	○	⊗	⊗	⊗	⊗
Reliability		⊗	○	○	⊗	⊗	○
Environment		⊗	○	○	⊗	⊗	○

⊗ negative ⊗ positive ○ neutral

in Table 4, whereas those for the VTHL is presented by Table 5. It shall be reminded that not every variant was investigated to full detail and some were abandoned. However, the vast database available during this evaluation process allows transposing tendencies observed for fully investigated candidates to others. For instance, it can be expected with good confidence that hydrocarbon-fueled variants will always lead to higher gross lift-off masses than hydrogen-fueled ones, irrespective of recovery method.

It is emphasized that the evaluation was performed within each overall recovery category, which is within VTVL and within VTHL separately. This does not allow comparing the evaluations of a VTVL variant to a VTHL variant. For instance, it is expected that test effort for a VTVL engine will be significantly higher than for a VTHL engine since the former has to offer deep throttling capabilities representing considerable design challenges and which will have to be validated by additional test runs not necessary for engines with only limited throttling requirements.

Overall, the hydrogen-fueled variants received the best evaluation. It shall be noted that since all RTLS variants have been discarded from further considerations due to their excessive lift-off mass, they were not subjected to the evaluation. Since no development program for propane as a rocket fuel for the relevant thrust class existed in Europe, these variants were also not considered for further investigation.

Fig. 8 Geometry and layout of selected RLV of the ENTRAIN study compared to Falcon 9 and Ariane 5

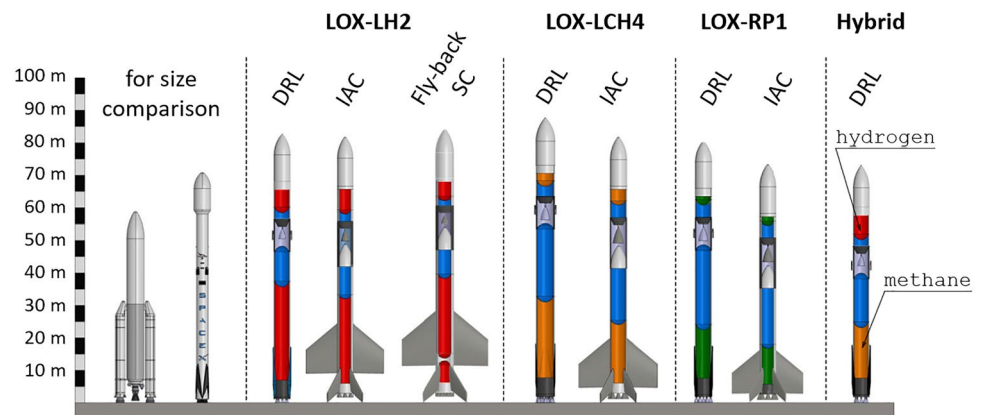


Table 5 Evaluation of VTHL variants

Recovery method		FB						IAC					
Fuel combination		C		H		RP1		C		H		RP1	
Engine cycle		GG	SC	GG	SC	GG	SC	GG	SC	GG	SC	GG	SC
Launch costs		⊗	○	○	○	⊗	○	○	○	○	⊕	○	○
Development costs	System	⊗	○	○	○	⊗	○	○	○	○	⊕	○	○
	Engine	○	⊗	⊕	○	○	○	○	⊗	⊕	○	○	○
Development risk		○	○	⊕	○	○	○	○	○	⊕	○	○	○
Growth/shrink potential		○	○	○	○	⊗	⊗	○	○	⊕	⊕	○	○
Mission flexibility		○	○	⊗	⊗	○	○	○	○	○	○	⊕	⊕
Reliability		⊕	○	○	○	⊕	○	○	○	○	⊗	○	○
Environment		⊗	○	○	⊕	⊗	○	⊗	○	○	⊕	⊗	○

⊗ negative ⊕ positive ○ neutral

The following section establishes the reasoning behind the evaluation result. It shall be highlighted that this reasoning is based on engineering judgement on a preliminary basis and against the backdrop of a limited data base available for each variant.

4.2.1 Recovery by vertical landing (VTVL)

For this landing strategy, the hydrogen variant sporting gas generator engine cycle came out winner of the selection process closely followed by the hydrogen variant with staged combustion engines. While the staged combustion engine variants received a favorable evaluation with respect to launch and system development costs compared to the gas generator cycle variant due to its smaller size, it generates additional challenges with respect to reliability due to the particular nature of the closed cycle engine that is difficult to master.

It shall be noted that RTLS was no longer considered during this evaluation process since the obtained performance was very disappointing leading to excessively large launch vehicles and to the conclusion that this recovery method was impracticable for GTO missions.

4.2.1.1 Launch, development costs and development risk Concerning launch and system development cost, those VTVL concepts with the lowest gross lift-off mass can be expected to have a certain advantage over other concepts. In ENTRAIN 1, no cost estimation was performed for each variant using the gross lift-off mass as a surrogate instead for the launch costs and the dry mass for the development cost. Most cost estimation tools used in preliminary design stages, like TRANSCOST [33] parametrize the development and launch costs based on a mass breakdown of the object in question. While development costs resulting from such a model are more linked to the dry mass, the gross lift-off weight of the system, albeit together with the dry mass, has a stronger impact on the launch costs.

This approach favors the better performing variants such as the hydrogen-fueled concept with staged combustion engine since these launchers tend to be smaller both in gross lift-off weight and dry mass compared to the hydrocarbon launchers as can be seen in Figs. 6 and 7.

Europe has extensive experience with hydrogen gas generator cycle engines placing this type of engine on the top of the ranking list with respect to the engine development costs and the development risks. Until recently, the staged combustion cycles using any of the two considered hydrocarbon fuels would have been ranked at the bottom for both the engine development costs as Europe lacked any significant experience for either staged combustion engine or the use of hydrocarbon fuel. While the Prometheus X engine, a methane-driven staged combustion engine, is still in its concept phase, [34], not enough to lift it up from the bottom of the ranking, this picture has changed with the successful test runs of the kerosene-driven staged combustion Helix engine of the private European company Rocket Factory Augsburg (RFA). This is the reason why kerosene staged combustion cycle was better evaluated with respect to its methane counterpart placing it in the neutral range.

As for the development risk, this has two-fold aspects. The first aspect is related to the technology readiness level (TRL) in Europe, partially covered already by the engine development cost criteria, and a global TRL. A low global TRL would imply that developers would have to tread unknown territory on many points with a high risk of discovering showstoppers. The mere existence of a foreign working engine can be considered as a proof of concept justifying a favorable evaluation with respect to development risk. Since recent developments (Raptor engine, Prometheus engine, and the Helix engine) showed that all considered propellant-engine cycle combinations are feasible. None was considered negatively leaving the hydrogen gas generator cycle on the top of the ranking due to thorough European expertise and all others neutral.

4.2.1.2 Growth and shrink potential The evaluation of the variants was principally based only on the sub-cooling capability of the propellants allowing storing more propellant quantity in the tanks with some impact on the structural design and flight control not assessed at this stage of the study. It was considered that other distinctive characteristics of the investigated variants did not allow discerning them with respect to better or worse growth and shrink potential at this stage of study.

Compared to hydrocarbon variants, the LOX/LH₂ fueled variants offer the best growth and shrink potential due to its higher sub-cooling capability. With sub-cooling propellant, more of it can be stored inside the same volume. The density of hydrogen being particularly sensitive to temperature offers an enhanced potential for increasing fuel mass without the need to modify the tank volume. It is obvious that this benefit has to be traded against any additional effort to maintain lower temperatures. This kind of analysis however was beyond the scope of the ENTRAIN 1 study.

For this criterion, the kerosene variants received the worst evaluation as, albeit also benefitting from sub-cooling, does so at a more restricted level than methane. Coupled to the fact that due to the lower mixture ratio of kerosene variants that for methane variants, these candidates even benefit less from a potential sub-cooling of oxygen.

4.2.1.3 Mission flexibility Concerning mission flexibility, the evaluation tendency is reversed with the kerosene variants being evaluated as the best performing one and the hydrogen variants receiving the worst evaluation. This evaluation is based on the judgment that concerning in-orbit waiting times for multi-boost missions, non-cooled fuels show superior handling qualities.

4.2.1.4 Reliability Concerning reliability, hydrocarbon-fueled variants were deemed to fare better than hydrogen-fueled ones since they require less effort in maintaining the fuel at extremely low temperatures, hence limiting the need for sophisticated insulation concepts that might fail. Additionally, gas generator engines are considered to be more reliable than closed cycle engines as they can run at lower combustion chamber pressure and Europe has decades of experience in operating these engines. This makes the hydrocarbon gas generator variants to be evaluated as more reliable than all other considered variants from a European perspective.

4.2.1.5 Environmental impact No specific analysis of the environmental impact nor a life cycle analysis of the launch vehicles from the time of production until its decommissioning could be performed within this parametric study. As a very simplified surrogate approach, smaller launchers are assumed to have advantages as far as the non-propellant

parts are concerned as it was considered that the smaller the launcher the less material and less energy is needed for production and less material may prove unrecyclable requiring special treatment.

Additionally, hydrogen combustion does not produce CO₂ and is as such more ecologically friendly than any hydrocarbon fuel as long as it is assumed that propellant production itself is ecologically friendly enough. This for instance would require that hydrogen production uses predominantly energy drafted from renewable sources. It was assumed that due to the increase of the share of renewable energies and the drive of the European Union to become CO₂-neutral by 2050 and by 2030 having reduced its CO₂ production to at least 55% with respect to the state at 1990, this would be the case by the time a European reusable launch system became operational. Additionally, the less fuel quantity needs to be produced, the less energy is consumed. This helps in reducing energy consumption and potential CO₂ production. Finally, propellant that can be produced on-site or near its place of consumption allows limiting transport costs and any ecological impact. These considerations led to the hydrogen staged combustion candidates being considered to be environmentally most friendly.

4.2.2 Recovery by horizontal landing (VTHL)

Similar reasoning applies to the VTHL variants when comparing cycles and fuel types. Additionally, two recovery methods were part of the evaluation. As the in-air capturing methods (IAC) lead to smaller launchers and offer higher flexibility and growth/shrink potential as, at least within some limits, the towing air plane can be deployed in a flexible way recovering the stage from various points irrespective of inclination and, to some extent, irrespective of distance to the landing spot. It was considered that fly-back variants offer a somewhat lesser flexibility as they rely on high-performance, but relatively low fuel-efficient adapted fighter engines compared to the highly efficient civil turbojet engines of the towing aircraft, and that due to the fixed design, the limits to the range that can be covered with the onboard fuel are more limited. However, the development risk for the in-air capturing is estimated to be noticeably higher as this technology has yet to be developed and demonstrated for this kind of application.

For this category of landing method again, the hydrogen-fueled variants were evaluated more favorably than their hydrocarbon-fueled counterparts. While for the fly-back recovery strategy, this difference is small. It becomes more pronounced for the variants relying on the in-air capturing method. Here, the differences in evaluation between staged combustion and gas generator are less obvious compared to the evaluation of the VTVL configurations.

5 Demonstrator roadmap

As highlighted in the introduction, the decision on the recovery mode is of strategic importance when developing a reusable launch system. This development has to be accompanied by developing demonstrators that support knowledge and competence acquisition as a means for development risk mitigation. Ideally, a demonstrator program is set up in parallel to the development program for the operational system while enabling mutual interactions of both programs. This demonstrator program has to be embedded in a technology development program that is dedicated to the acquisition of necessary or desired technologies.

At this stage, no firm commitment for a development of a reusable launch system, let alone a final decision on the preferred recovery mode has been taken in Europe. DLR is developing the Reusable Flight Experiment ReFEx, [35], a winged demonstrator with an emphasis on system design of a maneuverable winged re-entry vehicle mastering the transition from hypersonic to subsonic flight while retaining full controllability.

In addition to ReFEx, DLR is developing, in cooperation with CNES and JAXA, a demonstrator mirroring principal flight phases of a vertical take-off vertical landing reusable first stage, [36].

Both demonstrators are each dedicated to addressing technically challenging aspects specific to VTHL and VTVL reusable first stages. This approach of developing

and flying these two demonstrators will contribute to consolidating the knowledge of the challenges and attitudes of both recovery modes by hands-on experience complemented by further flight demonstration such as FALCon [31]. As these flight demonstrations are comparatively small and only partially covering a life cycle of an operational system, further and larger demonstrators have to follow.

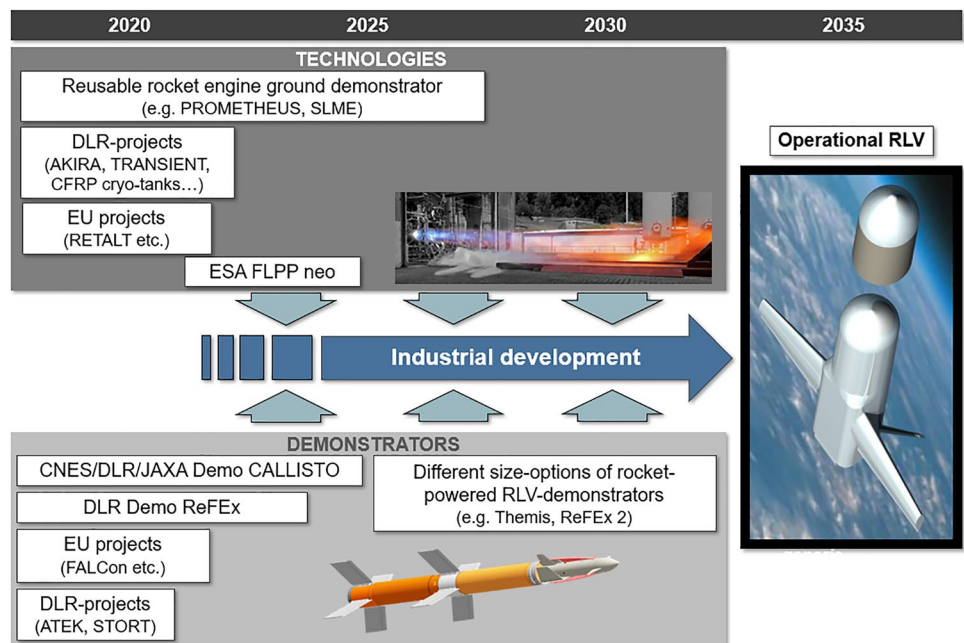
Parallel to this demonstrator activity, a variety of technology development projects are set up in DLR, either fully domestic funded or EU and ESA-funded ones. Such technology DLR projects are AKIRA, [37, 38], focusing on efficient stage return, reusable cryogenic tank insulation, and structural technologies for RLV stages and TRANSIENT, [38], a follow-up project to AKIRA focusing on cryogenic insulation technologies for RLV.

The development of a reusable engine, being of central significance for the operational system, is to be preceded by appropriate ground demonstrators such as the ESA-funded Prometheus demonstrator engine development [39].

Such a publicly funded program will benefit and accompany the industrial development of the operational system. It is clear that with advancing development, more and more industry involvement is needed for realizing some of the technology and demonstrator development program.

Figure 9 draws a potential roadmap arranging the various development strings currently underway and potential evolutions toward a European operation RLV.

Fig. 9 Potential roadmap toward an operational European TSTO with a reusable first stage



6 Conclusion

Europe's access to space currently relies solely on expendable launch systems. In the face of the successful introduction of reusability to the launch services in the United States, the increasing cost pressures and the questions of sustainability challenge any view of pursuing in Europe with expendable launch systems after a future decommissioning of Ariane 6 and Vega. Reusing the first stage is an obvious first but decisive step of introducing reusability to the European launch capability. While it may seem tempting to simply follow the approaches selected by US companies like SpaceX, it may be worthwhile to investigate alternatives prior to committing to a lengthy and costly development program. To this end, DLR initiated a large system study of two-stage-to-orbit heavy launch systems with a reusable first stage with a special focus on the recovery method. The main interest was to compare two entirely different recovery approaches: vertical landing and horizontal landing since the decision for one or the other entails entirely different architectures and would set Europe on diverging technology development paths. These two landing approaches were further diversified by considering specific recovery methods as well leading to two investigated recovery methods for each landing method.

Further key design parameters were identified and included in the concept matrix, such as fuel type and engine cycle. Common fuel types, such as cryogenic fuels (LOX/LH₂), methane (LOX/LCH₄), and kerosene (LOX/RP-1), were investigated. This was complemented for evaluation purposes by an investigation of propane (LOX/LC3H₈). Gas generator cycles, a technology well mastered by Europe since decades, were considered alongside staged combustion cycle engine for which a technology development program would be required.

For each variant, three staging points were fixed based on the propulsive ΔV delivered by the upper stage. A design loop involving mass estimation, aerodynamic database calculations, coupled trajectory optimization for ascent and re-entry and architectural studies were performed to obtain a convergent design for each variant.

A down-selection process compatible with the preliminary nature of the achieved design level was applied to the variants evaluating the relative performance of each one of them with respect to the selection criteria launch costs, development costs, development risk, growth/shrink potential, mission flexibility, reliability, and environment.

At the outcome of this down-selection process, one set of design parameters for two-stage-to-orbit launch system with a horizontally landing first reusable stage and one for that with a vertically landing first reusable stage were evaluated more favorably than other competing variants.

They both have in common to rely on hydrogen fuel that with respect to the selection criteria fare noticeably better than their hydrocarbon-fueled counterparts. While in terms of engine cycle, the gas generator cycle received overall a more favorable compared to staged combustion for the VTVL variants this distinction is less obvious for the VTHL category. For this latter category, the in-air capturing method ranked better than the VTHL concepts relying on fly-back for first stage recovery.

Finally, a possible development roadmap toward a European two-stage-to-orbit launch system was drafted for a commissioning of such a system by the year 2035 based on on-going technology development in Europe.

Author contributions I.D. prepared and revised the main manuscript, figures 4 and 5, tables 2 to 6, contributed to formatting of figures 6, 7, 8 and 9 S.S. prepared table 1 and figures 6, 7 (data and python script) and figure 8, contributed to tables 2, 3, 4 and (data) L.B and J.W. contributed to figures 6, 7 and 8 (data), contributed to tables 2, 3, 4 and 5 (data), contributed to sections 3 and 4 M.S. contributed to section 2, 3, 4 and prepared figure 9. S. S. contributed to the data generation on which the figures are based. All authors reviewed the manuscript.

Funding Open Access funding enabled and organized by Projekt DEAL.

Data Availability Datasets were generated to produce tables and figures in this manuscript. These can be made available on request under compliance to applicable laws.

Declarations

Conflict of interest The authors have no competing interests to declare that are relevant to the content of this article.

Open Access This article is licensed under a Creative Commons Attribution 4.0 International License, which permits use, sharing, adaptation, distribution and reproduction in any medium or format, as long as you give appropriate credit to the original author(s) and the source, provide a link to the Creative Commons licence, and indicate if changes were made. The images or other third party material in this article are included in the article's Creative Commons licence, unless indicated otherwise in a credit line to the material. If material is not included in the article's Creative Commons licence and your intended use is not permitted by statutory regulation or exceeds the permitted use, you will need to obtain permission directly from the copyright holder. To view a copy of this licence, visit <http://creativecommons.org/licenses/by/4.0/>.

References

1. De Concini, A., Toth, J.: The future of the European space sector How to leverage Europe's technological leadership and boost investments for space ventures, report for the European Commission by the European Investment Bank, 2019
2. James, T., Kevin, O., Wood, K.: A comparison of design decisions made early and late in development, 21st International Conference on Engineering Design, Vancouver, Canada, 2017

3. Bussler, L., Sippel, M., Dietlein, I.: Comparative Analysis of European Horizontal-Landing Reusable First Stage Concepts, CEAS Space Journal 2024, to be published
4. Wilken, J., Stappert, S.: Comparative Analysis of European Vertical-Landing Reusable First Stage Concepts, CEAS Space Journal 2024, to be published
5. Sippel, M., Wilken J.: Selection of Propulsion Characteristics for Systematic Assessment of Future European RLV-Options, CEAS Space Journal 2024, to be published
6. Stappert, S., Dietlein, I., Wilken, J., Bussler, L., Sippel, M.: Options for future european reusable booster stages: evaluation and comparison of VTHL and VTVL Return Methods, CEAS Space Journal 2024, to be published
7. Wilken, J., Herberhold, M.: Options for future reusable booster stages: evaluation and comparison of VTHL and VTVL costs, CEAS Space Journal 2024, to be published
8. Dujarric, C., Caporicci, M.: Conceptual studies and technology requirements for a new Generation of European launchers: Paper IAF-97-V. 3.03—"a FESTIP status report", Acta Astronautica 41.4-10, 219–228, August 1997
9. Anfimov, N., Kostromin, S., Kuczera, H., Sacher, P., Bayer, M.: ORYOL-FESTIP cooperation—Comparison of concepts and first conclusions, 8th AIAA International Space Planes and Hypersonic Systems and Technologies Conference, 1998, <https://doi.org/10.2514/6.1998-1544>
10. Kuczera, H., Johnson, C.: The Major Results of the FESTIP System Study, 9th International Space Planes and Hypersonic Systems and Technologies Conference, 1999, <https://doi.org/10.2514/6.1999-6001>
11. Iranzo-Greus, D., Deneu, F., Le-Coulis, O., Bonnal, C., Prel, Y.: Evolved European reusable space Transport (EVEREST)—System design process and current status, IAC-04-V.4.07, 55th International Astronautical Congress 2004, <https://doi.org/10.2514/6.IAC-04-V.4.07>
12. Iranzo-Greus, D., Deneu, F., Le-Coulis, O., Bonnal, C., Prel, Y.: Selection and design process of TSTO configurations, IAC-03-V.4.05, 54th International Astronautical Congress, 2003
13. Guédrón, S., Prel, Y., Bonnal, C., Rojo, I.: RLV concepts and experimental vehicle system studies: current status, IAC-03-V.6.05, 54th International Astronautical Congress, 2003
14. Filatyev, A.S., Buzuluk, V., Yanova, O., Ryabukha, N., Petrov, A.: Advanced aviation technology for reusable launch vehicle improvement. Acta Astronaut. **100**, 11–21 (2014)
15. Sippel, M., Klevanski, J., Burkhardt, H., Eggers, T., Božić, O., Langholf, P., Rittweger, A.: Progress in the Design of a Reusable Launch Vehicle Stage, AIAA 2002–5220, 2002
16. Sippel, M., Manfretti, C., Burkhardt, H.: Long-term/strategic scenario for reusable booster stages. Acta Astronaut. **58**, 209–221 (2006)
17. Patureau de Mirand, A., Bahu, J.-M., Louaas, E.: Ariane Next, a vision for a reusable cost-efficient European rocket, 8th European Conference for Aeronautics and Space Science, 2019, <https://doi.org/10.13009/EUCASS2019-949>
18. Sippel, M., Stappert, S., Callsen, S., Bergmann, K., Dietlein, I., Bussler, L.: Family of Launchers Approach vs. "Big-Size-Fits-All", IAC-22-D2.4.1, 73rd International Astronautical Congress, 2022
19. Marwege, A., Gülhan, A., Klevanski, J., Hantz, C., Karl, S., Laureti, M., De Zaiacomo, G., Vos, J., Jevons, M., Thies, C., Krammer, A., Lichtenberger, M., Carvalho, J., Paix~ao, S.: RETALT: review of technologies and overview of design changes, CEAS Space Journal 14:433–445, 2022, <https://doi.org/10.1007/s12567-022-00458-9>
20. De Zaiacomo, G., Blanco, A.G., Bunt, R., Bonetti, D.: Mission engineering for the RETALT VTVL launcher. CEAS Space Journal (2021). <https://doi.org/10.1007/s12567-021-00415-y>
21. Burkhardt, H., Sippel, M., Herbertz, A., Klevanski, J.: Kerosene vs Methane: A Propellant Tradeoff for Reusable Liquid Booster Stages, Journal of Spacecraft and Rockets Vol. 41, No. 5, September–October 2004, 762–769, <https://doi.org/10.2514/1.2672>
22. Dresia, K., Jentzsch, S., Waxenegger-Wilfing, G., Dos Santos Hahn, R., Deeken, J., Oschwald, M., Mota, F.: Multidisciplinary design optimization of reusable launch vehicles for different propellants and objectives, Journal of Spacecrafts and Rockets, 58(4), July 2021, <https://doi.org/10.2514/1.A34944>
23. Koelle, D. E.: SÄNGER II, A Hypersonic Flight and Space Transportation System, International Council of the Aeronautical Sciences, ICAS-88-1.5.1, 1988
24. Kopp, A., Stappert, S., Mattson, D., Olofsson, K., Marklund, E., Kurth, G., Mooij, E., Roorda, E.: The Aurora space launcher concept 2017 CEAS Space Journal <https://doi.org/10.1007/s12567-017-0184-2>
25. Baiocco, P.: Overview of reusable space systems with a look to technology aspects. Acta Astronaut. **189**, 10–25 (2021)
26. Jenkins, D. R.: Space Shuttle The History of the National Space Transportation System The First 100 Missions, Hardcover Third Edition, Sixth Printing, 2010, ISBN-13: 978-0-9633974-5-4
27. Chaudhary, A., Nguyen, V., Tran, H., Poladian, D., Falangas, E.: Dynamics and stability and control characteristics of The X-37, AIAA-2001-4383, AIAA GN&C Conference, Montreal, Canada (2001). <https://doi.org/10.2514/6.2001-4383>
28. SpaceX: Starship User Guide revision 1.0, March 2020
29. Stappert, S., Wilken, J., Bussler, L., Sippel, M., Karl, S., Klevanski, J., Hantz, C., Briese, L. E., Schnepfer, K.: European Next Ariane (ENTRAIN): a multidisciplinary study on a VTVL and a VTHL booster stage, IAC-19-D2.4.2, 70th International Astronautical Congress, 2019
30. Blair, J. C., Ryan, R. S., Schutzenhofer, L. A., Humphries, W. R.: Launch vehicle design process: characterization, technical integration, and lessons learned, NASA/TP—2001–210992, Nasa report, 2021
31. Sippel, M., Singh, S.; Stappert, S.: Progress Summary of H2020-project FALCon, aerospace europe conference—10th European Conference for Aeronautics and Space Sciences—9th CEAS, 2023
32. Godget, O., Mansouri, J., Breteau, J., Patureau de Mirand, A., Louaas, E.: Launch vehicle system studies in the "Future Launchers Preparatory Programme": the reusability option for ariane evolutions, 8th European Conference for Aeronautics and Space Science, 2019, <https://doi.org/10.13009/EUCAS S2019-971>
33. Koelle, D. E.: Handbook of cost engineering and design, revision 4, TransCostSystems, TCS-TR-200, no date
34. Espinosa-Ramos, A.; Taponier, V.: Towards a new class of engine for future heavy lift launch vehicles, Aerospace Europe Conference 2023—10th European Conference for Aeronautics and Space Science – 9th CEAS, 2023, <https://doi.org/10.13009/EUCASS2023-887>
35. Rickmers, P., Bauer, W., Stappert, S., Sippel, M., Redondo Gutierrez, J. L., Seelbinder, D., Bernal Polo, P., Razgus, B., Acquatella, P., Robens, J., Gäßler, B., Wartemann, V., Merrem, C., Ruhe, T., Elsäßer, H., Welter, M., Schmidt, A., Damp, L., Williams, P.: The Reusability Flight Experiment—ReFEx: From Design to Flight—Hardware, IAC-21-D2.6x65984, 72nd International Astronautical Congress, 2021
36. Krummen, S., Desmariaux, J., Yasuhiro, S., Boldt, M., Briese, L. E., Cesco, N., Chavagnac, C., Cliquet Moreno, E., Dumont, E., Ecker, T., Eichel, S., Ertl, M., Giagkozoglou Vincenzino, S., Glaser, T., Grimm, C., Illig, M., Ishimoto, S., Klevanski, J., Lidon, N., Mierheim, O., Niccolai, J.-F., Reershemius, S., Reimann, B., Riehmer, J., Sagliano, M., Scheufler, H., Schneider,

- A., Schröder, S., Schwarz, R., Seelbinder, D., Stief, M., Windelberg, J., Woicke, S.: Towards a Reusable First Stage Demonstrator: CALLISTO—Technical Progresses & Challenges, IAC-21-D2.6.1, 72nd International Aeronautical Congress, 2021
37. Sippel, M., Stappert, J., Wilken, J., Darkow, N., Cain, S., Krause, S., Reimer, T., Rauh, C., Stefaniak, D., Beerhorst, M., Thiele, T., Kronen, R., Briese, L. E., Acquatella, P., Schnepfer, K., Rissius, J.: Focused research on RLV-technologies: the DLR project AKIRA, 8th European Conference for Aeronautics and Space Sciences, 2019, <https://doi.org/10.13009/EUCAS S2019-385>
 38. Wilken, J., Callsen, S., Daub, D., Fischer, A., Liebisch, M., Rauh, C., Reimer, T., Scheufler, H., Sippel, M.: Testing combined cryogenic insulation and thermal protection systems for reusable stages, IAC-21-D2.5.4, 72nd International Aeronautical Congress, 2021
 39. Simontacchi, P., Remy, A., Humbert, E., Blasi, R., Espinosa, A., Caruana, J.-N.: PROMETHEUS®: Precursor of new low-cost rocket engine family, Aerospace Europe Conference—10th European Conference for Aeronautics and Space Sciences—9th CEAS, 2023,

Publisher's Note Springer Nature remains neutral with regard to jurisdictional claims in published maps and institutional affiliations.



Selection of propulsion characteristics for systematic assessment of future European RLV-options

Martin Sippel¹ · Jascha Wilken¹

Received: 31 December 2023 / Revised: 31 July 2024 / Accepted: 19 August 2024 / Published online: 18 September 2024
© The Author(s) 2024

Abstract

The propulsion system as the key-element of any space transportation concept is systematically investigated supporting a study on potential future European RLV. Different liquid propellant combinations are compared and evaluated. Subsequently, main stage rocket engines are defined for the two cycle options: open gas-generator and closed staged-combustion. Four different propellant combinations are considered all based on liquid oxygen (LOX) as oxidizer and with the fuel options liquid hydrogen (LH₂), liquid methane (LCH₄), liquid propane (LC₃H₈) and kerosene (RP1). These combinations result in eight different generic engines with sub-variants using different nozzle expansion ratios in first and upper stage application. Engine characteristics are similar, as far as conceivable, to be well-suited for the system level comparison of pre-defined RLV-launchers. However, characteristics are not necessarily identical as different engine architectures and propellants might make individual choices necessary. Engine performance characteristics are compared with similar existing engines when available. It is shown that closed-cycle staged combustion engines bring significant performance gains, particularly in sea-level operations. On the other hand, hydrocarbon- and open-cycle gas-generator engines offer a better thrust-to-weight-ratio than hydrogen and staged combustion cycle.

Keywords Rocket propulsion · Rocket propellants · Staged combustion cycle · Gas generator cycle

Abbreviations

A	(Cross section) area m ²
I _{sp}	(Mass) specific Impulse s (N s / kg)
M	Mach-number
p	Pressure MPa (bar)
T	Thrust N
m	Mass kg
W	Weight N
ε	Expansion ratio
FFSC	Full-flow staged combustion
FRSC	Fuel-rich staged combustion
FTP	Fuel turbo pump
LC ₃ H ₈	Liquid propane
LCH ₄	Liquid methane
LH ₂	Liquid hydrogen
LOX	Liquid oxygen
MCC	Main combustion chamber
MR	Mixture ratio

N.B.	Nota bene
OTP	Oxidizer turbo pump
ORSC	Oxidizer-Rich staged combustion
RP1	Rocket propellant (Kerosene)
SLME	SpaceLiner Main Engine
SSME	Space shuttle main engine
TET	Turbine entry temperature
VTHL	Vertical take-off horizontal landing
VTVL	Vertical take-off vertical landing
c, C	Chamber
fr	Frozen
s/l	Sea level
t	Throat
vac	Vacuum

1 Introduction

Reusability of launch systems is the key innovation element in early twenty-first century space transportation. The US-American-company SpaceX has demonstrated with Falcon 9 Block 5 that routine operation with multiple reuses of first stages is feasible and probably also cost effective. This major

✉ Martin Sippel
Martin.Sippel@dlr.de

¹ Space Launcher Systems Analysis (SART), DLR, Bremen, Germany

achievement by SpaceX shows one technical option, however, not necessarily the best technical option for Europe with its different mission scenario.

The Space Launcher System Analysis division SART of the German Aerospace Center (DLR) has performed a systematic investigation of promising options for a reusable first stage of a future European partially reusable launch vehicle. The final goal has been the determination of the impact of the different return methods on a technical, operational and economical level and the assessment of their relevance for a future European launch system. Within the first phase (called ENTRAIN 1, see also [1–4]) a wide variety of reusable first stages were investigated by DLR. This includes vertical take-off vertical landing (VTVL) with propulsive deceleration [2] and vertical take-off horizontal landing (VTHL) with winged stages and aerodynamic deceleration in the atmosphere [3].

The systematic assessment of future RLV-stages and technical options requires the definition of generic engines with similar baseline assumptions in order to reach maximum comparability. The underlying assumptions of all propulsion aspects and justification of certain choices are in focus of this paper. This includes an overview on the propellants and important engine performance characteristics which are compared to existing engines, whenever possible. Such cross validation is essential to generate realistic engine reference data to be used in a viable and meaningful preliminary launcher sizing.

The available literature on comparable engine data for different fuel choices and engine cycles is limited, even more so when considered from a European perspective. While comparative data for the combustion chamber performance alone is available for various propellant combinations in established literature [5], it doesn't contain generic data based on the analysis of entire engine cycles. In previous system optimization studies [6] the performance of closed cycles was derived from the combustion chamber performance without a detailed analysis of the entire cycle, while for the gas generator cycle the massflow through the gas generator was estimated via a regression over the combustion chamber pressure. The latter approach has the disadvantages of neither considering the individual propellant characteristics, gas generator conditions, nor the turbomachinery efficiencies and pressure ratios. A former DLR study already looked into the launcher system performance of entire engine cycles [7, 8], however, at the time was focused only on staged combustion methane and kerosene rocket engines. Another study with an industrial perspective on hydrocarbon propellants has been published as a conference paper [9].

In contrast to existing literature this manuscript aims to provide a database for staged combustion and gas generator rocket engines for four different fuel options (hydrogen, methane, propane and kerosene), all evaluated under realistic

and comparable assumptions for the engine cycle and thrust chamber performance.

2 Propellants

The main driver for chemical rocket engines to achieve high performance is by selection of the propellant combination. As long as thrust-levels are scaled with the engine massflow without running into design challenges, the (mass) specific impulse I_{sp} is representing chemical engine performance. Additional criteria are to be considered which are important but, nevertheless, are secondary to performance dominating spaceflight. These other high-level criteria for propellants are

- non- or low-toxicity of the propellants or reaction products,
- low or at least affordable production costs of the propellants,
- simple handling in ground operations and hence low operating costs, and not to forget
- energy efficiency in production, low environmental and climate impact (e.g. in CO_2 -equivalent)

It is well known that a compromise is to be found as no propellant combination has been identified fulfilling always the optimum conditions. In case of reusable stages only liquid-state propellant combinations are of interest. The easily available and cheap oxidizer is liquid oxygen (LOX) and corresponding fuels of interest are:

- Liquid hydrogen (LH2) and the hydrocarbons
- Liquid methane (LCH4)
- Liquid propane (LC3H8)
- Kerosene or rocket propellant (RP1)

These four fuels in combination with oxygen are most promising for modern launcher application and are selected for this study without performing extensive trade-offs with more exotic alternative fuels or oxidizers. The reason these propellant combinations are widely used, or at least being under extensive study is the fact that the high-level criteria listed are well met.

2.1 Key characteristics at typical operating points

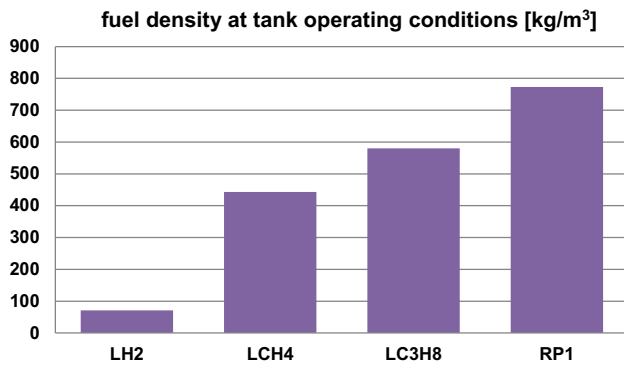
Note, all propellants with the only exception RP1 would be in gaseous state under the ambient conditions at all possible launch sites. For the practical use in launch vehicles, these propellants need to be liquified by significant cooling below ambient temperature which is represented

Table 1 Key propellant characteristics [10, 12]

	LOX	LH2	LCH4	LC3H8	RP1
Molar mass [g/Mol]	31.9988	2.01588	16.04	44.1	13.97
Typical tank filling conditions (1 bar pressure at sea-level)					
Temperature [K]	90.1	20.324	111.66	231.08	298.1
Density [kg/m ³]	1141.8	70.899	422.6	582	807
Thermodynamic characteristics					
Normal melting point [K]	54.361	13.957	90.68	85.47	223
Normal boiling point [K]	90.1878	20.369	111.63	231.08	400–500
Critical temperature [K]	154.581	33.145	190.5	369.8	956
Critical pressure [MPa]	5.043	1.2964	4.596	4.25	2.18
Critical density [kg/m ³]	436.1	31.262	162.8	224.9	232.3
Combustion heat [kJ/kg]	–	120,000	55,526	50,327	43,340

Table 2 Stoichiometric mixture ratio (MR) of propellants with LOX

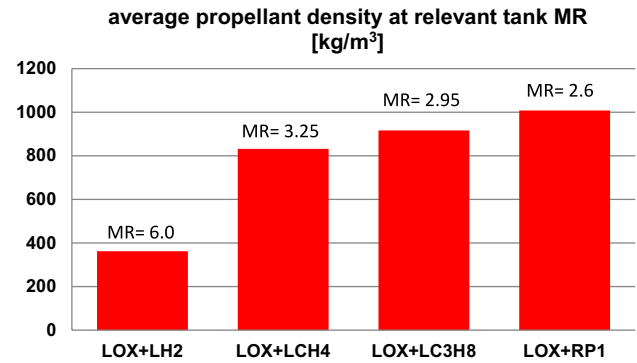
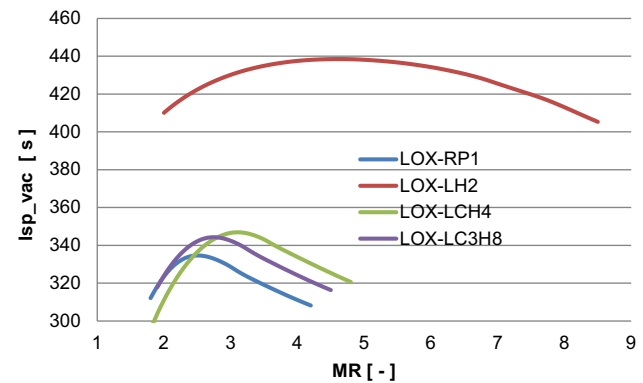
LH2	LCH4	LC3H8	RP1
7.936	3.989	3.628	3.403

**Fig. 1** Density at normal boiling point for cryogenic fuels and at ambient temperature for RP1

by the capital letter L in the names. Characteristic data are listed in Table 1.

The three hydrocarbon fuels methane, kerosene (RP1), and propane are relatively close in their characteristics. Methane represents the lowest density of the hydrocarbon propellants while Kerosene embodies the highest density. Kerosene (RP1) is more than 10 times denser than liquid hydrogen and even methane is about 6 times more dense than the lightest element at normal boiling point (Fig. 1).

The most commonly used oxidizer in launch vehicles is liquid oxygen (LOX) with a density at normal boiling point (90.15 K, 1 bar) at 1142 kg/m³. Relevant for stage sizing is not the density of the fuels alone (as shown in Fig. 1) but the average bulk density of the two propellant constituents, oxidizer and fuel at the resp. relevant mixture ratio (MR). MR of practical engines remain below the

**Fig. 2** Average density inside tanks of propellant combinations with LOX**Fig. 3** I_{sp} in vacuum as function of mixture ratio (MR) and different propellant combinations calculated for main combustion chamber

stoichiometric values listed in Table 2 and are defined with the engine investigations in Sects. 3.2–3.6. The lighter the fuel, the higher the mixture ratio and hence amount of relatively dense and heavy oxygen in the propellant combination. As a result, the average propellant density shows the same ranking order but much less pronounced with a factor of 2.5 between densest LOX-RP1 compared to LOX-LH2 (Fig. 2).

Figure 3 shows the dependency of vacuum specific impulse on the propellant mixture ratio calculated for chamber pressure p_c of 16 MPa and nozzle expansion ratio ϵ of 33. These are typical data, later being used in the work as a reference for the preliminary sizing of engines. Note the relatively close position of all hydrocarbon fuels compared to hydrogen and that the optimum I_{sp} -performance is found for all propellants below the stoichiometric MR as listed in

Table 2 because lighter molecules in the exhaust composition shift somehow the optimum position.

2.2 Relevant internal engine fuel characteristics

The following short summary of fuel characteristics is relevant for the correct and safe functioning of rocket engines. These play a minor role in the performance estimation and engine preliminary sizing but important to be kept in mind anticipating more detailed engine definition.

2.2.1 Thermal stability and coking

The decomposition of hydrocarbons takes place when a certain fluid temperature is exceeded in the case of heat transfer. Due to a defined property of the fuel for the combustion process and as coolant in the regenerative cooling system, this has to be prevented. Certain bulk- and wall temperature limitations have to be considered.

Thermal cracking of hydrocarbons is dependent on wall temperatures, flow rates and pressure. Molecules with higher atomic mass can be decomposed at lower heat input. It has been observed that higher pressures decrease the tendency of thermal decomposition of propellants and the temperature value for starting thermal decomposition is shifted towards higher values as the pressure is increased [10].

Coking is the deposition of carbon compounds to the cooling channel wall. These layers are increasing with time. It influences the heat transfer and hydrodynamic behavior as follows: heat transfer is reduced due to an increase of the coolant side thermal resistance with an increasing layer thickness of carbon deposition. Pressure loss is increased due to roughness elements on the cooling channel wall [10].

Single tube heat exchanger experiments have been accomplished to define certain wall temperature limits for the application of hydrocarbon fuels as coolant. It has been observed that for each fuel, a wide range of maximum acceptable wall temperatures is found. Coking of fuels is

dependent on the wall material and coatings such as gold plating, platinum plating, nickel plating and silver plating [10].

2.2.2 Potential chemical reactions with liner material

Corrosion of the liner wall material occurs if the fuel contains a certain part of sulfur. Copper corrosion produces rough wall layers with reduced thermal conductivity and causes an additional pressure loss in the cooling channels [10].

Contamination of sulfur and oxygen in the fuels are responsible for sulfurize and oxidize copper, which results in a deterioration of the copper wall. Carbon deposition from heated hydrocarbon fuels on a hot copper wall can cause copper corrosion [10].

Hydrogen embrittlement is a degradation of mechanical properties, especially in plasticity, of materials relevant for many metallic materials, including steel, aluminum (at high temperatures only), and titanium. High-pressure hydrogen gas, electrochemical hydrogen charging and corrosion reactions are the typical sources of hydrogen embrittlement in metals [11]. Prevention of hydrogen embrittlement can be based on surface coating and surface modification treatments or the modification of the material microstructure [11].

2.2.3 Pressure drop and heat transfer

The physical properties of the coolant are influencing the heat transfer. Good coolants are high density fluids with a high heat capacity c_p and low dynamic viscosity η . A comparison of the heat capacity of different coolants is given in Fig. 4 and of viscosity in Fig. 5 all in the typical operational range of regenerative cooling of high-performance rocket engines.

Fig. 4 Heat capacity of selected propellants [10, 12]

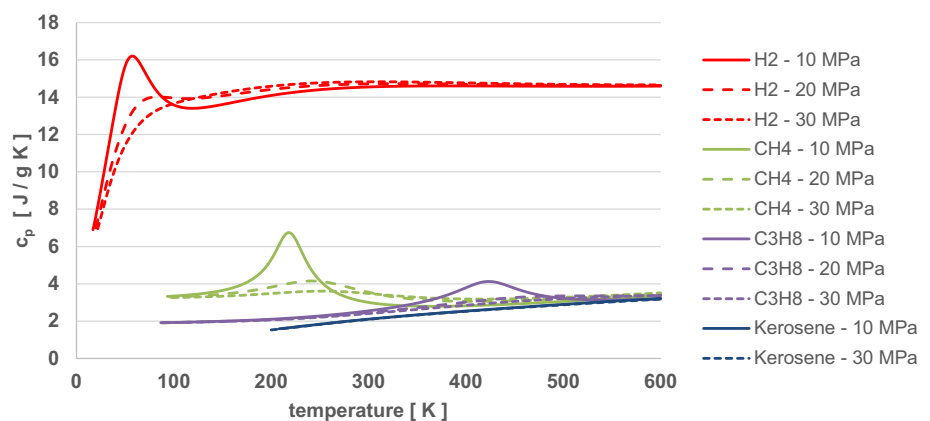
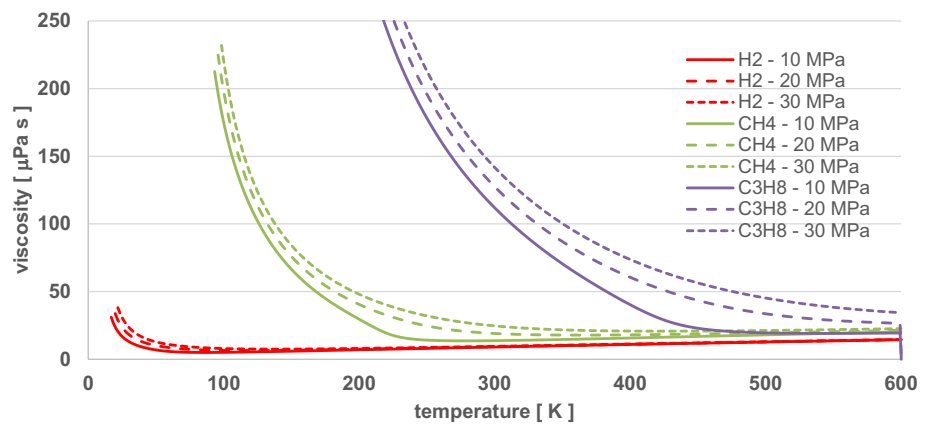


Fig. 5 Viscosity of selected propellants [12]**Table 3** Triple point conditions of cryogenic propellants [12]

	LOX	LH2	LCH4	LC3H8
Triple point temperature [K]	54.361	13.803	90.694	85.525
Tripe point density [kg/m ³]	1306.1	76.977	451.48	733.13
Density increase compared to filling conditions in Table 1	14.4%	8.6%	6.8%	26%

2.3 Key characteristics at triple point

Usually cryogenic propellants are loaded into the tanks at their boiling point under ambient pressure (already shown in Table 1). However, employing colder, subcooled propellants offers the benefit of increased density. Subcooled propellants are currently being used by SpaceX in both their currently operating Falcon 9 rocket as well as the Starship configuration under development.

The maximum density increases possible, while still remaining fully liquid, is given for the cryogenic propellants in Table 3. The increase is especially large for LOX and LC3H8. For RP-1 the lowest possible temperature (as well as properties such as the boiling point) are not easily defined since it is a mixture of various hydrocarbons. However, in principle the RP-1 can also be subcooled in order to increase the density, as is done for the Falcon 9.

While the increased density is beneficial for the structural index and thus performance of the vehicles, it comes at a price. Loading the propellants at boiling point has the benefit of a well-defined state throughout propellant loading. While propellant may evaporate, the body of fluid itself remains at the boiling point with a constant temperature and density. For a subcooled propellant, any heat influx will lead to thermal stratification which has to be well-understood and managed in order to arrive at useful values for the average propellant density (and thus actually loaded propellant mass on the launch pad) and the thermal residuals.

3 Main propulsion rocket engines

Despite the engines being generic, their selected technical characteristics for simulation are strongly oriented towards data of existing types or previous or ongoing development projects, whenever possible.

The two rocket engine cycles most commonly used in first or booster stages are included in the study:

- Gas-Generator-cycle (GG)
- Staged-Combustion cycle (SC).

Expander cycle engines which exclusively use the heat transferred to the fuel in the regenerative circuit to power the turbopumps have *not* been considered. The Japanese LE-9 in the H-3 launcher is the first application of this cycle in first or booster stages [13]. However, the H-3 is an expendable vehicle and the more demanding missions of reusable first stages make expander cycle engines less attractive for this application. DLR has looked in the past into the feasibility of such open expander engines (LOX-LH2) for reusable winged side-mounted boosters. Although, a converging design could be found under certain conditions at the time, its limitations were also revealed with the necessity to implement a vast combustion chamber generating sufficient heat transfer, highly efficient impulse turbines, and significantly larger tanks compared to gas generator cycle configurations because of the relatively low chamber pressure and engine mixture ratio [14, 15].

3.1 Numerical simulation methods

3.1.1 Chamber performance estimation

3.1.1.1 Ideal performance The baseline of all engine performance calculations is the theoretical rocket engine performance estimation for which the following assumptions are made for its calculation:

- adiabatic, isenthalpic combustion;
- adiabatic, isentropic (frictionless and no dissipative losses) quasi one-dimensional nozzle flow;
- ideal gas law;
- no dissipative losses.

This calculation approach for theoretical rocket engine performance is commonly used since decades and has been implemented in the famous NASA “Lewis code” developed in the 1960s by Zeleznik, Sanford Gordon and Bonnie J. McBride [16, 17]. The condition for chemical equilibrium can be stated in the minimization of Gibbs energy or the maximization of entropy. According to the second law of thermodynamics an isolated system is at equilibrium when entropy is constant and reaches its maximum [18, 19].

The analysis is started by obtaining the combustion chamber equilibrium composition assuming the isobaric-isenthalpic combustion, followed by calculation of the thermodynamics derivatives from the equilibrium solution [20]. The results include the number of moles for each species, combustion temperature, heat capacity, enthalpy and entropy of the reacting mixture, as well as specific heat ratio and velocity of sound. The calculation tools implement a thermodynamic analysis module which utilizes a free energy minimization approach to obtain the combustion composition for given propellant components and combustion conditions.

3.1.1.2 Models for non-ideal performance Ideal performance calculations provide an overestimation of actual engine performance. This is on the one hand related to less efficient open cycles that bring propellants to chamber pressure conditions (see following Sect. 3.1.2) and on the other hand is linked to constraints of the gas expansion process relevant for all cycles.

Those factors relevant for the liquid rocket engine pre-designs performed here are including:

- non- chemical equilibrium conditions,
- performance loss due to finite-area combustor,
- performance loss due finite rate chemical reaction kinetics,
- nozzle wall friction loss,
- nozzle divergence loss,
- performance change due to nozzle flow separation.

In ideal performance, the composition is assumed to attain its chemical equilibrium instantaneously. While this assumption is a good approximation in the combustion chamber, it is not realistic in rapid supersonic expansion. In “frozen” performance, composition is assumed to remain fixed at a certain combustion composition during expansion [18] and is no longer able transforming chemical into kinetic energy. The early CEC/CEA-codes of NASA offered

already the equilibrium and “frozen” performance calculation options with actual performance to be expected in between these upper and lower theoretical limits.

The consideration of finite rate chemical reaction kinetics is important for realistic rocket engine performance estimation. Assuming full chemical equilibrium along the complete nozzle can overestimate the I_{sp} by 10 s or more depending on the expansion ratio [5]. Usually it is recommended in rocket performance assessment that the combustion composition is assumed to remain fixed (“frozen”) at certain area- or pressure-ratios during expansion. A classic, however, slightly conservative assumption is “freezing” chemical composition at the nozzle throat. The commercially available rocket engine tool RPA (rocket propulsion analysis) recommends empirically derived values [21] depending on the combustion products at different supersonic area ratios A_{fr}/A_t (where A_{fr} is the cross-section after which chemical composition is assumed frozen):

- LOX–Kerosene (hydrocarbons): 1.3
- LOX–LH2: 3.0

These values are recommendations and the actual input is selected by the user potentially based on specific test data. This study is following the empirically-based data and assumes for the less well-known propellant compositions LOX–LCH4 and LOX–LC3H8 values between 1.9 and 2.

Other factors create additional losses compared to the ideal performance. These might simply be considered by correction factors derived from recalculation of existing engines. Such an approach had been implemented in the ASTOS launcher optimization tool within the ESA-funded CDO-project [22]. A more sophisticated method is used by tools like RPA [23] capable of predicting the delivered performance of a thrust chamber using semi-empirical relations to obtain performance correction factors more specific to engine design parameters.

Practical combustion chambers of large-scale engines have relatively small cross sections with contraction area ratios A_c/A_t of less than four. In this case the expansion of the gases is accompanied by significant acceleration and resulting pressure drop. The acceleration process in the chamber is assumed to be adiabatic, but not isentropic, and the pressure drop leads to the lower pressure at nozzle inlet p_c . This causes a small loss in specific impulse [20] which can be calculated. The iterative procedure for its computation in the so-called Finite Area Combustor is described in [21].

A correction factor that represents performance loss due to finite rate kinetics in the combustion chamber depends on propellant combination, oxidizer excess coefficient and chamber pressure [21].

In real thrust chambers the flow is mostly axisymmetric two-dimensional (or even three-dimensional), with a

viscous boundary layer next to the nozzle walls, where the gas velocities are much lower than the core-stream velocities, finite-rate chemical kinetics, and other factors which further reduce the real delivered performance [21]. The correction factor due to wall friction in boundary layer can be calculated according to the fluid dynamic relations of laminar and turbulent boundary layers.

A theoretical ideal nozzle would expand the flow fully parallel to the centerline. Such nozzles are unpractical for any launcher application and hence the nozzle exit angle $> 0^\circ$ is creating some flow divergence and related performance losses. The correction factor can be calculated depending on the nozzle type, expansion ratio and selected fractional length (see e.g. [21]).

The performance of flow separation inside the nozzle could be estimated by RPA [21]. In steady engine operation such flow separation caused by strong overexpansion should be avoided.

3.1.2 Cycle performance, size and mass estimation

All preliminary engine definitions have been performed by simulation of steady-state operation at 100% nominal thrust level using the DLR-tools *lrp* (liquid rocket propulsion) and *ncc* (nozzle contour calculation program) as well as the commercially available tool *RPA*. Any potential requirements specific to transient operations or deep-throttling are not considered in this early design study.

DLR's *lrp*-program has a long heritage of early rocket engine pre-sizing based on a selection of fixed internal engine flows combined with a rough estimation of engine size and empirically based mass estimation per major component. The commercially available program *RPA* (versions 2.2.3 and 2.3.2) [23, 24, 20] has been used as a second tool for crosscheck of results and for improved modelling of certain cycle variants like oxygen-rich pre-burner systems. The *RPA* engine cycle analysis module is capable of analyzing the operational characteristics of engine configurations, performing a power balance of the turbomachinery to achieve the defined combustion chamber pressure. *RPA* offers more sophisticated performance estimation methods [21] and can be operated by graphical user interface or by scripts. In the preliminary definition of the reusable rocket engines, both numerical tools are useful and complement each other.

The program *ncc* generates the internal thrustchamber contours of different bell-type nozzles based on the main combustion chamber (MCC) operating conditions and definition of characteristics like characteristic chamber length, nozzle fractional length, contraction- and expansion ratio, etc. Further, *ncc* can create input files for the

NASA code TDK [25] allowing conveniently subsequent analysis of boundary layer effects.

3.2 Baseline design assumptions

3.2.1 Programmatic requirements

Reliability and robustness are basic requirements, excluding any exotic technical options. Further, the propulsion system choice should be environmentally compatible with non- or low-toxic propellants and reaction products. This point has been addressed by the four selected propellants described in Sect. 2. Sustainability of space flight gains increasing importance. The life-cycle and climate impact of the propulsion system is a key element for all launchers and should be as low as possible. A quantitative assessment of the different options is going beyond the scope of this paper and should be addressed in future activities.

Development risks should be limited and potential concepts should build upon European expertise in operating engines or technology demonstration performed or ongoing. The propulsion system should, thus, be affordable in development but also later in manufacturing and launcher operations. The target for reusability is set between minimum of 5 to maximum 25 ignitions or flights. A quantified assessment of such high-level programmatic requirements is not pursued in the study.

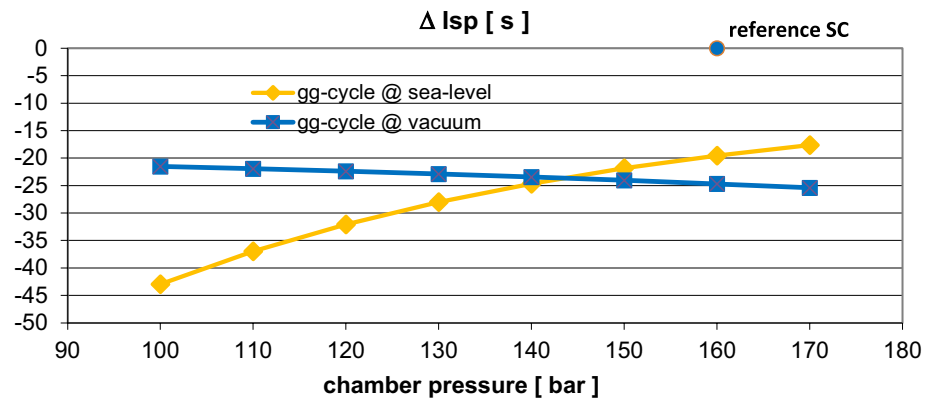
3.2.2 Technical requirements

3.2.2.1 Thrust level Common baseline assumption of all engines is a vacuum thrust in the 2200 kN-class. This a-priori-choice is keeping future heavy-lift launcher options in mind and is also set by the upgrade limits of European test infrastructure for liquid rocket engines. Most VTVL- and VTHL-launcher configurations described in [2, 3] have a lower thrust requirement. The engine massflows are scaled to the required thrust level of the individual RLV-concepts while I_{sp} -performance and engine thrust-to-weight ratios (T/W) are kept in [2, 3] on the values described below.

3.2.2.2 Chamber pressure In case of the staged-combustion engines, the main combustion chamber (MCC) pressure is commonly fixed for all propellant combinations at 160 bar (16 MPa). This moderate value in Russian or US perspective has been chosen considering the limited European experience in closed cycle high-pressure engines.

The chamber pressure for the gas-generator type is unlikely to be set on the same value of 16 MPa. Figure 6 shows the performance difference of the LOX-LH₂ gas generator engine as a function of MCC pressure compared to the reference staged combustion (SC) cycle at 160 bar (16 MPa). The difference in I_{sp} is shown for sea-level

Fig. 6 Trade study on main combustion chamber pressure sensitivity for GG-cycle on I_{sp} performance, sea-level (yellow), vacuum (blue)



(yellow) and vacuum conditions (blue) and typical nozzle expansion ratio of 30. The open cycle's performance is at least 15 to 20 s below the closed cycle but could degrade by 30 to 40 s if parameters are not carefully selected. Raising the main combustion chamber pressure of the open gas generator cycle beyond 100 bar is widening the I_{sp} -gap in vacuum when compared to the reference SC-point while for sea-level conditions the gap closes in. The explanation of this behavior is straight-forward and well known: Increasing the chamber pressure requires swelling the low-efficiency secondary flow powering the turbopumps and, consequently, does no longer allow improving overall engine performance in vacuum. At sea-level, the increased MCC-pressure results in higher nozzle exit pressure and delivers significantly improved performance despite elevated, less-efficient gas generator flow.

Subsequently, the main combustion chamber pressure for the gas-generator type is commonly set to 12 MPa. This pressure is not far from the useful upper limit of this cycle but is assumed necessary to achieve sufficient performance for the RLV stages. Europe has considerable experience in this range with Vulcain 2 operating at 11.7 MPa and the development risk of the additional slight increase is assessed as low.

3.2.2.3 Nozzle expansion ratio Nozzle expansion ratios are selected according to optimum performance but also requirements of safe throttled operations when landing VTVL-stages. For the first stage engines data are calculated for several expansion ratios from 20 for gas generator types up to 35 for the staged-combustion variants. The upper stage engines are derived from the first stage engines with the only difference being the increased nozzle expansion. The impact of this value is evaluated for expansion ratios of 120 and 180.

3.2.2.4 TET and cooling Turbine entry temperature (TET) target is set around 750 K and kept in all cases below 800 K to be compatible with the increased lifetime requirement

of reusable rocket engines. These assumptions are in the lower segment of the typical range of rocket engine TET. Reference [5] mentions an elevated range between 900 to 1200 K, however, not having any reusability in focus. The reusable SSME has preburner combustion temperatures of 739 K on the OTP-side and up to 983 K on the FTP-side [33].

Further, for all engines in this study regeneratively cooled combustion chambers supported by film cooling at the wall using small amount of fuel are assumed. Large down-stream nozzle extensions should use a combination of dump- and radiation cooling.

3.2.3 Design assumptions

Beyond the already described technical design requirements, some parameters need to be selected for the engine cycle analyses and engine pre-dimensioning. These are the turbomachinery efficiencies, gas-generator operating pressure and turbine pressure ratio in open cycles and internal line, valve and injector total pressure losses.

The parameters can be preselected and iteratively further optimized during the maturing engine design process. However, such an approach applied to the numerous engine configurations would go well beyond the scope of this study. Instead, typical engine component values have been selected but are not validated by sophisticated analyses. Data are similar within narrow limits but not identical for all types. An open cycle high pressure-ratio impulse turbine can't reach the same efficiency as the low pressure-ratio turbines in closed cycle engines.

The actually selected design parameters of the turbopumps are listed in the following together with the short engine descriptions. In case more elaborated turbomachinery data are available based on dedicated designs, the references are provided. Selection of the parameters within the narrow boundaries has only limited impact on performance

and mass estimation. The driving factors remain propellant combination, cycle and nozzle expansion ratio.

3.3 LOX-LH2 engines

The combination of liquid oxygen with liquid hydrogen delivers the highest practically achievable mass specific performance. Water as the reaction product is also the most environmentally compatible exhaust. The low bulk density due to the low density of hydrogen and its very low boiling temperature are the key challenges.

Europe has gained significant experience with these propellants in more than 50 years and has flown several hundred engines up to date (HM7 from 1979 to 2023 and Vulcain since 1996).

The selection of the engine mixture ratio (MR) has a major impact on overall performance. However, the optimum I_{sp} as shown for example in typical conditions in Fig. 3 is not exactly at the optimum of the launcher. If a new engine is designed for a dedicated launcher application, an iterative MR-optimization could be performed considering tank sizing or trajectory optimization. However, usually the vehicle is not yet well defined when engine MR is to be chosen. Nevertheless, a preliminary choice of the main combustion chamber MR close to the I_{sp} -optimum is recommended with small offset to the right, towards increased propellant density for reduced tank size.

This approach is followed for the hydrocarbon-based types described in the following sections. The case of the LOX-LH2 propellant combination is somehow special because of its low average bulk density as shown in Fig. 2. Therefore, both types have been set a-priori to an engine MR of 6.0 which is a good compromise between performance, acceptable propellant bulk density of the stage, and technical feasibility of the combustion process. This choice of 6.0 is

supported by the design of many existing LOX-LH2 main stages which are around this value.

As clearly visible in Fig. 7, the main combustion chamber operating points are off the optimum I_{sp} -performance, shifted to the right towards increased density. In case of the gas generator cycle chamber (blue curve) this shift is more pronounced into less favorable regions (6.77, indicated by red arrow). This shift is necessary in order to reach an engine MR of 6.0 because the turbines are driven by strongly hydrogen-rich hot gas. The closed cycle's MCC MR is, consequently, exactly at the engine mixture ratio of 6.0 because the secondary flow is not disturbing.

3.3.1 Open gas-generator cycle

The architecture of the open cycle is following the conventional approach with single gas generator and two separate turbopumps run in parallel. This is similar to the Vulcain engine and nominal gas generator pressure is selected at 11 MPa. The turbine power-pack data assumptions for the dual shaft design have been selected as follows:

- GG combustion temperature 780 K
- LOX turbine efficiency 48%
- LOX turbine pressure ratio 16.5
- LOX pump efficiency 75%
- LH2 turbine efficiency 53%
- LH2 turbine pressure ratio 16.9
- LH2 pump efficiency 75%

3.3.1.1 First stage engine performance assessment Based on these assumptions and the 2200 kN vacuum thrust requirement, three reference engines have been calculated with different nozzle expansion ratios (Table 4), all of potential interest for the RLV first stage application.

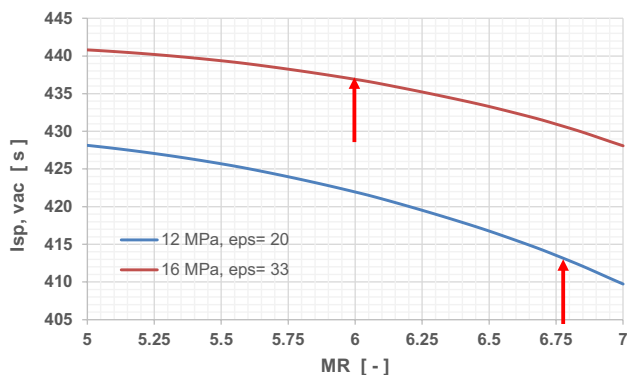


Fig. 7 Influence of LOX/LH2-mass ratio in main combustion chamber on $I_{sp,vac}$ chamber performance (red arrows indicating selected MCC design points)

Table 4 Performance data of LOX-LH2 gas generator cycle engines from lrp1.1 calculation

Nozzle expansion ratio	–	20	30	35
Sea level thrust	kN	1990.9	1893.6	1845.5
Vacuum thrust	kN	2200	2200	2200
Sea level spec. impulse	s	366.9	357.2	351
Vacuum spec. impulse	s	405.4	415	418.4
Chamber pressure	bar	120	120	120
Total engine mass flow	kg/s	553.3	540.45	536.11
gg mass flow	kg/s	20.9	20.4	20.2
Total engine mixture ratio	–	6	6	6
Chamber mixture ratio	–	6.77	6.77	6.77
Nozzle exit pressure	bar	0.7	0.412	0.34

Comparing the calculation methods in Table 4 with a computation using RPA of the engine with expansion ratio 20 shows a difference in I_{sp} performance at vacuum condition of less than 1.3 s (0.3%) and 4.5 s at sea-level (1.28%). These numbers give an indication on the level of uncertainty in the numerical performance calculation.

Another comparison of calculated performance with real operating engines is most suitable for the RS-68 which has been designed for a similar launcher application in Delta IV main and booster stage and which also has a relatively low expansion ratio. The calculated engine performance data of variant $\varepsilon = 20$ is found slightly below those published for the RS-68. The American engine has a slightly lower combustion pressure of 11.26 MPa while nozzle expansion is at 21.5. The vacuum I_{sp} is announced to reach 409 s [26]. The very large size of the RS-68 (2950 kN) with related potential efficiency gains should be taken into account in the comparison as well as uncertainty of its TET.

3.3.1.2 Upper stage engine derivative Using the same core engine in the upper stage in order to save cost is one of the baseline design drivers of the ENTRAIN TSTO configurations. Therefore, two upper stage engines with significantly increased nozzle expansion ratios of 120 and 180 have been defined using the $\varepsilon = 20$ design. Calculated engine performance is listed in Table 5. For the same mass flow, vacuum thrust increases by up to 10%. Items not listed are identical to the first stage engine. Note the gas generator conditions have not been changed for this calculation. A variation might offer the potential of slight improvements.

3.3.1.3 Engine size and mass The upper stage engines' thrustchambers have further been modeled using the tool ncc assuming parabolic nozzles with 66% fractional length. A sketch of the contours is visible in Fig. 8. Note the enormous size of the engines with a total length of beyond 7 m and exit diameter slightly below 5 m for the $\varepsilon = 180$ variant.

However, at the current state of investigations it is not possible to confirm that such a design is actually achievable. Anything similar has never been realized in the past and a launcher design based on a large upper stage engine having an expansion ratio of 180 would be subject to major development risk. In subsequent steps of the

Table 5 Performance data of LOX-LH2 gas generator cycle upper stage engines from lrp1.1 calculation

nozzle expansion ratio	—	120	180
vacuum thrust	kN	2389	2420
vacuum spec. impulse	s	440.4	446

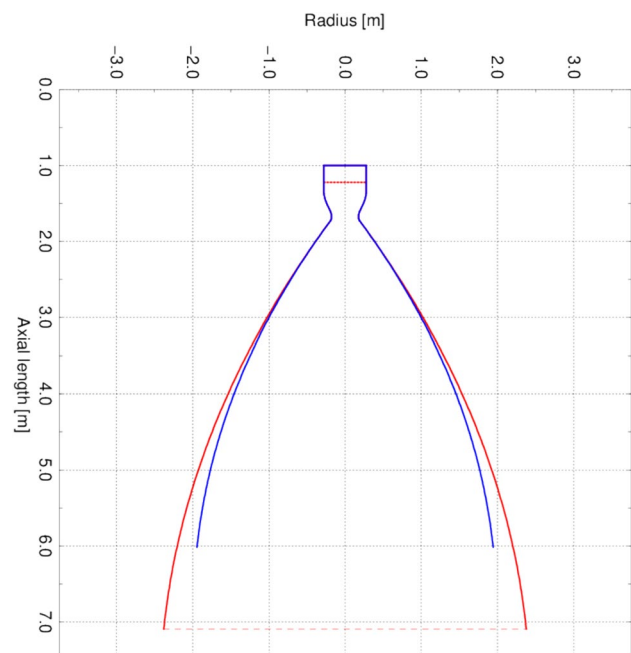


Fig. 8 Thrust chamber internal contours of LOX/LH2 GG-engine with nozzle expansion ratio 180 (red) and 120 (blue)

investigations, it has been decided to restrict the upper stage engine to an expansion ratio of 120.

The following rough geometry and mass data (Table 6) have been calculated using the tool lrp1.1.

3.3.2 Closed staged-combustion cycle

The staged combustion cycle reference engine is derived of the SLME (SpaceLiner Main Engine) under investigation for several years at DLR (e.g. [27–31]). A full-flow staged combustion cycle (FFSC) with fuel-rich preburner gas driving the LH2-pump and oxidizer-rich preburner gas driving the LOX-pump is a preferred design solution for the SLME.

In a full-flow staged combustion cycle the complete fuel and oxidizer flow rates are fed through one of the preburners after being pressurised by each turbo pump. Subsequently, the turbine gases are all injected in hot gaseous condition into the main combustion chamber (MCC).

The operational domain of the SLME has been preliminarily defined [30, 31]: The SLME in the SpaceLiner application is operating at $MR = 6.5$ during lift-off and is later throttled to $MR = 5.5$ by reducing the LOX-massflow. The intermediate SLME operating point O1 with a mixture ratio of 6 is typical for LOX-LH2 engines and with its moderate 16 MPa chamber pressure is used as the reference condition for the RLV-ENTRAIN-system studies.

The turbine power-pack data assumptions for the dual preburner, integrated powerhead design have been selected based on preliminary component sizing in [31]:

Table 6 Geometry and mass data of LOX-LH2 gas generator cycle engines

Nozzle expansion ratio	–	20	30	35	120	180
Total engine length	m	2.76	3.25	3.47	6.18	7.47
Nozzle exit diameter	m	1.62	1.96	2.11	3.97	4.86
Total engine mass	kg	2275.54	2287.18	2300.56	2955.9	3378.2
T_{vac}/W	–	98.55	98	97.48	82.4	73

Table 7 Performance data of LOX-LH2 staged combustion cycle engines from lrp1.1 calculation

Nozzle expansion ratio	–	23	33	35
Sea level thrust	kN	2024.3	1952.5	1938.2
Vacuum thrust	kN	2200	2200	2200
Sea level spec. impulse	s	394	387	385
Vacuum spec. impulse	s	428	436.5	437.8
Chamber pressure	bar	160	160	160
Total engine mass flow	kg/s	523.3	513.8	512.3
Engine mixture ratio	–	6	6	6
Nozzle exit pressure	bar	0.705	0.438	0.405
Power Pack conditions:				
Ox-rich preburner MR	–	≈ 130	≈ 130	≈ 130
Ox-rich preburner pressure	bar	262.9	262.9	262.9
Ox-rich preburner massflow	kg/s	408.7	401.2	400.1
Fuel-rich preburner MR	–	≈ 0.6	≈ 0.6	≈ 0.6
Fuel-rich preburner pressure	bar	266.2	266.2	266.2
Fuel-rich preburner massflow	kg/s	114.6	112.5	112.2

- Ox-rich preburner combustion temperature 775 K
- LOX turbine efficiency 87%
- LOX pump efficiency 86%
- Fuel-rich preburner combustion temperature 769 K
- LH2 turbine efficiency 92%
- LH2 pump efficiency 79%

N.B.: calculated performance of all closed cycles is independent of the internal architecture. Thus, a fuel-rich preburner variant like the one used in the SSME (space shuttle main engine) or proposed for the European SCORE-D demonstrator [32] would achieve the same I_{sp} as a Full-Flow-cycle engine. The difference is in engine complexity and has an impact on mass.

3.3.2.1 First stage engine performance assessment The requirements of the ENTRAIN study with tandem arrangement of stages (see [2, 3]) are not identical to the Space-Liner and therefore the baseline SLME had been adapted in its nozzle expansion ratio and was recalculated. Based on these assumptions and the 2200 kN vacuum thrust requirement, three reference engines have been calculated with different nozzle expansion ratios (see Table 7), all of potential interest for the RLV first stage application.

Table 8 Performance data of LOX-LH2 staged combustion cycle upper stage engines from lrp1.1 calculation

Nozzle expansion ratio	–	120	180
Vacuum thrust	kN	2317	2343
Vacuum spec. impulse	s	458.6	463

A comparison of calculated performance with real operating engines is suitable for the SSME (RS-25), originally been designed for the Space Shuttle and now used in the core stage of SLS. The SSME expansion ratio is 69 and achieves a vacuum I_{sp} of 452 s when operating at 109% thrust level with 21 MPa chamber pressure [33].

3.3.2.2 Upper stage engine derivative Following the ENTRAIN TSTO propulsion logic, two similar upper stage engines with significantly increased nozzle expansion ratio of 120 and 180 have been defined using the $\varepsilon = 33$ design. Calculated engine performance is listed in Table 8. For the same mass flow, vacuum thrust increases by about 6.2%. Items not listed are identical to the first stage engine.

3.3.2.3 Engine size and mass Rough geometry and mass data have been calculated using the tool lrp1.1 and are listed in Table 9. As all 1st-stage engines are scaled for 2200 kN vacuum thrust, the variant with larger expansion ratio has a slightly reduced mass flow and hence reduced throat diameter (approximately 3 mm difference or 1%).

T_{vac}/W is calculated approximately 24% below the gas generator cycle, however, under different assumptions in chamber pressure and nozzle expansion ratio. The explanation is mainly found in the more powerful and heavier turbopumps and the two high-pressure preburners.

3.4 LOX-RP1 engines

The combination of liquid oxygen with kerosene is by far the most commonly used propellant combination in spaceflight. Still today LOX-RP1 is the fuel choice of more than 50% of all rockets flown worldwide.

The spaceflight heritage of LOX-RP1 is impressive:

- Launching the first artificial satellite (R-7 rocket (8K71PS)),

Table 9 Geometry and mass data of LOX-LH2 staged combustion cycle engines

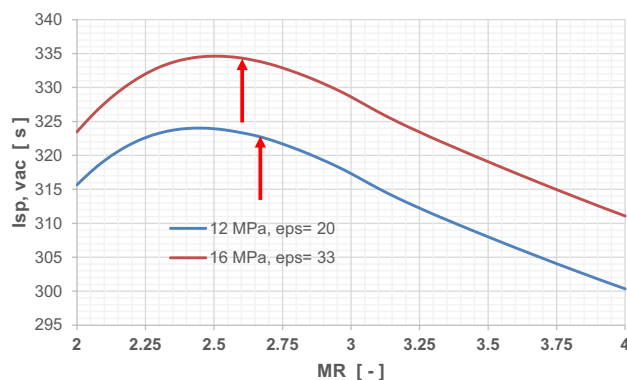
Nozzle expansion ratio	–	23	33	35	120	180
Total engine length	m	2.55	2.92	2.98	5	6
Nozzle exit diameter	m	1.49	1.77	1.82	3.37	4.12
Total engine mass	kg	3006	2992	2991	3362.2	3617.5
T_{vac}/W	–	74.6	74.9	74.95	70.2	66

- Launching the first man to space (R-7 rocket (8K72K)),
- Launching the first man to the Moon (S-IC first stage with F1-engine on Saturn V rocket),
- Achieving the highest operational chamber pressure (RD-180 engine on Atlas V),
- Powering the first operational RLV-booster stage (Merlin 1D engine on Falcon 9).

Early European experience exists with the British Blue Streak but was discontinued with the demise of the Europa rocket in the early 1970s.

The strategy in selecting combustion chamber operating points is different for hydrocarbon engines than for hydrogen engines. The reason is the increased sensitivity of I_{sp} to MR variations (see Fig. 3) in contrast to hydrogen, where the dependence is rather flat. Figure 9 shows the selected main combustion chamber operating points (red arrows) close to the optimum performance, slightly shifted to the right towards increased density. In case of the gas generator cycle (blue curve) this shift is a bit more pronounced into less favorable regions (2.66) because the turbines are driven by strongly fuel-rich hot gas. This choice helps avoiding the engine and hence tank mixture ratio dropping below 2.2. The closed cycle's MCC MR is exactly at the engine MR of 2.6.

Note, engine mixture ratio of the hydrogen engines had been set independent of the cycle to 6.0 (see Sect. 3.3) to keep average propellant density acceptable for the vehicle design. For all hydrocarbon engines the propellant density

**Fig. 9** Influence of LOX/RP1- mass ratio in main combustion chamber on $I_{sp,vac}$ chamber performance (red arrows indicating selected MCC design points)**Table 10** Performance data of LOX-RP1 gas generator cycle engines from lrp1.1 calculation

Nozzle expansion ratio	–	20	30	35
Sea level thrust	kN	1984	1884	1834
Vacuum thrust	kN	2200	2200	2200
Sea level spec. impulse	s	279	272	267
Vacuum spec. impulse	s	310	317	320
Chamber pressure	bar	120	120	120
Total engine mass flow	kg/s	723.4	706.1	700.3
gg mass flow	kg/s	47.2	46	45.7
Total engine mixture ratio	–	2.25	2.25	2.25
Chamber mixture ratio	–	2.66	2.66	2.66
Nozzle exit pressure	bar	0.72	0.42	0.34

is less a concern and instead performance becomes more important. Therefore, the chamber operating points are selected not far from the individual optimums.

3.4.1 Open gas-generator cycle

The architecture of the open cycle is following the typical approach with single gas generator and single shaft turbopump. This is similar to many famous gas-generator cycle RP1-engines like F1 or Merlin 1D. The nominal gas generator pressure is selected at 11 MPa. The turbine power-pack data assumptions have been selected as follows:

- GG combustion temperature 780 K
- turbine efficiency 50%
- turbine pressure ratio 7.5
- LOX pump efficiency 75%
- RP1 pump efficiency 75%

3.4.1.1 First stage engine performance assessment Based on these assumptions and the 2200 kN vacuum thrust requirement, three reference engines have been calculated with different nozzle expansion ratios (Table 10), all of potential interest for the RLV first stage application.

Another performance calculation has been executed for the engine with expansion ratio 20 by using the cycle analysis tool RPA 2.23 under identical assumptions. Comparing the two calculation methods shows a difference in I_{sp}

performance at vacuum condition of less than 1.3 s (0.3%) and 4.5 s at sea-level (1.28%).

A comparison of calculated performance with real operating engines is most suitable for the SpaceX Merlin 1D which has been designed for a similar launcher application in Falcon9 main- and with increased nozzle expansion ratio in the upper stage. The calculated engine performance of the engine with nozzle area ratio 20 is found very similar to data published for the Merlin 1D. Although chamber pressure of the latest and most powerful Merlin 1D+ is not exactly known, under considerations for the thrustchamber geometry and published thrust level of the -1D, a combustion chamber pressure of 12 MPa is realistic. The 1D+ vacuum I_{sp} is announced to reach 311 s. In combination with nozzle expansion of 16, the Merlin would show a slightly better performance than the ENTRAIN engine. However, missing information on the turbopump system of Merlin makes the exact comparison difficult.

3.4.1.2 Upper stage engine derivatives Upper stage engines with significantly increased nozzle expansion ratios of 120 and 180 have been defined using the $\varepsilon=20$ design. Calculated engine performances are listed in Table 11. For the same mass flow, vacuum thrust increases by up to 10%. Note the gas generator conditions have not been changed for this calculation. A variation might offer the potential of slight improvement.

3.4.1.3 Engine size and mass For the gas generator engines rough geometry and mass data (Table 12) have been calculated using the tool lrp1.1. Note the calculated high T_{vac}/W ratios of above 100 for the lower stage engines, still below what is claimed by SpaceX for its Merlin 1D.

Table 11 Performance data of LOX-RRP1 gas generator cycle upper stage engines from lrp1.1 calculation

Nozzle expansion ratio	–	120	180
Vacuum thrust	kN	2397	2430
Vacuum spec. impulse	s	338	342

Table 12 Geometry data of LOX-RP1 gas generator cycle engines from lrp1.1 calculation

Nozzle expansion ratio	–	20	30	35	120	180
Total engine length	m	2.93	3.45	3.67	6.5	7.85
Nozzle exit diameter	m	1.65	1.99	2.14	4.03	4.94
Total engine mass	kg	1978	1982	2016	2716	3175
T_{vac}/W	–	113.4	112.2	111.2	89.9	78

In subsequent launcher system investigation, it has been decided again to restrict the upper stage engine to an expansion ratio of 120 because of the enormous size of the larger variant with $\varepsilon=180$ would be subject to major development risk.

3.4.2 Closed staged-combustion cycle

The staged combustion cycle is derived of the NPO Energomash RD-120 (11D123) with oxidizer-rich preburner. In case of hydrocarbon staged combustion cycle engines, the oxygen-rich pre-combustion allows for significantly lower turbine pressure ratios compared to fuel-rich preburners in otherwise similar engine architectures [34]. The driving factor is the product of specific enthalpy and turbine gas massflow which is higher for oxygen-rich gas. All Russian closed cycle RP1-engines of the last 50 years are following this design approach.

The power-pack conditions have been selected as follows:

- Ox-rich preburner combustion temperature 750 K
- LOX turbine efficiency 75%
- LOX pump efficiency 75%
- RP1 pump efficiency 75%

Table 13 Performance data of LOX-RP1 staged combustion cycle engines from lrp1.1 and RPA 2.3 calculations

Nozzle expansion ratio	–	23	33
Sea level thrust	kN	2021	1948
Vacuum thrust	kN	2200	2200
Sea level spec. impulse	s	301	296
Vacuum spec. impulse	s	327.7	334.3
Chamber pressure	bar	160	160
Total engine mass flow	kg/s	684.55	670.95
Engine mixture ratio	–	2.6	2.6
Nozzle exit pressure	bar	0.77	0.48
Power Pack conditions:			
Ox-rich preburner MR	–	≈ 51.4	≈ 51.4
Ox-rich preburner pressure	bar	314.9	314.9
Ox-rich preburner massflow	kg/s	504.1	494.1

3.4.2.1 First stage engine performance assessment Based on the same 2200 kN vacuum thrust requirement as for LOX-LH2, two reference engines have been calculated with different nozzle expansion ratios (see Table 13), both of potential interest for the RLV first stage application. RPA is capable of calculating an oxygen-rich preburner staged combustion cycle. Overall engine performance estimated by RPA is found very close to Irp1.1 results with largest deviations again in sea-level conditions. Relative difference here is less than 0.53% while in vacuum the relative difference is less than 0.006% (0.02 s).

3.4.2.2 Upper stage engine derivative Similar to the previous sections, upper stage engines with significantly increased nozzle expansion ratios have been defined using the $\varepsilon=33$ first stage configuration for area ratio 180 and a smaller one with $\varepsilon=120$. Calculated engine performance is listed in Table 14. For the same mass flow, vacuum thrust increases by up to 7%. Items not listed are identical to the first stage engine.

The Russian upper stage engine RD-120 (11D123) by NPO Energomash has a similar chamber pressure of 16.28 MPa and an oxygen-rich preburner architecture. The calculated specific impulse of the smaller engine with $\varepsilon=120$ is close to the vacuum I_{sp} of RD-120 of 350 s which has a slightly smaller nozzle expansion ratio of 114.5 [35].

3.4.2.3 Engine size and mass Calculated geometry and mass data of the staged combustion engines are listed in Table 15. As the first stage engines are scaled for 2200 kN vacuum thrust, the variant with larger expansion ratio has a slightly reduced mass flow and hence reduced throat diameter. The staged combustion engines are more compact despite the increased expansion ratios due to the higher nominal chamber pressure.

T_{vac}/W is calculated approximately 30% below the gas generator cycle, however, with different assumptions in chamber pressure and nozzle expansion ratio. The explanation is again related in the more powerful and heavier turbopumps and the high-pressure preburner. T_{vac}/W of the variant with expansion 33 is slightly above the engine with expansion 23 because of the latter's slightly larger massflow and hence size of major components.

Table 14 Performance data of LOX-RP1 staged combustion cycle upper stage engine from Irp1.1 calculation

Nozzle expansion ratio	–	120	180
Vacuum thrust	kN	2323	2350
Vacuum spec. impulse	s	353	357

Table 15 Geometry data of LOX-RP1 staged combustion cycle engines

Nozzle expansion ratio	–	23	33	120	180
Total engine length	m	2.6	3	4.87	6.57
Nozzle exit diameter	m	1.50	1.78	3.4	4.15
Total engine mass	kg	2825	2809	3179	3602
T_{vac}/W	–	79.3	79.8	74.5	66.6

3.5 LOX-LCH4 engines

Several initiatives are currently working on engines with the propellant combination LOX-Methane. Although proposed several times in the past, this “softly cryogenic” blend has only recently in July 2023 been realized in an operational Chinese small launcher: ZQ-2 of LandSpace [36]. On the other end of the spectrum, SpaceX is developing its Super-Heavy & Starship with increasing success.

N.B.: all calculations are carried out for pure Methane as a fuel, which however is costly to produce. Depending on the available blend, LOX-LNG might be acceptable as a substitute with almost similar performance. Sulfur included in the natural gas from some sources needs to be removed before its liquefied state LNG can be used as a rocket fuel. In this case a clear standard definition of composition is required as it has been defined for kerosene as RP1 in the US or RG1 in Russia.

The main combustion chamber mixture ratios of the LOX-LCH4 combination have been selected close to their optimum I_{sp} (indicated by red arrows in Fig. 10), however, slightly shifted towards increased MR to reach increased bulk density. This approach is the same as for all hydrocarbon engines (see previous Sect. 3.4) and different to the one used for LOX-LH2 engines.

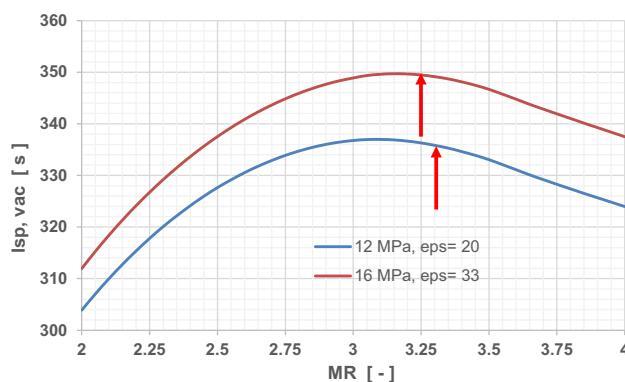


Fig. 10 Influence of LOX/LCH4- mass ratio in main combustion chamber on $I_{sp,vac}$ chamber performance (red arrows indicating selected MCC design points)

The selected MCC-MR of the gas generator engine is 3.3 while MCC-MR in case of the staged combustion thrust-chamber is set to 3.25.

3.5.1 Open gas-generator cycle

The gas generator operates methane-rich and its hot gas powers the single shaft turbine. Major characteristics are derived of the PROMETHEUS-Demonstrator [37] but the baseline assumptions remain similar to all other engines of the system study. The nominal gas generator pressure is selected at 11 MPa. The turbine power-pack data assumptions for the single shaft design have been selected as follows:

- GG combustion temperature 780 K
- turbine efficiency 50%
- turbine pressure ratio 16.5
- LOX pump efficiency 75%
- CH₄ pump efficiency 75%

3.5.1.1 First stage engine performance assessment Based on these assumptions and the 2200 kN vacuum thrust requirement, three reference engines have been calculated with different nozzle expansion ratios (Table 16), all of potential interest for the RLV first stage application.

Another performance calculation has been executed for the smaller engine with expansion ratio 20 by using the cycle analysis tool RPA 2.23. Baseline assumptions are mostly identical to the lrp-calculations but the internal iteration process is different. Inducer efficiencies are assumed at only 70% (no separate value in lrp1.1) while turbine efficiency is raised to 54%. Comparing the two calculation methods shows a difference in I_{sp} performance at vacuum condition of 0.0 s (0.0%) and 0.8 s at sea-level (0.28%).

PROMETHEUS is a European engine under development with potential future application in first and upper stages

Table 16 Performance data of LOX-LCH₄ gas generator cycle engines from lrp1.1 calculation

Nozzle expansion ratio	–	20	30	35
Sea level thrust	kN	1984	1884	1834
Vacuum thrust	kN	2200	2200	2200
Sea level spec. impulse	s	289	281	276
Vacuum spec. impulse	s	320	328	331
Chamber pressure	bar	120	120	120
Total engine mass flow	kg/s	699.4	683.4	677.8
gg mass flow	kg/s	65.8	64.3	63.8
Total engine mixture ratio	–	2.5	2.5	2.5
Chamber mixture ratio	–	3.3	3.3	3.3
Nozzle exit pressure	bar	0.7	0.4	0.34

[37]. The characteristics of the engine with nozzle area ratio 20 are in comparable range as the engine should see similar applications. The similar Chinese TQ-12A [36] is operational and its announced sea-level I_{sp} almost exactly fits the performance of the gas generator engine with smallest nozzle in Table 16 (difference < 0.14%).

3.5.1.2 Upper stage engine derivative Upper stage engines with significantly increased nozzle expansion ratios of 120 and 180 have again been defined using the $\epsilon=20$ design. Calculated engine performances are listed in Table 17. For the same mass flow, vacuum thrust increases by up to 10.2%. Note the gas generator conditions have not been changed for this calculation. A variation might offer the potential of slight improvement.

3.5.1.3 Engine size and mass Geometry and mass data (Table 18) have been estimated using the tool lrp1.1. As all first stage engines are scaled for 2200 kN vacuum thrust, the variant with larger expansion ratio has a slightly reduced mass flow and hence reduced throat diameter. Note their high calculated T_{vac}/W ratios a little above 100, slightly below the LOX-RP1-engines. Note the enormous size of the engine with $\epsilon=180$, reaching a total length of almost 8 m and exit diameter slightly below 5 m. This is another example why such huge size upper stage engines are hardly feasible and in subsequent steps of the study the upper stage engines are restricted to an expansion ratio of 120.

3.5.2 Closed staged-combustion cycle

The staged combustion type is based on an oxidizer-rich preburner design with a single-shaft turbopump. The power-pack conditions have been selected as follows:

- Ox-rich preburner combustion temperature 750 K
- Turbine efficiency 75%
- LOX pump efficiency 79%
- CH₄ pump efficiency 78%

3.5.2.1 First stage engine performance assessment Based on the same 2200 kN vacuum thrust requirement as for LOX-LH₂, two reference engines have been calculated with different nozzle expansion ratios, both of potential interest

Table 17 Performance data of LOX-LCH₄ gas generator cycle upper stage engines from lrp1.1 calculation

Nozzle expansion ratio	–	120	180
Vacuum thrust	kN	2394	2425
Vacuum spec. impulse	s	348	353

Table 18 Geometry and mass data of LOX-LCH₄ gas generator cycle engines

Nozzle expansion ratio	–	20	30	35	120	180
Total engine length	m	2.98	3.49	3.72	6.54	7.89
Nozzle exit diameter	m	1.65	1.99	2.14	4.03	4.94
Total engine mass	kg	2126	2144	2161	2862	3319
T_{vac}/W	–	105	104	103	85.2	74.4

Table 19 Performance data of LOX-LCH₄ staged combustion cycle engines from lrp1.1 and RPA 2.3 calculations

Nozzle expansion ratio	–	23	33
Sea level thrust	kN	2016	1950
Vacuum thrust	kN	2200	2200
Sea level spec. impulse	s	314	308
Vacuum spec. impulse	s	342.5	349
Chamber pressure	bar	160	160
Total engine mass flow	kg/s	654.5	641.9
Engine mixture ratio	–	3.25	3.25
Nozzle exit pressure	bar	0.76	0.47
Power Pack conditions:			
Ox-rich preburner MR	–	58	58
Ox-rich preburner pressure	bar	320	320
Ox-rich preburner massflow	kg/s	509.1	499.3

for the RLV first stage application. Additional cycle performance analyses were run using RPA with overall engine performance found close to the lrp1.1 results. Relative difference in sea-level conditions is less than 0.01% (0.25 s) while in vacuum the relative difference is less than 0.55% (1.9 s). Data presented in Table 19 are a combination of both tools' results.

The best comparison to an existing LOX-LCH₄ staged combustion engine is probably the SpaceX Raptor. Raptor is operating in Full-Flow Staged Combustion-cycle (FFSC) similar to the SLME (see previous Sect. 3.3.2). The Raptor's sea-level or booster stage version has a nozzle expansion ratio of 34.34 close to the ENTRAIN reference engine but with a significantly higher chamber pressure of at least 250 bar and 300 bar in the latest Raptor variant 2 [38]. This explains the vacuum I_{sp} -values coming close while the sea-level I_{sp} of the ENTRAIN-reference being approximately 20 s below calculated Raptor (351.5 s / 328.7 s) [38] due to its relatively low nozzle exit pressure.

3.5.2.2 Upper stage engine derivative Similar to the previous ENTRAIN designs, upper stage engines with sig-

Table 20 Performance data of LOX-LCH₄ staged combustion cycle upper stage engine from lrp1.1 calculation

Nozzle expansion ratio	–	120	180
Vacuum thrust	kN	2323	2353
Vacuum spec. impulse	s	366	371

Table 21 Geometry data of LOX-LCH₄ staged combustion cycle engines

Nozzle expansion ratio	–	23	33	120	180
Total engine length	m	2.58	2.99	5.39	6.52
Nozzle exit diameter	m	1.49	1.77	3.38	4.14
Total engine mass	kg	2925	2908	3350	3673
T_{vac}/W	–	76.6	77.1	70.6	65.2

nificantly increased nozzle expansion ratios have been defined using the $\epsilon = 33$ first stage configuration. Calculated engine performance with nozzle area ratios 180 and 120 are listed in Table 20. For the same mass flow, vacuum thrust increases by up to 7%. Items not listed are identical to the first stage engine.

3.5.2.3 Engine size and mass The geometry and mass data listed in Table 21 have been calculated using the tool lrp1.1. The staged combustion engines are more compact despite the increased expansion ratios in the first stage application due to the higher nominal chamber pressure.

3.6 LOX-LC3H8 engines

The propellant combination of oxygen with propane has not yet been applied in the launcher sector. Characteristic specific impulse data is close to kerosene and methane, almost in the middle between both. Propane is also a “soft” cryogenic fuel, being in gaseous state under ambient conditions. Propane offers a higher bulk density compared to methane and its potential for densification was identified to be higher than that of methane (see Sect. 2.3, Table 3 and reference [39]).

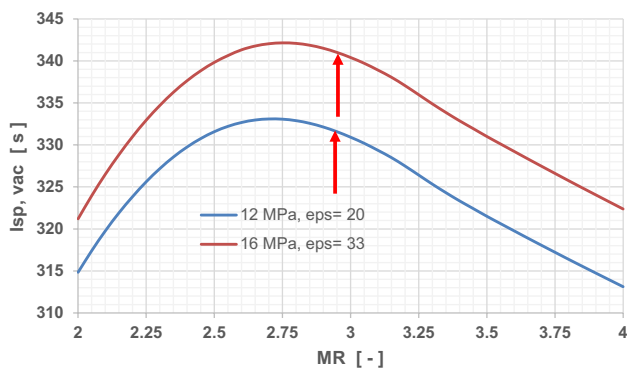


Fig. 11 Influence of LOX/LC3H8- mass ratio in main combustion chamber on $I_{sp,vac}$ chamber performance (red arrows indicating selected MCC design points)

Table 22 Performance data of LOX-LC3H8 gas generator cycle engines from lrp1.1 calculation

Nozzle expansion ratio	–	20	30
Sea level thrust	kN	1984	1884
Vacuum thrust	kN	2200	2200
Sea level spec. impulse	s	284	277
Vacuum spec. impulse	s	315	323
Chamber pressure	bar	120	120
Total engine mass flow	kg/s	710.8	693.8
gg mass flow	kg/s	46.4	45.3
Total engine mixture ratio	–	2.45	2.45
Chamber mixture ratio	–	2.93	2.93
Nozzle exit pressure	bar	0.72	0.42

The process for the selection of operational MR is the same as for the other hydrocarbon engines with MCC-MRs chosen at 2.95 and 2.93 close to their optimum I_{sp} as indicated by red arrows in Fig. 11.

3.6.1 Open gas-generator cycle

The gas generator operates propane-rich and its hot gas powers the single shaft turbopump. Major characteristics remain similar to the baseline assumptions to all other engines of the system study. The nominal gas generator pressure is selected at 11 MPa. The turbine power-pack data assumptions for the single shaft design have been selected as follows:

- GG combustion temperature 780 K
- turbine efficiency 50%
- turbine pressure ratio 16.5
- LOX pump efficiency 75%
- C3H8 pump efficiency 75%

Table 23 Performance data of LOX-LC3H8 gas generator cycle upper stage engine from lrp1.1 calculation

Nozzle expansion ratio	–	120	180
Vacuum thrust	kN	2398	2431
Vacuum spec. impulse	s	344	348

Table 24 Geometry and mass data of LOX-LC3H8 gas generator cycle engines

Nozzle expansion ratio	–	20	30	120	180
Total engine length	m	2.98	3.49	6.54	7.89
Nozzle exit diameter	m	1.64	1.99	4.03	4.93
Total engine mass	kg	2014	2034	2751	3208
T_{vac}/W	–	111.3	110.3	88.8	77.2

3.6.1.1 First stage engine performance assessment Based on these assumptions and the 2200 kN vacuum thrust requirement, two reference engines have been calculated with different nozzle expansion ratios (Table 22), both of potential interest for the RLV first stage application.

Another performance calculation has been executed for the smaller engine with expansion ratio 20 by using the cycle analysis tool RPA 2.32. Baseline assumptions are mostly identical to the lrp-calculations but the internal iteration process is different. Comparing the two calculation methods shows a difference in I_{sp} performance at vacuum condition of 0.54 s (0.18%) and 1.05 s at sea-level (0.37%).

The mini-launcher Spectrum currently under development at Isar Aerospace should use propane as fuel in both of its stages. The Aquila is a gas generator type engine using the LOX-LC3H8 combination and its expansion ratio is around 20. Very little information is available in the public on Aquila and, therefore, no performance comparison can be included here.

3.6.1.2 Upper stage engine derivative Upper stage engines with significantly increased nozzle expansion ratios of 120 and 180 have again been defined using the $\varepsilon=20$ design. Calculated engine performances are found in Table 23. For the same mass flow, vacuum thrust increases by about 10%. Items not listed are identical to the first stage engine. Note the gas generator conditions have not been changed for this calculation. A variation might offer the potential of slight improvement.

3.6.1.3 Engine size and mass Estimated geometry and mass data of the gas generator engines are listed in Table 24. Note also here the enormous size of the engine with expansion ratio of 180 reaching a total length of almost 8 m and exit

diameter slightly below 5 m. Further note the high calculated T_{vac}/W ratios of slightly above 110.

3.6.2 Closed staged-combustion cycle

The staged combustion type is based on an oxidizer-rich preburner design with a single-shaft turbopump.

The power-pack conditions have been selected as follows:

- Ox-rich preburner combustion temperature 750 K
- Turbine efficiency 75%
- LOX pump efficiency 75%
- C3H8 pump efficiency 75%

3.6.2.1 First stage engine performance assessment Based on similar assumptions as for all staged combustion cycles and the 2200 kN vacuum thrust requirement, two reference engines have been calculated with different nozzle expansion ratios (see Table 25), both of potential interest for the RLV first stage application.

Additional cycle performance analyses using RPA are found close to lrp1.1 results with largest deviations again in sea-level conditions. Relative difference is 3.1 s or less than 1.1% while in vacuum the relative difference is less than 0.5% (1.5 s).

No comparison to an existing LOX-LC3H8 staged combustion engine is available because this propellant-cycle combination has not yet been realized.

3.6.2.2 Upper stage engine derivative Upper stage engines with significantly increased nozzle expansion ratios have been defined using the $\varepsilon = 33$ first stage configuration. Calculated engine performance data of nozzle area ratio 180 and 120 are listed in Table 26. For the same mass flow,

Table 25 Performance data of LOX-LC3H8 staged combustion cycle engines from lrp1.1 and RPA 2.3 calculations

Nozzle expansion ratio	–	23	33
Sea level thrust	kN	2023	1952
Vacuum thrust	kN	2200	2200
Sea level spec. impulse	s	308	303
Vacuum spec. impulse	s	335	342
Chamber pressure	bar	160	160
Total engine mass flow	kg/s	668.7	668.7
Engine mixture ratio	–	2.95	2.95
Nozzle exit pressure	bar	0.8	0.5
Power Pack conditions:			
Ox-rich preburner MR	–	≈ 54.2	≈ 54.2
Ox-rich preburner pressure	bar	313.9	313.9
Ox-rich preburner massflow	kg/s	500.388	500.388

Table 26 Performance data of LOX-LC3H8 staged combustion cycle upper stage engine from lrp1.1 calculation

Nozzle expansion ratio	–	120	180
Vacuum thrust	kN	2327	2358
Vacuum spec. impulse	s	362	367

vacuum thrust increases by up to 7.1%. Items not listed are identical to the first stage engine.

3.6.2.3 Engine size and mass Preliminary geometry and mass data (Table 27) have been estimated using the tool lrp1.1 in a way similar as for all other engines. T_{vac}/W is calculated approximately 30% below the gas generator cycle, however, different assumptions in chamber pressure and nozzle expansion ratio. The explanation is mainly found in the more powerful and heavier turbopumps and the two

Table 27 Geometry data of LOX-LC3H8 staged combustion cycle engines from lrp1.1 calculation

Nozzle expansion ratio	–	23	33	120	180
Total engine length	m	2.9	3.25	5.39	6.52
Nozzle exit diameter	m	1.49	1.77	3.37	4.12
Total engine mass	kg	2691	2675	3114	3435
T_{vac}/W	–	83	83.5	76	69.9

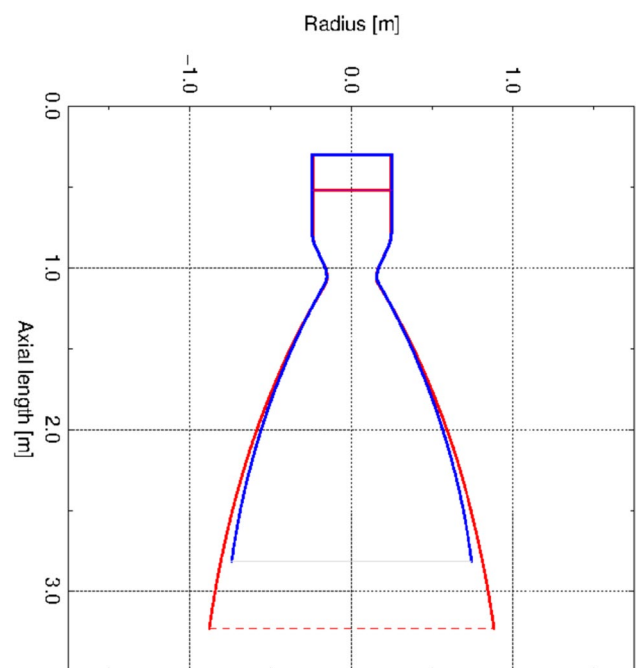


Fig. 12 Internal thrustchamber contours of LOX-LC3H8 staged combustion cycle engine $\varepsilon = 23$ (blue) and 33 (red)

high-pressure preburners. T_{vac}/W of the variant with expansion 33 is slightly above the engine with expansion 23 because of the latter's slightly larger massflow and hence size of major components.

The first stage engine-thrustchambers' internal flow contours as calculated by the DLR tool ncc under the assumption of parabolic nozzles with 80% fractional length are plotted as example of the staged combustion cycles in Fig. 12.

4 Engine data summary and evaluation

4.1 Impact of propellant combinations and cycle

The key performance drivers of chemical rocket engines are the choice of propellant combinations, the engine cycle and the nozzle expansion ratio. This section summarizes and compares data for the four selected fuels in combination with liquid oxygen and present these in a wide range of nozzle supersonic area ratios (15–180). Maximum achievable performances as well as characteristic differences are identified for the reference chamber pressure, mixture ratio and realistic design conditions previously described in Sects. 3.2–3.6.

The general trends of specific impulse of the open gas generator cycle engines with chamber pressure of 12 MPa are shown in Fig. 13 under vacuum and sea-level conditions. The largest nozzle expansion of 180 could provide up to $446 \text{ s } I_{sp}$ in vacuum for LOX-LH2 while hydrocarbon propellants are not exceeding 350 s. Sea-level operation at expansion beyond ratios of 45 risk flow separation inside the nozzle and thus cannot be operated in first stage applications, even at full throttle. Reduced thrust levels with lower chamber pressures, as potentially required for controlled vertical landing of stages, are further restricting the feasible nozzle expansion. In case of the smallest nozzle, the I_{sp} at sea-level might reach up to 370 s for LOX-LH2 and hydrocarbon propellants are approaching a maximum of 290 s when selecting Methane as fuel.

The curves of the propellant combinations shown in Fig. 13 are running almost with constant distances in the displayed nozzle expansion range. The differences in vacuum I_{sp} between LH2 and LCH4 is roughly 90 s (deviation $-3.6 \text{ s}, +6.2 \text{ s}$), between LCH4 and LC3H8 roughly 5 s ($-1 \text{ s}, +0.5 \text{ s}$) and between LCH4 and RP1 about 10 s ($-2 \text{ s}, +0.8 \text{ s}$). It is to be noted that such comparison is influenced by the assumption on the area ratio at which the chemical reactions are set to “frozen”. Although reality is more complicated, the empirically based ratios depending on propellant are held constant for all nozzle sizes which

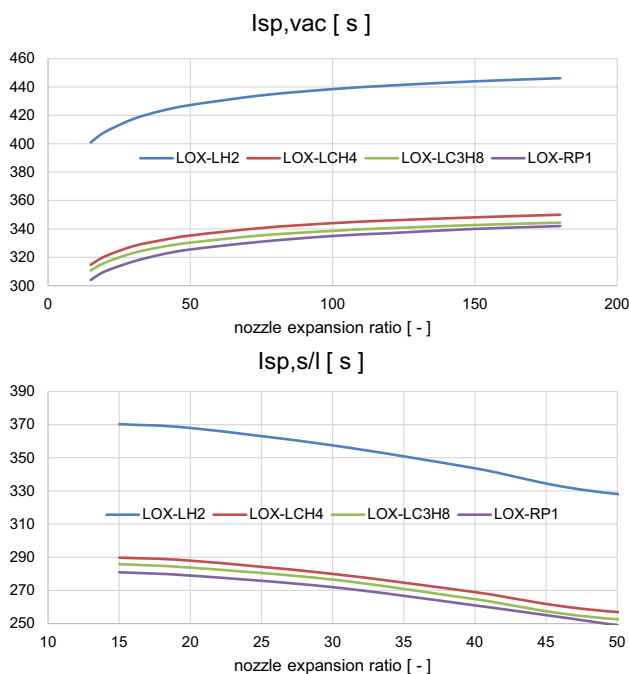


Fig. 13 Calculated specific impulse of open gas-generator cycle rocket engines as function of nozzle expansion ratio

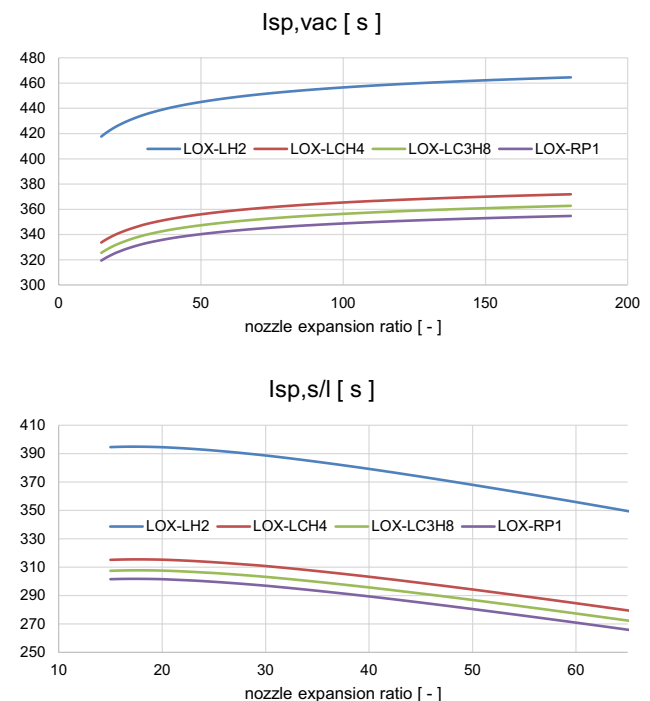


Fig. 14 Calculated specific impulse of staged-combustion cycle rocket engines as function of nozzle expansion ratio

Fig. 15 Calculated thrust-to-weight ratios of selected reference engines for first stage (top) and upper stage application (bottom)

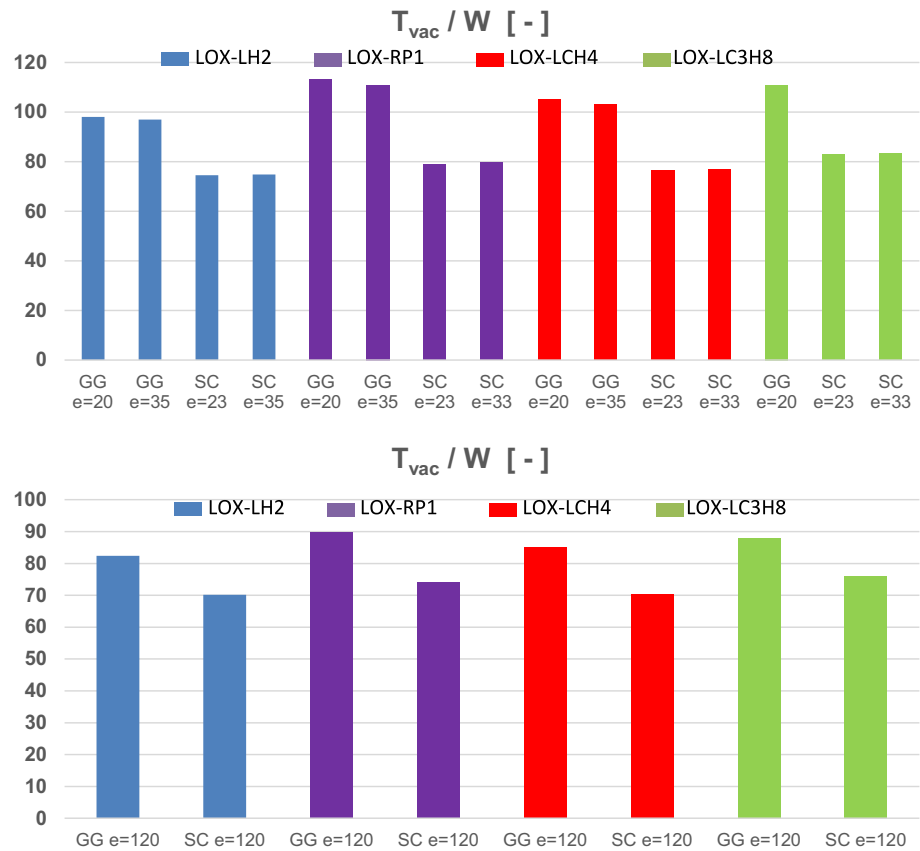


Table 28 Key performance data summary of selected first stage engines

	LOX-LH2 GG $\epsilon=20$	LOX-LH2 GG $\epsilon=35$	LOX-LH2 SC $\epsilon=23$	LOX-LH2 SC $\epsilon=35$	LOX-RP1 GG $\epsilon=20$	LOX-RP1 GG $\epsilon=35$	LOX-RP1 SC $\epsilon=23$	LOX-R1 SC $\epsilon=33$
Engine MR [-]	6	6	6	6	2.25	2.25	2.6	2.6
Sea level I_{sp} [s]	366	351	394	385	279	267	301	294
Vacuum I_{sp} [s]	405.5	418	428	437.8	310	320	327	334
Engine T_{vac}/W [-]	98.1	97	74.6	74.9	113	111	79	79.8
	LOX-LCH4 GG $\epsilon=20$	LOX-LCH4 GG $\epsilon=35$	LOX-LCH4 SC $\epsilon=23$	LOX-LCH4 SC $\epsilon=33$	LOX-LC3H8 GG $\epsilon=20$	LOX-LC3H8 SC $\epsilon=23$	LOX-LC3H8 SC $\epsilon=33$	
Engine MR [-]	2.5	2.5	3.25	3.25	2.45	2.95	2.95	
Sea level I_{sp} [s]	289	276	314	308	284	308	303	
Vacuum I_{sp} [s]	320	331	342.5	349	315	335	342	
Engine T_{vac}/W [-]	105	103	76.5	77	111	83	83.5	

Table 29 Key performance data summary of selected upper stage engines

	LOX-LH2 GG $\epsilon=120$	LOX-LH2 SC $\epsilon=120$	LOX-RP1 GG $\epsilon=120$	LOX-RP1 SC $\epsilon=120$	LOX-LCH4 GG $\epsilon=120$	LOX-LCH4 SC $\epsilon=120$	LOX-LC3H8 GG $\epsilon=120$	LOX-LC3H8 SC $\epsilon=120$
Engine MR [-]	6	6	2.25	2.6	2.5	3.25	2.45	2.95
Vacuum I_{sp} [s]	440.4	458.6	338	353	348	366	344	362
Engine T_{vac}/W [-]	82.4	70.2	89.9	74	85	70.5	88	76

is sufficient for supporting the preliminary launcher sizing approach.

Similar trends derived for the staged combustion cycle with p_c of 16 MPa and the four propellant combinations are shown in Fig. 14. The largest nozzle expansion of 180 could provide up to 464 s I_{sp} in vacuum for LOX-LH2 while hydrocarbon propellants might reach 372 s at best with LOX-LCH4 achieving a slight edge over propane and kerosene. At the low end with nozzle ratio 15 the engines are slightly underexpanding even at sea-level. If not required by geometrical constraints, no rationale is found to choose a nozzle with area ratio below 18 in case of the staged combustion cycle with 16 MPa chamber pressure.

Similar to the gas generator cycle, the curves of the propellant combinations shown in Fig. 14 are running almost with constant distances in the displayed nozzle expansion range. The differences in vacuum I_{sp} between LH2 and LCH4 is roughly 90 s (deviation -6 s, $+2.6$ s), between LCH4 and LC3H8 roughly 8.5 s (with small deviations < 1 s) and between LCH4 and RP1 about 12 s (-1.4 s, $+1.7$ s). Note, the overall tendencies are robust while small deviations are subject to simplified assumptions on the chemical reactions in supersonic flow which should be treated with caution.

The impact of the cycle on performance has been checked assuming the typical chamber pressures of 12 MPa for the gas generator and 16 MPa for the staged combustion engines. The closed cycle brings a gain of 18–22 s in vacuum I_{sp} . The advantage of an increased chamber pressure pays off even more in case of sea-level operations with a specific impulse gain for the staged combustion cycle between 20 s ($\epsilon = 15$) and 40 s ($\epsilon = 45$).

4.2 Engine performance reference data for system analyses

The intended reusable launcher system analyses [2, 3] require the preselection of the most promising engines out of those preliminarily defined in Sects 3.3–3.6. In general, first stage engines projected to be used for vertical landing in VTVL-RLV have a smaller nozzle expansion than those to implemented in VTHL. This choice allows deep-throttling of engines without risking flow-separation in the nozzle to safely perform a vertical landing at roughly stage-T/W around 1.0. Engines to be used in horizontal landing RLV (VTHL) do not face such restrictions and somehow larger nozzle area ratios can be selected driven by optimal launcher ascent flight performance.

Preliminary mass estimation of all engines has been performed on main subcomponent level using empirically derived relationships implemented in DLR's *lrp* program. The launcher designs of [2, 3] scale the engine massflows individually per vehicle that a suitable number of first

stage engines and a single upper stage engine of equivalent flow are defined. Vacuum thrust divided by engine weight is suitable for comparison of the different propellant and cycle options showing clear tendencies. The estimations deliver ambitious weight results compared to actual European heritage to date and the future will tell if such values are supported by actual engine design. On the other hand, announcements by SpaceX or weight targets of PROMETHEUS [37], are even exceeding the calculated values of this study.

The high thrust to weight ratios estimated for all gas generator cycle engines should be noted, reaching from 97 (LOX-LH2) to 113 (LOX-RP) for first stages (Fig. 15). The staged combustion cycle engines are between 25 and 30% below the open cycle due to the significantly raised pressure levels and turbopump power. A ranking comparison of T_{vac}/W between the propellants is slightly correlated with the bulk density. In this mass estimation the difference is less than 15% for similar engine types because the more complex LOX-LH2-engines with increased specific power required by the hydrogen pump and hence mass growth is widely compensated by the reduced massflow needed by this propellant combination for the same thrust level.

In case of the upper stage engines with large expansion nozzle, the differences between the propellants are even less pronounced with maximum difference less than 10%.

All key performance reference data of the first stage engines selected for the RLV system analyses are listed in Table 28. In a similar way the reference data of the upper stage engines are listed in Table 29.

5 Conclusion

Several variations of advanced liquid-propellant rocket engines have been performed to support an RLV-system study with reliable and realistic propulsion data. The three cryogenic propellants hydrogen, methane and propane as well as kerosene (RP1) have been used in combination with LOX as oxidizer. Open gas-generator cycle and closed staged combustion cycle types were defined with relevant chamber pressures and nozzle expansion ratios.

Expendable upper stage engines have been derived from the reusable first stage engines keeping all internal cycle parameters, however, with significantly increased nozzle size for improved performance. With the intention of maximizing I_{sp} , initially, nozzle expansion ratios have been extended up to 180. The extremely large nozzles of the high-thrust engines turn out to be challenging from manufacturing-, weight- and integration perspective. In order to keep realistic assumptions, the expansion ratios have been restricted to 120 losing roughly 5 s of vacuum I_{sp} .

A systematic comparison of the different engines in a large range of nozzle expansion shows the combination LOX-LH2 about 90 s ahead of LOX-LCH4 closely followed by LOX-LC3H8 and LOX-RP1 with the latter having a distance of roughly 10 s to methane. A closed-cycle staged combustion engine brings around 20 s I_{sp} gain in vacuum and up to 40 s in sea-level operations. However, the less performing hydrocarbon- and open-cycle gas-generator engines offer a better thrust-to-weight-ratio than hydrogen and staged combustion. The question which of the characteristics become dominating in future launchers needs to be addressed in multi-disciplinary investigations under consideration of relevant missions.

Therefore, the optimum engine for a future European partially reusable space transportation system cannot be selected solitarily out of engine characteristics. The pre-selected promising engine candidates of this paper are transferred to a system study on different types of partially reusable space transportation vehicles. This multidisciplinary study with sufficiently detailed analyses also on subsystem level should provide a reliable technical basis for the development decisions on the next generation of advanced launch vehicles.

Author contributions MS: performed all calculations, data post processing and analyses, has written almost the complete manuscript, reviewed the complete manuscript several times. reworked the complete manuscript. JW: reviewed the complete manuscript, contributed to the manuscript by research on state-of-the-art in similar propulsion analyses and contributed section on near triple point propellant characteristics and interest. checked the reworked manuscript.

Funding Open Access funding enabled and organized by Projekt DEAL.

Data availability No datasets were generated or analysed during the current study.

Declarations

Conflict of Interest The authors declare no competing interests.

Open Access This article is licensed under a Creative Commons Attribution 4.0 International License, which permits use, sharing, adaptation, distribution and reproduction in any medium or format, as long as you give appropriate credit to the original author(s) and the source, provide a link to the Creative Commons licence, and indicate if changes were made. The images or other third party material in this article are included in the article's Creative Commons licence, unless indicated otherwise in a credit line to the material. If material is not included in the article's Creative Commons licence and your intended use is not permitted by statutory regulation or exceeds the permitted use, you will need to obtain permission directly from the copyright holder. To view a copy of this licence, visit <http://creativecommons.org/licenses/by/4.0/>.

References

1. Dietlein, I., Bussler, L., Stappert, S., Wilken, J., Sippel, M.: Overview of system study on recovery methods for reusable first stages of future European launchers. CEAS Space J. (2024). <https://doi.org/10.1007/s12567-024-00557-9>
2. Wilken, J., Stappert, S.: Comparative analysis of european vertical-landing reusable first stage concepts. CEAS Space J. (2024). <https://doi.org/10.1007/s12567-024-00549-9>
3. Bussler, L., Sippel, M., Dietlein, I., Wilken, J., Stappert, S.: Comparative analyses of European horizontal-landing reusable first stage concepts. Submitted to CEAS Space Journal (2024)
4. Stappert, S., Dietlein, I., Wilken, J., Bussler, L., Sippel, M.: Options for future european reusable booster stages: evaluation and comparison of VTHL and VTVL return methods. Submitted to CEAS Space Journal (2024)
5. Sutton, G.P., Biblarz, O.: Rocket Propulsion Elements. John Wiley & Sons, Hoboken (2016)
6. Castellini, F.: Multidisciplinary Design Optimization for Expendable Launch Vehicles, Ph.D. Thesis. Polytechnic University of Milan, Milan (2012)
7. Burkhardt, H., Sippel, M., Herbertz, A., Klevanski, J.: Comparative Study of Kerosene and Methane Propellant Engines for Reusable Liquid Booster Stages, 4th International Conference on Launcher Technology Space Launcher Liquid Propulsion, Liege (Belgium) (2002)
8. Burkhardt, H., Sippel, M., Herbertz, A., Klevanski, J.: Kerosene vs methane: a propellant tradeoff for reusable liquid booster stages. J. Spacecr. Rockets (2004). <https://doi.org/10.2514/1.2672>
9. Preclik, D., Hagemann, G., Knab, O., Brummer, L., Mäding, C., Wiedmann, D., Vuillermoz, P.: LOX/Hydrocarbon Propellant Trade Considerations for Future Reusable Liquid Booster Engines, AIAA 2005–3567, 41st AIAA/ASME/SAE/ASEE Joint Propulsion Conference & Exhibit, Tucson, Arizona (2005)
10. Burkhardt, H., Herbertz, A., Sippel, M., Woschnak, A., Riccius, J.: Evaluation of green propellants for space applications, WP 2200: propulsion requirements, DLR-IB 647–2, SART TN-003/2004 (2004), Available at <https://elib.dlr.de/1716/1/SART-TN3-2004.pdf>
11. Li, X., Ma, X., Zhang, J., et al.: Review of hydrogen embrittlement in metals: hydrogen diffusion, hydrogen characterization, hydrogen embrittlement mechanism and prevention. Acta Metall. Sin. **33**, 759–773 (2020). <https://doi.org/10.1007/s40195-020-01039-7>
12. NN: NIST Chemistry WebBook, SRD 69, <https://webbook.nist.gov/chemistry/fluid/>. <https://doi.org/10.18434/T4D303>
13. Maeda, T., Onga, T., Tamura, T., Negoro, N., Okita, K., Kobayashi, T., Kawashima, H.: Firing Tests of LE-9 Development Engine for H3 launch vehicle, IAC-19-C4.1.4, 70th International Astronautical Congress (IAC), Washington D.C., United States, 21–25 October 2019
14. Sippel, M., Herbertz, A., Haeseler, D., Götz, A.: Feasibility of High Thrust Bleed Cycle Engines for Reusable Booster Applications; 4th International Conference on Launcher Technology & Space Launcher Liquid Propulsion, Liege (2002)
15. Sippel, M., Herbertz, A., Manfletti, Ch., Burkhardt, H., Imoto, T., Haeseler, D., Götz, A.: Studies on Expander Bleed Cycle Engines for Launchers, AIAA 2003–4597, 39th AIAA/ASME/SAE/ASEE Joint Propulsion Conference and Exhibit, Huntsville, Alabama (2003)
16. Zeleznik, F.J., Gordon, S.: A general IBM 704 or 7090 computer program for computation of chemical equilibrium compositions, rocket performance, and Chapman-Jouguet detonations. NASA TN D-1454 (1962)

17. Gordon, S., McBride, B.J.: Computer program for calculation of complex chemical equilibrium compositions, rocket performance, incident and reflected shocks, and Chapman-Jouguet detonations, NASA SP-273, 1971, Interim Revision (1976)
18. Gordon, S., McBride, B.J.: Computer program for calculation of complex chemical equilibrium compositions and applications I. Analysis. NASA-RP-1311 (1994)
19. Gordon, S., McBride, B.J.: Computer program for calculation of complex chemical equilibrium compositions and applications II. User's manual and program description. NASA RP-1311-P2 (1996)
20. Ponomarenko, A.: RPA - Tool for rocket propulsion analysis, C++ Implementation (2010)
21. Ponomarenko, A.: RPA: tool for rocket propulsion analysis, assessment of delivered performance of thrust chamber, (v.1). https://www.rocket-propulsion.com/downloads/pub/RPA_AssessmentOfDeliveredPerformance.pdf (2013). Accessed March 2013
22. Gangami, F., Sippel, M., Dumont, E.: Statistical analysis and classification of rocket motor efficiency, thrust to mass ratio and structural index, internal report SART TN-007/2009
23. Ponomarenko, A.: RPA - Tool for Rocket Propulsion Analysis, Space Propulsion 2014. Cologne, Germany (2014)
24. Ponomarenko, A.: RPA: Tool for Rocket Propulsion Analysis, Thermal Analysis of Thrust Chambers. https://www.rocket-propulsion.com/downloads/pub/RPA_ThermalAnalysis.pdf (2012). Accessed July 2012
25. Nickerson, G. R., Dang, L. D., Coats, D. E.: Engineering and programming manual: two-dimensional kinetic reference computer program (TDK), NASA-CR-178628 (1985)
26. RS-68, <https://en.wikipedia.org/w/index.php?title=RS-68&oldid=838191803> (2018). Accessed May 20, 2018
27. Sippel, M., Yamashiro, R., Cremaschi, F.: Staged combustion cycle rocket engine design trade-offs for future advanced passenger transport, ST28-5, Space Propulsion 2012, Bordeaux (2012)
28. Yamashiro, R., Sippel, M.: Preliminary design study of staged combustion cycle rocket engine for spaceliner high-speed passenger transportation concept, IAC-12-C4.1.11, Naples (2012)
29. Sippel, M., Schwanekamp, T., Ortelt, M.: Staged Combustion Cycle Rocket Engine Subsystem Definition for Future Advanced Passenger Transport, Space Propulsion 2014. Cologne, Germany (2014)
30. Sippel, M., Wilken J.: Preliminary Component Definition of Reusable Staged-Combustion Rocket Engine, Space Propulsion 2018 conference, Seville (2018)
31. Sippel, M., Stappert, S., Pastrikakis, V., Barannik, V., Maksiuta, D., Moroz, L.: Systematic Studies on Reusable Staged-Combustion Rocket Engine SLME for European Applications, Space Propulsion 2022. Estoril, Portugal (2022)
32. Jeaugey, I., Montheillet, J., Reichstadt, S., Ghouali, A., Dantu, G.: System engineering presentation of the european staged combustion demonstrator score-D, Space Propulsion 2012, Bordeaux (2012)
33. NN: Space shuttle main engine orientation, Boeing Rocketdyne propulsion & power, space transportation system training data (1998)
34. Deeken, J., Herbertz, A.: Vergleich von Expanderzyklusvarianten und Turbomaschinenanordnungen in Raketentriebwerken unter Verwendung des Zyklusanalyseprogramms LRP, DLR-IB 647-2004 /07, SART TN-013/2004, internal report in German (2004)
35. RD-120, <https://en.wikipedia.org/wiki/RD-120> (2020). Accessed May 22, 2020
36. LandSpace: creator of commercial space transportation systems, fact sheet, undated (2023)
37. P. Simontacchi: Prometheus: precursor of new low-cost rocket Engine Family, Space Propulsion 2018 conference, Seville (2018)
38. Wilken, J.; et al: Critical Analysis of SpaceX's Next Generation Space Transportation System: Starship and Super Heavy, 2nd HiSST: International Conference on High-Speed Vehicle Science Technology, Bruges (2022)
39. Wilken, J., Scelzo, M., Peveroni, L.: System Study of Slush Propellants for Future European Launch Vehicles, Space Propulsion 2018 conference, Seville (2018)

Publisher's Note Springer Nature remains neutral with regard to jurisdictional claims in published maps and institutional affiliations.



Options for future European reusable booster stages: evaluation and comparison of VTHL and VTVL return methods

Sven Stappert¹ · Ingrid Dietlein¹ · Jascha Wilken¹ · Leonid Bussler¹ · Martin Sippel¹

Received: 20 February 2024 / Revised: 30 August 2024 / Accepted: 7 October 2024 / Published online: 4 November 2024
 © The Author(s) 2024

Abstract

In the past, the majority of system studies on reusable space transportation performed within Europe focused on concepts relying on lift-generating wings for recovery. Recently, vertically landing concepts similar to those deployed successfully by SpaceX have moved to the center of technical attention. Both recovery and landing strategies have their pros and cons and it is not obvious what would be a sound choice for Europe. Therefore, the German Aerospace Center DLR initiated a parametric system study, named ENTRAIN, that evaluates the impact of different return options on the launcher design on a technical level: the vertical take-off, vertical landing method (VTVL) as used by SpaceX compared to the vertical take-off, horizontal landing (VTHL) method as used for the Space Shuttle. Within this study, launchers were designed using different propellant combinations, staging velocities and engine cycles. The designed launchers are evaluated in this paper regarding performance, technical difficulties, operational aspects, size, mass and complexity.

Keywords ENTRAIN · VTVL · VTHL · Reusability · RLV · Space Transportation

List of symbols

α	Angle of attack [°]
c_e	Effective exhaust velocity [m/s]
Δv	Velocity increment [m/s]
F_D	Aerodynamic drag force [N]
F_T	Thrust force [N]
g_0	Earth gravitational acceleration constant [m/s ²]
γ	Flight path angle [°]
I_{sp}	Specific impulse [s]
μ	Earth standard gravitational parameter [m ³ /s ²]
Π	Payload fraction [–]
r	Radius [m]
R	Ratio between inert mass to final mass [–]
t	Time [s]
m	Mass [kg]

Abbreviations

CSG	Centre spatial Guyanais
DLR	Deutsches Zentrum für Luft- und Raumfahrt

DRL	Downrange landing
ELA	Ensemble de lancement Ariane
ELV	Expendable launch vehicle
ENTRAIN	European next reusable Ariane
EU	European union
FALCon	Formation flight for in-air launcher 1st stage capturing demonstration
FB	Fly-back
GG	Gas generator
GLOM	Gross lift-off mass
GTO	Geostationary transfer orbit
HL	Horizontal landing
IAC	In-air capturing
IMR	Inert mass ratio
LC3H8	Liquid propane
LCH4	Liquid methane
LEO	Low Earth orbit
LH2	Liquid hydrogen
LOX	Liquid oxygen
MECO	Main engine cutoff
RLV	Reusable launch vehicle
RP1	Rocket propellant-1 (kerosene)
RTLS	Return-to-launch-site
SC	Staged combustion
SI	Structural index
STS	Space transportation system
TPS	Thermal protection system

✉ Ingrid Dietlein
ingrid.dietlein@dlr.de

¹ Space Launcher System Analysis (SART), Institute of Space Systems, Deutsches Zentrum für Luft- und Raumfahrt, Bremen, Germany

TSTO	Two stage to orbit
T/W	Thrust-to-weight ratio
US	United States
VL	Vertical landing
VTHL	Vertical take-off, horizontal landing
VTVL	Vertical take-off, vertical landing
X-TRAS	Expertise Raumtransport

1 Introduction

Reusability in space travel has already been a topic since the earliest spacefaring years in the twentieth century. The idea of recovering and reusing launch systems or particular stages was however not turned into reality until the Space Shuttle or Space Transportation System (STS) was first launched in 1981, see right side of Fig. 1. The Space Shuttle orbiter returned from space and landed horizontally on a runway using wings to create sufficient lift for deceleration and maneuvering. However, the Space Shuttle program turned out to be not as economically successful as hoped. In contrast, launch costs were even higher compared to an expendable launch vehicles (ELV), which, however, can partially be attributed to the fact that the Space Shuttle was a crewed system with a reusable orbital stage. A very similar approach was adopted by the Soviet Union with their Buran system which was at least partially derived from the US Space Shuttle but which never saw operations.

After the retirement of the Space Shuttle, space transportation relied exclusively on expendable systems. Numerous studies and concepts for reusable launch systems were performed by various actors but none of them were realized. A short overview of major European studies on RLV can be found in [1].

It took several years until a new reusable launch vehicle (RLV) became operational in the twenty-first century. The successes of SpaceX (with Falcon 9 and Falcon Heavy, see left side of Fig. 1) and Blue Origin (New Shepard) in landing, recovering and reusing their respective booster stages by means of retro-propulsion have shown

the possibility of developing, producing and operating launchers with reusable first stages at low launch service costs. This has raised the interest to investigate the impact of developing reusable launchers in Europe as a way to lower the launch costs and stay competitive in the evolving launch market.

Reusability for launch systems can be achieved through a broad range of different approaches, each offering unique advantages, but also technical challenges. Understanding and evaluating the impact of those different recovery and reuse methods on a technological, operational and economic level is of essential importance to choose a technology that is adaptable to a European launch system.

The study ENTRAIN (European Next Reusable Ariane) was conducted within the X-TRAS project of DLR [1] to assess the potential of reusable booster stages in future European launchers. During this study, the impact of different recovery and reusability options on system level was investigated. It focuses solely on first-stage recovery since recovery and reuse of orbital stages is generally more difficult and technically challenging due to the high energy state of an orbital stage.

Additionally, an upper stage is usually smaller than the first stage and so is the recovered hardware. As such, the value of the recovered hardware is higher for a first than for an upper stage. So, consequently, mastering first stage recovery is recommended as the first step before facing orbital stage recovery. In addition, all investigated vehicles are vertical takeoff launchers as no launch vehicle with horizontal take-off is yet operational and for which the development of additional technologies such as take-off compatible gear and wings would be required.

The results of the ENTRAIN study are presented in a series of papers, [1, 4–7], including this one, each with a specific focus. Whereas [1] provides an overview of the study, the context of the study and its motivation, [4] will give details on the choice and design of the propulsion systems used for the launchers while [5, 6] will focus on the design of the VTVL and VTHL launch system with details on the selected design process and assumptions

Fig. 1 Two prominent reusable launch stages: the Falcon heavy side boosters landing vertically, [2], and the Space Shuttle orbiter during the final approach landing horizontally, [3]



Copyright: NASA

used for the design itself. A cost assessment was performed as well of which the results can be consulted in [7].

The mission requirements were identical for all launchers (refer to section 2 for details) to allow maximum comparability as far as possible. In addition, further design choices such as the propellant combination, the rocket engine cycle, the staging velocity and the engine cycle were also subject to parametric change. Following this study and design logic, a broad range of launchers with reusable first stages were designed. In this paper, a comparison of vertical take-off vertical landing (VTVL) versus vertical take-off horizontal landing (VTHL) with respect to certain evaluation parameters is performed to firstly identify the impact of the design choices on a system level (mass, performance, re-entry loads, etc.) and thus, secondly, select and identify superior design choices most suitable for a potential reusable launch vehicle.

It shall be noted that in this paper, the focus was set on comparing results from the design process without the intention of pre-selecting one concept over the other. Other aspects such as reliability, complexity or operational costs have not been part of the comparison in this paper. An evaluation based on an extended set of criteria such as reliability, launch costs etc. is presented in [1].

2 RLV design and comparison methods

Two different recovery and landing options were considered in the ENTRAIN study which are summed up in Fig. 2: VTVL and VTHL, further subdivided into two landing methods each.

VTVL always features propulsive maneuvers by reigniting the rocket engines in flight and, thus, re-ignitable and throttleable engines would need to be developed. Two different landing options were examined for VTVL: Return-to-launch-site (RTLS) and downrange landing (DRL). For a launch from Kourou, RTLS stages also land back in Kourou whereas for a downrange landing the landing site is assumed in the Atlantic Ocean, thus requiring a seagoing barge. In general, RTLS requires three propulsive maneuvers, a boost-back burn to revert the horizontal velocity, an optional re-entry burn to limit re-entry loads and the final landing burn whereas DRL requires only two burns, the re-entry burn and the landing burn. These two landing options for VTVL recovery are schematically depicted in Fig. 3.

It shall be pointed out that during the course of the study the investigation of the RTLS return option was discontinued as its performance proved disappointing under the selected study requirements (see [1, 5]).

For horizontally landing systems, two recovery options were considered: In-air-capturing (IAC) or Fly-back (FB), see Fig. 4. The former is a DLR-patented technology [8]

Fig. 2 Return options considered in the ENTRAIN study (return-to-launch-site later abandoned due to low performance within selected study requirements)

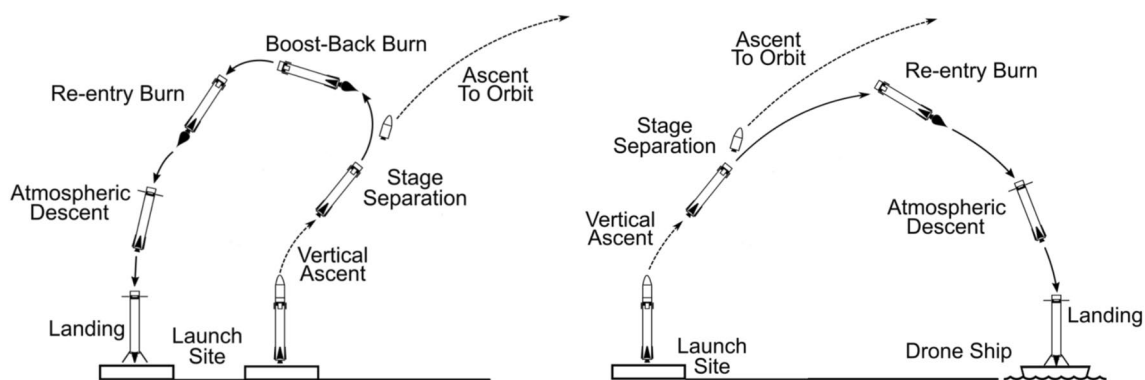
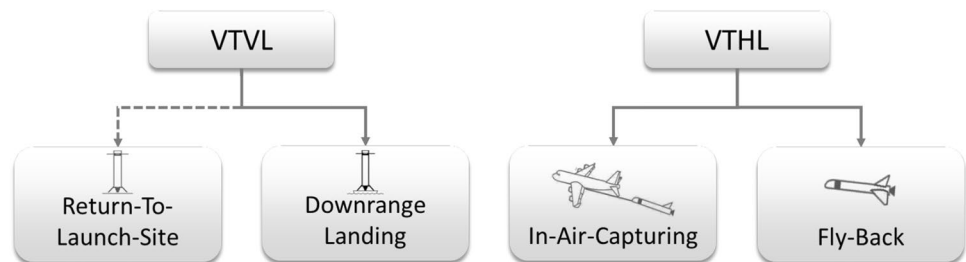


Fig. 3 Return strategies for VTVL: return to launch site (left) and downrange landing (right)

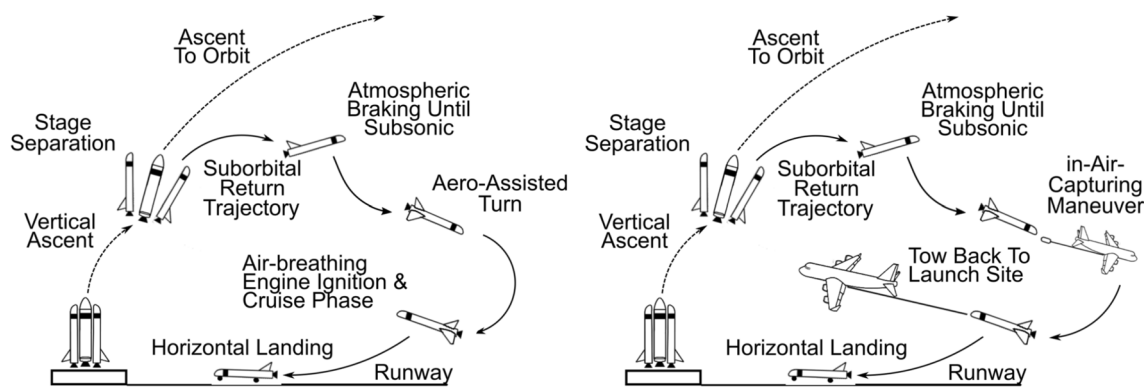


Fig. 4 Return strategies for VTHL: fly-back (left) and in-air capturing (right)

which has been under investigation in the EU Horizon 2020-funded project FALCon [9]. This approach is based on the idea to have a towing aircraft loitering in the designated area while the winged RLV stage transitions to subsonic, steady glide and starts descending on a constant flight path angle. The towing aircraft, equipped with a capturing device attached to a rope, matches speed and flight path angle to allow for the RLV stage to dock to the capturing device. Then, the RLV stage can be pulled back to any landing site where it detaches and lands autonomously. This method offers the advantage that no additional propellant or propulsion hardware is necessary for the first stage. Further details on this technology can be found in [9, 10]. The aerodynamic shapes of the winged stages have been pre-designed to ensure maneuverability and controllability throughout the entire velocity range from hypersonic to subsonic flight regimes [6].

Fly-back methods are based on the idea to equip the returning RLV stage with airbreathing turbo-engines that are ignited once the vehicle is at subsonic velocity. Thus, the stage can return autonomously to its landing site at the expense of additional propulsion hardware and propellant mass.

The presented study focused on recovery methods deployed on operational or prototype launchers (like on launchers of SpaceX, Space Shuttle or Buran) or the in-Air capturing method, a technology invented and developed in-house. These methods are well suited for large launch

systems such as those considered here. There are of course more recovery methods that are investigated or developed around the world. In [11], several recovery methods were investigated for large launch vehicles as well with a special focus on costs. Other recovery methods used such as parafoil deployment for the MIURA 1 rocket, [12], are more suitable for small or suborbital vehicles.

All RLVs were subject to the same high-level mission requirements shown in Table 1.

A thrust-to-weight ratio (T/W) of 1.4 at lift-off was targeted. This value was estimated, based on past experience, to be a sound compromise between launcher performance and implemented total thrust while fixing this value which accelerated the design process considerably.

After separation from the first stage, the upper stage accelerates until reaching an intermediate orbit (Low Earth Orbit or LEO transfer orbit) with a perigee altitude between 140 and 150 km and an apogee altitude of about 290 m to 330 km depending on the variant. These transfer orbits with an optimized argument of perigee allow reaching an altitude of 250 km at a latitude of zero degree where the GTO insertion boost is to be performed. Upon reaching the perigee altitude of the desired GTO when the position coincides with the equator the upper stage performs a second boost maneuver inserting itself and the payload into the desired GTO with the appropriate argument of perigee of 180° . Figure 5 provides a schematic depiction of this insertion strategy not reflecting the true relative dimensions of the orbits and Earth

Table 1 Design requirements for the RLV design process

Payload	7500 kg \pm 150 kg
Orbit	GTO (250 km \times 35,786 km \times 6°) via an intermediate transfer orbit
Launch site	CSG Kourou
Architecture	Two stage to orbit (TSTO) configuration in serial configuration with common bulkhead tanks on both stages, common diameter for first and second stage
Engines	Same engines in both stages but different nozzle expansion ratios

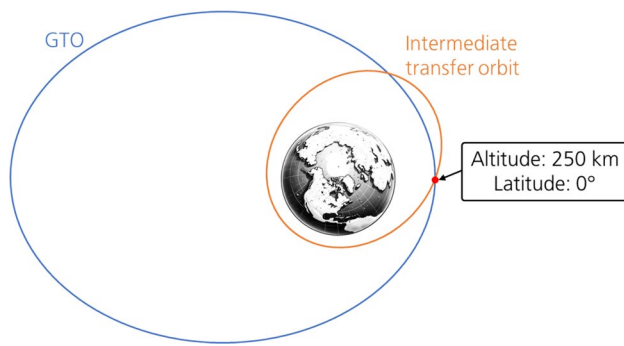


Fig. 5 Schematic presentation of the ENTRAIN insertion strategy

Table 2 Design matrix of ENTRAIN study with nomenclature abbreviations

Design parameter	Description	Nomenclature
Return method	VTVL downrange landing	VL DRL
	VTVL return-to-launch-site	VL RTLS
	VTHL in-air-capturing	HL IAC
	VTHL fly-back	HL FB
Propellant	LOX/LH2	H
	LOX/LCH4	C
	LOX/LC3H8	C3H8
	LOX/RP1	RP1
	1st stage: LOX/LCH4, 2nd stage: LOX/LH2	Hybrid
Engine cycles	Staged combustion (SC)	SC
	Gas generator (GG)	GG
Upper stage Δv	6.6 km/s (Mach 10–12)	Hi
	7.0 km/s (Mach 8.5–9.5)	Med
	7.6 km/s (Mach 6.0–7.5)	Lo

and the fact that both the intermediate transfer orbit and GTO are not sharing the same orbital plane.

Additionally, to the return method, further design parameters were subject to variation, thus rendering a vast combination of modelled and investigated RLV stages. The overall design matrix of all combinations of this study is shown in Table 2.

At this point the use of upper stage (propulsive) velocity increment (Δv) as a design parameter defining the staging

point between the first and second stage shall be explained. A larger upper stage Δv reduces the Δv requirement for the first stage leading to smaller first stages. This effect is not entirely linear as a larger upper stage represents a heavier weight for the first stage to accelerate. Due to losses such as gravity losses suffered during ascent it is a parameter where an optimum is expected to exist and hence the staging “point” (the upper stage Δv) is one of the major key design parameters. To simplify the calculation process such a detailed optimization shall however not be attempted within this study phase. Instead, three staging points that are three different upper stage Δv values are set with the expectation that the staging optimum will be within the range set by these three points or at least close to its borders. Consequently, this upper stage Δv corresponds to a Δv of the first stage that varies depending on the investigated variant. Depending on trajectory optimization, losses encountered during ascent etc. the separation will occur at different altitudes and velocities even for identical first stage Δv . Consequently, the Mach number at which the separation occurs may vary within a certain range. Table 2 indicates the Mach number range as obtained by trajectory optimization for the investigated variants. It shall be noted that the propulsive Δv in the nomenclature as presented within this paper does not include any losses which however were considered during trajectory optimization and therefore included in the overall performance and design of each variant.

Table 3 provides an overview of the investigated variants within the study.

For each investigated concept and the selected staging points the stages were sized in an iterative approach. The respective design procedures and processes are described for VTVL systems in [5] and for VTHL systems in [6].

For the relevant system design, the dedicated modelling of the rocket engines is of outstanding importance to achieve reliable performance data. Therefore, the definition of reference propulsion systems and related validation are described in [4].

2.1 Nomenclature of launcher configurations

The vast range of launchers considered within this study requires a nomenclature that facilitates distinguishing the vehicles with respect to the design space parameters. This

Table 3 Investigated variants

Return strategy		LOX/LH2		LOX/LCH4		LOX/RP1		LOX/LC3H8	
		GG	SC	GG	SC	GG	SC	GG	SC
VL	RTLS	●	●	●	●	●	●	–	–
	DRL	●	●	●	●	●	–	●	–
HL	FB	●	●	●	●	●	●	–	–
	IAC	●	●	●	●	●	●	●	–

nomenclature is shown in Table 2. Mainly, the return methods and engine cycles are plainly abbreviated whereas for propellants a substitute letter for each propellant combination is chosen. Each stage's propellant loading is indicated by this letter followed by a number representing the propellant loading in metric tons. Last, the separation velocity is indicated by either a "Hi" for high, "Med" for medium and "Lo" for low first stage separation velocity.

As an example, a launcher featuring vertical landing with downrange landing, LOX/LH2 in both stages, gas generator engines and an upper stage Δv of 7.0 km/s corresponding to a separation Mach number between 8.5 and 9.5 would be dubbed: *VL DRL H GG Med*.

2.2 Metrics for comparing VTHL and VTVL launchers

This section describes metrics used for comparison of the investigated systems.

2.2.1 GLOM, dry mass and payload fraction

The gross lift-off mass (GLOM) is used as an indicator of the overall performance of the system. Since all launchers are designed for the same reference payload to Geosynchronous Transfer Orbit (GTO), the heavier the system, the lower the payload fraction. This ratio is defined as the ratio between payload mass and GLOM as follows:

Payload Fraction

$$\Pi = \frac{m_{\text{payload}}}{m_{\text{GLOM}}} \quad (1)$$

In addition, it is important to note that the costs of launch vehicles scale mainly with dry mass.

2.2.2 Structural index and inert mass ratio

Structural Index (SI) and Inert Mass Ratio (IMR) are two performance parameters that are always aimed to be minimized in launcher design. According to the rocket equation, stages with low structural index, defined as the ratio between the stages dry mass to the stage propellant mass, are more efficient. These performance parameters are defined as

$$SI = \frac{m_{\text{dry}}}{m_{\text{propellant}}} \quad (2)$$

and

$$IMR = \frac{m_{\text{inert}}}{m_{\text{GLOM, stage}}} = \frac{m_{\text{GLOM, stage}} - m_{\text{prop, ascent}}}{m_{\text{GLOM, stage}}} \quad (3)$$

Here, the inert mass is defined as any mass of the stage that does not contribute to the acceleration of the payload. For a VTVL system, any propellant that is required for re-entry maneuvers is accounted as inert mass. The inert mass ratio is a direct indicator of performance since it is linked to the Tsiolkovsky rocket equation (here expressed for the first stage):

$$\Delta v_{\text{stage 1}} = g_0 I_{\text{sp}} \ln \frac{m_{\text{GLOM, stage 1}} + m_{\text{GLOM, stage 2}}}{m_{\text{inert, stage 1}} + m_{\text{GLOM, stage 2}}} \sim \ln \frac{1}{IMR1} \quad (4)$$

As Eq. (4) shows, a lower inert mass ratio increases the achievable Δv of the stage, or in the case of predefined Δv , reduces the required mass ratio.

2.2.3 Re-entry loads

The major difference between the return trajectory of an RLV to an ELV stage is obvious: whereas the latter is dispensed and the re-entry has no influence on the mission whatsoever (disregarding the application of a safety constraint on the impact point of the non-orbital stage), an RLV stage has to re-enter in a controlled manner to keep the loads low and to allow a controlled landing at a dedicated landing site. Hence, the separation and re-entry parameters have a significant influence on the re-entry loads experienced.

Loads experienced during ascent and re-entry such as dynamic pressure, heat flux and load factor are to be addressed by imposing constraints on the trajectory and by the design, e. g. by adding a suitable thermal protection system (TPS) and to set up adequate refurbishment and maintenance operations after recovery. While imposing constraints on the trajectory leads to lower loads and thus limits the need for specific design adaptations it usually costs launcher performance that might require a scaling up of the design to meet performance targets. At the same time not imposing trajectory constraints may lead to higher system complexity, higher system mass and increased refurbishment effort.

It is clear that these loads, specifically the heat flux, load factor and dynamic pressure are important metrics of comparison. Considering that the re-entry loads are particularly relevant for RLV vehicles this section will focus on a comparison of the investigated variants with respect to these re-entry loads.

For the present study following trajectory constraints were imposed for the descent:

For VTVL

- The dynamic pressure has to be smaller than 200 kPa,
- The lateral acceleration is to be lower than 3 g, and
- The heat flux rate calculated according to the Fay-Riddell equation using a uniform nose radius of 0.5 m shall not exceed 200 kW/m². The decision to base the heat flux

rate on an identical nose radius irrespective of the geometry was motivated by enabling the use of the heat flux rate as a comparative value that allows sorting the VTHL concepts with respect to the experienced heat load.

For VTHL

- Maximum lateral load factor is set to 4 g, whereas
- No specific constraint on dynamic pressure or heat flux were imposed during descent. These loads were however considered during the design process.

The different approach with respect to constraints for VTHL and VTHL is owed to the different design processes for both types of vehicles. The wings for the RLV stage of the VTHL launchers were sized, amongst others, to limit re-entry loads to acceptable levels while the thermal protection system (TPS) was dimensioned such that the temperature on the metal surface remains within acceptable limits.

The angle of attack during re-entry is adapted such that the lateral load factor n_z respects the imposed limit of 4 g. This, simultaneously, has a limiting effect on dynamic pressure and heat flux since the load factor, intimately linked to the aerodynamic force, is a function of dynamic pressure while the stagnation heat flux rate depends on the same parameters (density, velocity) as the dynamic pressure.

For VTHL the imposed constraints shall ensure that only a light TPS cover is needed for the rear part of the launcher which further benefits from the fact that due to the active control of the re-entry burn the management of re-entry loads is more straightforward than for aerodynamically controlled vehicles. Further details can be found in [5, 6].

3 Launcher data comparison

In this paragraph, the ENTRAIN RLV systems resulting from the convergent design process are compared to each other with respect to the parameters mentioned in the previous section.

3.1 Layout and size

A selection of the conceptual RLVs of the ENTRAIN study is shown in Fig. 6. For the launchers shown in this picture the Δv of the second stage is identical (~ 7 km/s) for all designs. Generally, the launchers are larger compared to the Ariane 5 or Falcon 9. The differences to the Falcon 9 can be explained by the higher target GTO performance as RLV (7.5 tons) whereas the difference between Ariane 5 is explained by the variation in architecture as “2 1/2-stage” (central stage with side boosters) expendable vehicle and the high density of solid propellants in the side-mounted EAP-boosters.

On a general basis, while the VTHL variants are equipped with landing legs and aerodynamic control devices such as grid fins (both depicted in folded position) on the first stage, the VTHL have each a delta wing, dual fins and a landing gear not shown here.

As can be seen, the diameter of the VTHL are generally larger than the VTHL. These configurations require considerable amounts of fuel to perform the boosts during re-entry hence an increased need for storage volume compared to VTHL that uses its wings for deceleration. The diameter for VTHL has been set such that the length-to-diameter ratio was about 15. Used diameters for VTHL range from 5.0 to 6.1 m, for VTHL from 5.0 to 6.0 m. No specific requirements on the ratio of length to diameter were imposed on the VTHL design to ease the achievement of static trim during the aerodynamic layout. Obtained length-to-diameter ratios range from 7.5 to 9.2 for the VTHL variants.

Fig. 6 Geometry and layout of selected RLV of the ENTRAIN study compared to Falcon 9 and Ariane 5

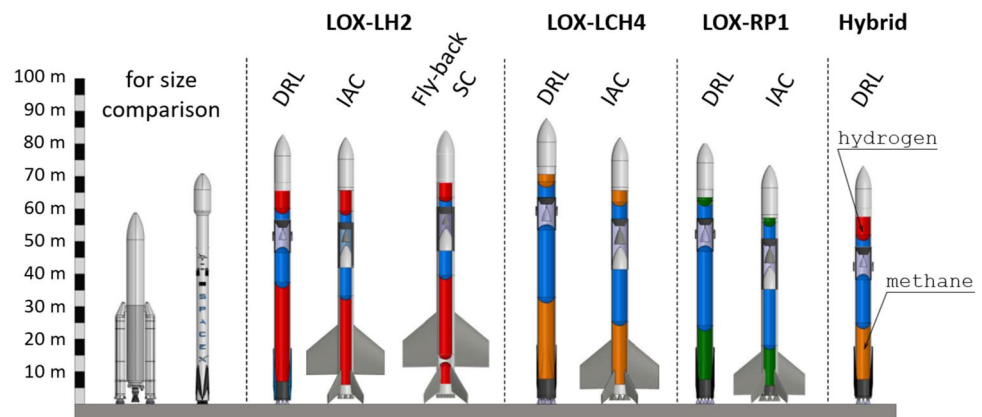


Fig. 7 Gross lift-off mass of the RLVs of the ENTRAIN study

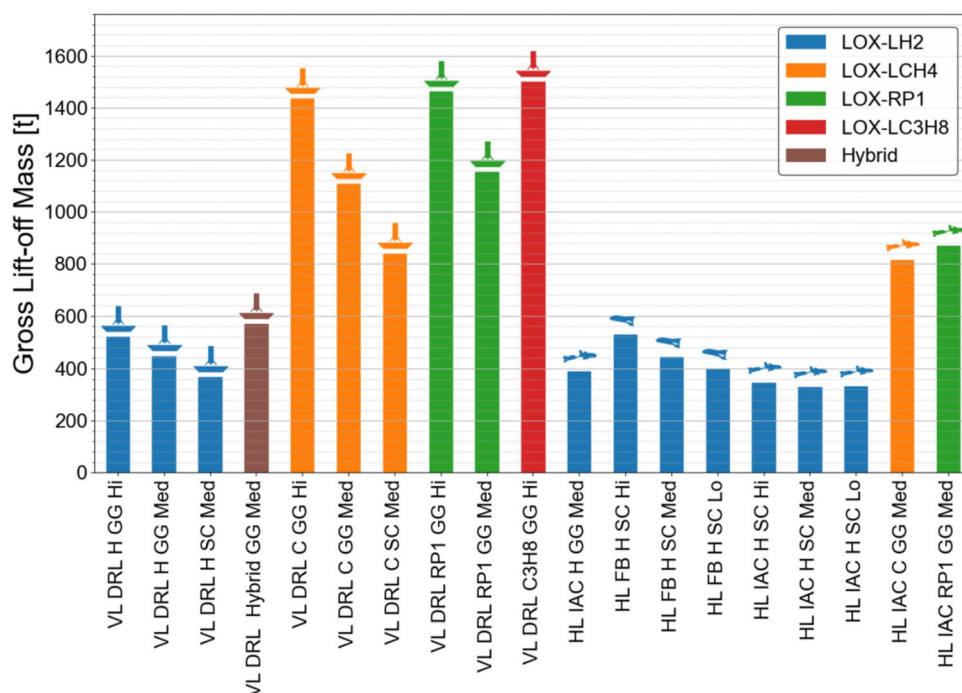
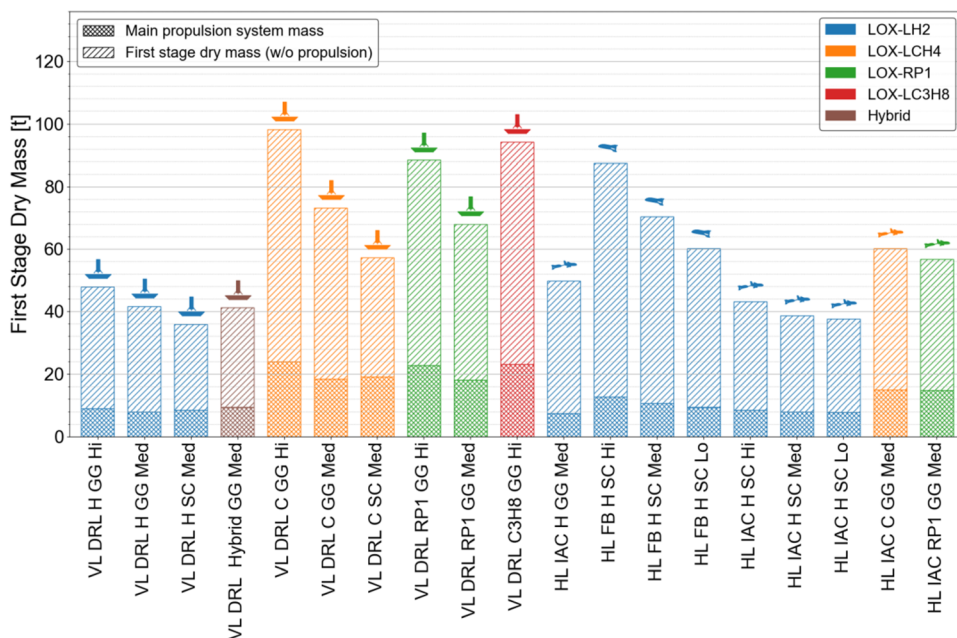


Fig. 8 First-stage dry masses of the RLVs of the ENTRAIN study



3.2 Mass

The mass comparisons from Figs. 7, 8 offer further insight into the impact of the different design options on the mass budget. As could be expected the hydrocarbon-fueled variants exceed by far the LOX/LH2-fueled ones in terms of Gross Lift-off Mass (GLOM) irrespective of recovery method. This is to be expected since the LOX/LH2 propellant combination offers a significant advantage in specific

impulse of approximately +90 s to +110 s [4]. Nonetheless, LOX/LH2 systems tend to have higher structural indexes as a direct consequence of a larger volume and size for a given propellant mass due to the low bulk density of the propellant combination. The ENTRAIN study results clearly show that the positive impact of higher specific impulse outvalues those negative impacts of the LOX/LH2 combination.

Additionally, the effect of the mass increase in hydrocarbons systems is even more pronounced in the case of vertical

First, for VTVL stages an increase in separation velocity increases the fuel demand for the return maneuvering as more energy has been accumulated by the system that has to be dissipated to limit re-entry loads. For instance, the separation velocity. For the LOX/LH2 variants with gas generator (GG), passing from the “Medium” class (Med) with a separation velocity of the first stage of 2.87 km/s

Figure 8 shows the first stage dry mass which is the part that will be recovered for a later reuse. The global tendencies already observed for the gross lift-off mass are reflected for the VTVL variants. The first-stage dry masses of hydrocarbon-fueled VTVL variants are significantly higher than those for LOX/LH2-fueled variants or for the variant with a mixed fuel combination. For VTHL, the dry mass relationship between LOX/LH2 and hydrocarbon is less important than observed for the take-off mass. This

shows that the better bulk density of hydrocarbon cannot compensate for the performance loss due to the fuel.

For the VTHL variant, a similar tendency is observed with respect to the fuel type although not as strong as observed for the VTVL options. As can be seen in Fig. 8, the hydrocarbon VTHL launchers result in higher values for the first stage dry mass than when using liquid hydrogen. A lower specific impulse as for hydrocarbon fuels leads directly to the need for additional fuel to deliver the required Δv for ascent but also for the re-entry deceleration in case of a VTVL in accordance with the rocket equation. A higher re-entry fuel mass, in turn, increases the separation mass at the end of the ascent flight of the first stage. Using again the rocket equation, this higher main engine cut-off (MECO) mass further increases the Δv requirement and hence more fuel for the first stage ascent boost phase. This effect is not as strong for VTHL, since no or only little fuel is needed for the re-entry phase limiting the impact of the fuel type to the ascent phase.

Unsurprisingly, variants using staged combustion engines (SC) yield configurations that show higher performance than their counterparts using gas generator engines (GG) leading to smaller launchers. This is a direct consequence of the better specific impulse and in line with what can be expected from the rocket equation.

The first stage main propulsion system masses strictly follow this trend observed for the gross lift-off mass and the first stage dry mass itself as can be seen in Figs. 7, 8. This is only natural as the required thrust for take-off scales linearly with the lift-off mass as the thrust-to-weight ratio was set to a fixed value of 1.4 for this design process and the propulsion mass roughly scales with the thrust.

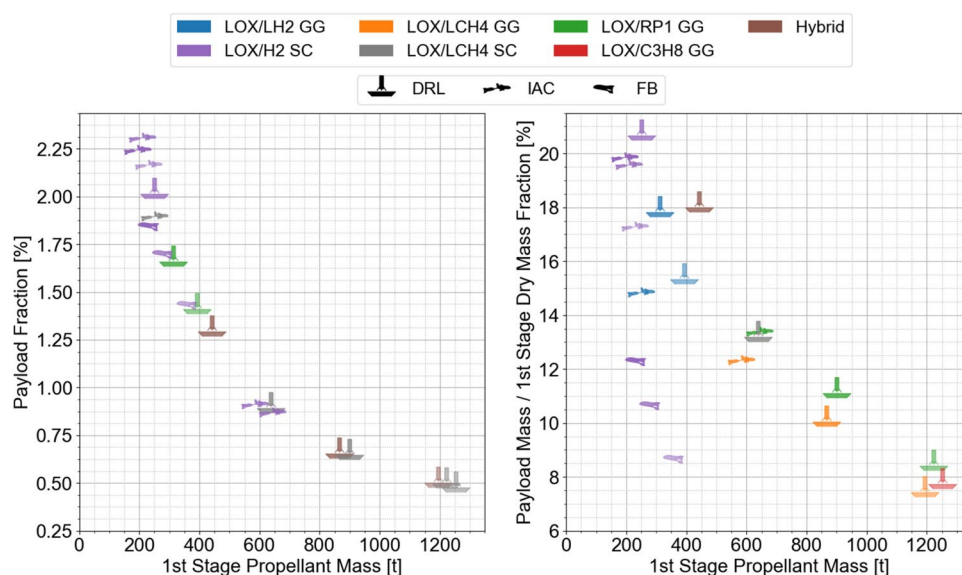
3.3 Performance

As performance indicators, the structural index (SI), the inert mass ratio (IMR) and payload ratio are used. Figure 9 shows the SI and IMR with respect to the RLV stage propellant mass. Some major conclusions can be drawn from the plots. As expected, the lowest structural index is achieved by the VTVL hydrocarbon launchers. For VTHL, the lowest structural index is achieved by using In-Air-Capturing in combination with hydrocarbon fuels. The structural index of fly-back variants naturally is higher than that of IAC stages, as the additional air-breathing propulsion system adds significant mass to the system.

As a direct indicator of performance capability with regard to mass, the inert mass ratio and payload ratio serve as means of rating the overall efficiency of the launcher. The lowest overall inert mass ratios are achieved by using In-Air-Capturing in combination with hydrocarbon launchers. This means that the accelerated “dead” mass, which includes dry mass, propellant residuals and optional return propellant, is lowest compared to all other methods.

The payload ratio offers additional insight. The superiority of LOX/LH2-based VTHL IAC concepts is evident offering the lowest propellant mass and highest payload ratio (see Fig. 10). The trade-off between payload fraction and inert mass ratio is the best of all possible combinations. The second-best option using the performance indicators is VTVL with downrange landing and LOX/LH2. Of VTVL hydrocarbon launchers, the best compromise is offered by the hybrid system as it features a decent payload efficiency with moderate propellant mass combining the denser LOX/LCH4 propellant combination of the first stage with the high-Isp LOX/LH2 combination in the 2nd stage. Considering overall

Fig. 10 Payload fraction (left-hand side) and payload to 1st stage dry mass fraction (right-hand-side) of the ENTRAIN RLVs; separation velocity is indicated by the transparency of the markers, with high transparency indicating higher separation velocity



efficiency, the hydrocarbon VTVL systems are the worst possible combination with the lowest payload efficiency and the highest mass. Comparing the three investigated hydrocarbon fuels, it can be observed that the IMR and the SI is improved. Considering the payload fraction, the results are a bit more mixed and a clear tendency difficult to identify.

Additionally, the separation velocity has a higher impact on VTVL systems performance, with a negative effect on efficiency for an increase in said velocity. Once again, the reason for this stronger pronunciation in VTVL systems is the strong impact of the propulsive handling of return maneuvering.

Note that the Falcon 9 vehicle in comparison offers a surprisingly good payload ratio due to a very low first-stage structural mass.

Among the winged concepts, the fly-back variants show noticeably higher first-stage structural indexes and higher inert mass fractions and a smaller payload mass fraction than those VTHL concepts relying on in-air capturing for first-stage recovery. This can be explained by the fact that significant parts of the recovery hardware for the in-air capturing method is outsourced to a towing aircraft. In opposition to that, the fly-back concepts have to carry the jet engines and its fuel for the cruise back to the landing runway.

Irrespective of the recovery methods, the inert mass ratio for winged concepts is almost insensitive to separation conditions contrary to the structural index that decreases with increasing separation velocity as can be seen on the right side of Fig. 9. For the in-air-capturing variants the first stage propellant mass used during ascent is quite insensitive to the separation point as well and consequently the inert mass ratio, too. This at a first glance surprising observation can be explained such that the staging points are very close to the optimal staging point. Indeed, the staging point of the Medium class (separation Mach number 9) is close to this optimum from a propellant loading and mass point of view. This means that increasing or lowering the staging velocity has only a minor impact on the overall mass around this optimum. This is a direct consequence also from a mathematical point of view as the gradient of the value with respect to the parameter should be flat near the optimum. For the fly-back configuration, the investigated staging points are farther away from the optimum and hence the propellant masses vary accordingly. While the structural index decreases with increasing fuel mass as expected this is not the case for the inert mass ratio which is almost constant. This can be explained by the additional return fuel of which more is needed for the fly-back maneuver the farther away the first stage re-enters the atmosphere which is the case for those launchers with a higher separation velocity. Further details can be found in [6].

Comparing variants with staged combustion engines (marked as SC in the figures) to their counterparts with gas

generator engines, the better engine performance is mirrored by a smaller IMR and SI but also higher payload mass fractions (roughly a 10–15% improvement with respect to these metrics). The payload fraction is roughly identical, with the exception of the IAC configurations for which the LOX/LCH₄ launcher yields better results.

3.4 Re-entry trajectory profile

Figures 11–15 show key parameters of the re-entry trajectories for the investigated launchers.

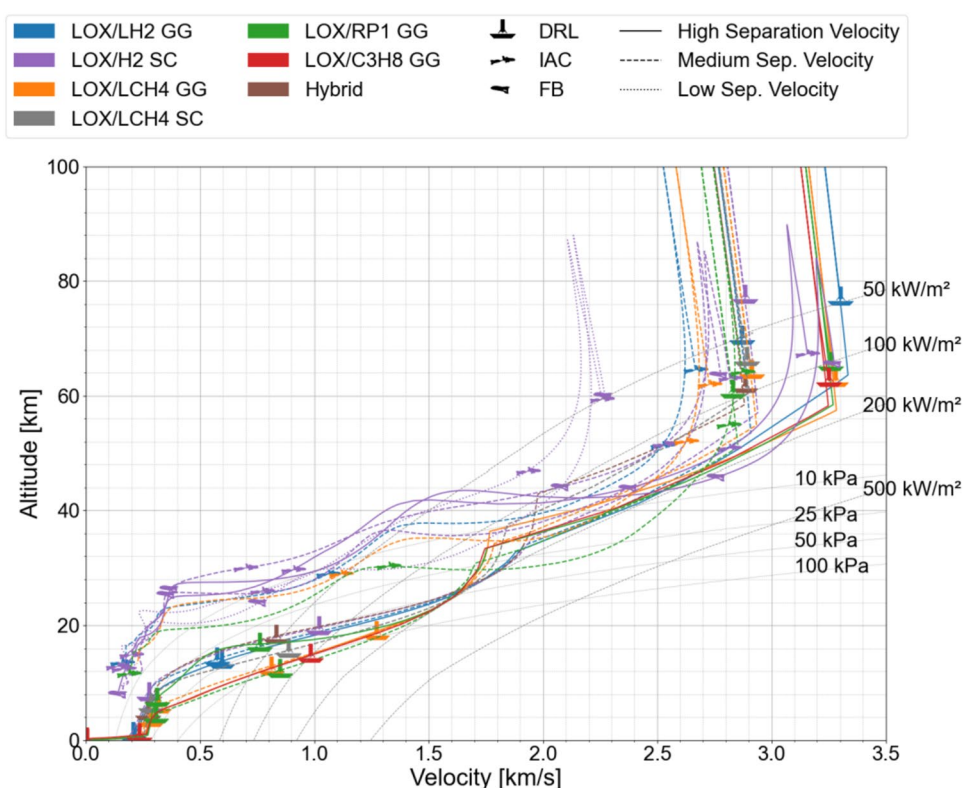
The plot in Fig. 11 presents the evolution of altitude as a function of relative velocity. It further shows the isolines for different dynamic pressures and heat flux with respect to a nose radius of 0.5 m, which is also the reference radius used for the stagnation point heat flux calculation for each stage. Thus, the heat flux values are not reflecting the actually maximum heat flux values at stage parts with a low radius such as the engine nozzle for VTVL or wing and fin leading edges for VTHL but allow the direct comparison between the different stages.

The separation point of the first stage is located on the right side of this graph at maximum or almost maximum velocity (point marked with the corresponding symbol). The stage is still on an ascent path albeit without propulsive assistance. As a consequence, the altitude still increases while the vehicle slows down under the effects of gravity until reaching its apogee. After having passed its maximum altitude point the stage picks up speed again while descending. As this occurs at high altitudes, aerodynamic forces are generally negligible where the only external force is gravity so that the ascent and descent path of this ballistic high-altitude arc coincide in this representation. It is only when the density becomes significant enough to generate a meaningful aerodynamic force that the ascent and descent path diverge.

The rather sharp edge observed for VTVL stages at the exit of the ballistic arc is due to the firing of the engines for the re-entry burn maneuver. Here the VTHL trajectories are smoother as the deceleration is accomplished by aerodynamic forces that depend on the angle of attack but also on velocity and density and hence altitude.

The deceleration of the VTVL launchers is achieved via a re-entry burn of which the ignition and extinction event is optimized in such a way that consumption is as low as possible while limiting the estimated stagnation heat flux to 200 kW/m² and dynamic pressure to 200 kPa. The former value was based on the reversed engineered SpaceX SES 10 mission trajectory which experienced a similar maximum heat flux. It was observed that the optimizer always attempted to delay the ignition as compatible with the heat flux limits to exploit aerodynamic deceleration as much as possible. The re-entry burn is

Fig. 11 Re-entry altitude versus relative velocity of ENTRAIN RLV first stages



characterized by the sudden change in velocity gradient with respect to altitude ($\delta v/\delta z$). Prior to this burn, the altitude decreases rapidly with only a moderate increase of velocity under the effects of the gravitational force in the course of this free-fall situation. During the deceleration boost the rate of decent is strongly reduced as is the velocity. At the end of this boost, the gravitational force takes over anew leading again to a larger decrease in altitude with only little impact on velocity until aerodynamic forces become more dominant that considerably reduces the decent rate and velocity.

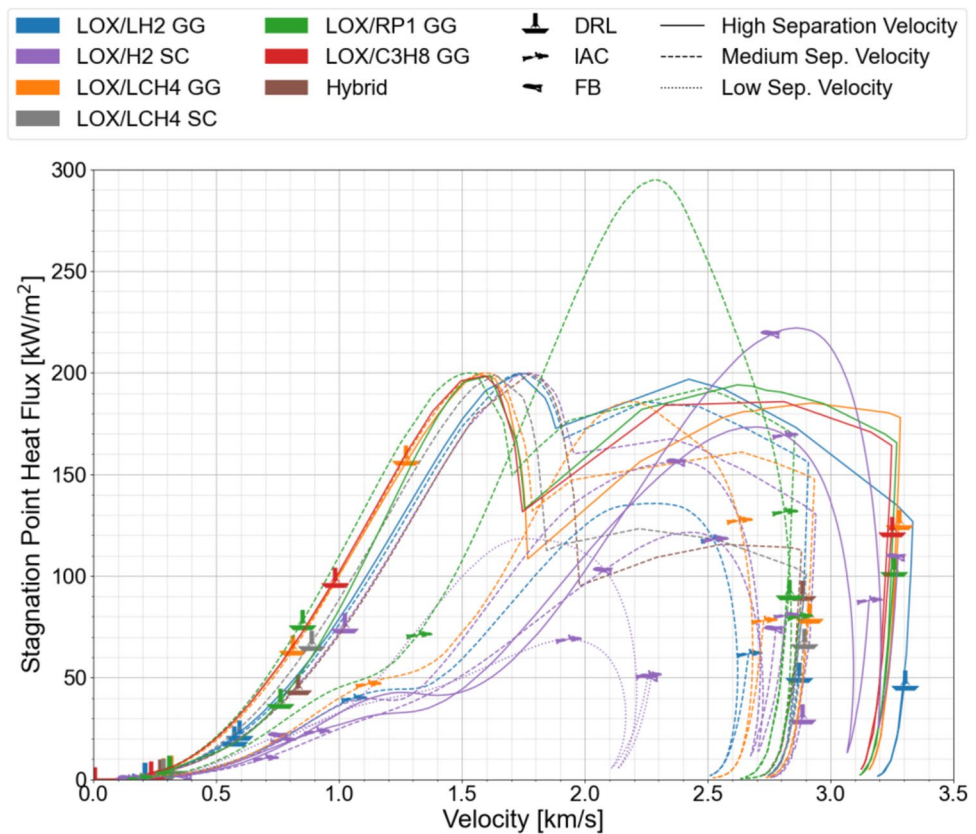
Contrary to that, the VTHL launchers have a more gradual deceleration profile. In the re-entry trajectory profile, it can be observed that the VTVL launchers follow a more or less similar velocity-altitude profile due to the fact that an estimated stagnation point heat flux of 200 kW/m^2 and a maximum dynamic pressure of 200 kPa were set. The VTVL trajectories most critical re-entry load value is this maximum heat flux which gets close to the 200 kW/m^2 isoline from re-entry until around 1.5 km/s for all trajectories. Interestingly, the hydrocarbon launchers experience the first heat flux peak shortly before the beginning of the re-entry burn whereas the LOX/LH2 launchers only get close to the 200 kW/m^2 mark during the aerodynamic flight. This can be explained by the lower ballistic coefficient of the LOX/LH2 stages and the lower gradient of velocity reduction through the re-entry burn. This combination is

advantageous for the fuel consumption during the re-entry since more velocity can be shed by aerodynamic forces in the case of LH2 VTVL. The heat flux rate is presented in Fig. 12.

Again, the separation point is located here on the right side at maximum or near maximum velocity marked by the corresponding symbol. During the ballistic ascent heat flux decreases until the altitude reaches its climax. Beyond that point, the heat flux increases as the vehicle descends further into denser atmosphere. The firing of the engines during the re-entry burn maneuver of the VTVL stages allows the limitation of the stagnation heat flux as seen by the pronounced flattening of the curves for these stages. The behavior is different for the VTHL where the deceleration and consequently the stagnation heat flux relies on the aerodynamic forces themselves depending on density as a function of altitude and velocity.

For VTHL re-entry, the trajectory profile is highly dependent on the separation parameters and the system mass. The heavy hydrocarbon stages with higher ballistic coefficient and high re-entry flight path angle experience the highest re-entry heat flux values. In this study, the LOX/RP1 stage showed the highest re-entry heat flux of nearly 300 kW/m^2 . The thermal protection system (TPS) for this stage is the heaviest of all VTHLs, not only due to the re-entry loads but due to the rather large surface area that has to be protected. A re-design of this concept to eliminate

Fig. 12 Re-entry stagnation point heat flux versus relative velocity of ENTRAIN RLV first stages



this behavior was not attempted at this stage to avoid such a large dip into denser atmosphere layers which could be achieved for instance by enlarging the wings. This in turn could reduce the TPS thickness. Whether this would lead to a lower TPS mass due to reduced thickness or to an increase in it due to the larger wing area would be part of the evaluation. However, this re-evaluation is not expected to topple the conclusion of the comparison with respect to the fuel type.

In Fig. 13 the evolution of the dynamic pressure during re-entry is provided. Again, the LOX/RP1 VTVL concept loads stand out as exceeding significantly the values of other VTHL concepts.

Comparing VTHL and VTVL globally, it can be seen that the dynamic pressure experienced by VTVL concepts are by a factor larger than two higher than those for the VTHL concepts after the re-entry burn. This explains the deceleration observed in Fig. 11 during atmospheric descent after the termination of the re-entry burn for these launchers. For a development program, this factor is to be considered during the design process as during high dynamic pressure phases comparatively small disturbances in angle of attack can lead to fairly big aerodynamic moments which may lead to high bending moments and potentially the need of adequately dimensioned means for attitude control.

While for the stagnation point heat flux and the dynamic pressure the VTVL launcher exhibit considerably higher loads during re-entry, this tendency is reversed for the lateral load factor as can be observed in Fig. 14. While the VTHL variants generate lift and hence lateral load factor throughout the entire re-entry trajectory this only occurs after the re-entry boost for the VTVL launchers that use lift during this phase for flight path corrections whereas no angle of attack is assumed during the boost phases. As a note, it shall be mentioned that the sign of this parameter is related to the orientation of the velocity vector with respect to the respective body-fixed coordinate frame. As the VTVL re-enter with the “rear” first that is with the engine side the angle of attack is a value in the vicinity of 180° .

The difference in re-entry strategy is also noticeable in the evolution of the axial load factor as depicted in Fig. 15. During the first part of the re-entry the axial load factor due to engine thrust dominates the evolution for VTVL launchers whereas this value is lower for VTHL. After termination of the re-entry burn, the drag generation at low or absent angle of attack is responsible for the significant axial load factor for VTVL launchers. The final sharp rise in axial load factor corresponds to the landing boost. The opposing sign of the axial load factor value for VTHL and VTVL resides

Fig. 13 Re-entry dynamic pressure versus relative velocity of ENTRAIN RLV first stages

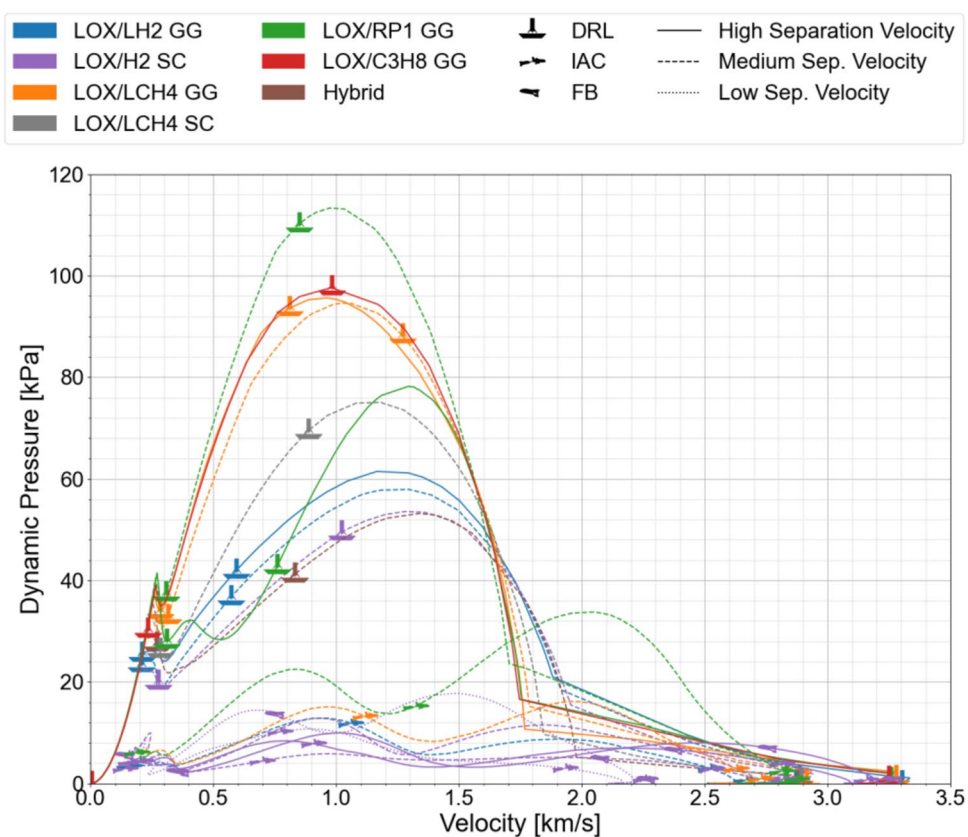


Fig. 14 Re-entry lateral load factor versus relative velocity of ENTRAIN RLV first stages

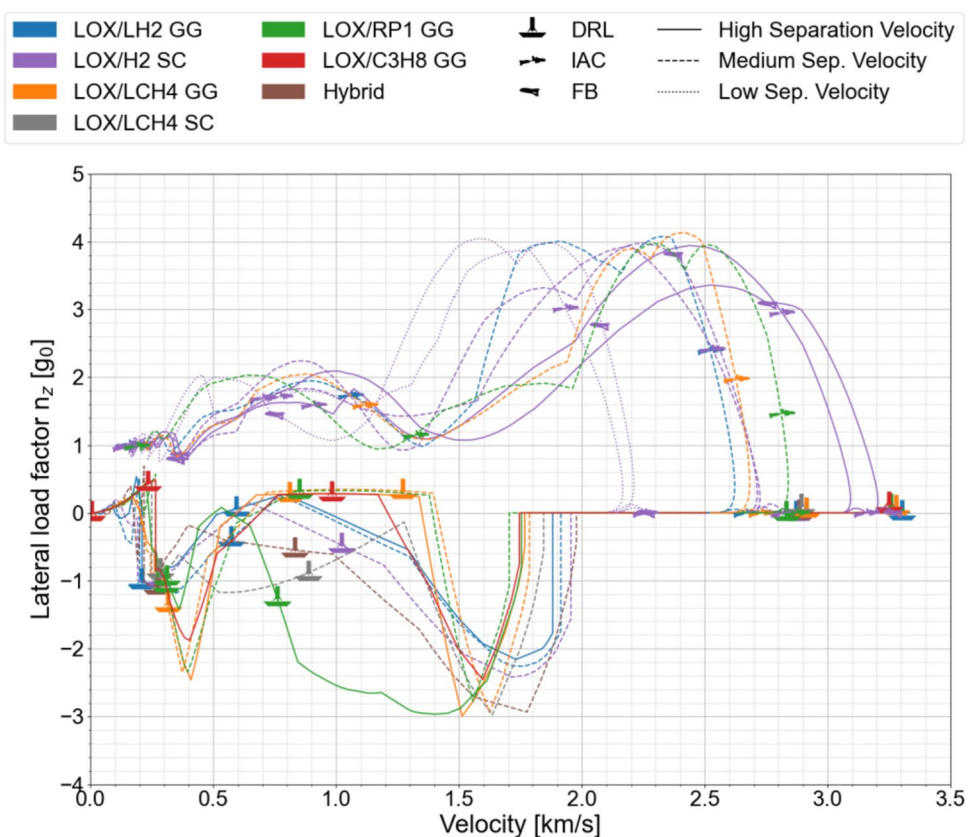
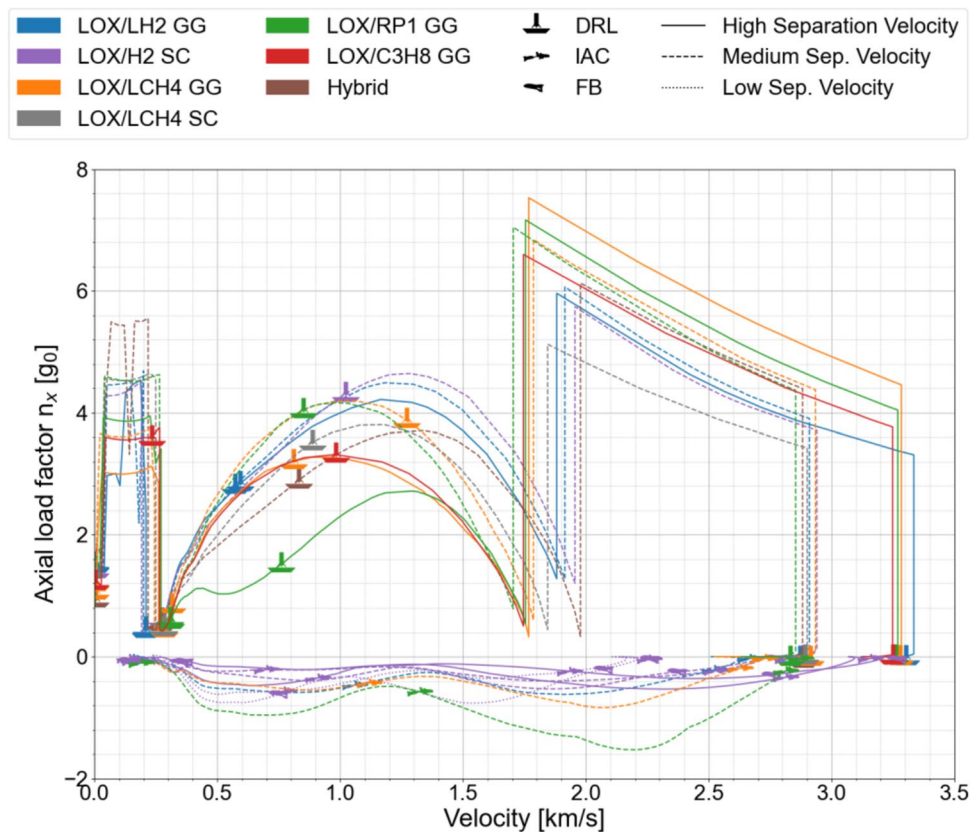


Fig. 15 Re-entry axial load factor versus relative velocity of ENTRAIN RLV first stages



in the fact that while the axial load factor for the VTHL during re-entry points from the nose to the rear where the rocket engines are located this is the opposite for the VTVL for which the first stage descent is performed engines first.

3.5 Reusable first stage Δv and mass ratios

An additional way of looking at the performance of the reusable first stages is the comparison of their Δv and mass ratios. These parameters are connected by the well-known rocket equation. Since the contribution of the Earth's rotation to the inertial velocity is small this part will be neglected for the following considerations. As a consequence, only the increase in relative velocity to will be considered. This leads to the following simplified formulation of the rocket equation:

$$\Delta v_{Gross} = \Delta v_{rel,Net} + \Delta v_{Loss} = c_e \ln(m_i/m_f) = c_e \ln(R) \quad (5)$$

In the above equation, R is the ratio between initial and final configuration mass, c_e is the first stage-specific impulse and gross Δv is the sum of net Δv and Δv losses. The Δv losses consist of gravity, atmospheric drag and thrust losses.

This formulation allows evaluating the achieved Δv_{rel} at any point of the trajectory by calculating the instantaneous

mass ratio R where m_i is the take-off mass and thus constant and m_f the current launcher mass.

Using this approach, the net Δv_{rel} as a function of mass ratio for VTVL and VTHL first stages with medium separation velocity can be compared to each other as shown in Fig. 16. The data shown is based on optimized ascent trajectories.

All reusable first stages shown in Fig. 16 are those for the Med separation velocity class (see Table 2) and reach a velocity of around 2.8 km/s. Obviously, in the case of the hydrocarbon systems this is only possible through an increased mass ratio which allows compensating the lower specific impulse of LOX/RP1 and LOX/LCH4.

Relating the net Δv_{rel} to the specific impulse allows obtaining a fully dimensionless representation of first-stage velocity evolution and to compare it to the ideal evolution in case of zero losses which is equivalent to the natural logarithm of the mass ratio. This is shown in Fig. 17 for Med separation velocity class stages. In the visualization shown in Fig. 17, the dimensionless losses are the difference between the ideal evolution (black dashed line) and the dimensionless net velocity. The dimensionless net Δv_{rel} of the different RLV stages is almost exclusively a function of mass ratio and the difference in the staging between hydrocarbon and LOX/LH2 configurations becomes evident. The comparison of dimensionless net Δv_{rel} to the ideal trend in

Fig. 16 Ascent net Δv vs. mass ratio for medium separation velocity RLV first stages

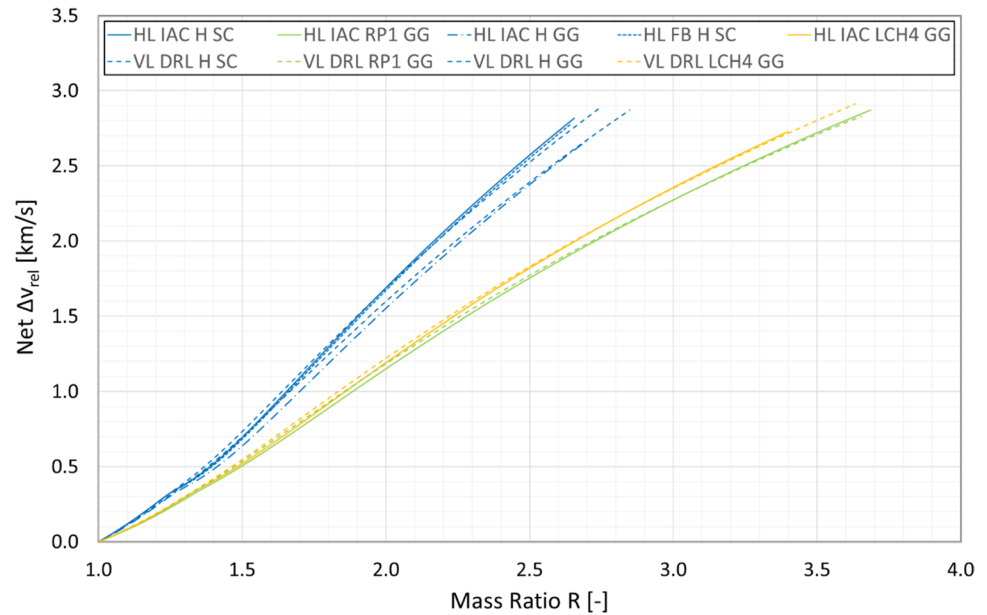
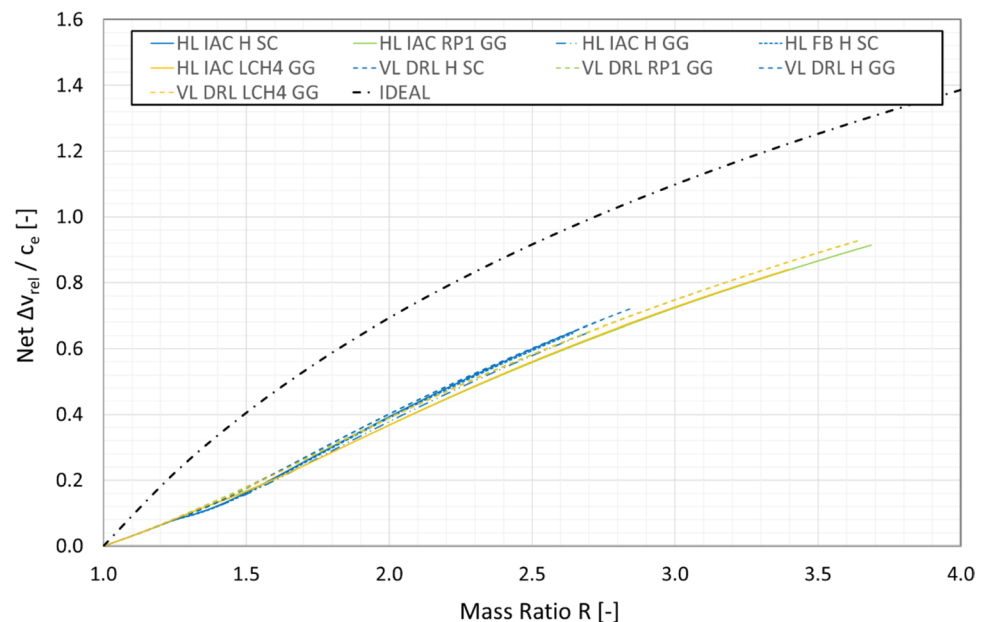


Fig. 17 Dimensionless ascent net Δv vs. mass ratio for medium separation velocity RLV first stages



case of zero velocity losses shows that up to a mass ratio of approximately 1.75 the dimensionless losses are surpassing the net velocity while for mass ratios beyond 1.75 the net velocity starts to dominate the overall gross velocity sum. Also, the maximum increase of dimensionless net Δv_{rel} is found at a mass ratio of around 1.75. At this point, the launchers are already beyond the maximum in dynamic pressure, have relatively low flight path angles and thus have already encountered the majority of first stage Δv losses. Significant differences in both final mass ratio and final dimensionless velocity are present between the LOX/LH2

and hydrocarbon configurations. While the LOX/LH2 first stages have final dimensionless velocities of 65% to 70% at mass ratios of approximately 2.7, the hydrocarbon configurations have final velocities between 85 and 92% at mass ratios between 3.4 and 3.7.

Going to higher mass ratios to be able to achieve the required separation velocity in the case of hydrocarbon first stages is increasingly less advantageous from the point of view of Δv generation and contributes to the explanation of the observed high GLOM and low payload fractions for the hydrocarbon launchers. Another related

aspect of importance is the staging at configuration level, both in terms of stage number and distribution of propellant between the stages. The number of stages as well as the first stage separation velocity have been fixed in the frame of the general study assumptions and the (negative) effect of this decision on the configuration performance is stronger for hydrocarbon configurations as compared to the LOX/LH2 systems. It shall be however kept in mind that the decision to set three fixed staging points instead of a dedicated staging point optimization was motivated to accelerate the iteration process since the focus of the study was on trade-off of key design parameters such as engine cycle and fuel choice and in no way a preemption of a dedicated staging point optimization for a final system design.

Gravitation, aerodynamic drag and thrust orientation deviating from the inflight velocity contribute to these ascent Δv losses. Thrust loss in this context is understood as the part of thrust not available for velocity increase as illustrated by the vector diagram of Fig. 18.

Neglecting again the contribution of Earth rotation, these losses are determined using the relationships as in equations 6, 7, and 8.

- Gravity loss:

$$\Delta v_{gravity} = - \int_0^{t_{MECO}} \frac{\mu}{r(\tau)^2} \cdot \sin \gamma(\tau) d\tau \quad (6)$$

where μ is the Earth gravitation constant and is $3.986004418 \times 10^{14} \text{ m}^3/\text{s}^2$, $r(t)$ the instantaneous distance from

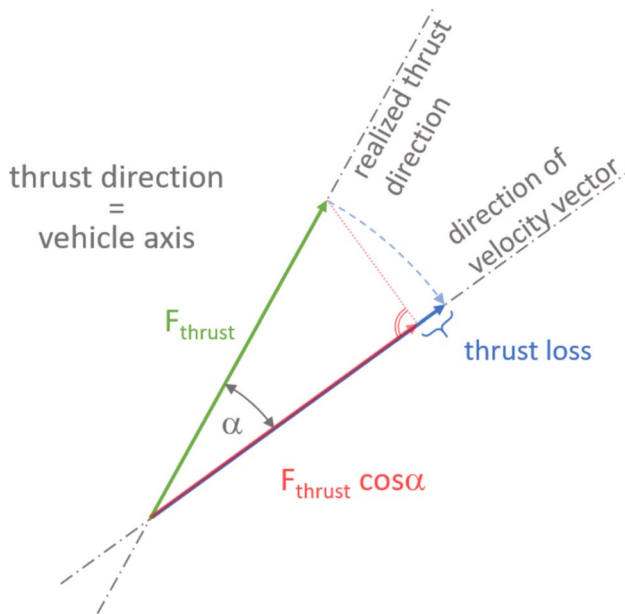


Fig. 18 Thrust loss, vector diagram

the Earth's center and γ the flight path angle. Integration is performed from lift-off to engine cut-off of the first stage.

- Aerodynamic drag loss:

$$\Delta v_{drag} = - \int_0^{t_{MECO}} \frac{F_D(\tau)}{m_{sys}(\tau)} d\tau \quad (7)$$

where F_D is the drag force and m_{sys} the instantaneous system mass. Integration is performed from lift-off to engine cut-off of the first stage.

- Thrust loss: This loss is interpreted as the reduction of thrust along the velocity direction due to non-alignment with the velocity vector. Assuming coinciding thrust vector and vehicle longitudinal axis this occurs when the angle of attack is non-zero.

$$\Delta v_{thrust} = - \int_0^{t_{MECO}} \frac{F_T(\tau)}{m_{sys}(\tau)} [1 - \cos \alpha(\tau)] d\tau \quad (8)$$

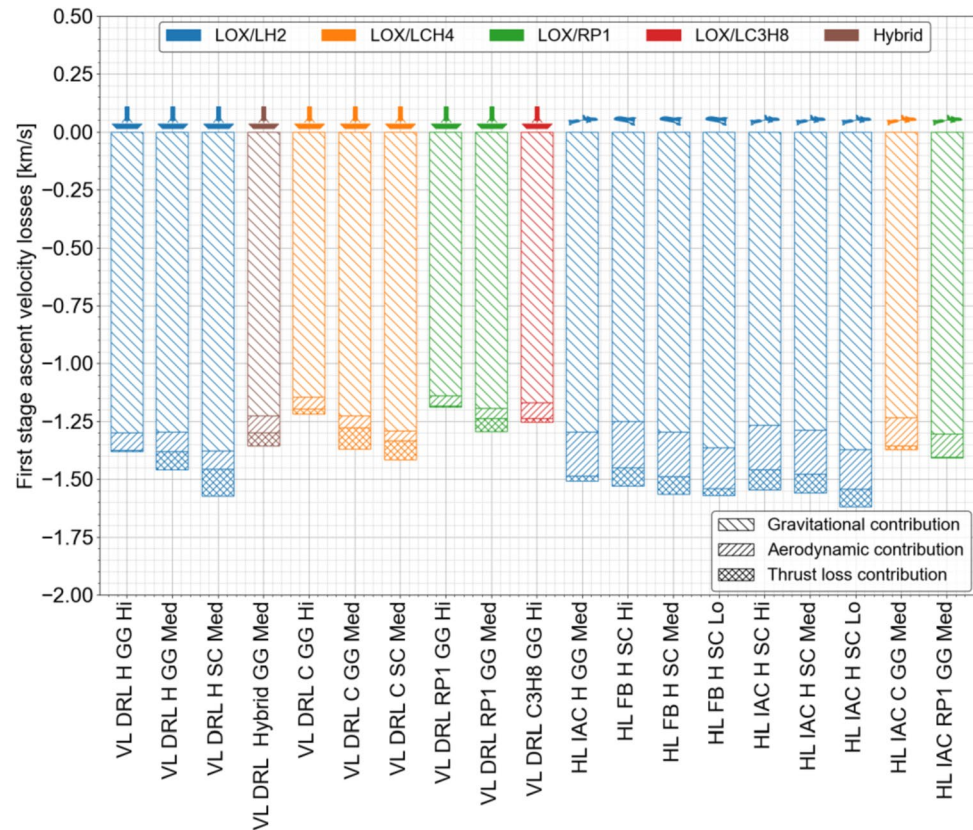
where F_T is the instantaneous thrust force, m_{sys} the instantaneous system mass and α the instantaneous angle of attack. Overall, these losses are of similar magnitude, irrespective of the configuration and recovery method. Three observations however are considered noteworthy with respect to the topic of this paper:

- Losses during the first stage ascent are dominated by gravity losses. Drag plays a minor role during atmospheric ascent which is in line with the general expectation for concepts with vertical lift-off.
- The investigated LOX/LH2 concepts show, on a general basis, a slightly higher velocity loss due to gravitation and drag than the hydrocarbon variants or the mixed fuel configuration.
- Unsurprisingly, the VTHL show a noticeably higher drag loss than the VTVL concepts since the wings generate additional drag compared to the VTVL variants.

Certain thrust losses are also expected due to the fact that both the aerodynamic moment during ascent and wind gusts have to be compensated by thrust vector control. These are expected to be more pronounced for winged vehicles than for non-winged ones although it is not expected that these effects become dominant with respect to the vehicle performance and are hence neglected at this stage. Figure 19 presents the numerical values of the ascent velocity losses.

While VTHL mostly relies on aerodynamic means to reduce energy, VTVL additionally requires engine burns to reduce the velocity. The engine burn contribution to velocity changes can be calculated by equation 9:

Fig. 19 Ascent net Δv contributions for investigated first stages



$$\Delta v_{engine} = - \int_0^{t_{MECO}} \frac{F_T(\tau)}{m_{sys}(\tau)} \cos \alpha(\tau) d\tau \quad (9)$$

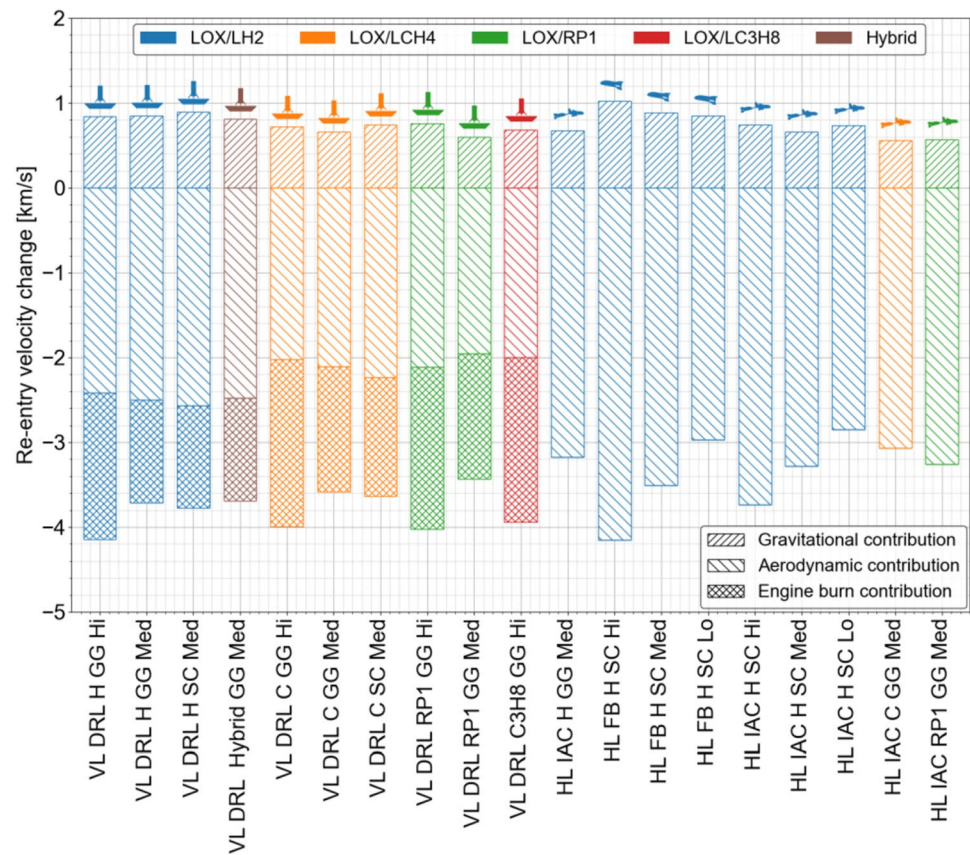
Interestingly, the VTVL stages still shed the majority of the velocity by aero-braking despite the important role of the propulsive deceleration maneuvers. The lower the ballistic coefficient of the stage the higher the share of aero-braking Δv with respect to that of propulsive Δv . This again plays in favor of the LOX/LH2 stages with low ballistic coefficients. Here, almost two-thirds of the whole deceleration are achieved by aero-braking whereas hydrocarbon launchers have a slightly less aero-braking to propulsive ratio of around 60%, see Fig. 20 for a detailed breakdown of reentry velocity contributions. This implies not only that hydrocarbon launchers require a larger propulsive deceleration due to the higher ballistic coefficient it also requires even more fuel due to the comparatively lower specific impulse of this fuel compared to LOX/LH2.


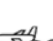
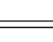
Two aspects are to be noted with respect to Fig. 20:

- The propulsive return flight for the fly-back variants is not represented within this figure as the propulsive force is in its large majority used to simply compensate

the aerodynamic drag and does only marginally modify the velocity if at all. The use of highly efficient air-breathing propulsion makes it difficult to compare the corresponding velocity contribution to those variants relying entirely on rocket propulsion from a vehicle design perspective. A very high-velocity contribution of the engine burn for an air-breathing propulsion would not be indicative of a very high fuel consumption due to the high efficiency of this propulsion system where thrust is generated drawing from external sources in the shape of oxygen present in the air.

- As the propulsive return flight for the fly-back variants is not represented within this figure this applies to the drag contribution as well. Consequently, the bar “aerodynamic contribution” does not include the drag contribution during this specific phase for these variants. Since thrust does not contribute much to the velocity as it is compensated by the drag force the opposite is true as well: drag does not contribute much to the velocity as it is compensated by the thrust force.

Fig. 20 Descent net Δv contributions first stages**Table 4** Comparison matrix for the ENTRAIN RLVs

					Mass Indicators		Performance Indicators			Re-Entry				
					GLOM	1st stage dry mass	Structural Index RLV stage	Inert Mass Ratio RLV stage	Payload Ratio	Max Heat Flux	Max Q			
					Propellant	Engine Cycle	Separation Velocity	[t]	[t]	[%]	[%]	[%]	[kW/m²]	[kPa]
VTVL Downrange Landing		LOX/LH2	SC	Med	367	35.9	14.4	19.7	2.03	200.1	53.6			
			GG	High	519	47.9	12.2	20.2	1.43	199.8	61.5			
				Med	447	41.7	13.4	19.4	1.68	199.7	57.9			
		Methane	SC	Med	839	57.3	9.0	16.0	0.91	199.2	75.1			
			GG	High	1434	98.1	8.2	17.7	0.52	199.4	95.7			
				Med	1107	73.2	8.5	15.8	0.67	199.8	94.6			
		Propane	GG	High	1500	94.2	7.5	16.7	0.49	198.5	97.7			
		RP1	GG	High	1463	88.4	7.2	16.1	0.52	198.7	78.2			
Med	1153			68.1	7.6	14.7	0.66	199.9	113.3					
Hybrid	GG		Med	570	41.2	9.3	15.9	1.31	199.8	53.2				
VTHL In-Air- Capturing		LOX/LH2	SC	High	344	43.2	18.9	17.8	2.17	173.4	8.4			
				Low	329	38.7	18.7	17.6	2.31	121.5	5.8			
					332	37.6	19.5	18.2	2.24	68.8	10.7			
		GG	Med	389	49.8	20.0	18.6	1.90	135.7	12.9				
			Methane	GG	Med	814	60.2	10.4	11.3	0.91	185.8	16.2		
				RP1	GG	Med	871	56.7	8.8	10.0	0.87	295.0	33.8	
VTHL Flyback		LOX/LH2	SC	High	529	87.5	23.9	23.5	1.44	222.1	9.9			
				Med	442	70.4	24.7	23.4	1.70	156.3	12.8			
				Low	401	60.2	25.3	23.5	1.85	118.4	17.8			

3 worst performing candidates

worse than average

better than average

3 best performing candidates

^{*} This value slightly violates the imposed constraint on maximum heat flux but was considered to be acceptable.

4 Discussion

The comparison of the ENTRAIN launch vehicles from a mass, performance and re-entry loads perspective shall now be bundled together to allow a quantitative evaluation on all those levels. Therefore, the parameters gross lift-off mass (GLOM), dry mass, SI, IMR, payload ratio and re-entry maximum heat flux and dynamic pressure are used to evaluate the vehicles as shown in Table 4. The cells are color-coded to reflect the placement of each vehicle with respect to other vehicles. The top or best three launchers of each category are represented by dark green, the bottom or worst three launchers in dark red. Further, all launchers better than average are coloured in pale green, while all worse than average are coloured in pale red.

Using this classification scheme, the following conclusions can be drawn:

- LOX/LH2 in any case and regardless of the return method offers better than average GLOMs, leading to lighter launch vehicles. Contrary, using any hydrocarbon fuel combination (LOX/LCH4, LOX/LC3H8, LOX/RP1) leads to worse than average GLOMs. A hybrid concept for VTVL offers potentially better than average take-off mass. The best option is VTHL IAC with LOX/LH2 and staged combustion. High separation velocity increases GLOM within the range of the investigated separation velocities.
- Considering absolute dry mass, most LOX/LH2-driven vehicles are better than average with the exception of Fly-back VTHL stages due to the additional turbofan hardware needed.
- The structural index is best for hydrocarbon-fuelled VTVL systems and worst for VTHL Fly-back systems. VTVL systems generally feature lower structural indexes.
- Hydrocarbon-fuelled options show generally better Inert Mass Ratios than their LOX/LH2-fuelled counterparts. The highest IMR is observed for the investigated LOX/LH2-fuelled Fly-back options.
- The payload ratio is best for VTHL IAC LOX/LH2 systems and better than average again for all other LOX/LH2 launchers. VTVL with hydrocarbons are the worst combination considering payload efficiency.
- While the structural index of IAC-stages is worse than VTVL-stages with DRL, the Inert Mass Ratios are significantly better for IAC in all cases. Hydrocarbon-powered stages would gain most in improving IMR when switching to IAC-return mode.
- Maximum re-entry heat flux and dynamic pressure is lowest for VTHL IAC versions and generally lower than average for most VTHL versions. However, this is partly due to the fact that the re-entry loads are managed differ-

ently for both versions. VTVL controls maximum heat loads by propulsive braking (e.g. re-entry burn) while VTHL are more sensitive to re-entry conditions and favour shallower trajectories for aero-braking (a detailed explanation is shown in [6]). Hence, the VTVL could also be limited to lower maximum re-entry heat fluxes but at the expense of more descent propellant leading to the need for iterative design scale-up to achieve the required 7.5 t of payload into GTO.

Taking all those considerations into account one could conclude that either a LOX/LH2 launcher with a first stage landing downrange or winged first stage using In-Air-Capturing are the best options performance-wise. Those vehicles are in almost all considered categories better than average. Specifically, the winged IAC-stages are positioned among the top three systems in the majority of the categories. Remarkably, a hybrid approach for VTVL is also almost in all categories better than average, thus offering a decent compromise between low bulk density propellants but less performance for the lower stage (LOX/LCH4), and high specific impulse but higher structural mass for the upper stage (LOX/LH2).

The analyses show that any hydrocarbon-fuelled vehicle is almost always worse than average in most of the categories except for the RLV-stage structural index. The effect of higher bulk density of the hydrocarbons cannot outweigh the lower performance compared to the LOX/LH2 combination thus leading to the observed high GLOMs and structural masses. This effect is most pronounced for VTVL vehicles since their mass budget is much more dependent on engine efficiency because of their more demanding mission Δv .

The performance-wise most interesting concepts also reach the lowest estimated launch costs for an extensive range of payload scenarios, as demonstrated in [7].

5 Conclusion

In this paper, the results of the DLR ENTRAIN study were used to assess the impact of recovery methods on reusable launchers on a system level, to identify and to compare different options for launch vehicles. A broad range of configurations had been iteratively sized to a set of mission requirements and design features that are of potential interest for a future European RLV. The main mission requirements are a payload mass of 7.5 t to GTO, a two-stage orbit architecture and similar engines in both stages. Further design parameters include the return method with vertical and horizontal landing, the choice of propellant combination, the engine cycle and the staging velocity of the first stage.

The focus of this paper is the comparison of VTVL and VTHL methods against the background of the selected design space. This comparison was performed on different levels: mass, performance and re-entry loads.

The most favourable combination of design parameters for the reference mission is either a LOX/LH2 VTHL IAC or VTVL DRL launcher with GG- or SC-cycle engines. The better specific impulse of the LOX/LH2 propellant combination outweighs the higher structural indexes due to the low bulk density of these propellants for all return methods. In contrast, the use of hydrocarbons for any return option generally increases take-off mass and absolute dry mass and decreases the payload efficiency. This is even more valid for VTVL systems where the specific impulse has not only an impact on the Δv capacity during ascent but also during the descent burns. A potential compromise between the low bulk density of hydrocarbon propellant combinations and the high specific impulse of LOX/LH2 is to design the launcher as a hybrid concept where the first stage is driven by LOX/LCH4 and the second stage by LOX/LH2.

The VTHL methods with fly-back require additional propellant and air-breathing engines needed for the return flight rendering it performance-wise less interesting than its IAC counterparts. As with VTVL, the use of hydrocarbon fuel leads to significantly higher gross lift-off masses and higher first-stage dry masses. This additionally loaded fuel mass has to compensate for the loss of specific impulse with respect to LOX/LH2 which in turn leads to larger stages with increased wing sizes and larger landing gears and higher TPS mass.

This study comparing different RLV first-stage return methods and propulsion options is the first of its kind on system level. The underlying assumptions and constraints are made transparent. Any systematic reassessment under modified mission or design assumptions is encouraged to further improve understanding of advanced space launch vehicle design.

Author contributions S. St., J.W., L. B. provided technical data S. St. and I. D. wrote the main manuscript text of the paper with contributions from M. S. and L. B. S. St., I. D. and L. B. prepared the images and tables, except those in Fig. 1 that come from external sources All authors reviewed the manuscript.

Funding Open Access funding enabled and organized by Projekt DEAL.

Data availability Datasets were generated to produce tables and figures in this manuscript. These can be made available on request under compliance to applicable laws.

Declarations

Conflict of interest The authors have no competing interests to declare that are relevant to the content of this article.

Open Access This article is licensed under a Creative Commons Attribution 4.0 International License, which permits use, sharing, adaptation, distribution and reproduction in any medium or format, as long as you give appropriate credit to the original author(s) and the source, provide a link to the Creative Commons licence, and indicate if changes were made. The images or other third party material in this article are included in the article's Creative Commons licence, unless indicated otherwise in a credit line to the material. If material is not included in the article's Creative Commons licence and your intended use is not permitted by statutory regulation or exceeds the permitted use, you will need to obtain permission directly from the copyright holder. To view a copy of this licence, visit <http://creativecommons.org/licenses/by/4.0/>.

References

1. Dietlein, I., Bussler, L., Stappert, S., Wilken, J., Sippel, M.: Overview of system study on recovery methods for reusable first stages of future European launchers. CEAS Space J (2024). <https://doi.org/10.1007/s12567-024-00557-9>
2. [https://commons.wikimedia.org/wiki/File:Falcon_Heavy_Side_Boosters_landing_on_LZ1_and_LZ2_-_2018_\(25254688767\).jpg](https://commons.wikimedia.org/wiki/File:Falcon_Heavy_Side_Boosters_landing_on_LZ1_and_LZ2_-_2018_(25254688767).jpg)
3. https://commons.wikimedia.org/wiki/File:Atlantis_is_landing_after_STS-30_mission.jpg
4. Sippel, M., Wilken J.: Selection of propulsion characteristics for systematic assessment of future European RLV-options, CEAS Space Journal 2024, accepted for publication
5. Wilken, J., Stappert, S.: Comparative analysis of European vertical-landing reusable first stage concepts. CEAS Space J (2024). <https://doi.org/10.1007/s12567-024-00549-9>
6. Bussler, L., Dietlein, I., Sippel, M.: Comparative analysis of European horizontal-landing reusable first stage concepts, CEAS Space Journal 2024, under review
7. Wilken, J., Herberhold, M., Sippel, M.: Options for future European reusable booster stages: evaluation and comparison of VTHL and VTVL costs, CEAS Space Journal 2024, submitted for publication
8. Patentschrift (patent specification) DE 101 47 144 C1: Verfahren zum Bergen einer Stufe eines mehrstufigen Raumtransportsystems, <https://patents.google.com/patent/DE10147144C1/en> released 2003
9. Sippel, M., Singh, S., Stappert, S.: Progress summary of H2020-project FALCon, Aerospace Europe Conference – 10th European Conference for Aeronautics and Space Sciences – 9th CEAS, (2023), <https://doi.org/10.1007/s12567-023-00512-0>
10. Stappert, S., Singh, S., Funke, A., Sippel, M.: Developing an innovative and high-performance method for recovering reusable launcher stages: the in-air capturing method. CEAS Space J (2023). <https://doi.org/10.1007/s12567-023-00512-0>
11. Gogdet, O., Mansouri, J., Breteau, J., Patureau de M.A., Louaas, E.: Launch vehicle system studies in the “future launchers preparatory programme”: the reusability option for Ariane evolutions. 8th Eur Conf Aeronaut Space Sci. (2019), <https://doi.org/10.13009/EUCASS2019-971>
12. PLD space: Miura 1 payload user's guide 1.3, 2018

Publisher's Note Springer Nature remains neutral with regard to jurisdictional claims in published maps and institutional affiliations.



Comparative analyses of European horizontal-landing reusable first stage concepts

L. Bussler¹ · I. Dietlein¹ · M. Sippel¹

Received: 5 April 2024 / Revised: 5 September 2024 / Accepted: 7 October 2024 / Published online: 24 October 2024
© The Author(s) 2024, corrected publication 2024

Abstract

Partially reusable two-stage-to-orbit (TSTO) launch configurations have been investigated on system level by DLR in the ENTRAIN study which encompasses an examination of both vertical takeoff horizontal landing (VTHL) and vertical takeoff vertical landing (VTVL) reusable first stages. A target payload performance of 7.5 Mg into GTO is selected as the common mission requirement of all concepts. In this paper, the preliminary designs of TSTO configurations consisting of a winged reusable first stage and an expendable upper stage are presented and discussed. The considered propellant combinations include LOX/LH2, LOX/LCH4 and LOX/RP-1. Configurations based on staged combustion and gas generator cycle engines are analyzed. The focus of the presented preliminary analyses is on the overall performance of the space transportation system, the design and architecture of the winged reusable first stage and the comparison and evaluation of different VTHL configurations.

Keywords RLV · VTHL · Reusability · Space transportation systems

Abbreviations

AoA	Angle of attack
CAC	Calculation of aerodynamic coefficients
DOF	Degrees of freedom
ENTRAIN	European next reusable ariane
FB	Fly-Back
FPA	Flight path angle
GEO	Geostationary earth orbit
GG	Gas generator
GLOM	Gross lift-off mass
GTO	Geostationary transfer orbit
IAC	In-air-capturing
LCH4	Liquid methane
LH2	Liquid hydrogen
LOX	Liquid oxygen
RLV	Reusable launch vehicle
RP-1	Rocket propellant 1 (kerosene)
SC	Staged combustion
TSTO	Two-stage-to-orbit
US	Upper stage
VTHL	Vertical take-off horizontal landing

Nomenclature

Isp	Specific impulse [s]
L/D	Lift-to-drag ratio [-]
T/W	Thrust-to-weight ratio [-]
ΔV	Delta velocity [km/s]
ϵ	Expansion ratio [-]

1 Introduction

The presented work is part of a general, systematic analysis of RLV configurations in DLR, [1–5]. This investigation is motivated by an aspiration to identify suitable and advantageous concept designs for a future European reusable launch system. This sequence of papers deals with first stage reusability only, upper stage reusability is not considered. In any case, prior to any reuse the stage has to be recovered. This necessity poses the question of how to recover those parts of the space transportation system that shall be reused, which recovery strategy is promising and what are the technologies to be developed. For this purpose, DLR has committed a large system study comparing different two-stage-to-orbit (TSTO) concepts including both winged reusable first stages and non-winged reusable first stages landing vertically, see [1–5] for more details.

The focus of the present paper is on RLV systems with winged reusable first stages. Winged reusable first stages

✉ L. Bussler
Leonid.Bussler@dlr.de

¹ DLR Institute of Space Systems, Robert-Hooke-Straße 7,
28359 Bremen, Germany

landing horizontally need additional hardware in form of wings, empennage and landing gears and for some concepts air-breathing propulsion along with additional fuel. This increases the mass of the first stage and thus reduces the overall payload performance of the transportation system. However, several advantages as compared to vertical landing RLV stages exist. First, no additional rocket propellant for atmospheric reentry and a vertical landing of the stage needs to be foreseen in the design of the reusable stage. Furthermore, no additional rocket propellant needs to be accelerated during the ascent prior to being consumed along the descent trajectory. The wing allows a safe, non-propelled atmospheric reentry with controlled mechanic and thermal loads as well as a horizontal, aircraft-like landing on a runway. If air-breathing propulsion is installed on the winged reusable first stage, the operating radius of the stage is significantly increased with the achievable range depending on the aerodynamic and propulsion efficiency as well as the amount of air-breathing propulsion fuel. Two return options for winged reusable first stages are considered in this work: a fly-back (FB) booster-type stage returning to launch site by means of its own air-breathing propulsion and a stage returned to launch site through the IAC method.

The patented In-air-capturing (IAC) intends the winged reusable stages to be caught in the air and towed back to their launch site without any necessity of an own propulsion system. The idea has performance similarities with the vertical Down-Range Landing mode of VTVL stages. After decelerating to subsonics, the reusable stage is awaited by an adequately equipped capturing aircraft, offering sufficient thrust capability to tow a winged launcher stage with restrained lift-to-drag ratio. Significant progress in maturing the technology was reached in the Horizon 2020 project *FALCon* by performing sophisticated full-scale and lab-scale flight experiment simulations, [6]. A schematic illustration of the two different return options is shown in Fig. 1 (left FB, right IAC).

Numerous studies of reusable space transportation systems in and outside Europe have been performed in the past. The French space agency CNES studied two-stage configurations targeting 7.5 Mg to GTO, [7]. Amongst others, the analyzed systems were the Two-Stage-To-Orbit concept EVEREST and a semi-reusable concept RFS. In both cases, LOX/LH₂ as propellant combination was used on the reusable stages. The reusable first stage (RFS) had a separation Mach number of around 13.5, while EVEREST was a Mach 6 separation concept. In [8] an overview of reusable systems with a focus on technology aspects of European programs is given. In addition, first stage reusability is considered to be a way to reduce launch cost. However, the need for further critical technology maturation is emphasized. One of the most detailed investigations in the area of winged, horizontally landing systems performed in the past in DLR in cooperation with German industry has been the ASTRA Liquid Fly-Back Booster (LFBB) study, [9]. The liquid boosters were meant as an option to replace the solid boosters of the Ariane 5 and relied on LOX/LH₂ gas generator propulsion. Separation of the boosters was foreseen to take place around Mach 6 and air-breathing propulsion using H₂ as fuel should have allowed a powered flight back to launch site. More recently, a reusable booster system has been studied in the U.S. and findings and recommendations concerning a number of technical, economical and operational aspects of RLV have been identified and formulated in [10]. A multidisciplinary approach is followed in [11]. In this work, winged RLV architectures are analyzed. While both glide-back and fly-back configurations are studied, finally the conclusion is drawn that the fly-back concept is a promising option. Within ESA's Future Launchers Preparatory Programme (FLPP), system studies to identify promising evolutions of the Ariane 6 launch vehicle towards a partially reusable launcher have been performed and are described in [12].

The content of the performed analysis presented in this paper is the technical assessment of partially reusable space

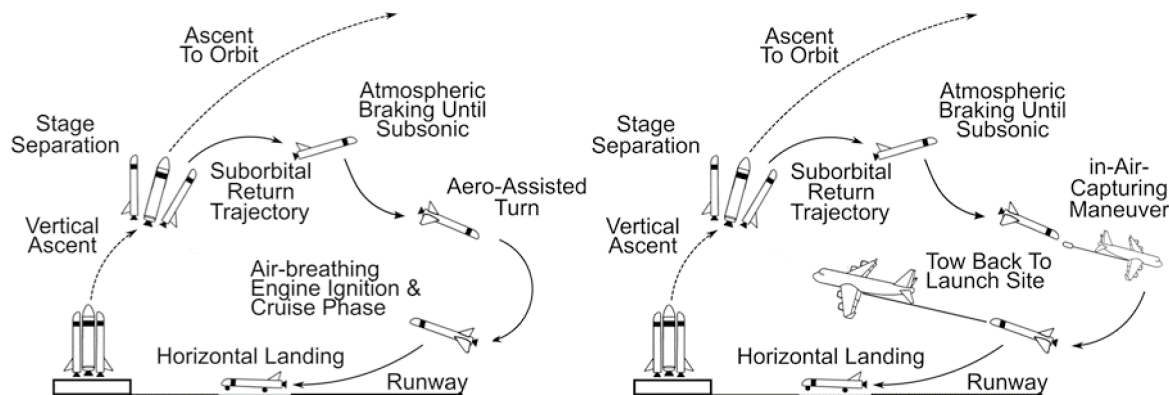


Fig. 1 Return options for winged reusable first stages

transportation systems with winged reusable first stages. An important aspect of the work performed is to ensure comparability of the analyzed configurations by maintaining identical requirements w. r. t. launch site, target orbit, thrust-to-weight ratio (T/W) at launch, system architecture and payload mass, see also [1]. The ultimate objective is a contribution to the selection of feasible, promising and advantageous future European space transportation system concepts. The reference mission used for the predesign of various configurations consists of delivering 7.5 Mg to a geostationary transfer orbit (GTO) following a launch from Kourou. A unique feature of the presented work is its balanced compromise between the depth of the analysis for a specific configuration and the breadth of scope in terms of including different RLV stage return options, propellant combinations, engine cycles and staging velocities. Together with identical study requirements and assumptions, this compromise allows analyzing a greater number of potentially promising configurations on the one hand, and, on the other hand, performing a downselection based on sufficiently detailed calculations of all relevant aspects of a partially reusable space transportation system.

2 Description of study assumptions, requirements and methods applied

2.1 Study assumptions and general requirements

To identify the different configurations without ambiguity, a specific nomenclature is used. This configuration nomenclature specifies the type of fuel (RP1 = kerosene, C = methane, H = hydrogen), the rocket engine cycle (GG = gas generator, SC = staged combustion), the reusable first stage separation velocity class (Hi = high separation velocity, Med = medium separation velocity, Lo = low separation velocity) and the specific first stage return method (IAC = In-Air-Capturing, FB = fly-back). More details can be found in [1].

The following space transportation configurations with winged reusable first stages landing horizontally are analyzed and presented in this paper:

- Winged reusable first stages with fly-back capability (FB):
 - LH2/LOX SC with 6.6, 7.0 and 7.6 km/s upper stage ΔV
- Winged reusable first stages without fly-back capability, needing to perform either a down-range landing or rely on additional means as In-Air-Capturing (IAC):
 - LH2/LOX SC with 6.6, 7.0 and 7.6 km/s upper stage ΔV
 - LH2/LOX GG with 7.0 km/s upper stage ΔV

- LCH4/LOX GG with 7.0 km/s upper stage ΔV
- RP-1/LOX GG with 7.0 km/s upper stage ΔV

Parameters that are considered important to obtain comparable reusable first stages are: thrust-to-weight ratio (T/W) at launch and upper stage delta velocity (ΔV). A T/W of 1.4 is fixed for all configurations. Upper stage nominal ΔV s of 6.6, 7.0 and 7.6 km/s are considered for hydrogen staged combustion VTHL configurations. An upper stage ΔV of 7.0 km/s is used for all remaining configurations. The above ΔV values refer to nominal changes in velocity during powered flight, ΔV losses due to gravity, atmospheric drag and thrust orientation are not included. The upper stage ΔV is chosen to define the staging point of the launcher. Given a certain total mission velocity increment, the upper stage ΔV as well defines the ΔV of the reusable first stage. However, the upper stages are all classical, expendable rocket stages and hence using the ΔV of these conceptually similar systems is obvious. Details concerning the selection of upper stage ΔV s are given in [1].

The propellant combinations under investigation are LOX/LH2, LOX/LCH4 and LOX/RP-1. The liquid rocket engine propellant feed cycles considered are the staged combustion (SC) and gas generator (GG) cycles. Another important aspect is the assumption of the same fuel/oxidizer combination for the reusable first stages and the expendable upper stages. Also, the same type of engine with different expansion ratios ϵ is used for the lower and upper stages. The number of stages is set to two for all analyzed configurations regardless of the propellant combination. Tandem staging is used for all configurations. First and upper-stage diameters are identical. The propellant tanks of the reusable first stage as well as the expendable upper stage share a common bulkhead.

The principal study assumptions are summarized below:

- Reference mission: delivery of 7500 ± 150 kg to GTO
- Two stage, tandem staging configurations
- T/W of 1.4 at launch
- Geostationary Transfer Orbit (GTO) parameters: 250 km \times 35,786 km, 6° inclination
- Launch site: Kourou, French Guyana, 52.77° W / 5.24° N

For RLV stages a system mass margin of 14% is applied to all components except the propulsion subsystem. For expendable upper stages a margin of 10% is applied to all components except the propulsion subsystem. For components of the propulsion subsystem, a margin of 12% is applied for both RLV and expendable stages. Propellant reserves of 0.9% relative to the ascent propellant mass are foreseen for all fuel/oxidizer combinations. In addition, a propellant reserve of 25% is foreseen for the subsonic cruise

flight towards the launch site for winged fly-back boosters. The amount of fly-back propellant reserve is oriented upon the ASTRA LFBB configuration, see [9].

It should be noted that performance-wise winged reusable first stages without fly-back capability are equivalent to configurations landing down range of the launch site. From an RLV stage performance point of view no additional hardware and/or fuel for a flight back to the launch site are foreseen in the design of these stages. Furthermore, no consideration of any operations to bring the stages back to the launch site is performed within this study. In the following, the In-Air-Capturing method is the assumed method for return to the launch site of these RLV stages without fly-back capability.

2.2 Mass modelling and structural analysis

For the mass model definition, a combination of empirical methods and preliminary structural analysis based on selected load cases and structural concepts is used. The empirical mass estimation methods are based on stage loads and masses as well as geometrical parameters of the respective component. For the structural analysis, beam theory and methods for stiffened shells are used. Load cases considered for structural analysis have been limited to ascent load cases. Masses of major structural elements as tanks, inter stage structures and thrust frames are obtained by structural analysis. An example of a structural analysis result is shown in Fig. 2. Apart from the visualization of the entire system structure (except for the wing and empennage) a close view on one of the tanks including the chosen stringer and frame geometries (not to scale) is shown. Empirical methods are

applied for the majority of the remaining elements of the mass models. In particular, the VTHL first stages wing mass is determined with empirical methods. Dimensioning parameters are lateral acceleration, stage dry mass as well as wing area, span and maximum thickness of the wing (root airfoil section).

The following ascent load cases are considered for the structural analysis:

- Maximum dynamic pressure
- Maximum product of dynamic pressure and AoA
- Maximum acceleration
- Launch pad in presence of wind loads, launcher full and pressurized
- Pad release

Tanks are modelled as stringer-frame stiffened common bulkhead tanks from aluminum alloy AA2219. Tank pressures are between 3 and 4 bars. Aerodynamic forces are computed with empirical methods. Wing forces are introduced as discrete forces acting at several points along the wing root chord. A safety factor of 1.25 is applied.

2.3 Trajectory simulation and optimization

The ascent and descent trajectories are calculated using the DLR in-house tool TOSCA (Trajectory Optimization and Simulation of Conventional and Advanced Space Transportation Systems), [13]. This tool allows the calculation of ascent and descent trajectories flown by launchers, spacecraft and reentry vehicles through the solution of the equations of motion of a point mass (3 DoF). The atmospheric

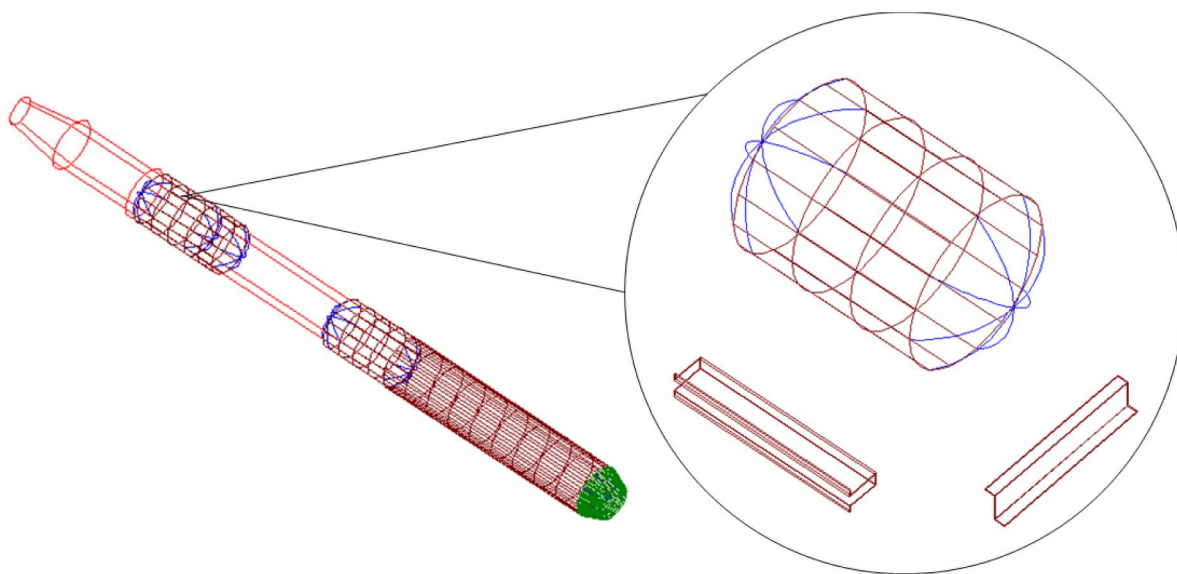


Fig. 2 An example of RLV first and ELV upper stage structural design

model used is oriented on the NRLMSISE00 model for Kourou, [14]. In all simulations, no wind is considered.

Ascent trajectory optimization is performed with a direct method and is based on Sequential Quadratic Programming (SQP). The payload mass delivered to orbit is the optimization objective while pitch rate, thrust angle (w. r. t. velocity), bank angle and thrust throttling are possible control variables. Furthermore, additional constraints can be defined. For the present study pitch rate and thrust angle are used as controls. Axial acceleration is in general limited to 50 m/s^2 . Rocket engines are throttled upon reaching this boundary. It is important to note that due to the requirement that the line of apsides of the GTO ellipse has to be in the equatorial plane, upper stage (US) flight is split into two thrust phases with a ballistic phase in between, see Fig. 3. The initial part of the ascent thus consists of the first stage thrust phase followed by the first thrust phase of the upper stage and allows reaching an intermediate orbit that is followed until crossing the equator. There, the upper stage is reignited and apogee reaches GEO altitude. Only the first part of the ascent towards the intermediate orbit is optimized, the second thrust phase of the upper stage is simulated. For most of the configurations the intermediate orbit has a perigee altitude of around 140 km, an apogee altitude of around 330 km and an inclination of 5.9° . Second phase upper stage delta velocity is approximately 2.4 km/s. The ascent trajectory of the VTHL reusable first stage concepts is on the one hand optimized with the objective of maximum payload to target

orbit, on the other hand, the trajectory is constrained considering the peak thermal loads during atmospheric reentry of the reusable stage. In particular, it is attempted to lower the flight path angle at separation by increasing the pitch rate as long as dynamic pressure at separation is below 1 kPa and upper stage thrust angle (w. r. t. velocity) is able to balance out the higher pitch rate. This approach results in small losses of payload mass but significantly reduces the thermal loads during the subsequent reentry phase.

No reentry trajectory optimization is performed for the VTHL reusable first stages. The reentry trajectories are iteratively simulated. Control of normal acceleration is achieved by variation of angle of attack. A limit of 4 g is set for the normal acceleration. Bank angle is varied to initiate a turn and achieve the desired heading towards the launch site.

Following the atmospheric reentry and turn, air-breathing engines are used for a powered return to launch site in case of the fly-back configurations. The amount of fuel required for the subsonic return flight depends on the stage mass, the distance to be travelled, the efficiency of the air-breathing propulsion system, the aerodynamic performance of the fly-back booster in the subsonic regime as well as the flight Mach number and altitude. Initially, the return cruise flight using air-breathing propulsion was simulated with a 4 DoF approach to determine the fly-back fuel mass, see [15]. Currently, a simplified approach using the Breguet equation with average values of aerodynamic and propulsion efficiency coming from the detailed simulations is used to calculate

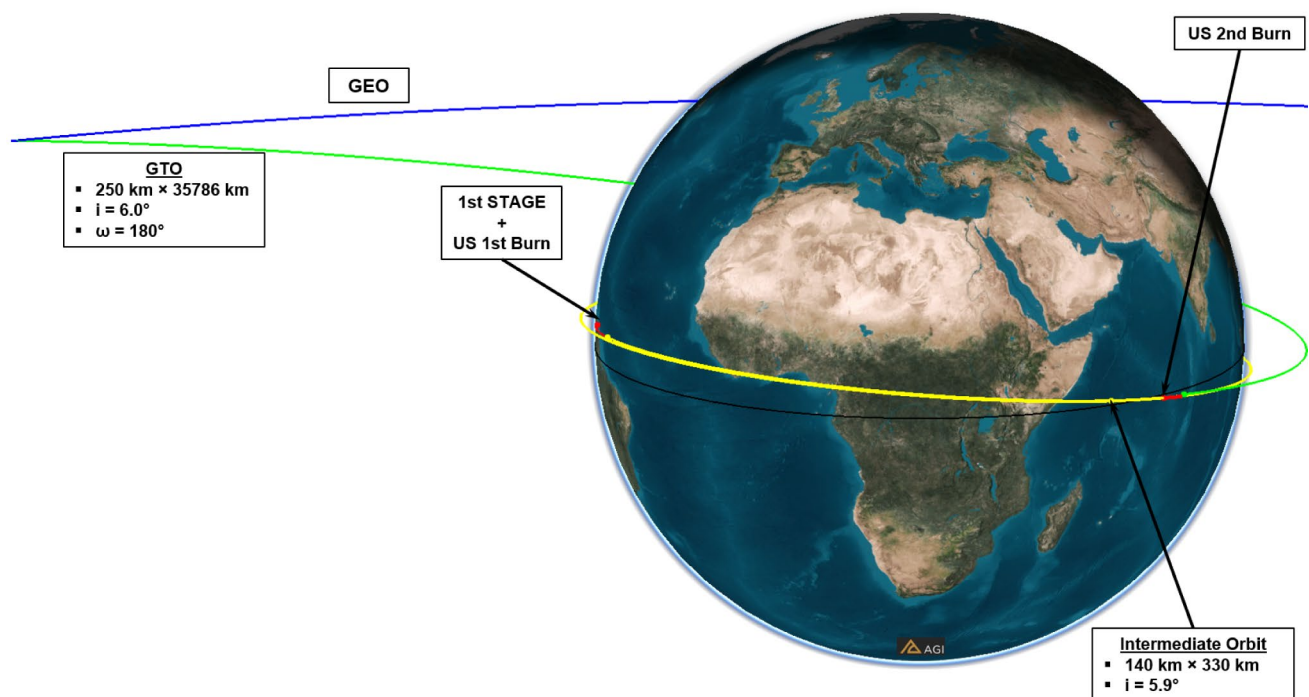


Fig. 3 Strategy followed for the ascent of the VTHL configurations

the fly-back fuel mass. For the in-air-capturing, the capture and tow-back are not simulated as this portion has, apart from the hardware to be installed on the returning stage, no impact on the launcher performance. The aforementioned hardware is considered within the mass budget.

2.4 Modelling of aerodynamics, aerothermodynamics and thermal protection system

Aerodynamic forces and moments are modelled with DLR in-house tools CAC (Calculation of Aerodynamic Coefficients) and HOTSOSE (Hot Second Order Shock Expansion). These programs allow the fast calculation of aerodynamic coefficient maps required for trajectory simulations depending on the angle of attack, Mach number and altitude or Reynolds number. CAC is used for ascent aerodynamics and the sub- and supersonic regimes of the reentry. HOTSOSE is used in the hypersonic regime of the reentry.

CAC is based on empirical and analytical methods and follows a superposition approach for obtaining total aerodynamic coefficients for a certain geometry. The methods implemented can be based on relationships from potential theory such as e. g. lifting-line theory for wing lift calculation as well as empirical relationships resulting from experimental work. More information on the theoretical

background and the methods applied within the CAC program can be found in [16] and [17].

HOTSOSE is a tool for hypersonic aerodynamics and aerothermodynamics. The implemented aerodynamical methods are based on inviscid surface inclination methods applicable in hypersonic flow. Within the tool, e.g. the modified Newtonian method and the second-order shock expansion method are used. Besides modelling air as an ideal gas, the consideration of high-temperature effects in HOTSOSE is possible. Functions for the thermodynamic and transport properties are implemented for chemically reacting air in equilibrium. Apart from aerodynamic coefficients as functions of angle of attack and Mach number, temperature and heat flux distributions can be obtained. Surface temperature is user-specified or calculated based on the assumption of radiation adiabatic equilibrium. An exemplary surface temperature distribution is shown in Fig. 4. More details can be found in [18].

The Thermal Protection System (TPS) is a crucial component for VTHL configurations. In the frame of the current study, the mass of the thermal protection system is estimated based on the selected TPS materials and the thermal loads experienced during atmospheric reentry. The VTHL first stages discussed in this work employ TPS materials such as Space Shuttle-type Flexible Reusable Surface Insulation (FRSI), Tailorable Advanced Blanket Insulation (TABI) and Alumina Enhanced Thermal Barrier (AETB) ceramic tiles as well as ceramic matrix composites (CMC) for highly loaded

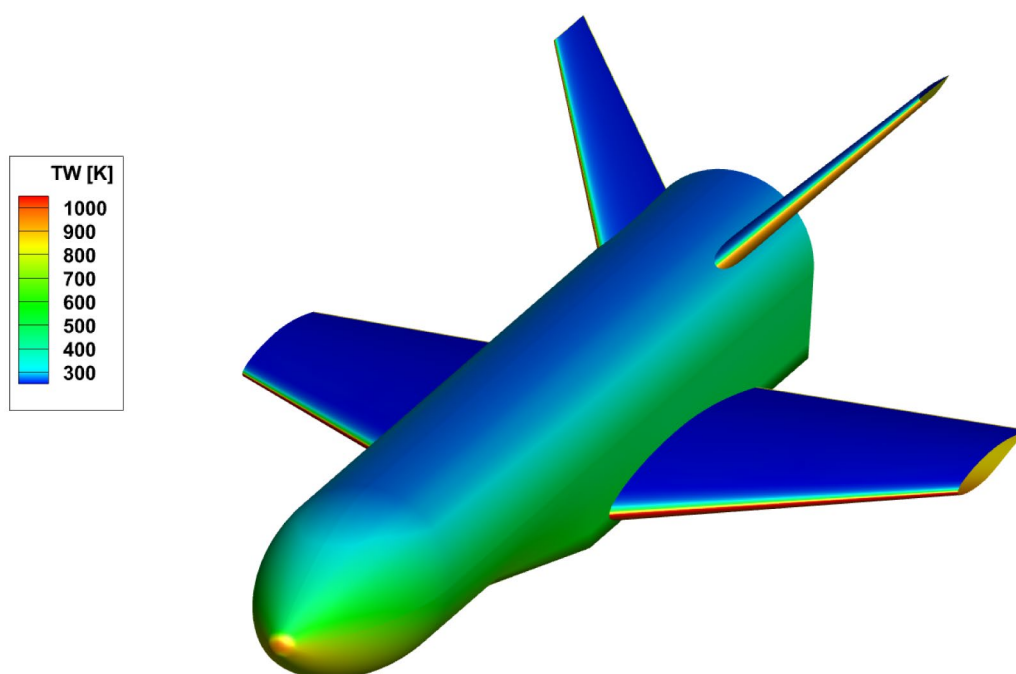


Fig. 4 Example of HOTSOSE results in the form of equilibrium temperature distribution – first stage of H SC Lo IAC configuration (altitude = 47 km, AoA = 46 deg, Ma = 5.9)

areas. A more detailed description of these materials can be found in [19]. The external thermal loads are determined with the tool HOTSOSE. Following the determination of the external loads and the definition of a maximum acceptable temperature limit beneath the thermal protection, the TPS thickness and mass are iteratively calculated assuming one-dimensional heat transfer. Radiation adiabatic equilibrium is assumed for the outer wall.

2.5 Propulsion and propellant supply system

To ensure comparability of the designed launchers, generic engines with identical baseline assumptions are needed for the systematic assessment and comparison of future RLV stages. The selected technical characteristics of these generic engines are oriented towards data of existing types as well as previous or ongoing development projects, [3]. The two rocket engine cycles most commonly used in first or booster stages are included in the study:

- Gas-Generator cycle (GG)
- Staged-Combustion cycle (SC)

The main combustion chamber (MCC) pressure is commonly set to 12 MPa for the gas-generator type. This pressure is not far from the useful upper limit of this cycle but is assumed necessary to achieve sufficient performance for the RLV stages, [3]. In the case of staged combustion engines, the MCC pressure is fixed at 16 MPa. This moderate value has been chosen considering the limited European experience in closed-cycle high-pressure engines, [3]. Nozzle expansion ratios in the first stage are selected according to optimum performance. Expansion ratio is set to 35 for both gas generator and staged combustion engines. The upper-stage engines are derived from the first stage engines with the only difference being the expansion ratio. Its value is set to 120 as a reasonable first assumption and considering inter-stage structure length requirements.

All preliminary engine definitions have been performed by simulation of steady-state operation at 100% nominal thrust level using the DLR tools LRP (Liquid Rocket Propulsion) and NCC (Nozzle Contour Calculation) as well as the commercial tool RPA (Rocket Propulsion Analysis). Any

potential requirements specific to transient operations are not considered in this early design study. Turbine entry temperature (TET) is set around 750 K and kept in all cases below 800 K to be compatible with the increased lifetime requirement of reusable rocket engines, [3]. Further, all engines considered in this study are designed with regeneratively cooled combustion chambers and regenerative or dump-cooling of the downstream nozzle extensions. Table 1 presents the mixture ratio (MR), the sea level (SL) and vacuum (Vac.) specific impulse (Isp) for the first and upper stage rocket engines considered within the study. More details on the performed rocket propulsion analysis can be found in [3].

The propellant supply system including feedlines, fill/drainlines and the pressurization system was modelled using the DLR in-house tool PMP. This program is able to calculate the respective masses for these systems by calculating the propellant and pressurizing gas flow throughout the whole mission and thus sizing the required hardware. Autogenous pressurization is assumed for all configurations except the LOX/RP-1 systems. Here the RP-1 tanks are pressurized with helium. The tool also calculates the mass of the cryogenic insulation of the tanks. It is important to note that insulation was only considered a necessity in the case of LOX/LH2 launchers due to the low temperature of LH2. In the case of hydrocarbon launchers, no insulation is used since it adds mass and it is assumed that it is technically feasible to fly cryogenic propellants without insulation (e. g. Falcon 9 with LOX/RP-1). This assumption is to be verified by a thermal analysis beyond the scope of this study.

In the case of FB as a reusable first stage return-mode, air-breathing engines are used for the return cruise flight. Their efficiency, i.e. their specific fuel consumption or specific impulse, is important not only from an RLV, but also from an overall configuration design point of view. The specific impulse of air-breathing engines depends on the type of fuel and is one of the main drivers for fly-back fuel mass. While kerosene would be a classic choice its specific impulse is in the area of 4000 s, whereas hydrogen potentially offers a specific impulse of more than 10000 s for typical turbofan engines at subsonic Mach numbers.

Thus, the selected air-breathing engines for FB configurations within this study are modified EJ200 of MTU Aero Engines without afterburner that can be operated with

Table 1 First and upper stage rocket engine data, [3]

Propellants	First Stage				Upper Stage			
	LOX/RP-1	LOX/LCH4	LOX/LH2		LOX/RP-1	LOX/LCH4	LOX/LH2	
Cycle	GG	GG	GG	SC	GG	GG	GG	SC
MR [-]	2.25	2.5	6	6	2.25	2.5	6	6
SL Isp [s]	267	276	351	385	—	—	—	—
Vac. Isp [s]	320	331	418	438	338	349	440	459

hydrogen after minor modifications, see [20]. Furthermore, they have a high specific thrust and thrust-to-weight ratio. Thrust and specific fuel consumption characteristics of EJ200 have been calculated with DLR in-house air-breathing propulsion tool. The calculated installed thrust characteristics as a function of altitude for subsonic Mach numbers from 0 to 0.8 is shown in Fig. 5. A summary of calculated EJ200 characteristics is given in Table 2.

3 Preliminary design of VTHL configurations

In this section, the preliminary design of the VTHL configurations as well as specific aspects of winged reusable first stage design are discussed. All analyzed configurations are two-stage systems and use tandem staging. A selection of configurations with a nominal upper stage delta velocity of 7.0 km/s is shown in Fig. 6.

The following structural segments are considered within the mass model and/or structural analysis for all analyzed configurations (top to bottom): payload fairing, upper stage fuel tank, upper stage oxidizer tank, upper stage thrust frame, interstage structure, lower stage oxidizer tank, lower stage fuel tank, lower stage wing, lower stage thrust frame, rear skirt. The length of the interstage structure is influenced by the length of the upper stage engine and the first stage nose structure. First stage nose structure length is set to 7 m for all configurations. Upper stage engine expansion ratio is fixed to $\varepsilon = 120$ for all studied variants, [3]. However, depending on the choice of propellant combination and first

Table 2 EJ200 calculated installed characteristics for operation with H₂ at return flight conditions

Ma [-]	Altitude [km]	Thrust [kN]	sfc [g/kN s]	Isp [s]
0.3	4.0	35	9.01	11,300
0.4	5.0	32	9.30	11,000
0.5	6.0	29	9.57	10,700
0.6	7.0	26	9.78	10,400
0.7	8.0	23	9.91	10,300

stage separation velocity and thus the efficiency as well as the thrust requirement for the upper stage engine, its nozzle size can differ substantially. Stage diameters are between 5.0 and 6.0 m and overall configuration height is between 70 and 83 m.

3.1 Winged reusable first stage architecture

The general layout of a VTHL reusable first stage is shown in Fig. 7 exemplified by the H SC Med IAC stage. The LOX tank is shown in blue, while the LH₂ tank is shown in red. All analyzed VTHL first stages are equipped with a single delta wing and a V-tail. The single delta wing uses an RAE 2822 airfoil and has a leading-edge sweep angle of 40 degrees. The chord lengths of the main wing and V-tail are functions of the stage length. Identical ratios of chord length to overall stage length are used for all configurations. From the point of view of pure subsonic aerodynamic performance, a straight wing with a high aspect ratio would be

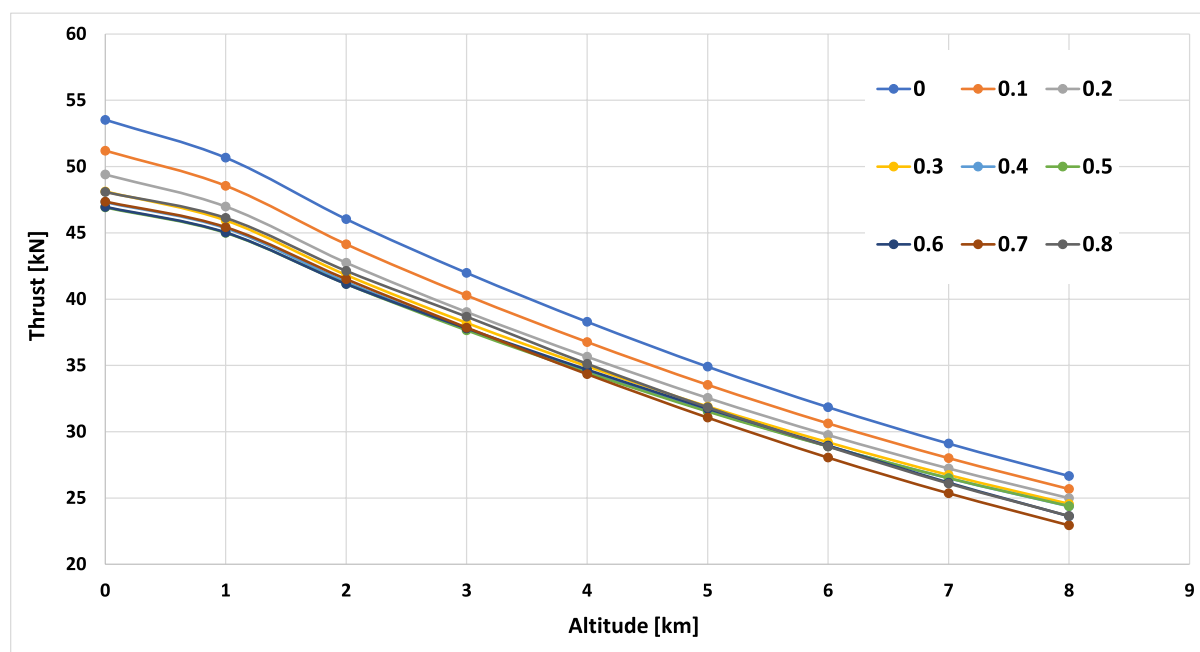


Fig. 5 Calculated installed thrust characteristics of EJ200 turbofan

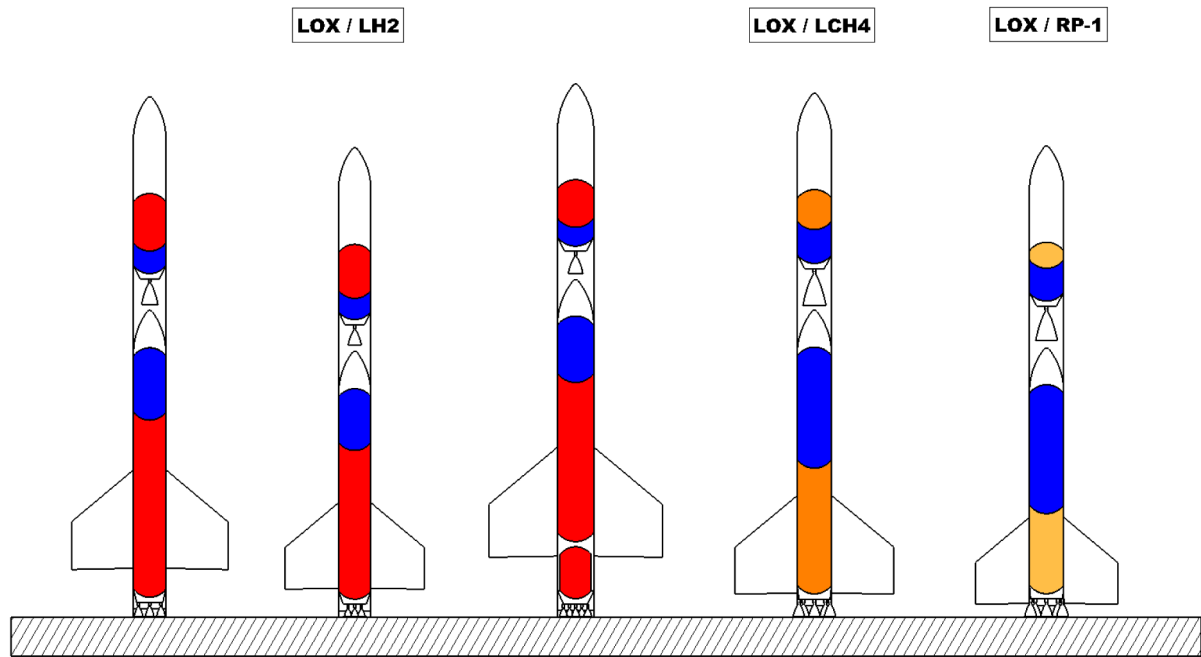


Fig. 6 VTHL configurations with 7.0 km/s upper stage delta velocity, LOX = blue, LH2 = red

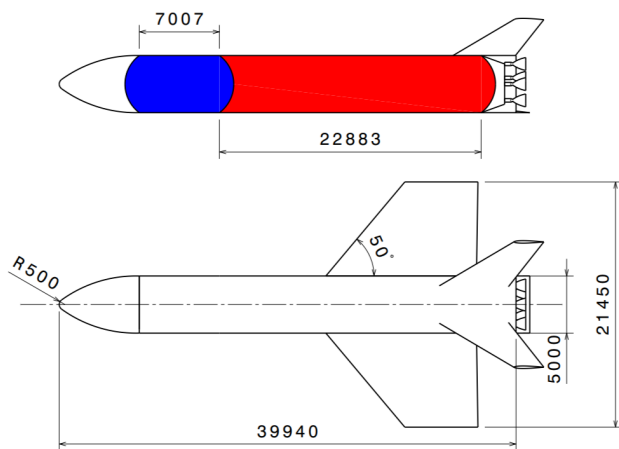


Fig. 7 H SC Med IAC VTHL reusable first stage, LOX = blue, LH2 = red (unit of length: mm)

advantageous. However, this is not realistic for an RLV stage with a fixed wing. The analyzed single delta wing fly-back stages have L/D ratios between 5 and 6 at subsonic Mach numbers. Typical trimmed lift-to-drag ratios of the analyzed VTHL winged reusable first stages are shown in Fig. 8 for subsonic, supersonic and hypersonic Mach numbers.

Several aspects have an influence on the stage diameter: the dimensions of the payload to be transported, the accommodation of first stage rocket engines and the desired length-to-diameter ratio of the first stage. The first two aspects are setting lower limits for the stage diameter. For VTHL

configurations a length-to-diameter ratio of 9 is considered desirable for the winged reusable first stage for aerodynamic stability and trimmability reasons. A body flap and wing flaps are used for aerodynamic control. The body flap is used exclusively in the hypersonic regime and is deflected only downward. The minimum stage diameter considered for the presented VTHL configurations is 5.0 m. The nose segment radius is 0.5 m for all analyzed configurations. In the case of FB as return mode, air-breathing engines are located in the nose segment (see box in Fig. 9) and an additional non-integral fly back fuel tank is placed behind the main, integral LH2 tank, see Fig. 9. Between four and six air-breathing engines are used on FB stages.

3.2 Design iteration loop

This subchapter presents the design iteration loop followed by the iterative preliminary analysis. Independent of the VTHL return option, the analysis iteration is initiated with a design that is based on an initial guess and experience with similar or comparable configurations. Propulsion data, a mass model and an aerodynamics model allow a first ascent trajectory simulation and optimization. This is the case for either of the two considered return options, namely fly-back (FB) and In-Air-Capturing (IAC). Flow charts for both of the analyzed VTHL return options are shown in Fig. 10 and Fig. 11.

After the first ascent trajectory calculation, the performance in the defined target orbit is assessed. In case the payload

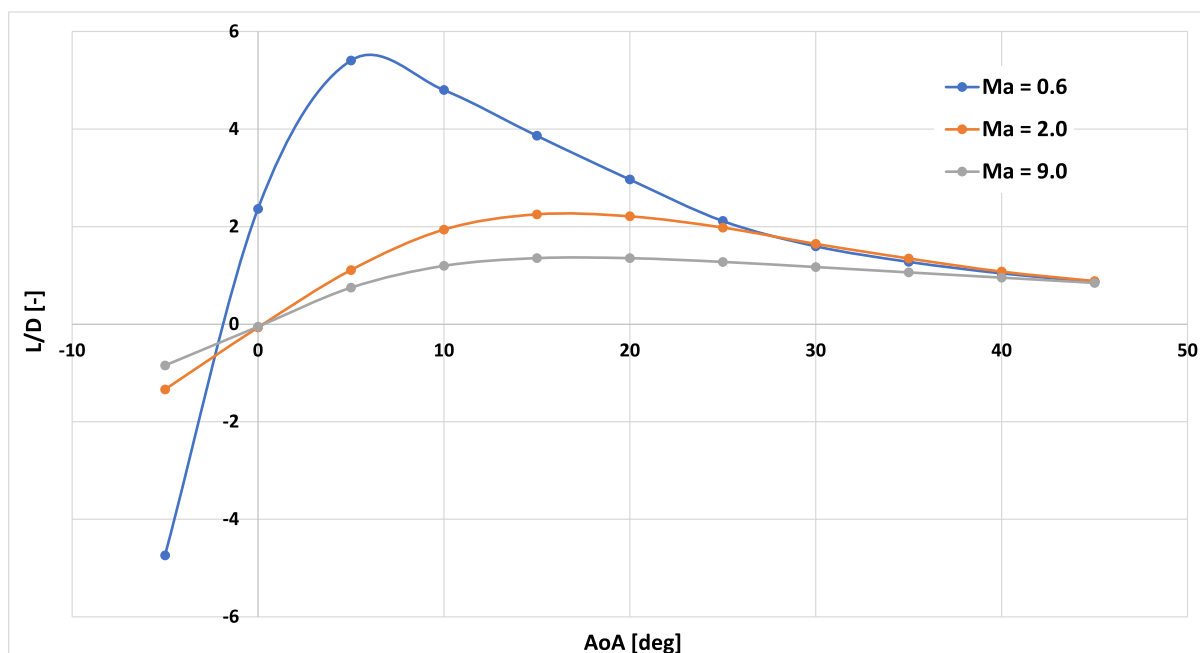
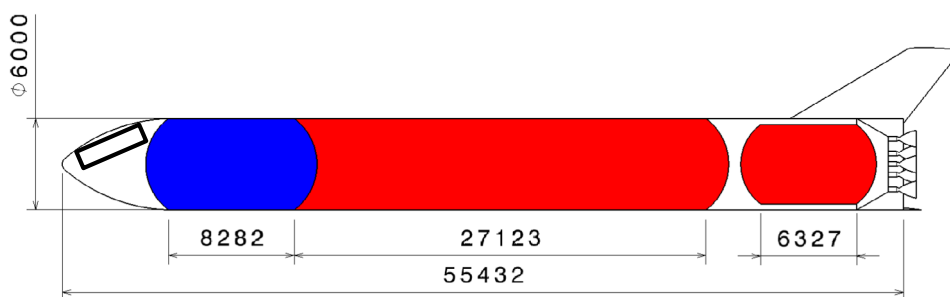


Fig. 8 Trimmed lift-to-drag ratios of winged RLV stages

Fig. 9 H SC Hi FB VTHL reusable first stage, LOX = blue, LH2 = red



target is not met, a reiteration of the ascent performance is done until the resulting payload mass, the overall configuration and also the particular stages are compliant with the defined requirements. The necessary adaptations can include changing the ascent propellant masses, the rocket engine thrust as well as the geometry of the configuration. Once the payload performance is within the defined boundaries, a calculation of the winged reusable first stage descent trajectory can be performed. The state at separation of the first stage defines the initial conditions of the descent calculation. Depending on the particular reentry trajectory and the associated aerothermal loads, the thermal protections system (TPS) mass is determined and compared with the current value in the mass model. Convergence is reached when no substantial difference exists between the thermal protection system mass calculation based on the latest reentry trajectory and the TPS defined in the previous step of the mass model. In contrast to the IAC configurations whose design iteration loop includes

ascent and atmospheric reentry calculations only, in the case of FB the return cruise flight back to the launch site with air-breathing engines is as well calculated and part of the iteration, see Fig. 11. This means that depending on the distance to the launch site after performing the atmospheric reentry and turn, the stage mass, the specific impulse of the air-breathing engines as well as the trimmed subsonic lift-to-drag ratio a fly-back fuel mass is calculated that is again input to the mass model and the entire design iteration loop is continued until convergence is achieved, see Fig. 11.

4 Results

4.1 Overview on investigated configurations

In this work, nine VTHL configurations are analyzed. A data summary of the nine converged VTHL configurations

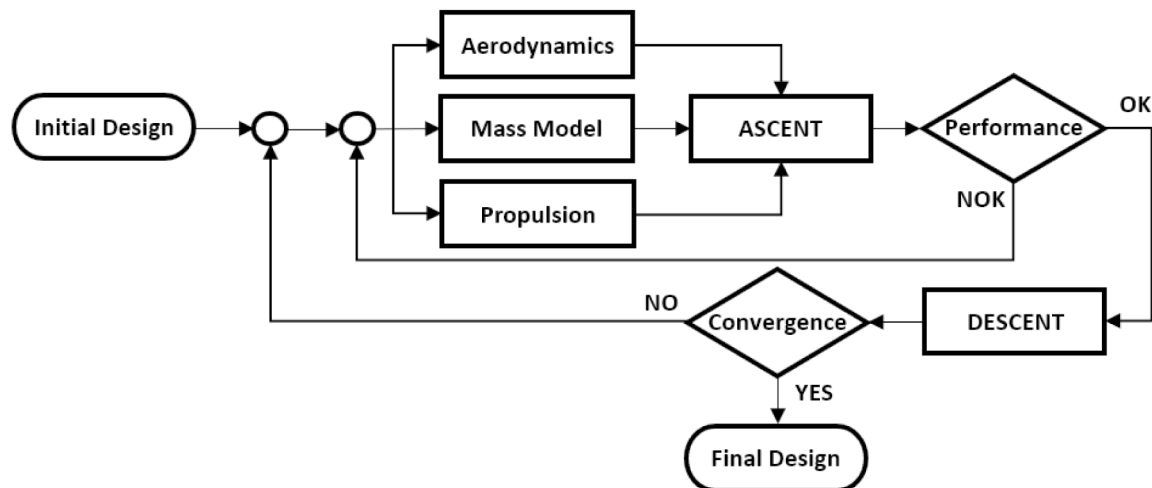


Fig. 10 Design iteration loop for IAC systems

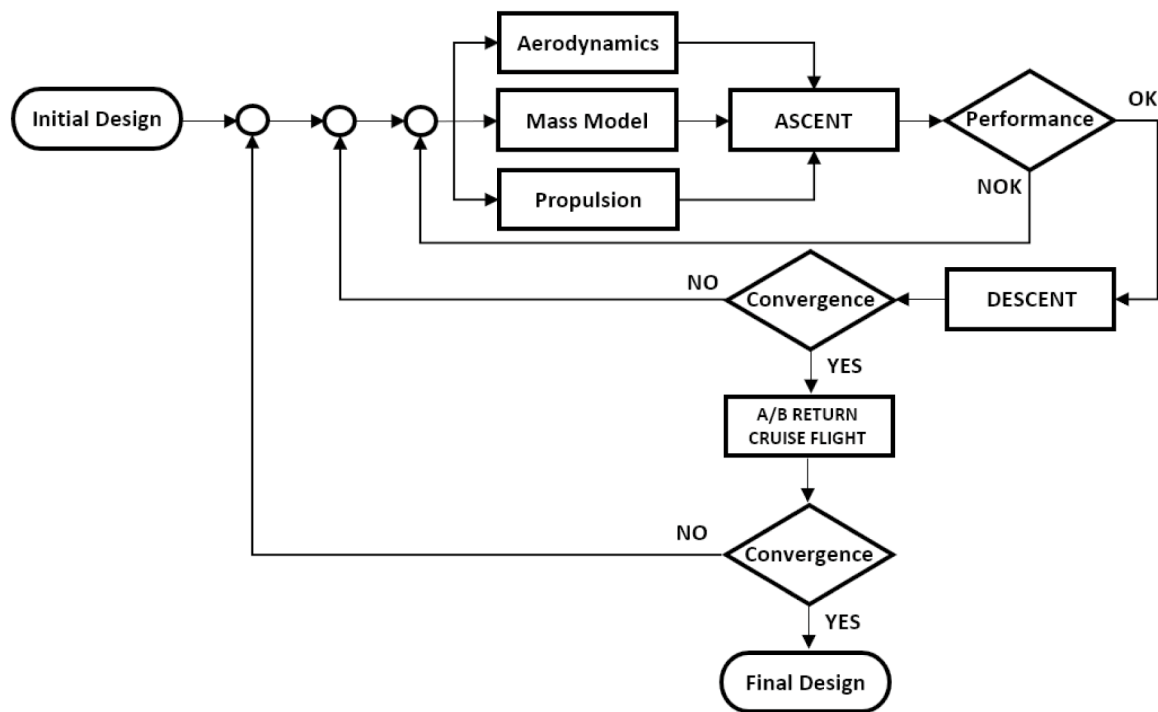


Fig. 11 Design iteration loop for FB systems

is given in Table 3. Six out of them are relying on staged-combustion rocket engines, the remaining ones are using gas-generator engines. One configuration each uses LOX/LCH4 and LOX/RP-1 as propellant combination, the remaining ones are LOX/LH2 designs. For all designs

the same propellant combination is used on the RLV and the expendable upper stage, hybrid configurations are not investigated. Gross lift-off masses (GLOM) span a range from approximately 330 Mg to 870 Mg, the corresponding payload fractions are between 0.9% and 2.3%.

Table 3 Summary of investigated VTHL configurations

		LH2 SC			LH2 SC			LH2 GG	LCH4	RP-1
Return Option		FB	FB	FB	IAC	IAC	IAC	IAC	IAC	IAC
Engine Cycle	–	SC	SC	SC	SC	SC	SC	GG	GG	GG
2nd stage Δv	[km/s]	6.6	7.0	7.6	6.6	7.0	7.6	7.0	7.0	7.0
First Stage Separation Velocity Class	–	Hi	Med	Lo	Hi	Med	Lo	Med	Med	Med
Winged Reusable First Stage										
Ascent Propellant	[Mg]	350	275	230	225	205	190	245	575	635
Total dry mass	[Mg]	83.0	66.3	55.7	40.1	35.4	33.8	45.3	53.2	49.5
Propulsion mass	[Mg]	20.9	17.4	14.8	8.6	8.1	8.0	7.7	15.1	14.9
No. of engines	[–]	9	7	5	7	6	5	7	9	9
Single Engine Thrust (sea level)	[kN]	814	870	1098	681	757	908	766	1246	1323
Expendable Upper Stage										
Ascent Propellant	[Mg]	57.5	68.1	83.4	56.4	64.6	83.2	73.3	150.0	150.4
Total dry mass	[Mg]	6.1	6.3	7.2	5.4	5.8	6.8	6.0	7.7	7.5
Propulsion mass	[Mg]	1.7	1.8	2.2	1.4	1.6	1.9	1.4	2.3	2.3
Engine Thrust (vacuum)	[kN]	967	1035	1304	810	900	1080	961	1574	1674
Launcher Configuration										
Height	[m]	82.7	80.5	80.9	72.4	70.8	71.7	78.9	78.3	70.2
Diameter	[m]	6.0	5.6	5.2	5.0	5.0	5.0	5.0	5.3	5.3
Payload to GTO	[Mg]	7.59	7.52	7.41	7.46	7.59	7.46	7.38	7.43	7.58
GLOM	[Mg]	528.9	442.4	400.8	344.4	328.8	332.5	389.3	814.5	870.9
P/L Fraction	[%]	1.4	1.7	1.8	2.2	2.3	2.2	1.9	0.9	0.9

4.2 Configuration and stage mass

To begin with, the Gross Lift-Off Masses (GLOM) of all analyzed configurations are shown in Fig. 12. The configurations are ordered by decreasing overall gross lift-off mass also making the distinction between reusable first stage and expendable upper stage.

It is remarkable that the hydrocarbon fuel configurations are by far the heaviest launchers. With a GLOM of 871 Mg and 815 Mg respectively, both the kerosene and the methane IAC configuration show lift-off masses of more than 800 Mg. In contrast, the hydrogen SC configurations using the IAC return option have a GLOM of around 330 Mg only. A relatively high GLOM from 401 to 529 Mg is found in the case of the configurations having reusable first stages employing the fly-back return method, with GLOM increasing significantly with first stage separation velocity. Gross lift-off masses below 400 Mg all belong to hydrogen IAC configurations. Here the GG configuration shows a GLOM of 389 Mg whereas the SC configurations using hydrogen as fuel and IAC as a return method have lift-off masses that are even approximately 15% lower.

The reusable first stage dry mass is shown in Fig. 13. Apart from showing the total dry mass of the RLV stage, Fig. 13 also displays the mass of the first stage rocket engines and its relative fraction within the total dry mass. The mass of rocket propulsion and its fraction play a role from the

point of view of cost estimation since rocket engines represent a large portion of a reusable stage's value. Looking at the comparison of reusable first stage dry mass, the highest dry mass values going from 83 to 56 Mg are obtained by FB configurations. Methane and kerosene first stages have overall dry masses of 53 Mg and 49 Mg respectively with corresponding rocket engine mass fractions of 28% and 29.7% which are the highest among all considered configurations. While the hydrogen gas-generator configuration has a total dry mass of 45 Mg and an engine fraction of 16.6%, the hydrogen staged combustion configurations using In-Air-Capturing as the first stage return option have the lowest dry masses of 40 Mg to 34 Mg. The corresponding rocket engine fractions are 21% to 23.1% in this case. For the hydrogen staged combustion FB and IAC configurations with different first stage separation velocities, dry mass increases with separation velocity while the rocket engine fraction is slightly decreasing.

4.3 Reusable first stage reentry trajectories and loads

The calculation of reusable first stage reentry trajectories is an essential part of the presented analysis. In general, loads experienced by the reusable stage when reentering the atmosphere have a major influence on the technical feasibility of the transportation system and its potential economical

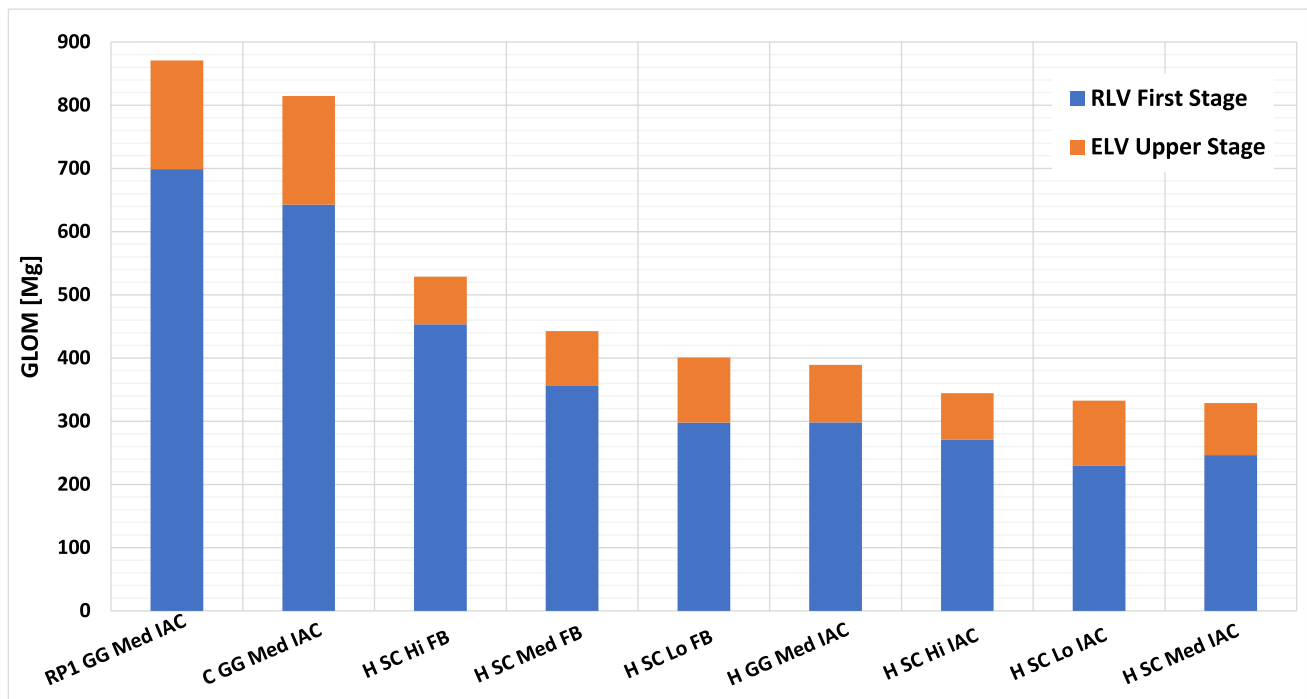


Fig. 12 Gross lift-off mass of analyzed VTHL configurations

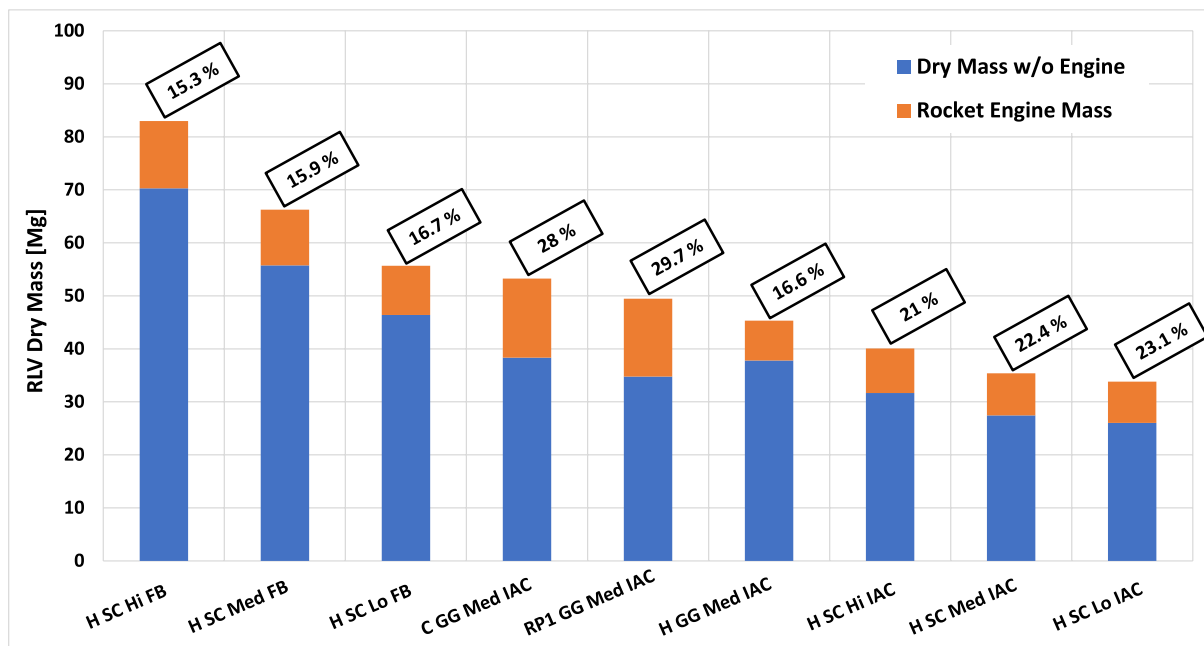


Fig. 13 RLV stage dry mass incl. rocket engine mass fraction

attractiveness. Keeping the loads low is thus imperative. In particular, the thermal protection system mass of all analyzed winged reusable first stages was determined based on reentry trajectory calculations and the related aerothermal loads present along the flight path. In addition, the fly-back

fuel mass is a direct consequence of the distance to launch site resulting from the reentry trajectory calculation.

Reentry trajectory shape and loads are strongly dependent on the initial conditions at the beginning of the atmospheric reentry of the reusable first stage. Table 4 lists the

separation conditions, in particular velocity, altitude and flight path angle (FPA). The flight path angle at separation is positive and initially the reusable first stages continue to climb, however, after passing the apogee, approximately the same flight path angle magnitude is present when the stages begin to decelerate entering denser layers of the atmosphere. Thus, the flight path angle at separation has a strong influence on the reentry trajectory and the encountered mechanical and thermal loads. Therefore, for the ascent trajectories optimized for maximum payload in the target orbit also constraints for the pitch rate at launch are imposed. These constraints lead to reductions in flight path angle magnitude and only limited losses of payload performance. A threshold

of 1 kPa for dynamic pressure at separation is respected as well to ensure a safe separation of the reusable first stages.

Reentry trajectories of all analyzed RLV stages are shown in Fig. 14 in terms of altitude as a function of Mach number. In this Mach-Altitude map the three different separation velocity classes are clearly identifiable. After first stage separation at altitudes between 60 and 67 km, the stages continue to climb reaching apogee altitudes up to 130 km, although in most of the cases the maximum altitude does not surpass 90 km.

When reaching denser layers of the atmosphere, the maximum stagnation point heat flux is reached at Mach numbers between 5.5 and 9.0 at altitudes between 30 and 50 km. The evolution of nose stagnation point heat flux along the reentry trajectory for all analyzed RLV stages is shown in Fig. 15 over the free-stream Mach number. Stagnation point heat flux is calculated using an empirical relation for a radius of 0.5 m which is the nose radius of the analyzed reusable first stages. Apart from the nose stagnation point heat flux, dynamic pressure and lateral load factor are also in the focus of the reentry trajectory analysis. For all reentry trajectories a limit of 4.0 is set for the lateral load factor n_z . Maximum values of n_z , dynamic pressure and stagnation point heat flux seen by the RLV stages during reentry are shown in Table 5.

Concerning dynamic pressure and heat flux the following is observed. Looking at the FB and IAC staged combustion configurations, one can see that with lower separation velocity maximum heat flux tends to decrease while the dynamic

Table 4 Summary of RLV separation conditions

RLV Stage	Velocity [km/s]	Altitude [km]	FPA [deg]
H SC Hi FB	3.28	65.6	9.0
H SC Med FB	2.78	63.8	12.4
H SC Lo FB	2.27	60.1	17.5
H SC Hi IAC	3.16	67.4	10.5
H SC Med IAC	2.82	63.1	11.8
H SC Lo IAC	2.26	59.5	17.3
H GG Med IAC	2.67	64.6	17.5
C GG Med IAC	2.73	62.1	20.0
RP1 GG Med IAC	2.87	64.1	21.2

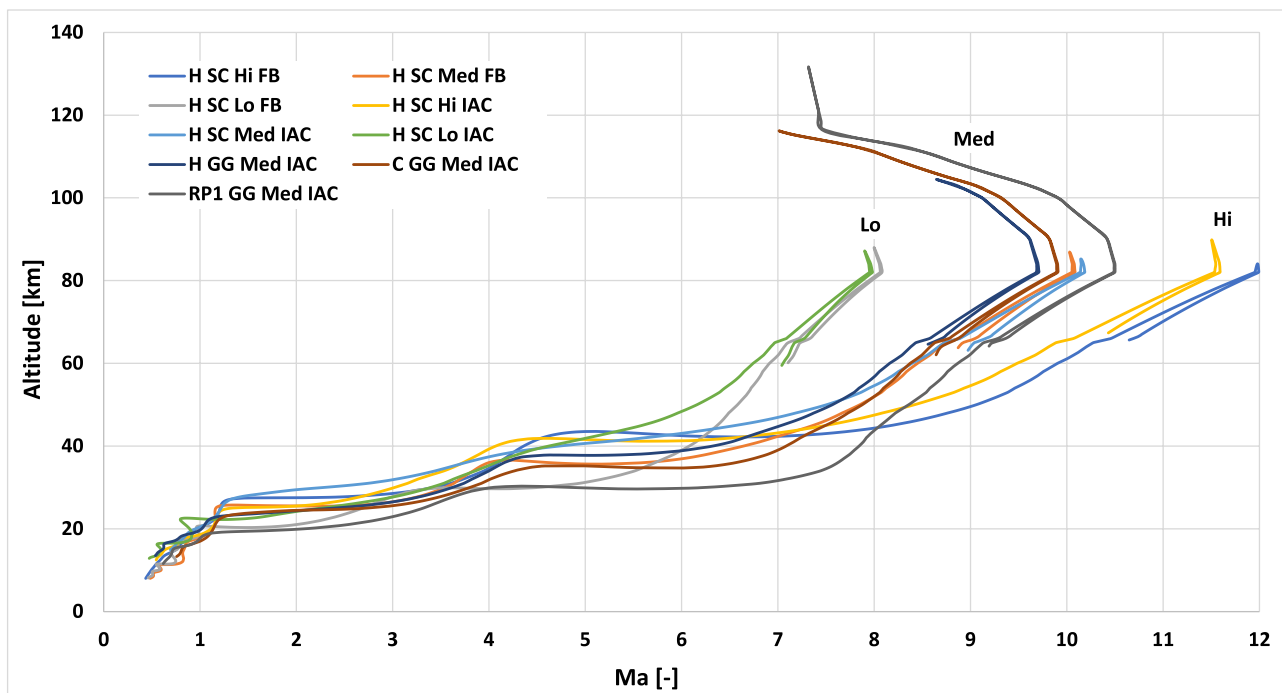


Fig. 14 Mach-altitude profiles of RLV stage reentry trajectories

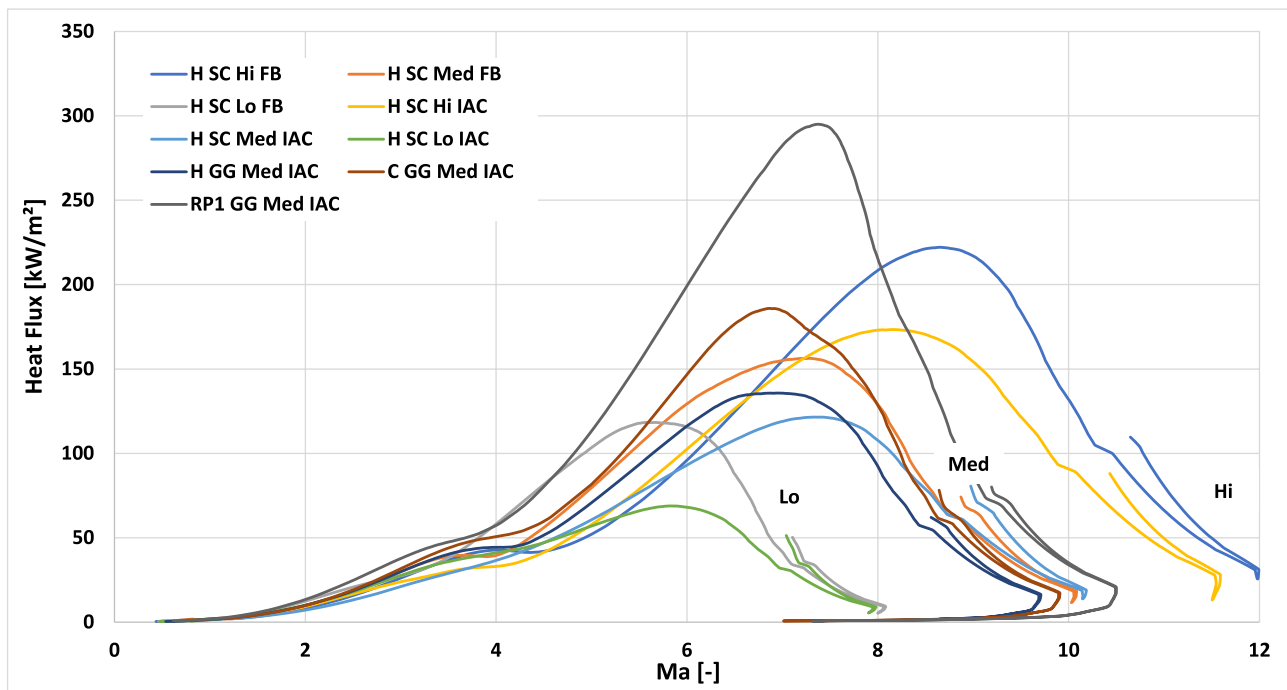


Fig. 15 Nose stagnation point Heat flux along RLV stage reentry trajectories

Table 5 Summary of maximum loads along reentry trajectories of RLV stages

RLV Stage	n_z [-]	P_{dyn} [kPa]	\dot{q} [kW/m ²]
H SC Hi FB	3.4	9.9	222
H SC Med FB	4.0	12.8	156
H SC Lo FB	4.0	17.8	118
H SC Hi IAC	3.9	8.4	173
H SC Med IAC	3.9	5.8	122
H SC Lo IAC	3.9	10.7	69
H GG Med IAC	4.1	12.9	136
C GG Med IAC	4.1	16.2	186
RP1 GG Med IAC	4.0	34	295

pressure tends to increase. The former is explained by the strong correlation between velocity and stagnation point heat flux. The latter is explained considering the flight path angle at separation, see Table 4. A strong increase of flight path angle magnitude is present with shorter first stage burn durations and lower separation velocities. This leads to steeper reentry trajectories and mostly higher peak dynamic pressures (proportionality to the square of velocity), while for the heat flux the influence of velocity is dominating (proportionality to the cube of velocity).

For the majority of the stages maximum heat flux and dynamic pressure stay below 200 kW/m² and 20 kPa respectively. However, in the case of the kerosene reusable first

stage a maximum heat flux of 295 kW/m² and a dynamic pressure of 34 kPa are reached although its separation velocity class is medium. On the one hand, this is due to the high separation flight path angle of more than 21 deg (see Table 4) that leads to a steep reentry trajectory and a high apogee altitude (see Fig. 14). On the other hand, the ballistic coefficient of the kerosene stage is relatively high compared to the hydrogen first stages. Among the IAC stages the kerosene configuration has the most compact dimensions and at the same time the highest dry mass. This leads to a deep dive into the atmosphere and the observed relatively high maximum values of heat flux and dynamic pressure. An aerodynamic redesign might be considered in the future to improve this situation. It is important to note that in any case the preliminary RLV stage sizing is consistent as the encountered loads are used for the mass estimation of TPS.

5 Discussion of results

In this chapter, the results of the performed analysis are regarded from different points of view concentrating on a specific aspect of launch vehicle performance and/or reusable launch vehicle design. These aspects are the following: general performance characteristics of the transportation system, propellant combination and rocket propulsion efficiency, launch vehicle staging, winged reusable first stage return option and rocket engine cycle. This is done in line

with the formulated overall objective of this analysis that is to contribute to the identification of promising future European transportation systems.

5.1 Launch vehicle performance

The importance of the general launch vehicle performance might be considered secondary from a cost engineering point of view frequently brought up in connection with partially reusable space transportation systems. Apart from the complexity and the difficulties associated with cost estimation for partially reusable launch vehicles, this completely would neglect the fact that partially reusable systems need as well to be attractive from a performance point of view to become competitive. In general, reusability of any kind reduces the performance of a launch vehicle. Therefore, in the case of reusable systems the selection of high-performance design options has an even higher significance than in the case of expendable launch vehicles.

One way to compare different launch vehicle configurations is to focus on the ratio of the payload mass that is delivered to the target orbit and the lift-off mass of the transportation system. This so-called payload fraction is defined as:

$$\Pi = \frac{m_{P/L}}{m_{GLOM}} \quad (1)$$

For the configurations analyzed in this work the payload mass is fixed to $7.5 \text{ Mg} \pm 150 \text{ kg}$ so that variations in payload fraction are completely due to variations in gross lift-off

mass. However, the use of the dimensionless payload fraction is preferred since both payload mass and GLOM are reflected and even a comparison with other launch vehicles, that might have different payload masses and might serve different missions, would become possible.

The payload fraction of all analyzed configurations is shown in Fig. 16. First, there is a remarkable difference in payload fraction between the hydrocarbon configurations and the most performant hydrogen staged combustion variants. While the methane and kerosene configurations have payload fractions of 0.9% the maximum payload fraction achieved by the H SC Med IAC configuration is 2.3%, a factor of 2.6. Also noteworthy is the performance of the hydrogen staged combustion FB configurations, that are able to achieve payload fractions of 1.4% to 1.8% despite the disadvantages associated with this specific return option. It should be noted that among all analyzed configurations the FB stages are the only ones that are able to reach the launch site by their own means. While the hydrogen gas generator configuration achieves a payload fraction of 1.9%, the H SC IAC configurations show payload fractions of 2.2% to 2.3%. It is important to note the evolution of performance with separation velocity class. In case of the H SC IAC stages the highest performance is reached for the medium separation velocity class. This is in contrast to the evolution of payload fraction for the FB configurations, here a clear trend of growing performance with decreasing separation velocity of the reusable first stage exists. This is a clear reference to the staging optimum of the respective configuration type. In case of the H SC IAC configurations the optimum is covered

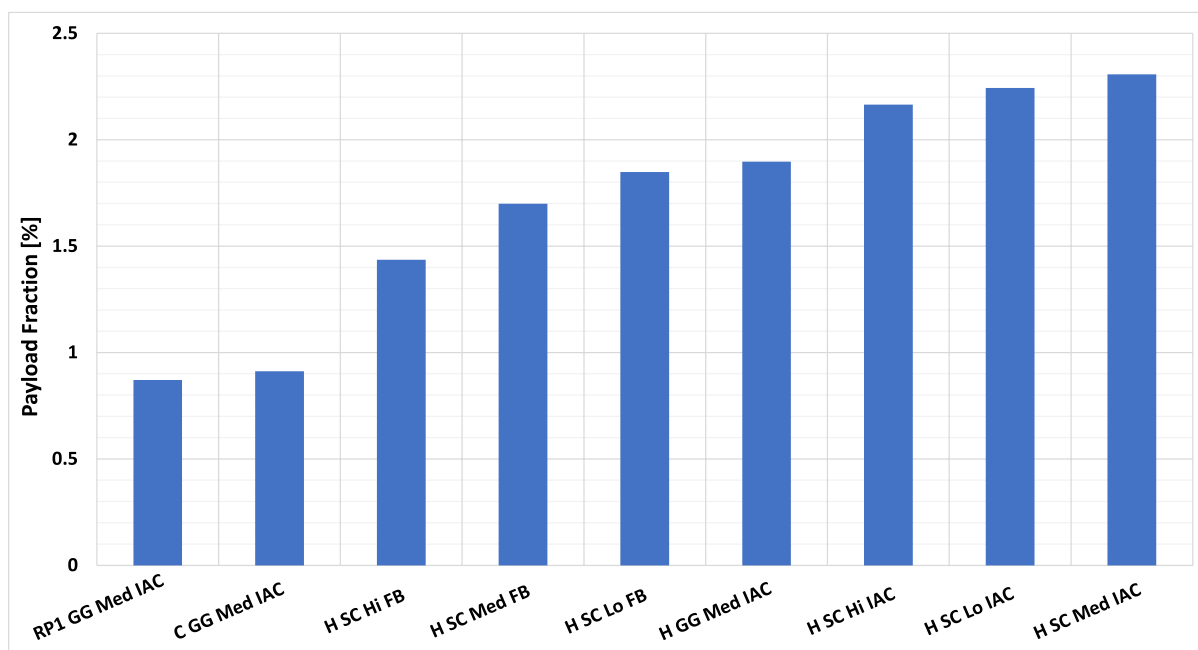


Fig. 16 Payload fraction of analyzed VTHL configurations

by the chosen separation velocity range, in case of H SC FB this is not the case.

Any attempt to explain the obtained overall launch vehicle performance expressed in terms of the payload fraction necessarily has to start with the well-known rocket equation:

$$\Delta v + \Delta v_{Loss} = c_e \ln m_i/m_f = c_e \ln R \quad (2)$$

The sum of the velocity change communicated to the launch vehicle and the delta velocity losses is equal to the product of the average specific impulse (expressed in the dimension of velocity) and the natural logarithm of the mass ratio. Mass ratio R is to be understood as the ratio of initial to final mass of the configuration.

While the significance of aspects like propulsion efficiency and staging is obvious, the gross delta velocity that needs to be delivered by the launch vehicle configuration stages and that includes the losses as well requires attention. The gross delta velocity including losses of all analyzed configurations is shown in Fig. 17. The bar chart shows the velocity changes actually performed by first and upper stages as well as the respective losses. The relevant losses are gravity, aerodynamic drag and thrust losses.

The defined nominal target orbit is a 1.5 km/s (remaining delta velocity to GEO) geostationary transfer orbit. The resulting gross delta velocity for the studied configurations is therefore between 11.2 km/s and 11.5 km/s. This variation is primarily due to different ascent trajectories and the associated losses. Small variations in the final orbit and payload mass have an additional, but minor effect. The delta velocity

without losses, i.e. the actual velocity change, is between 9.8 km/s and 9.9 km/s. According to the defined and analyzed first stage separation velocity classes, the gross delta velocity of the reusable first stages is between 3.5 km/s and 4.6 km/s, including losses of 1.1 km/s to 1.3 km/s. Obviously, the biggest share of the delta velocity contribution is performed by the expendable upper stages. Their gross contribution is between 6.8 km/s and 7.9 km/s with relatively small losses of 240 m/s to 330 m/s. It is important to observe that, independent of the separation velocity class, the methane and kerosene configurations have the lowest first stage velocity losses of 1.1 km/s which is around 85% of the losses of the hydrogen configurations. This can be explained by the higher levels of thrust and mass flow of the hydrocarbon first stages as well as their relatively short burn time. In general, the first stage velocity losses are dominated by the gravity losses, while aerodynamic losses have a minor contribution. However, the effect of aerodynamic drag is reduced in the case of the hydrocarbon stages due to their still relatively high masses around the maximum of dynamic pressure during the ascent flight. Therefore, the fraction of aerodynamic losses is 9.4% to 11.1% for the hydrocarbon stages, whereas in the case of the hydrogen it is 14.5% to 14.9%.

5.2 Propellant combination and rocket propulsion efficiency

The effect of the choice of the propellant combination and the rocket propulsion efficiency on the outcomes of the presented work is apparent. However, a clear separation

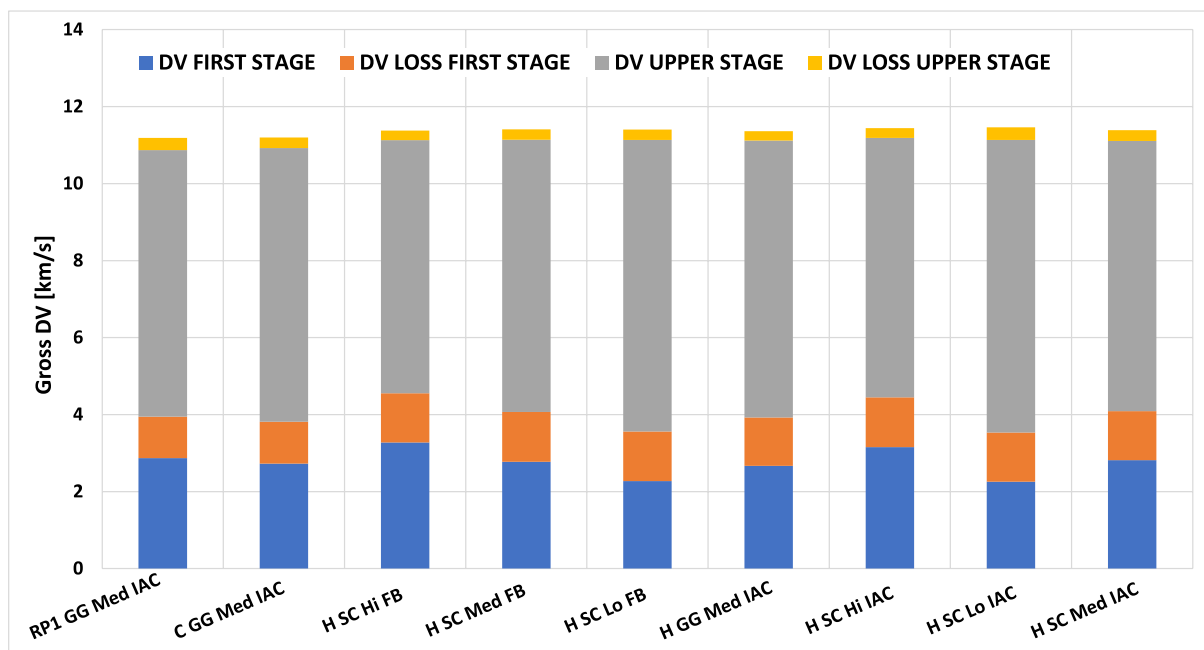


Fig. 17 Total gross delta velocity of analysed VTHL configurations during ascent

and isolation of this effect is not fully possible because the results for a certain configuration are under the influence of several, partially mutually dependent design aspects. In addition, due to limitations in the study scope not all details could have been analyzed. Thus, in the following mass results will be discussed for configurations having the same RLV stage return option and separation velocity class.

In Fig. 18 the specific impulse in dimensions of velocity is shown for the configurations having medium first stage separation velocity. Reusable first stage and expendable upper stage specific impulse is displayed. All shown variants use the IAC reusable first stage return method. The propellant combinations are RP1/LOX, LCH4/LOX and LH2/LOX. For hydrogen two rocket engine cycles, staged combustion and gas generator, are included, kerosene and methane configurations use the gas generator cycle only. The upper stage specific impulse is simply the vacuum specific impulse of the upper stage engines, whereas the shown first stage specific impulse is an effective specific impulse calculated with the rocket equation from velocity and mass data based on the optimized ascent trajectory. An overall specific impulse range from 3000 m/s to 4500 m/s is covered.

The lowest specific impulse values are those of the kerosene configuration with an upper stage Isp of 3310 m/s and a first stage effective Isp of 3020 m/s. The methane configurations' Isp is at 3420 m/s and 3120 m/s respectively. When going to hydrogen with gas generator cycle the efficiency significantly rises up to 4320 m/s for the upper and 3960 m/s

for the reusable first stage. Efficiency in the case of hydrogen with staged combustion engines goes up even higher to values of 4500 m/s and 4190 m/s. Thus, hydrocarbon configurations have an Isp that is more than 25% lower than the Isp of the hydrogen stages. This is a significant drawback of hydrocarbon configurations in tendency leading to launchers with higher ascent propellant loadings and consequently also higher dry and overall lift-off masses.

A direct consequence of the reduced rocket propulsion efficiency is a necessary increase in mass ratio. The number of stages for the launchers analyzed in this study is limited to two and the only way to achieve similar delta velocities in the presence of a low Isp is to increase the mass ratio. This applies to both the reusable first stage as well as the expendable upper stage. The resulting final mass ratios at stage burnout for the reusable and expendable stages are shown in Fig. 19. While in the case of hydrogen staged combustion the mass ratios of the upper and first stage are 5.3 and 2.7 respectively, the kerosene configurations' upper stage needs a ratio of 9.2 and its first stage a ratio of 3.7 to perform the defined mission of bringing 7.5 Mg of payload to GTO. According to the rocket equation, the delta velocity depends on the natural logarithm of the mass ratio, see Eq. (2). Therefore, increases in mass ratio are less efficient for high values of R . However, due to the fixed number of stages low specific impulse necessarily requires higher mass ratios. This leads to the substantial GLOM increase observed for hydrocarbon configurations.

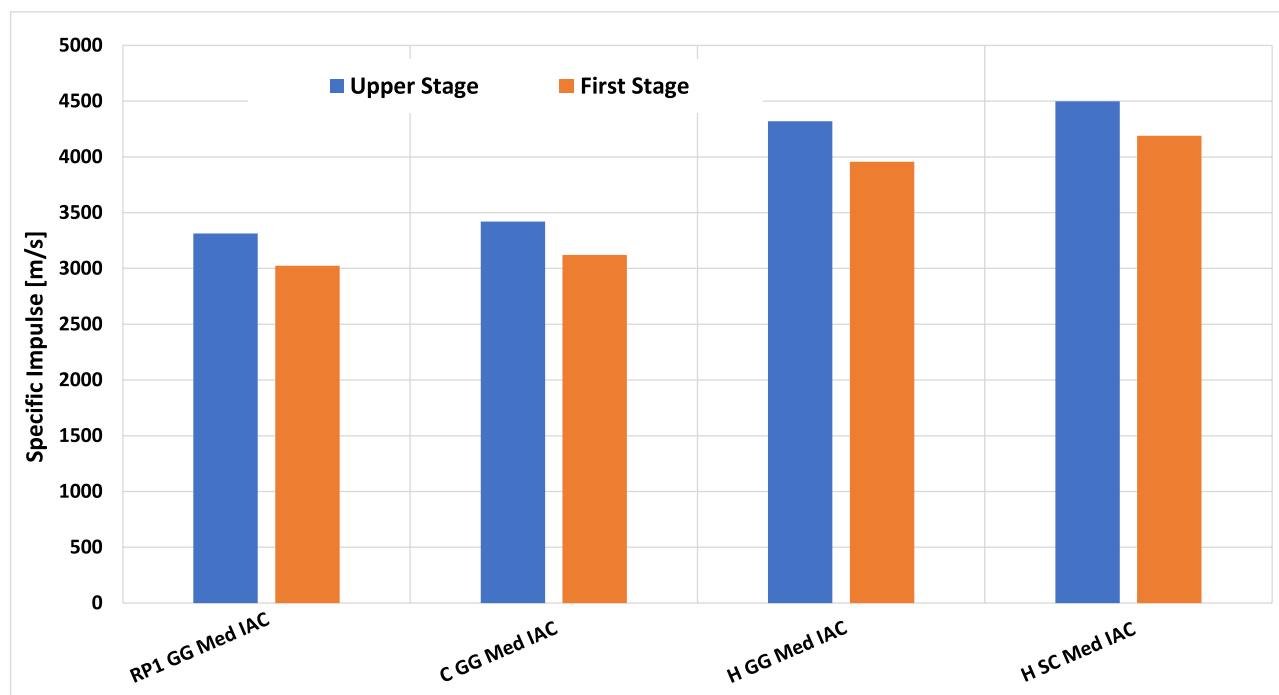


Fig. 18 Rocket propulsion efficiency for medium separation velocity variants

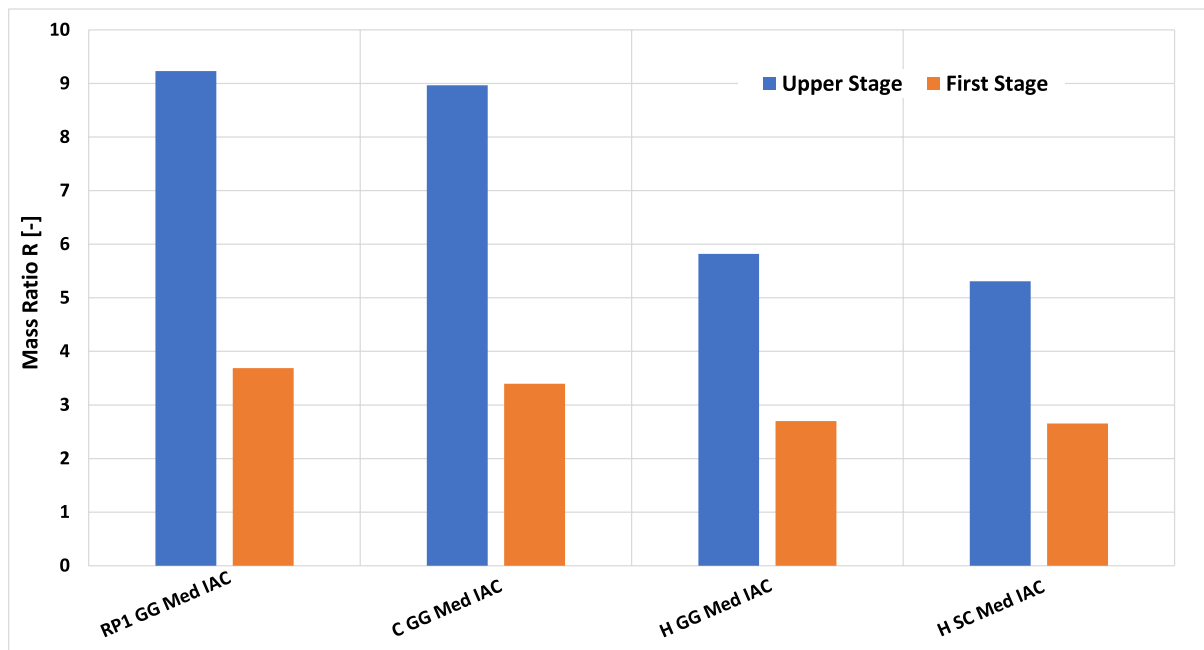


Fig. 19 Mass ratios for medium separation velocity variants

The non-dimensional GLOM for medium separation velocity IAC configurations is shown in Fig. 20 in reference to the maximum GLOM reached by the kerosene RLV. Since the propulsion efficiency of kerosene and methane is very similar, only a small difference in lift-off mass is observed. The methane configuration therefore shows a GLOM that is at 94% w.r.t. the reference. In contrast to that, the hydrogen

gas generator configuration with I_{sp} values of around 4000 m/s has a relative GLOM of just 45%. Finally, in the case of hydrogen staged combustion the advantages of the most efficient rocket propulsion lead to a relative GLOM of 38% as compared to the configuration using kerosene as fuel.

In addition to the comparison of GLOM, a comparison of reusable first stage dry mass is as well important due to the

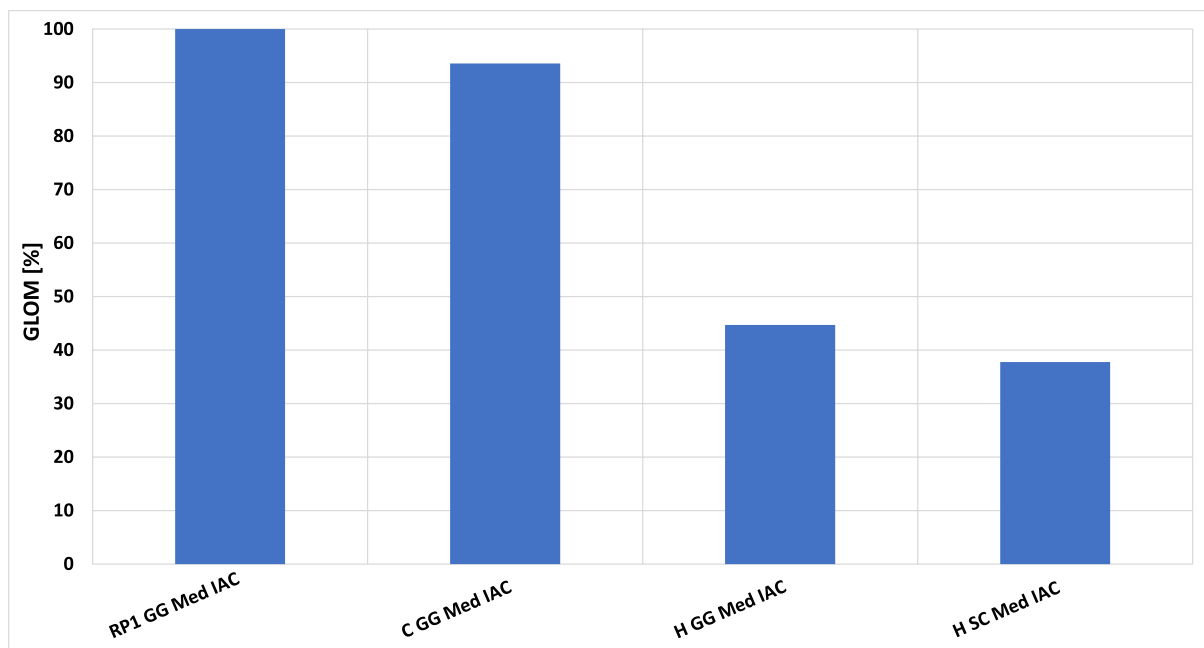


Fig. 20 Non-dimensional GLOM of medium separation velocity IAC configurations

significance of dry mass in the frame of cost estimations. A comparison of dry mass is shown in Fig. 21, a breakdown of dry mass in structural, subsystem, propulsion and thermal protection mass is shown. As in case of GLOM, hydrocarbon configurations again have the highest masses with the difference that methane has a dry mass slightly higher than kerosene. This is first of all because the structural mass in case of methane is higher as compared to kerosene. The Isp is higher by around 10 s in case of methane and thus the first stage ascent propellant loading is lower by approximately 60 Mg. However, the methane configurations fuel tank mass is higher by a factor of more than 1.5 due to its lower density relative to RP-1. As well remarkable is the fact that the hydrogen gas generator stage has a higher structural mass than the hydrocarbon variants. This is due to differences in stage length and diameter. Due to their higher diameters and shorter stage lengths (in addition to the higher fuel density as compared to hydrogen) the hydrocarbon RLV stages are less susceptible to bending and thus have relatively low structural masses. However, this is not enough to make up for their high propulsion system masses and the overall dry mass of hydrocarbons is still higher than the dry mass of the hydrogen gas generator stage. The reason for the very high propulsion system masses in the case of methane and kerosene is related to the requirement of an equivalent T/W ratio of 1.4 for all configurations. Thus, the low Isp of kerosene and methane leads to high GLOM which leads to a high thrust requirement which in turn leads to heavy rocket propulsion systems. While methane and kerosene have rocket engine fractions of 28% and 30%, in the case of the hydrogen stages

the rocket engine fractions decrease down to 17% in the case of the gas generator cycle and down to 22% in the case of the staged combustion cycle. Due to its high specific impulse, the hydrogen staged combustion stage is still lowest both in overall dry mass as well as concerning the structural mass.

Finally, the important conclusion has to be drawn that in the frame of the defined constraints of the study at hand, not only do the hydrocarbon configurations have the highest GLOM, they as well show the highest RLV stage dry masses and the highest rocket engine fractions.

5.3 Launch vehicle staging

In general, two aspects are important in the context of launch vehicle staging, the number of stages and the distribution of propellant between the particular stages. The number of stages is a design choice usually made with the goal of using as few stages as possible. For the distribution of propellant between the stages a theoretical optimum leading to minimum lift-off mass and maximum payload fraction exists.

In the frame of the performed analysis, the number of stages is set to two for all analyzed configurations. The distribution of propellant between reusable and upper stages is oriented upon three separation velocity classes to obtain comparable separation conditions for the winged reusable stages. However, these predefined separation velocity classes do not necessarily correspond to an optimal distribution of propellant between the first and upper stage. This is illustrated by the comparison of GLOM for the configurations

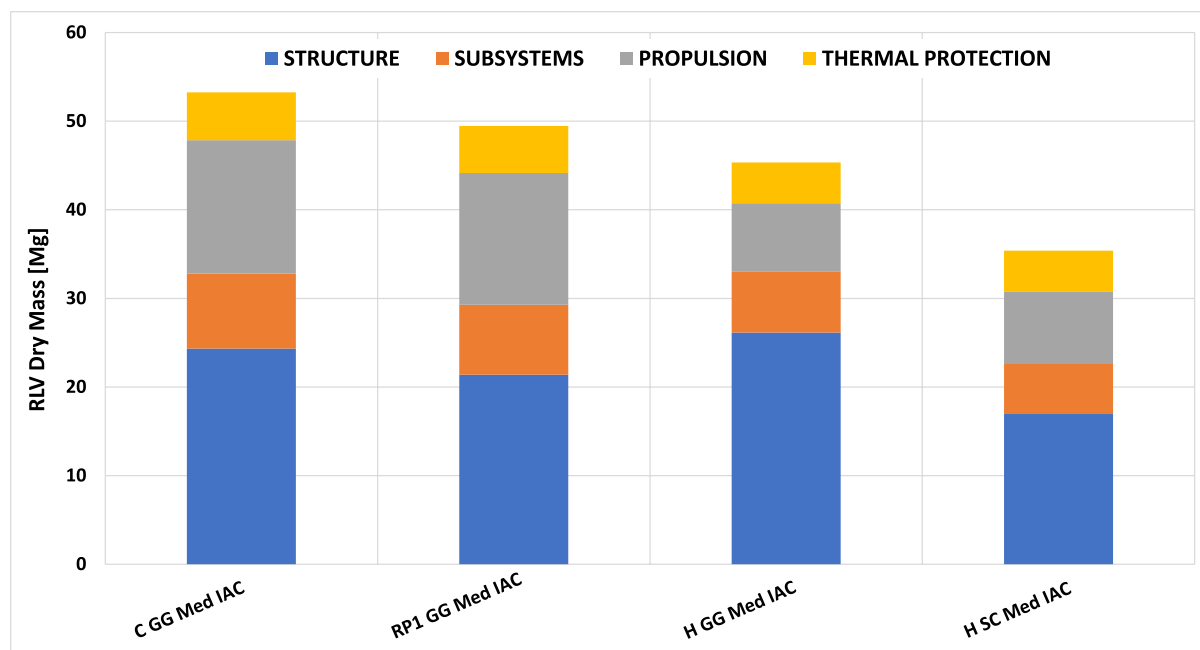


Fig. 21 Comparison of dry mass of medium separation velocity RLV (IAC) stages

using hydrogen as fuel and staged combustion as rocket engine cycle as shown above in Fig. 22.

All GLOM values are with respect to the GLOM of the Hi class FB configuration, which is 529 Mg. The Med IAC configuration shows a minimum in GLOM of 62%, although the difference as compared to Lo and Hi configurations with 63% and 65% is small. The fact that the GLOM of IAC configurations is almost insensitive to the separation velocity class is a standalone feature of this type of RLV. This is clearly not the case for the FB configurations. In case of FB there is a strong increase of GLOM instead. With the Lo and Med configurations having 76% and 84% GLOM respectively, an optimum cannot be seen within the chosen separation velocity range. The reason of the strong GLOM increase with first stage separation velocity is the fact that FB reusable stages contain additional hardware as air-breathing propulsion, a fly-back fuel tank and of course the fly-back fuel itself. The mass of this additional hardware and the fuel depend on the mass of the stage and the distance to launch site that needs to be flown using the air-breathing propulsion. Most likely, an optimum with regard to GLOM finds itself at a first stage separation velocity slightly below the Lo conditions, see Fig. 22. Thus, the comparison of configurations and stages with the same first stage separation velocity in certain cases does neglect the aspect of optimal staging. It is important to note, that the decision to focus on fixed staging points was taken in order to enable a faster design process in the frame of the general constraints of the performed analysis, see [1] and [4].

Concerning the number of stages for the analyzed configurations, an exactly defined point from which on a change to a three-stage configuration would be advantageous from

a practical design point of view does not exist. However, the comparison of mass ratios shown in Fig. 19 suggests that at least for the hydrocarbon configurations an additional stage might be advantageous in terms of performance. This is important both from the point of view of performance as well as fuel comparison.

5.4 RLV Stage Return Option

In general, for the choice of the return option of a winged reusable first stage several aspects might be considered. Apart from the technical feasibility of the concept and its potential ability to serve defined mission scenarios, possible economic advantages related to the reusability of the first stage play an important role. But aspects like autonomy, flexibility and responsiveness also deserve consideration. Within this work only a preliminary, technical analysis for the return options Fly-Back and In-Air-Capturing is performed. For the return options FB and IAC analyzed in this work, three first stage separation velocities are considered. Depending on the first stage separation velocity and reentry mass of the stage, the descent of the reusable first stage results in different distances to launch site after the reentry. In Fig. 23 the RLV stage reentry mass is shown over the distance to launch site for the return methods FB and IAC. The resulting distances to launch site differ only slightly among FB and IAC as long as the separation velocity class remains the same. For the Lo separation velocity class the distance to the launch site is roughly 500 km, in the case of the Med class it is approximately 700 km and for the Hi class it is around 900 km. The reentry mass shown in Fig. 23 is the first stage dry mass plus the first stage residuals and reserves in the

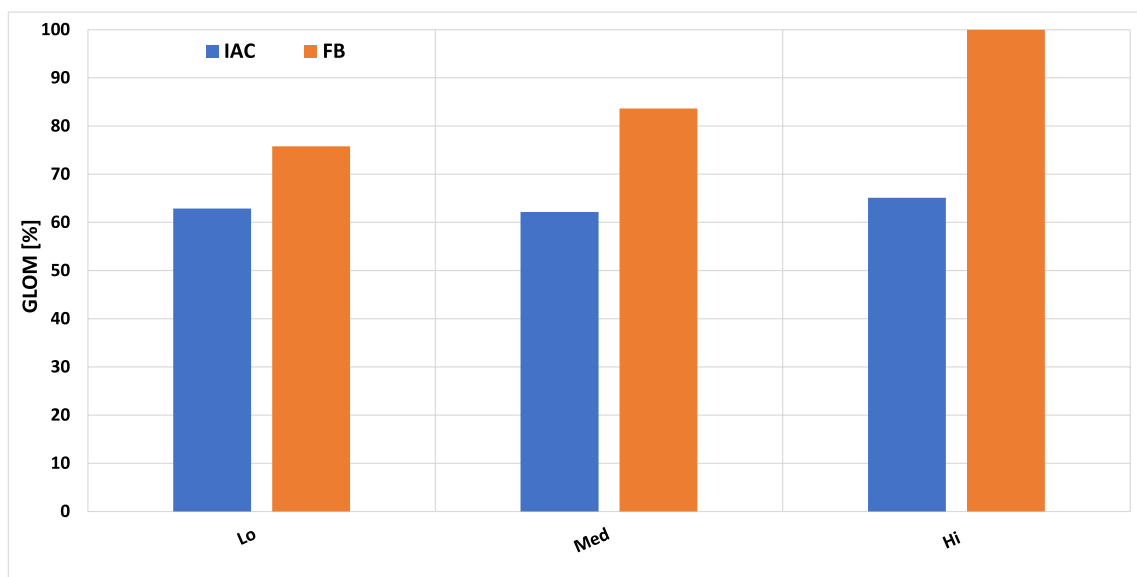


Fig. 22 Comparison in relative GLOM of hydrogen staged combustion configurations

case of IAC. For FB, the fly-back fuel mass is also part of the reentry mass. FB fuel masses of 4.5 Mg, 6.7 Mg and 11 Mg are required for the Lo, Med and Hi classes. Comparing the reentry mass, a similar trend as for the GLOM exists. In the case of FB a strong increase of reentry mass with first stage separation velocity is present, whereas for IAC only a weak correlation of reentry mass with first stage separation velocity is visible. In general, FB stages have significantly higher reentry masses than the IAC stages, e.g. for the Med class a factor of approximately two is observable, see Fig. 23. This is due to the additional hardware and fly-back fuel required in the case of FB as a return option. In Fig. 24 a comparison of the reentry mass for the Med IAC and Lo FB hydrogen staged combustion configurations is shown. The comparison of different separation velocity classes is justified because of the staging at or close to the optimum. In the case of FB, additional hardware and fuel are required. The FB hardware (FB H/W) consists of the FB fuel tank and the air-breathing propulsion. The FB hardware and fuel represent 11% and 7% of the total FB reentry mass, see Fig. 24

5.5 Rocket engine cycle

The effect of the choice of rocket engine cycle is primarily visible within a comparison of dry mass and rocket engine mass. The dry mass of the stage is to a certain extent an indicator for cost. However, the most valuable components of a launcher stage are its liquid rocket engines, so that mass units of dry mass are not enough for a cost estimation, the type of component representing a certain fraction of dry mass is important as well. Therefore, a comparison of RLV

stage dry mass and its rocket engine mass and fraction is performed for the medium separation velocity class IAC hydrogen first stages to evaluate the effect of rocket engine cycle choice, see Fig. 25. The dry mass of the SC stage is around 35 Mg, whereas the GG stage has a dry mass about 10 Mg higher. The staged combustion cycle has the advantage of higher specific impulse. The disadvantage of staged combustion engines is their higher mass. The configurations analysed in this work are designed for a common T/W the launch of 1.4. However, the rocket engine mass of the SC stage is 7.9 Mg and thus higher as the rocket engine mass of the GG stage, which is 7.5 Mg only. This is the more remarkable as the GG configuration has a higher GLOM. The GLOM of the H SC Med IAC configuration is 329 Mg, whereas the H GG Med IAC has a GLOM of 389 Mg. This means, that despite a higher dry mass and a higher GLOM, the absolute mass of rocket engines is slightly lower for the GG reusable first stage. The reason for this is the higher rocket engine T/W of gas generator engines as compared to staged combustion engines. While the T/W of SC is around 75, in the case of GG the engine T/W goes up to 97, see [3] for more details. This also contributes to the differences in rocket engine fractions that can be observed for the SC and GG stages.

6 Summary and conclusions

In this work, nine partly reusable two-stage-to-orbit VTHL configurations with the mission of delivering 7.5 Mg to GTO are analyzed. The studied space transportation

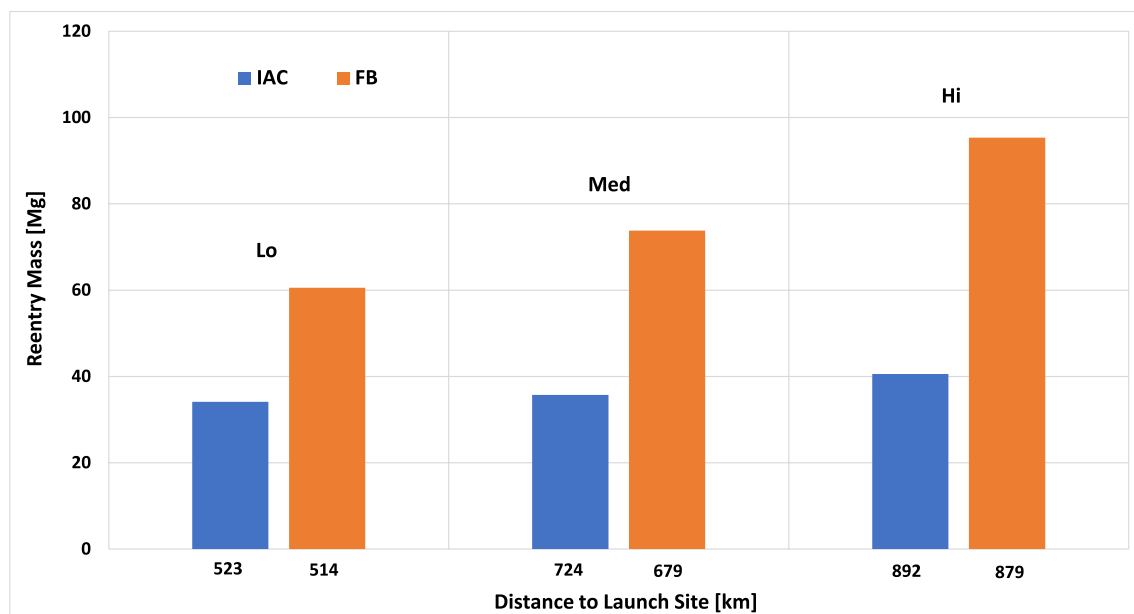


Fig. 23 RLV stage reentry mass and distance to launch site after reentry

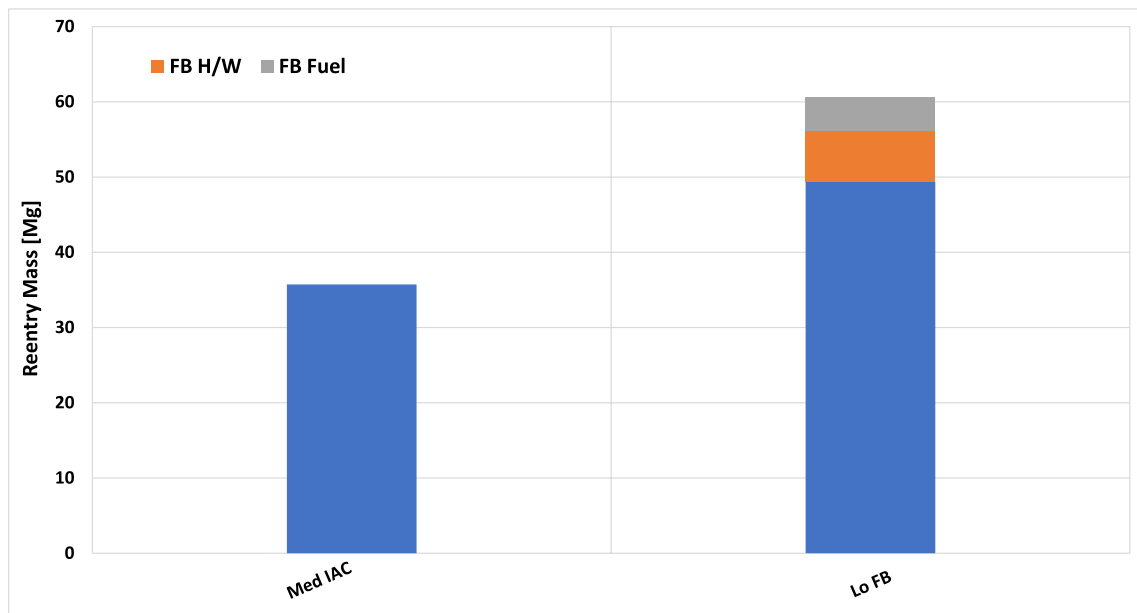


Fig. 24 Reentry mass comparison FB vs. IAC

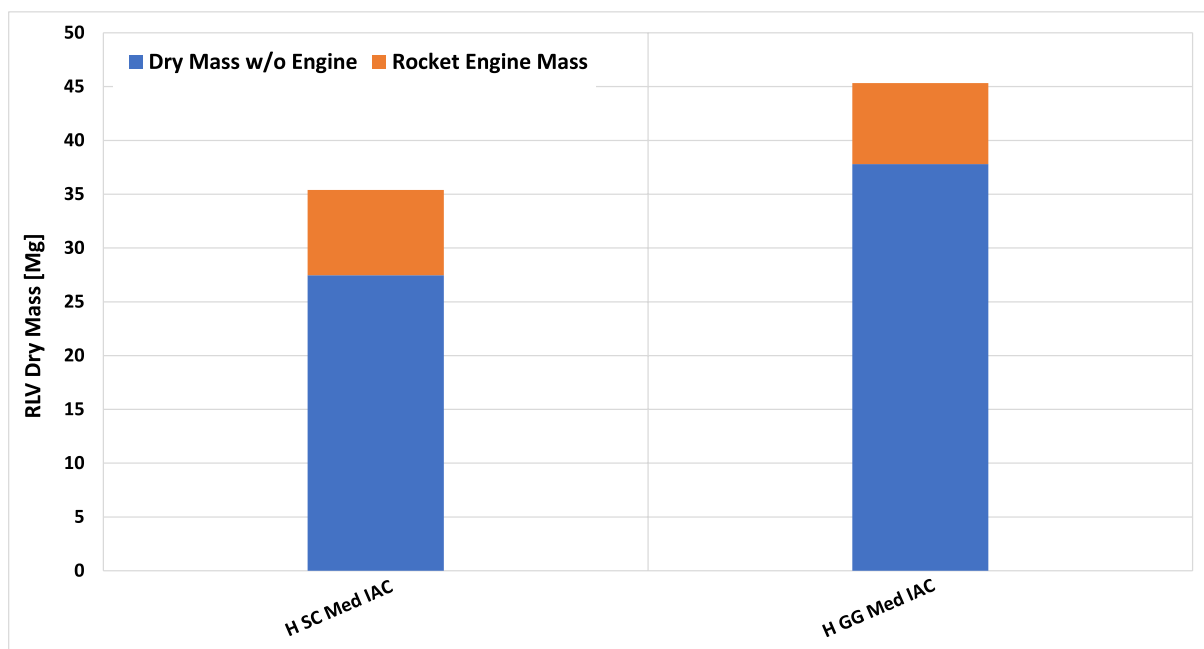


Fig. 25 Effect of rocket engine cycle on RLV stage dry mass

configurations consist of a winged reusable first stage and an expendable upper stage. The fuel/oxidizer combinations considered are LH₂/LOX, LCH₄/LOX and RP-1/LOX. Staged combustion and gas generator liquid rocket engine cycles are scaled in thrust within the iterative design process. Two return options for the winged reusable first stages, Fly-Back (FB) and In-Air-Capturing (IAC) are analyzed.

The following conclusions can be drawn from the presented results of the preliminary design of the studied RLV configurations: first, two-stage methane and kerosene configurations with winged reusable first stages do have GLOM higher by a factor of 2.1 as compared to hydrogen configurations. The reduction of payload fraction as compared to the most efficient hydrogen staged combustion configurations is as well by a factor of more than two. Furthermore, the

hydrocarbon stages not only have the highest GLOM but also the highest dry masses and rocket engine fractions. This is a consequence of the reduced specific impulse in case of methane and kerosene. Also, it is quantified to what extent FB as return option is depending on reusable first stage separation velocity. An increase of almost 60% in reentry mass is observed. In the case of IAC, only a very weak correlation between GLOM and separation velocity exists. The IAC hydrogen staged combustion configurations are the most performant in terms of GLOM and payload fraction. These stages cannot perform a return to launch site by their own means, thus performance-wise all IAC configurations need to be seen as downrange landing systems.

As an outlook, an interesting trade-off between performance and complexity (cost) could exist in the case of hydrogen gas generator configurations having relatively high payload fractions and low rocket engine masses.

Author contribution L.B. performed the preliminary analysis for VTHL systems within the presented study including all aspects of the design loop. I.D. substantially participated in the definition of the study logic, assumptions and constraints and prepared Fig. 1. M.S. calculated the rocket engines used as orientation in the entire study, defined the air-breathing propulsion characteristics. All authors reviewed the manuscript.

Funding Open Access funding enabled and organized by Projekt DEAL.

Data availability Not applicable.

Declarations

Conflict of interest The authors declare that there is no conflict of interest regarding the publication of this paper.

Open Access This article is licensed under a Creative Commons Attribution 4.0 International License, which permits use, sharing, adaptation, distribution and reproduction in any medium or format, as long as you give appropriate credit to the original author(s) and the source, provide a link to the Creative Commons licence, and indicate if changes were made. The images or other third party material in this article are included in the article's Creative Commons licence, unless indicated otherwise in a credit line to the material. If material is not included in the article's Creative Commons licence and your intended use is not permitted by statutory regulation or exceeds the permitted use, you will need to obtain permission directly from the copyright holder. To view a copy of this licence, visit <http://creativecommons.org/licenses/by/4.0/>.

References

1. Dietlein, I., Bussler, L., Stappert, S., Wilken, J., Sippel, M.: Overview of system study on recovery methods for reusable first stages of future european launchers. CEAS Space Journal (2024). <https://doi.org/10.1007/s12567-024-00557-9>
2. Wilken, J., Stappert, S.: Comparative analysis of european vertical-landing reusable first stage concepts. CEAS Space Journal (2024). <https://doi.org/10.1007/s12567-024-00549-9>
3. Sippel, M., Wilken, J.: Selection of Propulsion Characteristics for Systematic Assessment of Future European RLV-Options, CEAS Space Journal 2024. <https://doi.org/10.1007/s12567-024-00564-w>
4. Stappert, S., Dietlein, I., Wilken, J., Bussler, L., Sippel, M.: Options for Future European Reusable Booster Stages: Evaluation and Comparison of VTHL and VTVL Return Methods, CEAS Space Journal 2024. <https://doi.org/10.1007/s12567-024-00571-x>
5. Wilken, J., Herberhold, M., Sippel, M.: Options for Future European Reusable Booster Stages: Evaluation and Comparison of VTHL and VTVL Costs, CEAS Space Journal 2024. <https://doi.org/10.1007/s12567-024-00577-5>
6. Stappert, S., Singh, S., Funke, A., Sippel, M.: Developing an innovative and high-performance method for recovering reusable launcher stages: the in-air capturing method, CEAS Space Journal 2023
7. Guédron, S., Prel, Y., Bonnal, C., Rojo, I.: RLV concepts and experimental vehicle system studies: current status, IAC-03-V.6.05, 54th International Astronautical Congress, 2003
8. Baiocco, P.: Overview of reusable space systems with a look to technology aspects. Acta Astronaut. **189**(2021), 10–25 (2021)
9. Sippel, M., Manfretti, C., Burkhardt, H.: Long-term/strategic scenario for reusable booster stages. Acta Astronautica, Volume 58, Issue 4, February 2006.
10. Reusable Booster System: Review and Assessment, Aeronautics and Space Engineering Board, National Research Council, Washington D.C., 2012
11. Balesdent, M., et al.: Multidisciplinary design and optimization of winged architectures for reusable launch vehicles. Acta Astronaut. **211**, 97–115 (2023). <https://doi.org/10.1016/j.actaastro.2023.05.041>
12. Gogdet, O., Mansouri, J., Breteau, J., Patureau de Mirand, A., Louaas, E. 2019. Launch Vehicles System Studies in the Future Launchers Preparatory Programme: The Reusability Option for Ariane Evolutions. EUCASS <https://doi.org/10.13009/EUCAS S2019-971>
13. Kayal, H.: Aufbau eines Vereinfachten Simulationsmodells für den Bahnaufstieg in der Großkreisebene, DLR-IB 318–93/05
14. Picone, J. M., et al.: NRLMSISE-00 empirical model of the atmosphere: Statistical comparisons and scientific issues. Journal of Geophysical Research: Space Physics 107.A12 (2002): SIA-15
15. Klevanski, J., Sippel, M.: Quasi-Optimal Control for the Reentry and Return Flight of an RLV. 5th International Conference on Launcher Technology, Madrid 2003
16. Klevanski, J., Sippel, M.: Beschreibung des Programms zur Aerodynamischen Voranalyse CAC Version 2, DLR IB 647–2003/04, SART TN-004 / 2003, DLR Cologne 2003
17. Finck, R.D.: USAF Stability and Control DATCOM, AFWAL-TR-83–3048
18. Reisch, U., Streit, T.: Surface Inclination and Heat Transfer Methods for Reacting Hypersonic Flow in Thermochemical Equilibrium, DLR IB 129–96/10, Braunschweig 1996
19. Myers, D.E. et al.: Parametric Weight Comparison of Advanced Metallic, Ceramic Tile and Ceramic Blanket Thermal Protection Systems. NASA TM-2000–210289
20. Waldmann, H., Sippel, M.: Adaptation Requirements of the EJ200 as a Dry Hydrogen Fly Back Engine in a Reusable Launcher Stage. ISABE-2005–1121, September 2005

Publisher's Note Springer Nature remains neutral with regard to jurisdictional claims in published maps and institutional affiliations.



Options for future European reusable booster stages: evaluation and comparison of VTHL and VTVL costs

Jascha Wilken¹ · Moritz Herberhold¹ · Martin Sippel¹

Received: 2 September 2024 / Revised: 8 November 2024 / Accepted: 9 November 2024 / Published online: 5 December 2024
© The Author(s) 2024

Abstract

As the space industry evolves towards more cost-effective solutions, the development of reusable launch vehicles has become a crucial focus for reducing launch costs. This study addresses the problem of identifying the most cost-effective reusable booster stage design for future European launch systems, comparing vertical takeoff, horizontal landing (VTHL) and vertical takeoff, vertical landing (VTVL) methods. Conducted under the ENTRAIN (Europe's Next Reusable Ariane) study by the German Aerospace Center (DLR), the research provides a detailed analysis of both recurring and non-recurring costs associated with various design configurations. The study explores different design degrees of freedom, including engine cycles, propellant combinations, and staging velocities, using a parametric cost model to evaluate the trade-offs involved in each configuration. Findings indicate that reusable configurations can achieve significant cost reductions across a wide range of market scenarios, and offer slight total cost benefits even for the smallest herein considered launch markets. The results further show that the hydrogen-fueled configurations investigated within ENTRAIN offer lower costs compared to the hydrocarbon-fueled alternatives. In addition, the study highlights the sensitivity of launch costs to factors such as market conditions, reuse cycles, and refurbishment efforts, offering insights for future European space launcher development.

Keywords Reusable launchers (RLV) · VTVL · VTHL · Cost modeling · Launch market uncertainty · Market scenarios

1 Introduction

As the Ariane 6 enters service, the future trajectory of launcher development in Europe remains uncertain. It is increasingly likely that the next major European launcher will incorporate partial reusability. However, when this study was initiated in 2018, several critical aspects of the new launcher architecture, such as vehicle staging, fuel selection, and engine cycle, were still undefined and remain so to this day. While qualitative arguments supporting various options are well established, their quantitative impact on the overall vehicle system and its costs are not fully understood. For instance, while hydrogen is known for its high specific impulse, it also poses challenges due to its extremely low boiling point and low density. Conversely, hydrocarbon fuels, which are denser, result in lower specific impulses.

The quantifiable effects of these competing qualitative factors on launcher performance have not been thoroughly established and may vary significantly across different use cases. Accurately assessing these impacts necessitates a comprehensive, multidisciplinary evaluation of the entire launcher system for each potential option.

The Europe's Next Reusable Ariane (ENTRAIN) study, performed by DLR, aims to fill this gap by providing a quantitative evaluation of options for a partially reusable European launch system, thereby establishing a solid technical foundation for future discussions. Although the study's scope and iterations preclude the use of high-fidelity methods such as computational fluid dynamics (CFD) or finite-element (FE) models, key subdisciplines are modeled using specialized conceptual design tools. For example, the evaluation of each launcher configuration includes structural design analysis, trajectory optimization for both ascent and descent, and modeling of the propellant tank along with associated feed, fill, and pressurization systems.

The study explores a range of design parameters, including staging velocity, fuel choice, engine cycle, and recovery method, to offer a comprehensive understanding of

✉ Jascha Wilken
jascha.wilken@dlr.de

¹ Space Launcher Systems Analysis, Institute of Space Systems, Deutsches Zentrum für Luft- Und Raumfahrt (DLR), Bremen, Germany

the trade-offs and potential advantages of various design choices.

The findings of this extensive study are documented in several publications. Reference [1] offers an overview of the study's methodology and its relation to other European initiatives. Reference [2] focuses on the propulsion datasets and the underlying rocket engine models. In Refs. [3, 4], the technical work done for the VTVL and VTHL stages is described and discussed, respectively. Reference [5] provides an in-depth comparison of different recovery methods.

In these publications, the discussions are limited to the technical data; however, the actual goal of a partially reusable launch vehicle is the reduction of launch cost. While technical data such as dry mass or total mass can be used as surrogates for the cost estimation, this approach neglects aspects influencing the recurring and non-recurring cost of the vehicles.

Within this work, an attempt is made to expand the previously purely technical analyses and to estimate the recurring and non-recurring cost associated with each investigated configuration and compare them to each other.

1.1 Study logic and high-level assumptions

The ENTRAIN study was structured into two parts: the first part concentrates on a comparative analysis of VTVL and VTHL launchers ensuring uniformity in the investigation level to prevent distortions from varied degrees of detail. Therefore, identical high-level requirements and assumptions are used for all configurations:

- 7000 kg + 500 kg margin payload to geostationary transfer orbit (GTO)
- Launch from Centre Spatial Guyanais (CSG), Kourou
- Two stage to orbit (TSTO) configurations
- Same propellant combination in both stages
- Same engines in both stages with exception of different nozzle expansion ratios.

In the VTVL launchers detailed in Ref. [3], an exception to the aforementioned two requirements is included: a hybrid launcher configuration. This unique configuration incorporates a methane-fueled lower stage and a hydrogen-fueled upper stage.

Based on these requirements, the following degrees of freedom were explored:

- Engine cycles: gas generator (GG) and staged combustion (SC)
- Recovery modes:
 - VTVL with retropropulsion landing on downrange barge (DRL)

- VTHL with in-air-capturing and subsequent towing by a waiting aircraft (IAC)
- VTHL with return to launch site (flyback) with integrated turbojet engines (FB)
- 2nd-stage Δv : 6.6 km/s, 7.0 km/s and 7.6 km/s
- Propellant combinations:
 - Liquid oxygen (LOX)/liquid hydrogen (LH2)
 - LOX/liquid methane (LCH4)
 - LOX/liquid propane (LC3H8)
 - LOX/kerosene, rocket propellant-1 (RP-1)

In the analysis of the staging variations, the upper stage Δv was chosen instead of the more commonly used separation Mach number, as explained in Ref. [1]. For reference, the upper stage Δv of 6.6 km/s, 7.0 km/s, and 7.6 km/s approximately correspond to a separation Mach numbers of 12, 10 and 7, respectively.

1.2 Why do cost estimation?

Cost estimations are notoriously unreliable in most fields, and especially so in spaceflight. Even the organizations with full access to detailed current cost data have not been able to reliably estimate the time and effort associated with future projects.

Yet, nowadays a desired reduction of cost is the main driver of the development of the next generation of launch vehicles, beyond the baseline goal of independent access to space. When examining the different options for a future European semi-reusable launch vehicle, the associated cost is a necessary part of the whole picture.

For mechanical engineering products, 75% of the manufacturing cost is committed by the decisions made in the conceptual design phase [6]. In these early design phases, especially for new products, the uncertainties of the cost estimation are very high. However, the information is absolutely critical for early decisions that will define a significant portion of the final cost. Therefore, in order to avoid early incorrect decisions, initial estimates are critical, even if their absolute results have to be interpreted with care. In later design phases, while the amount and quality of data is better, core design features are already frozen and only minor changes can be made.

This situation is further complicated by the lack of publicly available cost data. Even for publicly funded launcher systems, the actual recurring and non-recurring costs are often not disclosed. Without reliable cost data and estimations based on them, decision-makers are left to rely on information provided by potentially biased parties. Commercial entities, with a vested interest in promoting their existing portfolios, have little incentive to evaluate what

might be the best solution for society, which often funds their development projects.

The authors recognize their own potential biases as well, but hope that this publication can contribute to the ongoing discussion on these issues.

A partial remedy for the uncertainties in the cost estimation is a focus on relative cost comparison, which will be the case for this manuscript. Different future European launcher options are compared and thus, the absolute values are not the core result. Instead, the goal is to gain insights into the relative effect of the design options investigated within ENTRAIN on the total cost.

With this background and the mentioned caveats, herein an attempt is made to estimate the recurring and non-recurring cost of the vehicle concepts investigated within the ENTRAIN study. Section 2 briefly describes the investigated launch vehicles, with a focus on a number of expendable versions. The cost models employed are described in Sect. 3. The results are shown in Sect. 4 and discussed in Sect. 5. The caveats that apply to this analysis are discussed in Sect. 5.1.

2 Reference launchers

2.1 ENTRAIN configurations

A technical description of the VTVL and VTHL launchers and their major subsystems for which the cost estimation is done herein, is given in Refs. [3, 4]. The propulsion datasets are discussed in Ref. [2]. Sketches of some of the investigated launchers are shown in Fig. 1.

2.1.1 Nomenclature

The range of launchers considered in this study is categorized using a nomenclature that makes it easy to distinguish

Table 1 Design matrix of ENTRAIN study with nomenclature abbreviations

Design parameter	Description	Nomenclature
Return method	VTVL downrange landing	DRL
	VTHL in-air-capturing	IAC
	VTHL flyback	FB
	None (ELV)	EL
Propellant	LOx-LH2	H
	LOx-LCH4	C
	LOx-LC3H8	P
	LOx-RP1	K
Engine cycles	Staged combustion	SC
	Gas generator	GG
Upper stage Δv	6.6 km/s	Hi
	7.0 km/s	Med
	7.6 km/s	Lo

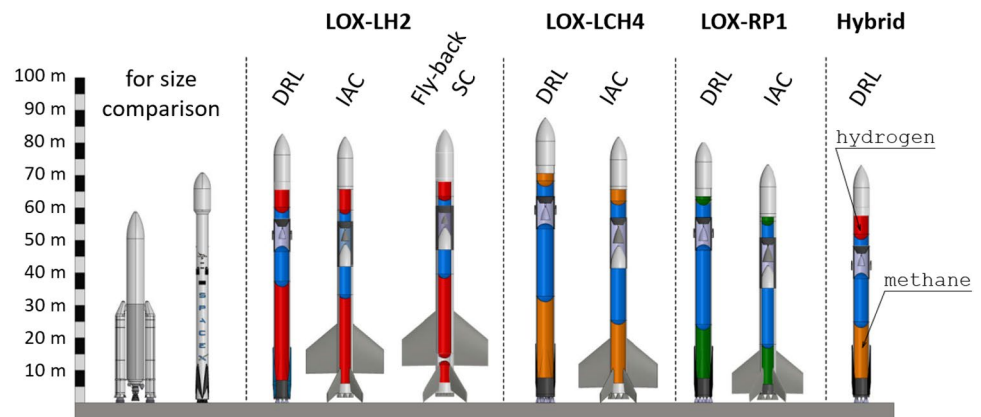
between vehicles based on key design space parameters, as outlined in Table 1. This nomenclature employs simple abbreviations for the return methods and engine cycles. In terms of propellants, each propellant combination is represented by a unique substitute letter. The first stage separation velocity is indicated by terms such as “Hi” for high, “Med” for medium, and “Lo” for low separation velocity.

For example, a launcher featuring vertical landing with downrange landing, LOX/LH2 in both stages, gas generator engines and an upper stage Δv of 7.0 km/s would be dubbed: *DRL HH GG Med*.

2.2 Expendable variants

To compare the cost of the investigated RLV launchers with that of traditional ELV launchers, five reference ELV configurations are designed. These adhere to the same requirements employed for the partially reusable launchers described in Refs. [3, 4]. This part of the study focuses on

Fig. 1 Sketch of selected launchers investigated within the ENTRAIN study, from Ref. [5]



the LOX/LH2 and LOX/LCH4 propellant combinations and the 7.0 km/s Δv upper stage. Both gas generator engines and staged combustion engines are examined. A hybrid configuration is also investigated. It features LCH4/LOX in the lower stage, and LH2/LOX in the upper stage and uses gas generator engines for both stages. The key parameters of the resulting ELV configurations are shown in Table 3.

Some systems required for recovering the first stage of VTVL configurations are unnecessary in an expendable configuration and are thus excluded from the mass model. These systems are the landing legs, the grid fins, the first stage reaction control engines and their fuel, as well as the insulation protection, and the thermal protection system. Eliminating these components reduces the stage's dry mass. In addition, no fuel must be reserved for the reentry burn and landing burn of the first stage, significantly reducing the required fuel amount. This further reduces the first stage dry mass, as it allows for smaller tanks. The number of first stage engines and the engine mass flow rate are adjusted to maintain an initial thrust-to-weight ratio of 1.4 across all configurations. The engine masses are changed to keep their thrust-to-weight constant at the values specified in Ref. [2]. As shown in Fig. 2, in total, the first stage dry mass of the ELV's first stage is reduced by one-third or more compared to the equivalent VTVL's first stage. A similar effect can be seen for the hydrogen VTHL stages. Only the IAC CC GG Med first stage shows a smaller dry mass difference of 15% to its expendable equivalent. The largest dry mass reduction is seen between DRL CC GG Med configuration and the ELV CC GG Med configuration, as the former uses the largest amount of fuel for its reentry and landing burn. Its dry mass shrinks by 38%.

The second stage's dry mass, also shown in Fig. 2, exhibits only minimal differences between the recovery methods, as all configurations shown use expendable upper stages

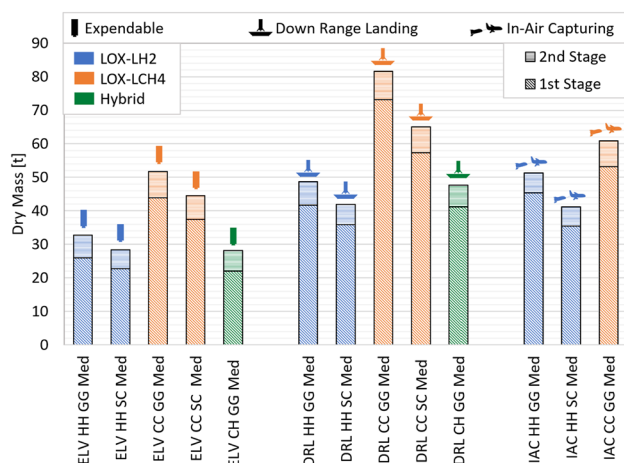


Fig. 2 Dry mass of configurations with different propellant combinations, engine cycles, and first stage recovery methods

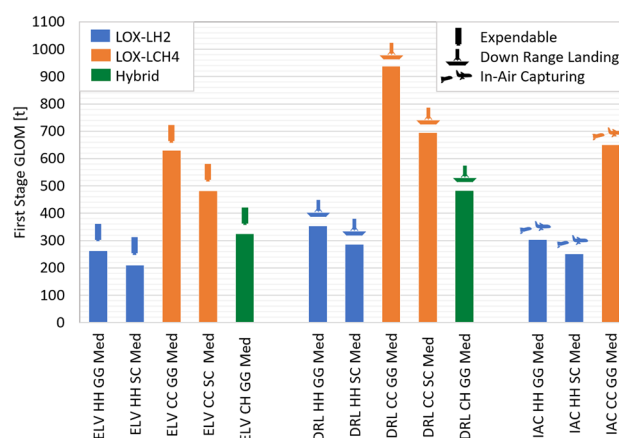


Fig. 3 GLOM of first stages with different propellant combinations, engine cycles, and recovery methods

with 7.0 km/s Δv . The minor variations arise from differing diameters and engine sizes.

Figure 3 illustrates a comparison of the Gross-Lift-Off-Masses (GLOM) for the investigated launchers. The difference in dry mass between the ELV and DRL configurations is reflected in the GLOM of both recovery methods. The GLOM of the IAC configurations is only slightly higher than the ELV's GLOM, as the IAC stages require no additional fuel for the recovery. The slight increase can be traced back to the higher dry mass of the winged first stages and the larger amount of fuel needed to accelerate that additional mass. When the GLOM of the ELVs is compared, the general trends previously observed for the RLVs (see Refs. [3, 4]) are retained. The LOX/LH2 configurations remain the smallest and lightest. Using LOX/LCH4 as propellant a configuration with more than twice the GLOM is necessary to accomplish the required GTO mission. The GLOM of the hybrid configuration sits in between, although closer to the LOX/LH2 GLOM. In addition, the use of staged combustion engines over gas generator engines lowers the GLOM by 20% and more.

2.3 Performance for SSO orbits

The transport of 7.5 t into GTO is the dimensioning use case for all configurations, but these missions represent only a portion of the global launch market [7]. To evaluate the economic performance of a launch system, its payload capabilities into Low-Earth-Orbits (LEO) have to be analyzed. However, the LEO group includes a wide range of orbits. These orbits have differing Δv budgets and consequently differing payload performances by the same launch system. The transport of a payload into a high SSO-orbit was chosen to represent this wide range of missions. Such an orbit requires a large Δv budget for a LEO mission, thus representing a conservative estimation of the launcher's LEO performance [8].

For the VTVL configurations the SSO payload with first stage RTLS is also investigated. The resulting SSO payloads, detailed in Fig. 4, are all close to 10 tons, showing minimal variations between different engine and fuel types.

- Engineering bottom-up
- Analogy estimation
- Parametric cost estimations



Factors such as system complexity, team experience, and technology readiness (TRL) are introduced into Eq. (1) for specific cost types.

Hereafter, a work-year cost of 370 k€ is assumed. This results from extrapolating the WYr cost data for Europe from TRANSCOST to the year 2022.

The following sections discuss the specific CER's chosen for each component as well as the fuel or engine-specific adaptations of the coefficients used in the CER's. The values of all coefficients used are given in Table 5 in the appendix. Unless specified, coefficients default to a baseline value of 1. For instance, the team experience factor f_3 is set at 1 to ensure comparability, as no specific entity for launcher implementation is defined.

As the ground infrastructure was not assessed during the technical analysis of the ENTRAIN study, the investment necessary for infrastructure build-up is not included in this cost analysis. The recurring cost associated with vehicle ground operations is modeled according to TRANSCOST.

3.1 Distortion introduced by relying on dry mass-based CERs

The models discussed in this chapter primarily focus on CERs based on the dry mass of components, which may lead to distortions when considered from the perspective of other relevant metrics.

For instance, rocket engines are typically evaluated based on their thrust class rather than dry mass. Comparing engines with equivalent thrust is more informative than comparing those with the same dry mass. For example, the thrust-to-weight (T/W) ratio for a methane-fueled gas generator engine is estimated at 105, whereas it is 75 for its staged combustion cycle counterpart (from [2]). Consequently, the dry mass relative to thrust level is approximately 31% greater for the staged combustion engine. Thus, despite using the same mass-based CER for both engines, the cost comparison changes significantly when thrust levels are considered. The staged combustion engines appear notably more expensive. The impact on costs varies depending on the exponent applied in the CER calculations. In this case, an exponent of 0.48 is used, indicating that the increased dry mass corresponds to an approximate 14% higher development cost for a staged combustion engine with the same thrust level, before any adjustment to the coefficients.

Similarly, when comparing stages with identical propellant loading, the structural index of the various design options results in different cost per propellant loading if the cost per dry mass is assumed to be identical. Assuming, for example, that a reference expendable hydrogen-fueled stage has a structural index of 9% and methane-fueled stage with the same propellant loading has a structural index of 5%, this results in the production cost of the methane stage

being 26% lower than a hydrogen-fueled stage with same propellant loading (including the effect of the production CER exponent).

The focus on dry mass as a primary cost driver in the development and production of components is justified, given its substantial influence on expenses. However, it is crucial to acknowledge the potential distortions this focus may introduce when applying CERs. To ensure that the CERs align with the intended modeling assumptions, it is essential to carefully select and adjust the coefficients and be aware of the distortions already inherent in use of dry mass as the scaling parameter.

3.2 Non-recurring costs

The development cost for a single component is calculated as

$$E_{\text{dev}} = f_1 \cdot f_2 \cdot f_3 \cdot a_{\text{dev}} \cdot M^{\alpha_{\text{dev}}} \quad (2)$$

Here, f_1 reflects technological readiness and complexity, f_2 is a technical quality factor, and f_3 represents team experience. The system engineering and integration effort (E_{sys}) of an entire launch vehicle with i components is calculated as

$$E_{\text{sys}} = (1.04^N - 1) \cdot \sum_1^i E_{\text{dev},i}$$

Here, N is the number of stages.

3.2.1 Core stage

The core stage component consists of all elements classically found on expendable launch vehicles for which historical data exist. For the development effort of the core stage itself, the updated CER from Ref. [12] was used.

The f_1 factor of all expendable stages is set to 0.7, to reflect that expendable cryogenic stages are state-of-the-art.

3.2.2 Reentry and landing hardware

The CER's based on historical stages do not include landing and reentry hardware, as the underlying stages were expendable. Depending on the recovery mode in question, the landing components consist of the landing gears or landing legs. Similarly, the reentry component can include either wings, grid fins or the thermal protection system. For the development effort of the landing and reentry hardware component, the cost estimations of the FESTIP studies [13] were used as the basis to generate specific CER's for these components. The resulting coefficients are given in the Appendix in Table 5.

3.2.3 Interstages

The interstages are modeled as separate components because they are jettisoned for the winged configurations in order to expose the aerodynamically more efficient nose, as can be seen in Fig. 1, and thus can't be considered part of the reusable first stage. The development effort for an interstage is estimated via a linear scaling with regard to the component mass based on the values given in Ref. [14] for the development of a sandwich-based interstage for the ARES-V launcher concept by NASA.

3.2.4 Propulsion

For the rocket propulsion elements, the CER's from TRANSCOST for modern pump fed engines were used for estimation of the development effort. In order to reflect the smaller European heritage of hydrocarbon-fueled engines, the f_1 factor is increased by 10%, while it is kept at 1 for hydrogen-fueled engines. f_1 is also increased by a further 10% for all closed-cycle engines, in addition to the implicit bias discussed above, this results in the development of staged combustion engine being ~25% more expensive than the development of an equal thrust gas generator cycle engine. For the recurring cost, the difference is ~15%.

For the airbreathing engines used in the FB cases, the effort assessed within the ASTRA [15] study was used. The same engines (EJ2000) are assumed therein and for the ENTRAIN FB configurations. As these engines already exist, only modifications to the design for the operation on hydrogen as the fuel are considered.

3.2.5 Guidance, navigation and control of reusable stages

Finally, a dedicated fixed cost component for the development of the guidance, navigation and control (GNC) systems necessary to safely decelerate and return the stages after separation is included. For the three recovery modes DRL, IAC and FB 2500, 2000 and 2200 WYr were budgeted for this effort. These values are rough assumptions and try to represent that for VTVL both propulsion and aerodynamic systems have to be mastered and that the flyback return mode includes the additional powered subsonic flight mode that also has to be included. No recurring costs are foreseen for this component, as the core stage already includes the mass of the electrical systems needed to execute the GNC algorithms.

3.3 Recurring costs

Recurring costs include production effort, prelaunch ground operations, and system costs. Production cost is calculated as

$$E_{\text{prod}} = f_4 \cdot a_{\text{prod}} \cdot M^{\text{X}_{\text{prod}}} \quad (4)$$

Here, f_4 accounts for cost reduction through series production, based on a learning factor p and production number n :

$$f_4(n) = n^{\frac{\ln p}{\ln 2}} \quad (5)$$

The effort for refurbishing a component is modeled as a fraction f_5 of the theoretical first unit (TFU) cost of the component:

$$E_{\text{prod,TFU}} = a_{\text{prod}} \cdot M^{\text{X}_{\text{prod}}} \quad (6)$$

$$E_{\text{refurb}} = f_{4,\text{refurb}} \cdot f_5 \cdot a_{\text{prod}} \cdot M^{\text{X}_{\text{prod}}} \quad (7)$$

As for the production cost, a learning effect which reduces the costs depending on the number of previously refurbished stages m is employed. The cost reduction, given in Eq. (8), is calculated similarly to Eq. (5), only with a specific p_{refurb} for this aspect. The learning factors for both the production and the refurbishment are assumed to be 0.85:

$$f_{4,\text{refurb}}(m) = m^{\frac{\ln p_{\text{refurb}}}{\ln 2}} \quad (8)$$

The effort of recovery of the stages is based on the analysis in Ref. [16]. Corrected for the herein assumed WYR cost of 370 k€, this results in a fixed recovery cost of ~850 k€ for DRL and IAC and ~310 k€ for the RTLS recovery. No scaling with dry mass of the returned stage is done here, as the infrastructure assumed in the derivation of these values is sufficient to handle the launchers of the size encountered within ENTRAIN.

3.3.1 Core stage

The core stage component consists of all elements classically found on expendable launch vehicles for which historical data exist. For the production effort, the original CER from TRANSCOST is used.

The main parameters governing the recurring cost of reusing a stage are the number of reuses and the refurbishment factor f_5 . To be competitive with VTVL stages, vehicles using VTHL technology must achieve a greater number of reuses while requiring less refurbishment effort. The baseline assumption for winged reusable stages is set at 50 reuses with a refurbishment factor of 2.3%, a figure derived from the Space Shuttle's historical data [10]. In contrast, VTVL stages are assumed to have a refurbishment factor of 5% and 25 reuses. Although specific values for the Falcon 9 are not available, as of 2020, the refurbishment and recovery costs were projected to be less than 10% of the new launcher

production costs, as noted in [17]. While 25 reuses have not achieved at this moment, it appears to be simply a matter of time until this is the case.

Given the inherent uncertainties in all these parameters, their impact is further explored through a parametric variation study detailed in Sect. 4.3.

3.3.2 Reentry and landing hardware

Just as for the development cost, as discussed in Sect. 3.2.2, for the production of the landing and reentry component, the cost estimations of the FESTIP studies [13] were used as the basis to generate specific CER's for these components. The resulting coefficients are given in the Appendix in Table 5.

The refurbishment factor and number of reuses are set to the same value as the for the core stage, discussed in Sect. 3.3.1.

3.3.3 Interstages

The interstages are modeled as separate components because they are jettisoned for the winged configurations in order expose the aerodynamically more efficient nose and thus cannot be considered part of the reusable first stage. The production effort for an interstage is estimated via a linear scaling with regard to the component mass based on the values given in Ref. [14] for the production of a sandwich-based interstage for the ARES-V launcher concept by NASA. Where applicable, the refurbishment factor and number of reuses are set to the same value as the for the core stage, discussed in 3.3.1.

3.3.4 Propulsion

For the propulsion elements, the CERs from TRANSCOST for modern pump fed engines were used for estimation of the production effort.

It is assumed that hydrocarbon-fueled engines have production costs approximately 30% lower per unit of thrust than hydrogen-fueled engines. One reason for this is the additional effort necessary for production of the complex hydrogen turbopump, while the hydrocarbon-fueled engines can be operated with a single turbine for both the fuel and oxidizer pumps. As the TRANSCOST model does not foresee a specific calibration factor for the production effort, a_{prod} for the hydrogen-fueled engines is set to $\sim 140\%$ of the values suggested for modern pump fed engines in TRANSCOST. Together with the implicit bias caused by the higher T/W of hydrocarbon engines, this results in a $\sim 30\%$ lower recurring cost for the hydrocarbon-fueled engines.

With regard to the reuse, the following assumptions are made: 20 reuses for engines on VTVL stages and 25 for those on winged stages, with refurbishment factors set at 7%

and 4%, respectively. The higher refurbishment requirement for VTVL stages accounts for the additional stresses—such as significant aerodynamic heat loads during reentry and multiple ignitions throughout a mission—that these engines endure. Given the inherent uncertainties in all these parameters, their impact is further explored through a parametric variation study detailed in Sect. 4.3.

For the airbreathing engines used in the FB configurations, the effort assessed within the ASTRA [15] study for production was used. The same engines (EJ2000) are assumed therein and for the ENTRAIN Flyback configurations. With regard to reuses, it is assumed that the engines are reused as often as the airframe into which they are integrated (50 times) and that no refurbishment between flights is necessary.

3.4 Evaluation of uncertain launch markets

In order to gain a complete picture of the cost associated with a given launch vehicle both the recurring and the non-recurring costs have to be considered. Obviously, the recurring cost depends heavily on the number of launches considered. Even the average cost of vehicle elements varies with the total number of produced elements, due to the learning factor considered.

In Ref. [11] a methodology was established that allows the consideration of uncertain market scenarios and includes a combinatorial optimization of the payloads onto the available launch options for minimal launch costs. While originally developed for the assessment of launch vehicles families, it is herein applied to the single launchers, essentially modeled as launch vehicles families with a single member. For the VTVL launchers, however, the single launcher offers different operational modes (DRL and RTLS), so in their case the family actually consists of the two variants.

3.4.1 Definition of launch market scenarios

Herein, a launch market scenario is defined by the following key characteristics:

- **Duration of scenario:** Reflecting the long lifespan of launch systems due to significant initial investments, the timeframe for assessing future launch needs is extensive. Longer durations introduce greater market uncertainties.
- **Probability of dedicated launch:** This factor considers the likelihood that a payload requires a dedicated launch due to specific needs such as security concerns, unique orbital requirements, or strict schedules.
- **Market share:** This denotes the percentage of payloads an organization successfully acquires in the competitive launch market. Herein, the market share for single payloads and for constellation payloads are varied separately.

- **Number of launch epochs:** Launch epochs model the intervals between launches to determine payload grouping for rideshare opportunities. Payloads are assigned to epochs randomly, affecting the feasibility of combining them in shared launches based on their time sensitivity.
- **Number and mass distribution of payloads:** Payloads are categorized by their intended orbits, such as Sun synchronous orbit (SSO) and geostationary transfer orbit (GTO). This classification influences the launcher's performance and the potential for rideshare missions, dictated by the compatibility of destination orbits.

Each scenario involves a randomly sampled set of payloads, each defined by mass, destination orbit, and the necessity for a dedicated launch. This structured approach allows for realistic simulation and analysis of market scenarios under varying conditions of uncertainty.

Herein, only GTO and SSO are considered as orbital destinations. Historically, these have been primary targets for non-constellation payloads and are likely to remain important due to their unique characteristics.

Table 2 Uncertainty parameters of launch scenario, all sampled uniformly

Parameter	Interval	Unit
No. of payloads for GTO per year	[7, 13]	—
No. of payloads for SSO per year	[11, 20]	—
No. of constellation payloads	[3000, 5000]	—
No. of epochs	[10, 80]	—
Dedicated launch probability	[0, 0.8]	—
Market share	[0.1, 1.0]	—
Payload mass GTO payload	[2500, 7000]	kg
Payload mass SSO payload	[300, 6500]	kg
Payload mass of constellation payloads	[400, 600]	kg

For constellation payloads, which are anticipated to form a large part of the future launch market, the specific orbital destination is often not fixed, and parameters can vary across the constellation. Due to the lack of comprehensive launcher performance data for all possible inclinations, SSO performance metrics are applied when assigning constellation payloads to launchers.

3.4.2 Uncertainties in future market scenarios

For the forthcoming results shown in Sect. 4, Table 2 outlines the parameter space for sampling individual scenarios, assuming a uniform distribution within defined intervals. These parameters, including the number of payloads and their masses for GTO and SSO orbits, are derived from 2023 ESA forecasts [18], considering only payloads accessible to a European launch provider. The maximum GTO payload mass is limited to 7 t, as this was the design target for the ENTRAIN study. An arbitrary uncertainty of approximately $\pm 30\%$ is assumed for payload numbers.

The parameters for the number of launch epochs, dedicated launch probability, and market share are designed to explore a broad range of possible future market conditions. The scenarios span 20 years, segmented into launch epochs ranging from a minimum of 3 months to a maximum of 2 years.

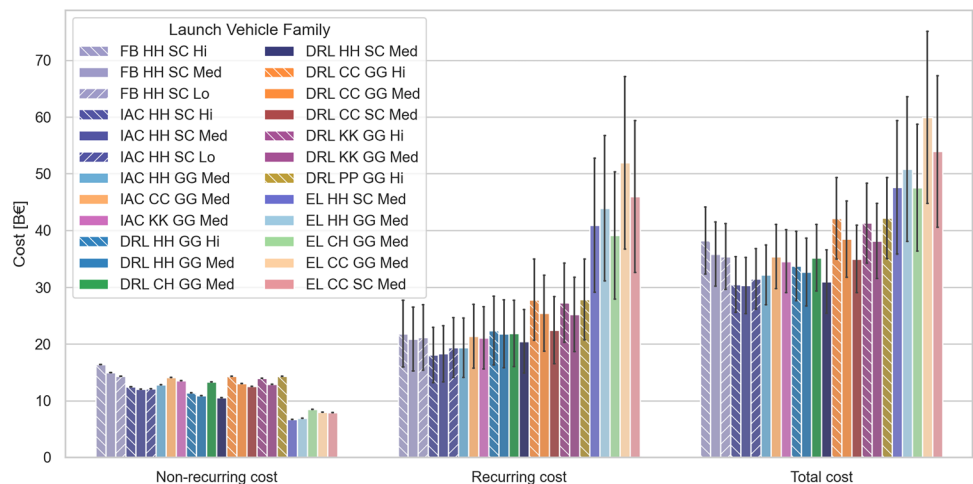
4 Results

This section includes the results of all vehicles subjected to the cost estimation methodology described in Sect. 3.

4.1 Results for all configurations

Figure 5 gives an overview over the cost estimation results. The magnitude of the total cost is substantial, but it has to be seen in context of the underlying launch scenarios. The

Fig. 5 Results overview all ENTRAIN configurations. The error bars indicate one standard deviation. As only uncertainties in the launch market are considered, the non-recurring cost does not show any variability. (e.c. 2022)



number of launches varies an order of magnitude ranging from 51 to 723 launches, corresponding to ~2.6 to ~36 launchers per year. Accordingly, there also is a significant spread in the total cost associated with each launcher. In most cases, the recurring cost is much larger than the non-recurring cost, especially for the fully expendable versions. It is noteworthy that under these assumptions, the ELV launchers are always costlier than their equivalent cousins, even in cases where the market share is small.

A more detailed breakdown of the development cost for each configuration is shown in Fig. 6.

The winged stages exhibit higher development cost than the equivalent DRL stages, even though their propellant loadings are smaller (as they do not require propellant for deceleration during reentry). This difference is driven by the higher mass of the reentry components and the associated costs. For the hybrid launchers, the impact of the additional engine development program on the development cost can also be clearly seen.

Figure 7 shows the average recurring launch cost of all configurations, which again puts the large total cost into perspective: per launch, the estimated costs of the configuration with a reusable first stage are lower than most currently operational systems.

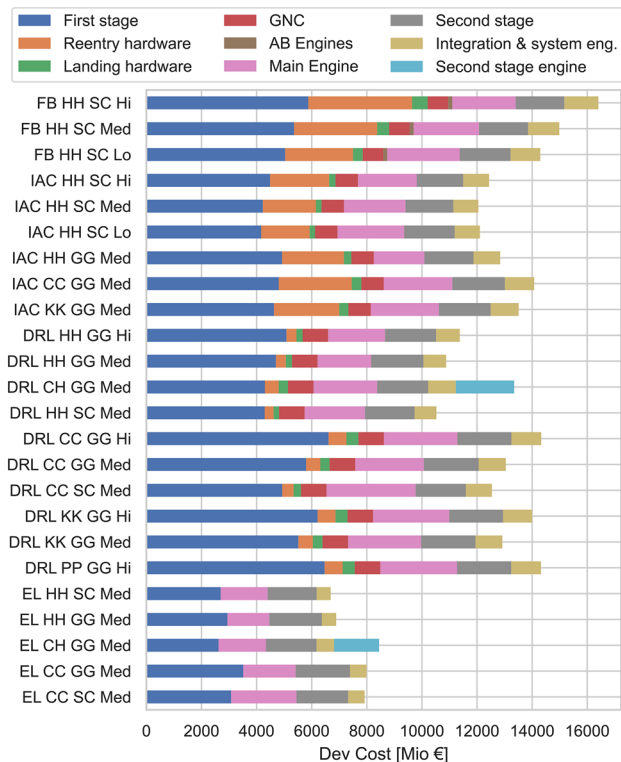


Fig. 6 Development cost breakdown of the launch vehicles investigated within the ENTRAIN study. (e.c. 2022)

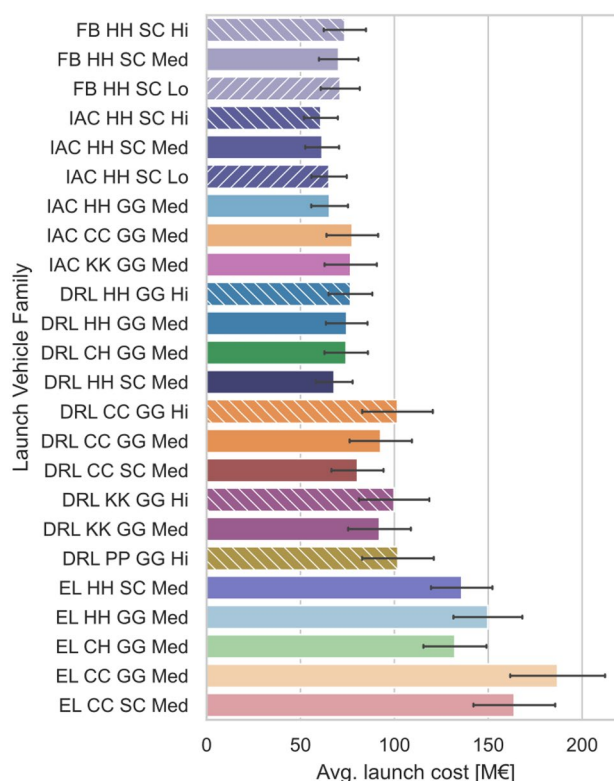


Fig. 7 Average launch cost of the launch vehicles investigated within the ENTRAIN study. The error bars indicate one standard deviation. (e.c. 2022)

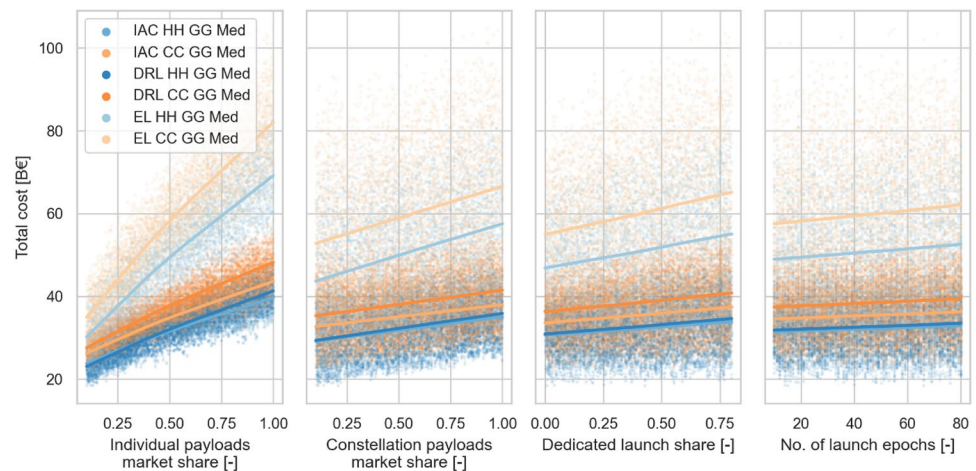
For the cases with a reusable first stage, the recurring cost of the first stage is significantly lower than the recurring cost associated with the second stage. Thus, an increase of reuses or reduction of refurbishment cost will not have a major impact in the total cost. Increase of the efficiency of all components and full reusability are the major pathways to reduce the cost significantly further.

4.2 Sensitivity to market scenario

For the sake of clarity in this section, and the next, only selected configurations will be shown and discussed. Methane- and hydrogen-fueled variants are selected with a focus on gas generator engines, as these are the development programs currently underway in Europe for large rocket engines.

In Fig. 8, the effect of the launch market uncertainties on the total cost for all assessed samples is shown. The resulting total cost for all 5000 samples is plotted over the four core uncertainties: Market share in individual payloads, market share for constellation payloads, share of payloads requiring a dedicated launch and the number of launch epochs. The rolling average is indicated by a solid line.

Fig. 8 Sensitivity to uncertain launch market parameters of selected ENTRAIN launchers. 5000 market scenario samples shown. (e.c. 2022)



As expected, the fully expendable variants fare worse, the larger the market share becomes. The IAC configurations exhibit a slightly shallower increase of cost with rising market share, due to the higher number of reuses and lower refurbishment factor assumed for them. For methane-fueled cases, the IAC option always is less expensive than the equivalent DRL launcher. In contrast, for the hydrogen-fueled versions, the comparison is very close, with a slight advantage for the VTVL configuration at lower market shares and vice versa at higher market shares.

The impact of the SSO payload capacity can be seen in the cost increase resulting from an increasing share of the constellation market. The methane-fueled launchers, with their higher SSO payload performance, as described in Sect. 2.3, have a slightly lower sensitivity towards this parameter.

In general, the sensitivity of the results towards the number of dedicated launches and the number of launch epochs is minor. As expected the fully expendable launchers are affected slightly more by the additional launches resulting from increased values of these parameters.

4.3 Sensitivity to parameters associated with reusability

Figure 9 shows the dependence of the total and recurring cost on the number of reuses and the refurbishment factor of the first stage and Fig. 10 shows the same parametric variation but for the engine reuses and refurbishment.

The parameters not being varied are kept at their reference values, as described in Sect. 3.3. Initially, increasing the number of reuses strongly impacts the total cost, however the effect flattens out after ~20 reuses for both engines and stages.

As discussed in Sect. 3.2.1, the IAC stages are required to have lower refurbishment factors and a higher number of

reuses to be competitive with their DRL equivalents. The results here essentially show the case if only one of these requirements is met, and in the other parameter, only parity is achieved.

For the engine reuses, the effect does not change the overall conclusions. However, for the stage itself, parity in either the number of reuses or the refurbishment factor lead to the hydrogen-fueled VL configuration being less costly than its IAC equivalent. This is not the case for the methane-fueled versions.

These parameter studies indicate that even with only one reuse of the stage the variants with IAC or DRL booster stages have similar costs than the ELV variants. However, this cost parity is due to the fact that engine reuse remains unaffected by this parameter variation. In the absence of these cost savings, an RLV with only a single reuse would naturally be significantly more expensive than its ELV counterpart.

5 Discussion

After a discussion of the study limitations in Sect. 5.1 and a comparison to real launchers in Sect. 5.2, the rest of the discussion is structured around the design degrees of freedom investigated within the ENTRAIN study: engine cycle, recovery mode, propellant and staging velocity. While some differences are small, others are significant enough that conclusions can be drawn with reasonable confidence, despite the uncertainties involved in the process.

5.1 Limitations

From a technical perspective, the uncertainties in the design of the launch vehicles, as discussed in Refs. [3, 4], apply

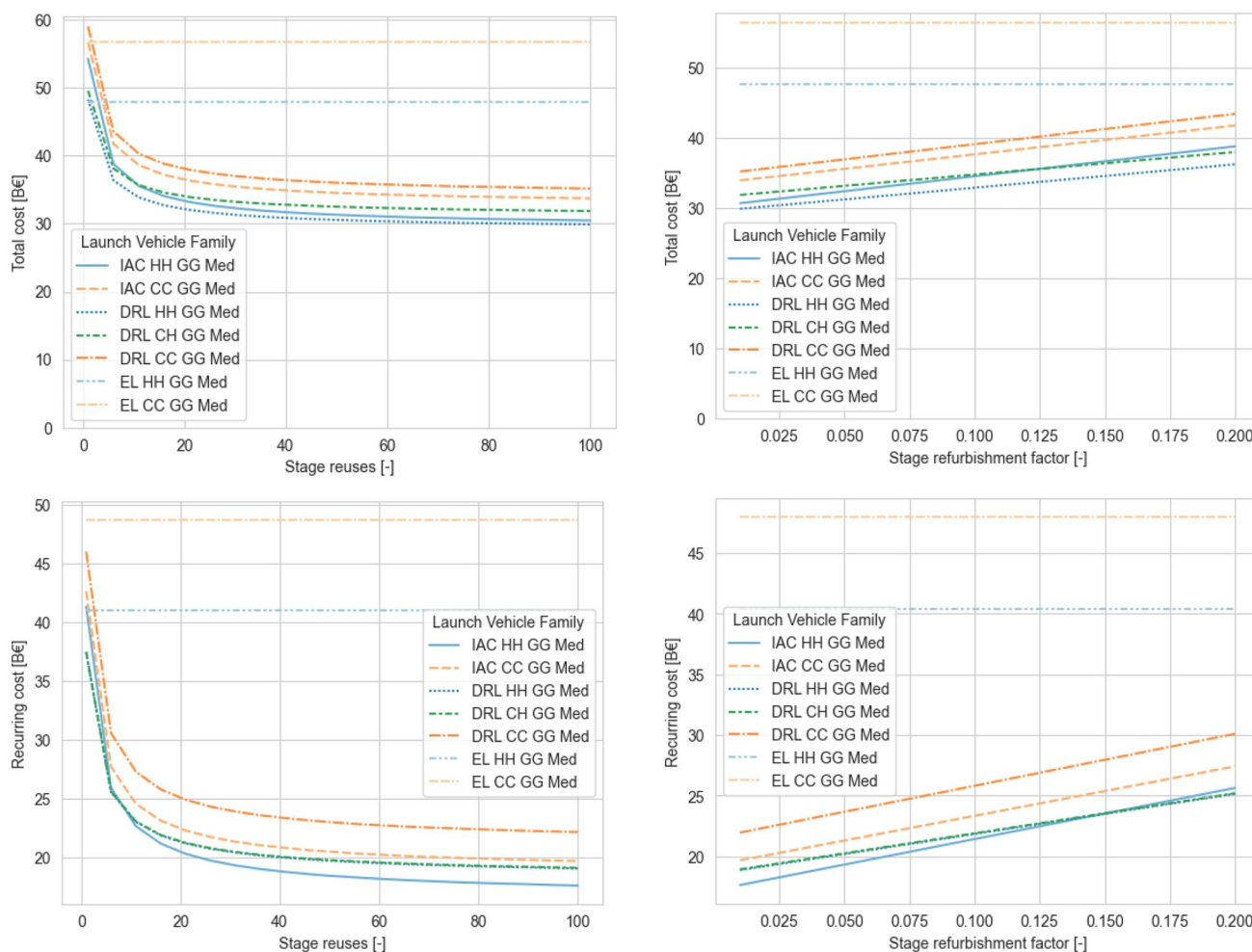


Fig. 9 Effect of stage reuse number and refurbishment factor on total and recurring cost of selected configurations. Average cost from 280 market scenario samples shown. (e.c. 2022)

here as well, since these launchers serve as input for the calculations herein. These uncertainties include potential errors in estimating subsystem masses and performance, as well as inaccuracies arising from the convergence limits of the iterative design process. Generally, the authors consider the uncertainties in the technical parameters as significantly smaller than the uncertainty in the absolute cost estimation.

5.1.1 Parametric cost modeling

In general, boiling down the cost estimation of such a complex project as the development and operation of a launch vehicle over decades to a handful of regression formulas necessarily neglects much of the details involved in the process. However, at the conceptual stage, these details are not available and thus a simplified assessment is necessary. For the relative comparison central to this work, accurately identifying the general cost drivers is essential, whereas precision in estimating absolute values is less critical.

5.1.1.1 Data basis The data used for the formulation of the CERs do not include the most modern launch vehicles, as their cost is usually not publicly known. Even for publicly funded development programs, the final effort is often not trivially available. Also, for the type of stages proposed within the ENTRAIN study, either no previously built stages exist (for the HL configurations) or very limited data is available for the few examples that have been flown (VL). For the CER's used for modeling of the landing and reentry hardware, the results of previous European studies are used, as described in Sect. 3. While these are the results of comparatively detailed cost breakdowns, actual data from operational vehicles would be preferable.

5.1.1.2 Choice of coefficients The selection of specific cost modeling parameters and scenarios reflects certain assumptions made by the authors. These choices, while made to the best of the author's knowledge, may introduce biases that favor certain configurations over others, poten-

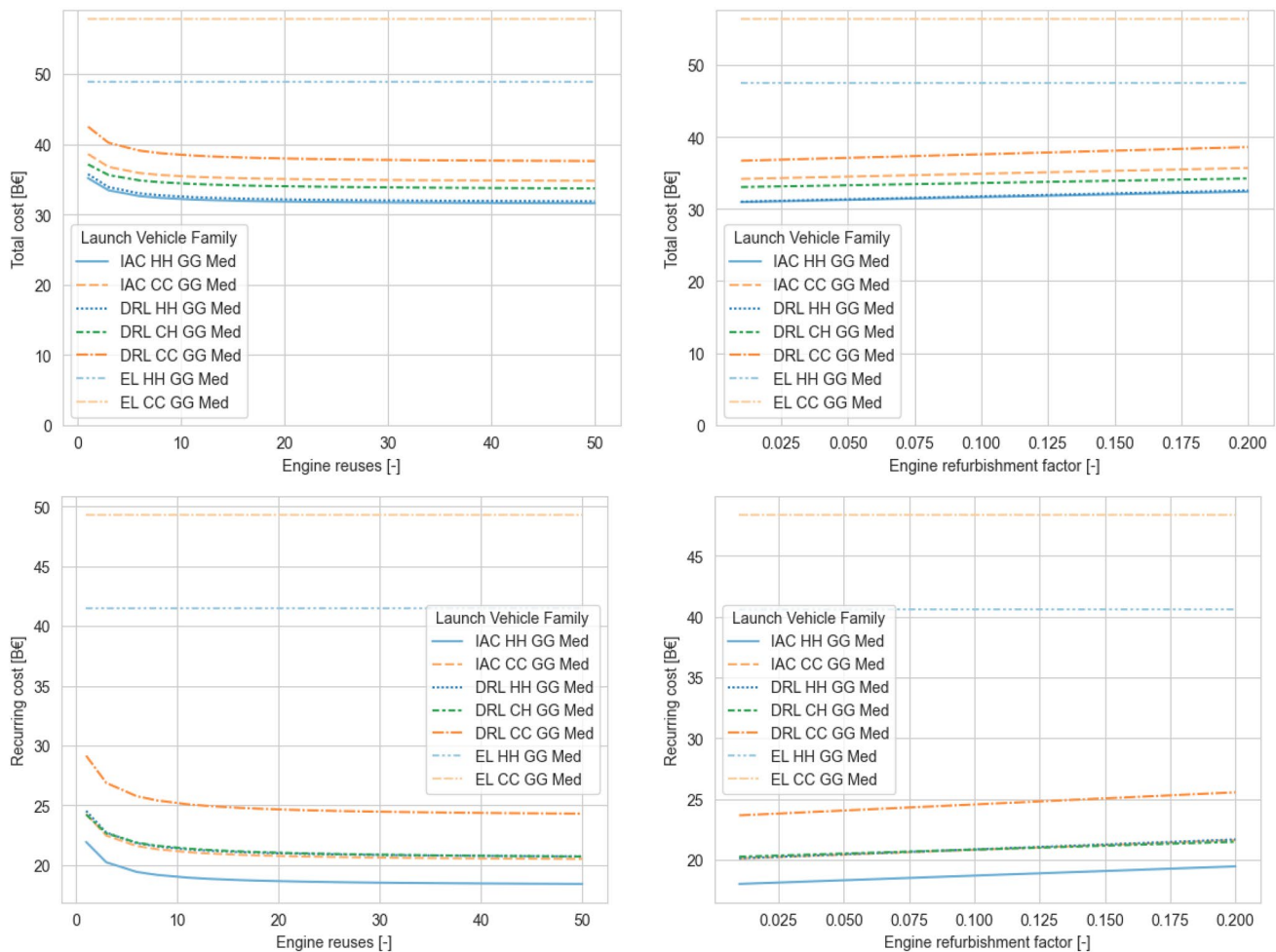


Fig. 10 Effect of engine reuse number and refurbishment factor on total and recurring cost of selected configurations. Average cost from 280 market scenario samples shown. (e.c. 2022)

tially influencing the study's conclusions. For the most uncertain parameters, the ones involving the cost of reusing a stage, a parametric variation was done and presented in Sect. 4.3 to illustrate scenarios beyond the reference assumptions.

5.1.2 Future launch markets

The launch markets considered, as shown in Sect. 3.4.2, span a substantial range, essentially covering an order of magnitude from 2.6 to 36 launches a year over 20 years. The different uncertainties cover a large possibility space. However, as with any prediction of the future, the actual launch market of the future might very well be different from what is expected. Since all these launch vehicles exhibit similar GTO payload capacities, changes in the

SSO market are more likely to cause significant distortions. For instance, hydrocarbon-fueled launchers have higher payload capacities for SSO orbits, so if the number of these payloads in the scenario increases significantly, their relative standing might improve, and conversely, it could decline if the number decreases.

5.2 Comparison with current launchers

5.2.1 Falcon 9

As SpaceX currently operates the only partially reusable launch vehicle, the Falcon 9, a comparison comes naturally. While SpaceX publishes prices [19] (currently 69.75 M\$), these of course are not identical to actual cost incurred. Currently, the internal cost of SpaceX is

speculated to be between 20 M\$ and 30 M\$ [20]. This is significantly lower than the average launch cost of the DRL KK GG Med configuration in the scenarios with the most launches (~ 66 M€). Multiple factors contribute to this:

- **Payload capacity:** The Falcon 9 can deliver 5.5 tons to GTO, compared to the 7.5-ton target for the ENTRAIN configurations.
- **Low dry mass:** The Falcon 9 uses technologies such as propellant densification and structures made of aluminum lithium that enable much lower low dry mass than estimated for the ENTRAIN configurations. The T/W ratio of the Merlin engine is also much higher than assumed for the kerosene fueled engines herein (as discussed in [2])
- **Higher launch cadence:** SpaceX's launch rate is currently about three times as high as the most optimistic launch market scenarios considered herein (~ 36 launches per year vs ~ 100 launches per year).
- **CER data basis:** The CERs used in this analysis are based on historical vehicles produced through government contracting, rather than the commercial approach used by SpaceX.

Taking these factors into account, the estimated recurring costs are in reasonable agreement with the real-world data currently available.

The non-recurring cost of the Falcon 9 is not directly comparable, as its design underwent continuous improvement, contrasting with the linear development programs traditionally used for launch vehicles. This continuous development approach differs from the assumptions underlying the CERs used in this study and the historical data they are based on.

5.2.2 Ariane 6

The development of the Ariane 6 has cost more than 4 B€ (mixed e.c.) [21]. This figure excludes the development of new rocket engines, as both the Vulcain and Vinci engines were previously developed and only adapted for this launcher. In addition, the development of the solid booster P120C is not included in these costs. The EL HH GG Med configuration within the ENTRAIN class is likely the most comparable launcher, with an estimated development cost of approximately €6.9 billion (2022 e.c.), which includes the development of a new main rocket engine. While the Ariane 6 boasts a higher payload capacity, its cryogenic stages are actually smaller, with propellant loadings of 140 tons and 31 tons compared to 230 tons and 75 tons for the ENTRAIN configuration.

This comparison suggests that the estimated development costs for the most similar ENTRAIN launcher align reasonably with the costs observed in the Ariane 6 development program.

5.3 Comparison of different engine cycles

Although, as discussed in Sect. 3.2.4, the chosen cost modeling approach leads to a 15% higher recurring cost and a 25% higher non-recurring cost per unit of thrust for staged combustion engines relative to their gas generator counterparts, the total cost results suggest that this premium is justified. Configurations with staged combustion engines consistently achieve approximately 6% lower total costs when fueled with hydrogen and 12% when fueled with methane.

The higher specific impulse of closed-cycle engines results in smaller launchers, particularly for the Δv -intensive VTVL stages, leading to overall cost reductions. This benefit extends to all components, including a reduction in thrust requirements, which compensates for much of the higher thrust-specific cost. Consequently, even the recurring engine costs are comparable between the two engine cycle options.

5.4 Comparison of different recovery modes

The comparison between different recovery modes is perhaps the most uncertain aspect discussed herein. No HL first stages have ever been operational for orbital missions, and only one operational launcher currently utilizes a VL first stage. Moreover, the actual costs associated with stage reuse in this case are not publicly available.

The difference between the IAC and DRL configurations largely depends on the specific impulse of the systems. For hydrogen-fueled configurations, the IAC return method has a slight total cost advantage (~ 2%) owing to its reduced recurring costs (~ 12% lower). However, this advantage is mostly offset by higher development costs (~ 14% higher).

For hydrocarbon-fueled configurations, the difference is more pronounced due to the impact of lower specific impulse on DRL vehicles and their larger total Δv budget. The recurring costs for IAC stages are about 19% lower, while the non-recurring costs are about 6% higher, resulting in an average total cost reduction of 9%.

Due to the higher assumed number of reuses and lower refurbishment factors (discussed in Sect. 3.3.1), IAC stages perform better in launch market scenarios with higher launch frequencies. However, the parametric studies in Sect. 4.3 demonstrated that merely achieving parity in even one of these requirements leads to higher total costs for IAC designs compared to hydrogen-fueled DRL stages. For methane-fueled versions, however, the advantage of IAC

stages is more robust, given the greater impact of the lower specific impulse.

With regard to the flyback configurations, they are always costlier than the equivalent IAC options with the difference in total cost increasing from 11 to 20% with increasing separation velocities.

5.5 Comparison of reusable and expendable launchers

As small as the differences are between the various RLV options, the difference towards the fully expendable launch vehicles is significant. The fully expendable launch vehicles are, on average, 36–41% more expensive than their equivalents with reusable first stages. Only in the most pessimistic launch scenarios do the ELV achieve similar total cost than their counterparts with reusable first stages, but in no case are their total costs actually lower. For example, in the scenario leading to the lowest launch costs, the DRL CC GG Med has a non-recurring cost of 13 B€ and an average launch cost of 186 €, the equivalent ELV EL CC GG Med has a development costs of 8 B€ and an average launch cost of 314 M€. In this case the breakeven point is at ~40 launches. As the scenario requires 51 launches in both cases, the DRL configuration ends up (slightly) ahead even in this extreme case.

It seems that the breakeven point is below the most pessimistic cases captured via the market uncertainties, so at less than 2.6 launches per year (over 20 years).

5.6 Comparison of different propellants

The full results shown in Sect. 4.1 contain four different fuel options; however, for the purpose of this discussion, the focus will lie on hydrogen and methane as the current discussion of the future heavy-lift European launcher is focused on these options. The results of methane and the other hydrocarbons are similar enough that the discussion remains applicable to the other cases.

All hydrogen-fueled launchers are less costly than their methane-fueled counterparts, which is noteworthy given that hydrogen engines have approximately 30% higher recurring costs per unit of thrust. The difference is particularly significant for versions with VTVL first stages and gas generator engines, where methane-fueled variants are about 18% more expensive than their hydrogen equivalents. The smaller thrust-specific cost of methane-fueled systems is outweighed by the significantly larger propellant load, which results in substantially increased dry mass and thrust requirements. For instance, the DRL CC GG Med configuration requires nearly 2.5 times the thrust of its hydrogen-fueled counterpart, DRL HH GG Med.

When staged combustion engines are used, the cost difference between hydrogen- and methane-fueled DRL configurations narrows but remains significant at 13%. Methane-fueled configurations, with their initially lower specific impulse, benefit more from the increase in specific impulse than hydrogen-fueled configurations.

In cases with an IAC first stage, the cost difference between the two fuel options is smaller, around 10%, as expected, since this return method demands less Δv . Although the ENTRAIN study did not evaluate any methane-fueled VTHL versions with staged combustion engines, the trends observed suggest that such a combination could be promising.

Continuing from the single-fuel launchers, the hybrid launchers, with a hydrogen-fueled upper stage and methane-fueled lower stage, remain competitive, even with the added cost of developing and producing two different engines. This results in 23% higher non-recurring costs, but only a minimal increase in recurring cost (0.3%), compared to the fully hydrogen-fueled version.

5.7 Comparison of different staging velocities

The sensitivity to staging varies significantly depending on the propellant choice and return method. This aligns with expectations from the rocket equation, as specific impulse and the total Δv budget largely determine the required total mass. As anticipated, the sensitivity is highest for hydrocarbon-fueled concepts with a VTVL first stage and lowest for hydrogen-fueled stages utilizing IAC and closed-cycle engines. Flyback configurations exhibit greater sensitivity to staging than IAC cases. Although the return flight in flyback configurations is powered by air-breathing engines and not directly linked to the main rocket propulsion, it still consumes fuel and, therefore, contributes to the overall Δv budget. As a result, higher staging velocities lead to increased stage sizes and, consequently, higher costs. This effect remains significant, even though this return method was only assessed for hydrogen-fueled configurations with closed-cycle engines, which, as mentioned earlier, are relatively insensitive to staging.

The IAC return method is better suited for higher separation velocities, while the development cost does also increase, the recurring cost falls sufficiently to compensate for this. In total cost, the medium and high separation velocity cases are almost identical.

For the configurations with vertically landing first stages, only the medium and high separation velocities were investigated within the ENTRAIN study. The low separation velocity lead to excessively large launchers for the hydrocarbon-fueled launchers due to the large Δv required of the upper stage in these cases, as described

in Ref. [3]. For these cases, the medium staging velocity results in the lowest costs. While the high separation velocity theoretically results in a larger reusable fraction, this benefit is more than equalized by the increase in first stage size driven by the additional Δv required for acceleration and deceleration.

6 Conclusion

Within this paper, a cost estimation of the launchers from the ENTRAIN study is presented. Designed for a 7.5 t payload into GTO, different propellant combinations, engine cycles and recovery methods of a reusable first stage were investigated and the cost for various combinations analyzed.

In addition to the partially reusable launchers, a number of expendable two-staged launchers were evaluated in order to quantify the advantage possible through a reusable first stage.

In general, the results herein show that even the cost of launchers cannot escape the tyranny of the rocket equation. Even though adaptations were made to account for differences between the different design options (i.e., the assumptions of lower thrust-specific production cost for hydrocarbon-fueled engines, or higher thrust-specific cost of staged combustion engines), the results largely follow the trends established in the analysis of the dry mass in the previous technical discussions. Due to the high-performance requirements resulting from serving a GTO mission with a two-staged vehicle including reuse of the first stage, any change in specific impulse has a large impact on the system size. Therefore, even though on a subsystem level, a specific design option might appear desirable and cost-beneficial, the resulting increase in total launcher size might negate the specific cost savings entirely.

The main takeaways are listed below, in order of the magnitude of the difference found:

- Across all 5,000 launch market scenario samples considered in this study, launchers with reusable first

stages enable significant cost savings compared to fully expendable versions.

- The use of hydrogen as a fuel results in significantly lower costs than fully hydrocarbon-fueled vehicles. The additional propellant and dry mass needed due to the lower specific impulse more than negate any potential cost benefits by lower production effort for hydrocarbon-fueled engines.
- The performance benefit of closed-cycle engines allows a reduction in overall stage size that results in lower total cost compared to the gas generator fueled version, even when considering increased thrust-specific development and production costs.
- Due to the nature of the parametric variation of the staging velocity, no exact staging optimum is identified. However, the medium separation velocity (ca. Mach 9) appears well suited. As expected, the sensitivity to the staging is higher the lower the specific impulse.
- With sufficiently low refurbishment costs and a high number of reuses, IAC first stages can amortize their additional development costs and become cheaper than the equivalent DRL stages. However, even in these cases, the differences are small, as the expendable fraction of the launch vehicles becomes the primary cost driver in both scenarios, making small differences in the costs of the reusable portions less impactful on the total cost. The comparison is clearer in the hydrocarbon-fueled cases, where IAC configurations show a greater advantage. This advantage arises from the reduced Δv budget of these missions using in-air-capturing technology compared to vertical landing, which particularly benefits lower specific impulse fuel options.

Appendix

See Tables 3, 4 and 5.

Table 3 Key parameters of investigated ELV launchers

Fuel	–	LH2	LCH4	Hybrid		
Engine cycle	–	GG	SC	GG	SC	GG
2nd-stage Δv	[km/s]	7.0	7.0	7.0	7.0	7.0
Staging category	–	Med	Med	Med	Med	Med
Designation	–	EL HH GG Med	EL HH SC Med	EL CC GG Med	EL CC SC Med	EL CH GG Med
<i>1st stage</i>						
Propellant loading	[t]	230	183	575	435	295
Total dry mass	[t]	26.0	22.7	43.9	37.4	22.0
Propulsion mass	[t]	6.4	6.7	13.1	13.9	6.8
No. of engines	[–]	7	7	11	9	7
Single engine thrust (sea level)	[kN]	711	572	992	949	802
<i>2nd stage</i>						
Propellant loading	[t]	75	64	148	125	70
Dry mass	[t]	6.7	5.7	7.8	7.1	6.1
Fairing	[t]	1.4	1.4	1.4	1.6	1.4
Propulsion mass	[t]	1.2	1.1	1.7	1.8	1.1
Engine thrust (vacuum)	[kN]	856	666	1198	1124	778
<i>Total launcher</i>						
Height	[m]	74.1	66.2	79.0	67.6	60.5
Diameter	[m]	5	5	5	5	5
Payload to GTO	[t]	7.57	7.55	7.41	7.54	7.51
GTO GLOM	[t]	355	291	799	627	411
Payload to SSO	[t]	15.0	13.8	18.5	17.5	14.6
SSO GLOM	[t]	362	297	810	637	419

Table 4 SSO Performance of selected ENTRAIN RLV launchers

Fuel	–	LH2	LCH4	Hybrid					
Engine cycle	–	GG	SC	GG	SC	GG	SC	GG	GG
2nd-stage Δv	[km/s]	7.0	7.0	7.0	7.0	7.0	7.0	7.0	7.0
Staging category	–	Med	Med	Med	Med	Med	Med	Med	Med
Designation	–	VL HH GG Med	VL HH SC Med	HL HH GG Med	HL HH SC Med	VL CC GG Med	VL CC SC Med	HL CC GG Med	VL CH GG Med
<i>SSO performance</i>									
Payload to SSO with RTLS	[t]	10.3	9.8	–	–	9.6	10.4	–	9.7
Payload to SSO	[t]	14.9	13.5	14.3	14.1	18.1	16.9	17.9	14.4
SSO GLOM	[t]	455	374	391	335	1119	845	826	577

Table 5 Coefficients and CER data used for parametric cost estimations

Launcher	Element	a_{dev}	x_{dev}	a_{prod}	x_{prod}	f_1	f_2	f_3	f_5	p	p_{refurb}	Reuses
FB_HH_SC_HI	First stage	331	0.377	1.84	0.59	1	1	1	0.023	0.85	0.85	50
	Reentry HW	0.899	0.972	1.901	0.59	1	1	1	0.023	0.85	0.85	50
	Landing HW	1.121	0.916	0.839	0.59	1	1	1	0.023	0.85	0.85	50
	GNC	2000	1	0	1	1	1	1	–	1	–	–
	A/B propulsion	0.432	1	0.029	1	1.1	0.73	1	0	1	0.85	50
	SL engine	277	0.48	1.2	0.535	1.1	0.73	1	0.04	0.85	0.85	25
	Interstage	0.079	1	0.005	1	0.7	1	1	–	0.85	–	–
	Second stage	331	0.377	1.84	0.59	0.7	1	1	–	0.85	–	–
	Vac. engine	277	0.48	1.2	0.535	1.1	0.73	1	–	0.85	–	–
FB_HH_SC_MED	First stage	331	0.377	1.84	0.59	1	1	1	0.023	0.85	0.85	50
	Reentry HW	0.899	0.972	1.901	0.59	1	1	1	0.023	0.85	0.85	50
	Landing HW	1.121	0.916	0.839	0.59	1	1	1	0.023	0.85	0.85	50
	GNC	2000	1	0	1	1	1	1	–	1	–	–
	A/B propulsion	0.432	1	0.029	1	1.1	0.73	1	0	1	0.85	50
	SL engine	277	0.48	1.2	0.535	1.1	0.73	1	0.04	0.85	0.85	25
	Interstage	0.079	1	0.005	1	0.7	1	1	–	0.85	–	–
	Second stage	331	0.377	1.84	0.59	0.7	1	1	–	0.85	–	–
	Vac. engine	277	0.48	1.2	0.535	1.1	0.73	1	–	0.85	–	–
FB_HH_SC_LOW	First stage	331	0.377	1.84	0.59	1	1	1	0.023	0.85	0.85	50
	Reentry HW	0.899	0.972	1.901	0.59	1	1	1	0.023	0.85	0.85	50
	Landing HW	1.121	0.916	0.839	0.59	1	1	1	0.023	0.85	0.85	50
	GNC	2000	1	0	1	1	1	1	–	1	–	–
	A/B propulsion	0.432	1	0.029	1	1.1	0.73	1	0	1	0.85	50
	SL engine	277	0.48	1.2	0.535	1.1	0.73	1	0.04	0.85	0.85	25
	Interstage	0.079	1	0.005	1	0.7	1	1	–	0.85	–	–
	Second stage	331	0.377	1.84	0.59	0.7	1	1	–	0.85	–	–
	Vac. engine	277	0.48	1.2	0.535	1.1	0.73	1	–	0.85	–	–
HL_HH_SC_HI	First stage	331	0.377	1.84	0.59	1	1	1	0.023	0.85	0.85	50
	Reentry HW	0.899	0.972	1.901	0.59	1	1	1	0.023	0.85	0.85	50
	Landing HW	1.121	0.916	0.839	0.59	1	1	1	0.023	0.85	0.85	50
	GNC	2200	1	0	1	1	1	1	–	1	–	–
	SL engine	277	0.48	1.2	0.535	1.1	0.73	1	0.04	0.85	0.85	25
	Interstage	0.079	1	0.005	1	0.7	1	1	–	0.85	–	–
	Second stage	331	0.377	1.84	0.59	0.7	1	1	–	0.85	–	–
	Vac. engine	277	0.48	1.2	0.535	1.1	0.73	1	–	0.85	–	–
	First stage	331	0.377	1.84	0.59	1	1	1	0.023	0.85	0.85	50
HL_HH_SC_MED	Reentry HW	0.899	0.972	1.901	0.59	1	1	1	0.023	0.85	0.85	50
	Landing HW	1.121	0.916	0.839	0.59	1	1	1	0.023	0.85	0.85	50
	GNC	2200	1	0	1	1	1	1	–	1	–	–
	SL engine	277	0.48	1.2	0.535	1.1	0.73	1	0.04	0.85	0.85	25
	Interstage	0.079	1	0.005	1	0.7	1	1	–	0.85	–	–
	Second stage	331	0.377	1.84	0.59	0.7	1	1	–	0.85	–	–
	Vac. engine	277	0.48	1.2	0.535	1.1	0.73	1	–	0.85	–	–
	First stage	331	0.377	1.84	0.59	1	1	1	0.023	0.85	0.85	50
	Reentry HW	0.899	0.972	1.901	0.59	1	1	1	0.023	0.85	0.85	50
HL_HH_SC_LOW	Landing HW	1.121	0.916	0.839	0.59	1	1	1	0.023	0.85	0.85	50
	GNC	2200	1	0	1	1	1	1	–	1	–	–
	SL engine	277	0.48	1.2	0.535	1.1	0.73	1	0.04	0.85	0.85	25
	Interstage	0.079	1	0.005	1	0.7	1	1	–	0.85	–	–
	Second stage	331	0.377	1.84	0.59	0.7	1	1	–	0.85	–	–
	First stage	331	0.377	1.84	0.59	1	1	1	0.023	0.85	0.85	50

Table 5 (continued)

Launcher	Element	a_{dev}	x_{dev}	a_{prod}	x_{prod}	f_1	f_2	f_3	f_5	p	p_{refurb}	Reuses
HL_HH_GG_MED	Vac. engine	277	0.48	1.2	0.535	1.1	0.73	1	–	0.85	–	–
	First stage	331	0.377	1.84	0.59	1	1	1	0.023	0.85	0.85	50
	Reentry HW	0.899	0.972	1.901	0.59	1	1	1	0.023	0.85	0.85	50
	Landing HW	1.121	0.916	0.839	0.59	1	1	1	0.023	0.85	0.85	50
	GNC	2200	1	0	1	1	1	1	–	1	–	–
	SL engine	277	0.48	1.2	0.535	1	0.73	1	0.04	0.85	0.85	25
	Interstage	0.079	1	0.005	1	0.7	1	1	–	0.85	–	–
	Second stage	331	0.377	1.84	0.59	0.7	1	1	–	0.85	–	–
HL_CC_GG_MED	Vac. engine	277	0.48	1.2	0.535	1	0.73	1	–	0.85	–	–
	First stage	331	0.377	1.84	0.59	1	1	1	0.023	0.85	0.85	50
	Reentry HW	0.899	0.972	1.369	0.59	1	1	1	0.023	0.85	0.85	50
	Landing HW	1.121	0.916	0.839	0.59	1	1	1	0.023	0.85	0.85	50
	GNC	2200	1	0	1	1	1	1	–	1	–	–
	SL engine	277	0.48	1.2	0.535	1.1	0.73	1	0.04	0.85	0.85	25
	Interstage	0.079	1	0.005	1	0.7	1	1	–	0.85	–	–
	Second stage	331	0.377	1.84	0.59	0.7	1	1	–	0.85	–	–
HL_KK_GG_MED	Vac. engine	277	0.48	1.2	0.535	1.1	0.73	1	–	0.85	–	–
	First stage	331	0.377	1.84	0.59	1	1	1	0.023	0.85	0.85	50
	Reentry HW	0.899	0.972	1.369	0.59	1	1	1	0.023	0.85	0.85	50
	Landing HW	1.121	0.916	0.839	0.59	1	1	1	0.023	0.85	0.85	50
	GNC	2200	1	0	1	1	1	1	–	1	–	–
	SL engine	277	0.48	1.2	0.535	1.1	0.73	1	0.04	0.85	0.85	25
	Interstage	0.079	1	0.005	1	0.7	1	1	–	0.85	–	–
	Second stage	331	0.377	1.84	0.59	0.7	1	1	–	0.85	–	–
VL_HH_GG_HI	Vac. engine	277	0.48	1.2	0.535	1.1	0.73	1	–	0.85	–	–
	First stage	331	0.377	1.84	0.59	1	1	1	0.06	0.85	0.85	25
	Interstage	0.079	1	0.005	1	1	1	1	0.06	0.85	0.85	25
	Reentry HW	0.899	0.972	1.901	0.59	1	1	1	0.06	0.85	0.85	25
	Landing HW	1.121	0.916	0.839	0.59	1	1	1	0.06	0.85	0.85	25
	SL engine	277	0.48	1.2	0.535	1	0.85	1	0.07	0.85	0.85	20
	GNC	2500	1	0	1	1	1	1	–	1	–	–
	Second stage	331	0.377	1.84	0.59	0.7	1	1	–	0.85	–	–
VL_HH_GG_MED	Vac. engine	277	0.48	1.2	0.535	1	0.85	1	–	0.85	–	–
	First stage	331	0.377	1.84	0.59	1	1	1	0.06	0.85	0.85	25
	Interstage	0.079	1	0.005	1	1	1	1	0.06	0.85	0.85	25
	Reentry HW	0.899	0.972	1.901	0.59	1	1	1	0.06	0.85	0.85	25
	Landing HW	1.121	0.916	0.839	0.59	1	1	1	0.06	0.85	0.85	25
	SL engine	277	0.48	1.2	0.535	1	0.85	1	0.07	0.85	0.85	20
	GNC	2500	1	0	1	1	1	1	–	1	–	–
	Second stage	331	0.377	1.84	0.59	0.7	1	1	–	0.85	–	–
VL_CH_GG_MED	Vac. engine	277	0.48	1.2	0.535	1	0.85	1	–	0.85	–	–
	First stage	331	0.377	1.84	0.59	1	1	1	0.06	0.85	0.85	25
	Interstage	0.079	1	0.003	1	1	1	1	0.06	0.85	0.85	25
	Reentry HW	0.899	0.972	1.901	0.59	1	1	1	0.06	0.85	0.85	25
	Landing HW	1.121	0.916	0.839	0.59	1	1	1	0.06	0.85	0.85	25
	SL engine	277	0.48	1.2	0.535	1.1	0.85	1	0.07	0.85	0.85	20
	GNC	2500	1	0	1	1	1	1	–	1	–	–
	Second stage	331	0.377	1.84	0.59	0.7	1	1	–	0.85	–	–
VL_HH_SC_MED	Vac. engine	277	0.48	1.2	0.535	1	0.85	1	–	0.85	–	–
	First stage	331	0.377	1.84	0.59	1	1	1	0.06	0.85	0.85	25

Table 5 (continued)

Launcher	Element	a_{dev}	x_{dev}	a_{prod}	x_{prod}	f_1	f_2	f_3	f_5	p	p_{refurb}	Reuses
VL_CC_GG_HI	Interstage	0.079	1	0.005	1	1	1	1	0.06	0.85	0.85	25
	Reentry HW	0.899	0.972	1.901	0.59	1	1	1	0.06	0.85	0.85	25
	Landing HW	1.121	0.916	0.839	0.59	1	1	1	0.06	0.85	0.85	25
	SL engine	277	0.48	1.2	0.535	1.1	0.85	1	0.07	0.85	0.85	20
	GNC	2500	1	0	1	1	1	1	–	1	–	–
	Second stage	331	0.377	1.84	0.59	0.7	1	1	–	0.85	–	–
	Vac. engine	277	0.48	1.2	0.535	1.1	0.85	1	–	0.85	–	–
	First stage	331	0.377	1.84	0.59	1	1	1	0.06	0.85	0.85	25
	Interstage	0.079	1	0.003	1	1	1	1	0.06	0.85	0.85	25
	Reentry HW	0.899	0.972	1.901	0.59	1	1	1	0.06	0.85	0.85	25
	Landing HW	1.121	0.916	0.604	0.59	1	1	1	0.06	0.85	0.85	25
	SL engine	277	0.48	1.2	0.535	1.1	0.85	1	0.07	0.85	0.85	20
	GNC	2500	1	0	1	1	1	1	–	1	–	–
	Second stage	331	0.377	1.84	0.59	0.7	1	1	–	0.85	–	–
VL_CC_GG_MED	Vac. engine	277	0.48	1.2	0.535	1.1	0.85	1	–	0.85	–	–
	First stage	331	0.377	1.84	0.59	1	1	1	0.06	0.85	0.85	25
	Interstage	0.079	1	0.003	1	1	1	1	0.06	0.85	0.85	25
	Reentry HW	0.899	0.972	1.901	0.59	1	1	1	0.06	0.85	0.85	25
	Landing HW	1.121	0.916	0.604	0.59	1	1	1	0.06	0.85	0.85	25
	SL engine	277	0.48	1.2	0.535	1.1	0.85	1	0.07	0.85	0.85	20
	GNC	2500	1	0	1	1	1	1	–	1	–	–
	Second stage	331	0.377	1.84	0.59	0.7	1	1	–	0.85	–	–
	Vac. engine	277	0.48	1.2	0.535	1.1	0.85	1	–	0.85	–	–
	First stage	331	0.377	1.84	0.59	1	1	1	0.06	0.85	0.85	25
	Interstage	0.079	1	0.003	1	1	1	1	0.06	0.85	0.85	25
	Reentry HW	0.899	0.972	1.901	0.59	1	1	1	0.06	0.85	0.85	25
	Landing HW	1.121	0.916	0.604	0.59	1	1	1	0.06	0.85	0.85	25
	SL engine	277	0.48	1.2	0.535	1.1	0.85	1	0.07	0.85	0.85	20
VL_CC_SC_MED	GNC	2500	1	0	1	1	1	1	–	1	–	–
	Second stage	331	0.377	1.84	0.59	0.7	1	1	–	0.85	–	–
	Vac. engine	277	0.48	1.2	0.535	1.1	0.85	1	–	0.85	–	–
	First stage	331	0.377	1.84	0.59	1	1	1	0.06	0.85	0.85	25
	Interstage	0.079	1	0.003	1	1	1	1	0.06	0.85	0.85	25
	Reentry HW	0.899	0.972	1.901	0.59	1	1	1	0.06	0.85	0.85	25
	Landing HW	1.121	0.916	0.604	0.59	1	1	1	0.06	0.85	0.85	25
	SL engine	277	0.48	1.2	0.535	1.21	0.85	1	0.07	0.85	0.85	20
	GNC	2500	1	0	1	1	1	1	–	1	–	–
	Second stage	331	0.377	1.84	0.59	0.7	1	1	–	0.85	–	–
	Vac. engine	277	0.48	1.2	0.535	1.21	0.85	1	–	0.85	–	–
	First stage	331	0.377	1.84	0.59	1	1	1	0.06	0.85	0.85	25
	Interstage	0.079	1	0.003	1	1	1	1	0.06	0.85	0.85	25
	Reentry HW	0.899	0.972	1.901	0.59	1	1	1	0.06	0.85	0.85	25
VL_KK_GG_HI	Landing HW	1.121	0.916	0.604	0.59	1	1	1	0.06	0.85	0.85	25
	SL engine	277	0.48	1.2	0.535	1.1	0.85	1	0.07	0.85	0.85	20
	GNC	2500	1	0	1	1	1	1	–	1	–	–
	Second stage	331	0.377	1.84	0.59	0.7	1	1	–	0.85	–	–
	Vac. engine	277	0.48	1.2	0.535	1.1	0.85	1	–	0.85	–	–
	First stage	331	0.377	1.84	0.59	1	1	1	0.06	0.85	0.85	25
	Interstage	0.079	1	0.003	1	1	1	1	0.06	0.85	0.85	25
	Reentry HW	0.899	0.972	1.901	0.59	1	1	1	0.06	0.85	0.85	25
	Landing HW	1.121	0.916	0.604	0.59	1	1	1	0.06	0.85	0.85	25
	SL engine	277	0.48	1.2	0.535	1.1	0.85	1	0.07	0.85	0.85	20
	GNC	2500	1	0	1	1	1	1	–	1	–	–
	Second stage	331	0.377	1.84	0.59	0.7	1	1	–	0.85	–	–
	Vac. engine	277	0.48	1.2	0.535	1.1	0.85	1	–	0.85	–	–
	First stage	331	0.377	1.84	0.59	1	1	1	0.06	0.85	0.85	25
VL_KK_GG_MED	Interstage	0.079	1	0.003	1	1	1	1	0.06	0.85	0.85	25
	Reentry HW	0.899	0.972	1.901	0.59	1	1	1	0.06	0.85	0.85	25
	Landing HW	1.121	0.916	0.604	0.59	1	1	1	0.06	0.85	0.85	25
	SL engine	277	0.48	1.2	0.535	1.1	0.85	1	0.07	0.85	0.85	20
	GNC	2500	1	0	1	1	1	1	–	1	–	–
	Second stage	331	0.377	1.84	0.59	0.7	1	1	–	0.85	–	–
	Vac. engine	277	0.48	1.2	0.535	1.1	0.85	1	–	0.85	–	–
	First stage	331	0.377	1.84	0.59	1	1	1	0.06	0.85	0.85	25
	Interstage	0.079	1	0.003	1	1	1	1	0.06	0.85	0.85	25
	Reentry HW	0.899	0.972	1.901	0.59	1	1	1	0.06	0.85	0.85	25
	Landing HW	1.121	0.916	0.604	0.59	1	1	1	0.06	0.85	0.85	25
	SL engine	277	0.48	1.2	0.535	1.1	0.85	1	0.07	0.85	0.85	20
	GNC	2500	1	0	1	1	1	1	–	1	–	–
	Second stage	331	0.377	1.84	0.59	0.7	1	1	–	0.85	–	–
	Vac. engine	277	0.48	1.2	0.535	1.1	0.85	1	–	0.85	–	–
VL_PP_GG_HI	First stage	331	0.377	1.84	0.59	1	1	1	0.06	0.85	0.85	25
	Interstage	0.079	1	0.003	1	1	1	1	0.06	0.85	0.85	25
	Reentry HW	0.899	0.972	1.901	0.59	1	1	1	0.06	0.85	0.85	25

Table 5 (continued)

Launcher	Element	a_{dev}	x_{dev}	a_{prod}	x_{prod}	f_1	f_2	f_3	f_5	p	p_{refurb}	Reuses
EL_HH_SC_MiED	Landing HW	1.121	0.916	0.604	0.59	1	1	1	0.06	0.85	0.85	25
	SL engine	277	0.48	1.2	0.535	1.1	0.85	1	0.07	0.85	0.85	20
	GNC	2500	1	0	1	1	1	1	–	1	–	–
	Second stage	331	0.377	1.84	0.59	0.7	1	1	–	0.85	–	–
	Vac. engine	277	0.48	1.2	0.535	1.1	0.85	1	–	0.85	–	–
	First stage	331	0.377	1.84	0.59	0.7	1	1	–	0.85	–	–
	Interstage	0.079	1	0.005	1	0.7	1	1	–	0.85	–	–
	SL engine	277	0.48	1.667	0.535	1.1	0.65	1	–	0.85	–	–
EL_HH_GG_MED	Second stage	331	0.377	1.84	0.59	0.7	1	1	–	0.85	–	–
	Vac. engine	277	0.48	1.667	0.535	1.1	0.65	1	–	0.85	–	–
	First stage	331	0.377	1.84	0.59	0.7	1	1	–	0.85	–	–
	Interstage	0.079	1	0.005	1	0.7	1	1	–	0.85	–	–
EL_CH_GG_MED	SL engine	277	0.48	1.667	0.535	1	0.65	1	–	0.85	–	–
	Second stage	331	0.377	1.84	0.59	0.7	1	1	–	0.85	–	–
	Vac. engine	277	0.48	1.667	0.535	1	0.65	1	–	0.85	–	–
	First stage	331	0.377	1.84	0.59	0.7	1	1	–	0.85	–	–
EL_CC_GG_MED	Interstage	0.079	1	0.005	1	0.7	1	1	–	0.85	–	–
	SL engine	277	0.48	1.2	0.535	1.1	0.65	1	–	0.85	–	–
	Second stage	331	0.377	1.84	0.59	0.7	1	1	–	0.85	–	–
	Vac. engine	277	0.48	1.2	0.535	1.1	0.65	1	–	0.85	–	–
EL_CC_SC_MED	First stage	331	0.377	1.84	0.59	0.7	1	1	–	0.85	–	–
	Interstage	0.079	1	0.005	1	0.7	1	1	–	0.85	–	–
	SL engine	277	0.48	1.2	0.535	1.21	0.65	1	–	0.85	–	–
	Second stage	331	0.377	1.84	0.59	0.7	1	1	–	0.85	–	–
	Vac. engine	277	0.48	1.2	0.535	1.21	0.65	1	–	0.85	–	–

Author contributions J.W. performed the cost analysis and wrote the majority of the manuscript. M.H. conducted the technical analysis related to the ELV launcher design and the SSO payload assessment for the ENTRAIN launchers, and authored the corresponding sections of the manuscript. M.S. contributed with conceptualization, supervision, and review of the manuscript.

Funding Open Access funding enabled and organized by Projekt DEAL.

Data availability No datasets were generated or analysed during the current study.

Declarations

Conflict of interest The authors have no relevant financial or nonfinancial interests to disclose.

LLM-Assisted Text Revision During the preparation of this work, the authors used ChatGPT 4o in order to revise the text. After using this tool/service, the authors reviewed and edited the content as needed and take full responsibility for the content of the publication.

Open Access This article is licensed under a Creative Commons Attribution 4.0 International License, which permits use, sharing, adaptation, distribution and reproduction in any medium or format, as long as you give appropriate credit to the original author(s) and the source, provide a link to the Creative Commons licence, and indicate if changes were made. The images or other third party material in this article are included in the article's Creative Commons licence, unless indicated otherwise in a credit line to the material. If material is not included in the article's Creative Commons licence and your intended use is not permitted by statutory regulation or exceeds the permitted use, you will need to obtain permission directly from the copyright holder. To view a copy of this licence, visit <http://creativecommons.org/licenses/by/4.0/>.

References

1. Dietlein, I., et al.: Overview of system study on recovery methods for reusable first stages of future European launchers. CEAS Space J. (2024). <https://doi.org/10.1007/s12567-024-00557-9>

2. Sippel, M., Wilken, J.: Selection of propulsion characteristics for systematic assessment of future European RLV-options. CEAS Space J. (2024). <https://doi.org/10.1007/s12567-024-00564-w>
3. Wilken, J., Stappert, S.: Comparative analysis of European vertical landing reusable first stage concepts. CEAS Space J. (2024). <https://doi.org/10.1007/s12567-024-00549-9>
4. Bussler, L., Sippel, M., Dietlein, I.: Comparative analysis of European horizontal-landing reusable first stage concepts. CEAS Space J. (2024). <https://doi.org/10.1007/s12567-024-00572-w>
5. Stappert, S., et al.: Options for future European reusable booster stages: evaluation and comparison of VTHL and VTVL return methods. CEAS Space J. (2024). <https://doi.org/10.1007/s12567-024-00571-x>
6. Ullman, D.G.: The Mechanical Design Process. McGraw-Hill, Boston (2003)
7. ESA Space Environment Report 2023, Technical Report, ESA Space Debris Office, 12.09.2023 (2023). https://www.sdo.esoc.esa.int/environment_report/Space_Environment_Report_latest.pdf
8. Vallado, D.A.: Orbital mechanics fundamentals. In: Blockley, R., Shyy, W. (eds.) Encyclopedia of Aerospace Engineering. Wiley (2010). <https://doi.org/10.1002/9780470686652.eae285>
9. Trivailo, O., Sippel, M., Şekercioğlu, Y.: Ahmet: Review of hardware cost estimation methods, models and tools applied to early phases of space mission planning. Prog. Aerosp. Sci. (2012). <https://doi.org/10.1016/j.paerosci.2012.02.001>
10. Koelle, D.E.: Handbook of Cost Engineering for Space Transportation Systems: Including TRANSCOST 8.2 Statistical-Analytical Model for Cost Estimation and Economical Optimization of Launch Vehicles. TransCostSystems (2013)
11. Wilken, J.: Cost estimation for launch vehicle families considering uncertain market scenarios. Acta Astronaut. **216**, 15–26 (2024). <https://doi.org/10.1016/j.actaastro.2023.12.035>
12. Stappert, S., Wilken, J., Calabuig, G.J.D., Sippel, M.: Evaluation of parametric cost estimation in the preliminary design phase of reusable launch vehicles. In: 9th European Conference for Aeronautics and Space Science (2022). <https://elib.dlr.de/187238/>
13. Kuczera, H., Sacher, P.W., Dujarric, Ch.: FESTIP system study—An overview. In: Space Plane and Hypersonic Systems and Technology Conference (1996)
14. Mann, T., et al.: Sizing and lifecycle cost analysis of an Ares V Composite Interstage. In: 53rd AIAA/ASME/ASCE/AHS/ASC Structures (2012)
15. Sippel, M., Herbertz, A.: Propulsion systems definition for a liquid fly-back Booster. In: 2nd European Conference for Aerospace Sciences (EUCASS), 2007-07-01–2007-07-06, Brussels, Belgium (2007)
16. Sippel, et al.: In-Air-Capturing Development Roadmap (Update), FALCon Deliverable D2.4 (2023). <https://elib.dlr.de/194602/>
17. Musk, E.: <https://x.com/elonmusk/status/1295883862380294144> (2020). Accessed 16 Aug 2024
18. ESA: Assessment of the launch service market demand: Forecast of the accessible launch service market demand. ESA/PB-ST(2023)31 (2023)
19. SpaceX: Capabilities & Services. <https://www.spacex.com/media/Capabilities&Services.pdf>. Accessed 29 Aug 2024
20. Lionnet, P.: SpaceX and the categorical imperative to achieve low launch cost. <https://spacenews.com/spacex-and-the-categorical-imperative-to-achieve-low-launch-cost/>. Accessed 29 Aug 2024
21. ESA: Overall Space Transportation Programmes Status Report, ESA/PB-ST(2024)1, February 2024

Publisher's Note Springer Nature remains neutral with regard to jurisdictional claims in published maps and institutional affiliations.